Fall 2021

# Fate and Transport of the Microbiome in Built Environments

Dahae Seong

# FATE AND TRANSPORT OF THE MICROBIOME IN BUILT ENVIRONMENTS

by

Dahae Seong

Bachelor of Science
Pukyong National University, 2013

Master of Science
Pukyong National University, 2015

---

Submitted in Partial Fulfillment of the Requirements

For the Degree of Doctor of Philosophy in

Civil and Environmental Engineering

College of Engineering and Computing

University of South Carolina

2022

Accepted by:

Shamia Hoque, Major Professor

Joseph Flora, Committee Member

Enrica Viparelli, Committee Member

R Sean Norman, Committee Member

Tracey L. Weldon, Interim Vice Provost and Dean of the Graduate School

# ACKNOWLEDGEMENTS

I would like to thank my esteemed supervisor – Dr. Shamia Hoque for her support, patience, and invaluable advice during my PhD study. Her guidance and advise carried me through all difficulties and made this work possible. I would also like to thank my committee members, Dr. Joseph Flora, Dr. Enrica Viparelli, and Dr. R Sean Norman, for your detailed comments and suggestions and all the encouraging words you have provided. I would also like to thank Dr. Qian Wang, Department of Chemistry and Biochemistry, for his kind advice and support during my research.

Most importantly, I would like to give special thanks to my family for their love and support. Without my family's support, care, and encouragement, it would not have been possible for me to achieve my educational goals. I am deeply grateful to my parents for always believing in me.

# ABSTRACT

Buildings are complex ecosystems evolving continuously. Indoor components such as occupants, ventilation system, and building structures influence the microbiome. To shed light on how the microbial population in a building will respond to such a fluid system, the fundamental interactions between microbes and the indoor ecosystem must be understood. Buildings are being designed as air-tight structures to save energy; however, this could lead to degradation of indoor air quality through indoor sources of contaminants and/or containment of pollutants in the room or introduce outdoor pollutants indoors depending on the ventilation conditions. In addition, transmission of infectious microbes in indoors threaten the health and well-being of people sharing the indoor spaces. Recent outbreak of severe acute respiratory syndrome coronavirus 2 (SARS-CoV-2) have brought to attention the significance of understanding indoor microbial fate and transmission mechanisms. This study focused on transitioning the existing body of knowledge on indoor environment and microbiome towards informing building design and generating insight into the mechanisms governing microbial fate and transport in indoor spaces.

An extensive literature review coupled with fractional factorial design approach was applied to identify bacterial families as bio-fingerprints of spaces for the first time. The bio-fingerprints allows the prediction of the possible bacteria present in a building space considering gender, age, and building usage. Field sampling at educational buildings extended knowledge of the influence of occupant characteristics, surface type and the influence of air exchange systems: vents, doors, and windows. While presence of occupants

resulted in an increase in particles and microbes, activity significantly influenced bacterial quantity from outdoor sources. Microbial levels were significant depending on whether the age group of the occupants was averaging under or over the 10-year-old, indicating that policies to improve indoor air quality need to account for the distinct nature of elementary schools while high schools and universities may have more similar traits. For surface materials, bacterial levels were lowest on metals and highest on carpets and, tiles. The ventilation system had minimal influence on the removal of microbes generated from indoor sources. The analysis highlighted possible dominance of wall and boundary effects on bacterial transport before occupants' influence take over. To gain better understanding of boundary effects and surface – microbes interactions, the influence of surface properties, surface types, external forces (inertial force and shear stress) were investigated. Enveloped viruses, vaccinia virus (VACV) and measles virus (MV), bacteria (*Corynebacterium* sp.) and bovine serum albumin (BSA) were applied. Quartz crystal microbalance with dissipation (QCM-D) was used to measure the change of mass on a range of 'ideal' surfaces for varying flow rates and to determine the adhesion kinetics governing the attachment and detachment process. Centrifugal experiments tested bacterial attachment and detachment from 'real' surfaces. Attachment and detachment kinetics were unique to each microbe-surface combination and shear stress magnitudes governed the extent of detachment.

*Keywords: Built environment, Indoor air, Surface, Microbiome, Ventilation, Adhesion*

# TABLE OF CONTENTS

# LIST OF TABLES

# LIST OF FIGURES

# CHAPTER 1. INTRODUCTION

People spend almost 90% of their lives indoors [1-3]. The Environmental Protection Agency (EPA) has established indoor air quality guidelines for structures and buildings and identified short- and long-term health effects. Immediate exposure to the contaminated indoor air can cause treatable problems such as eye soreness, nasal irritation, headaches, and fatigue. Long-term effects can give rise to respiratory diseases, heart disease, cancer or even can be fatal in severe cases [4]. After the outbreak of severe acute respiratory syndrome coronavirus 2 (SARS-CoV-2), *i.e.*, COVID-19 in 2019, the virus has spread rapidly across the world, infected over 250 million people, and contributed to the deaths of over 5 million people in the world [5]. This is not the first time that transmission of infectious microbes influenced public health and disrupted day to day life. In the 2000s, serious respiratory diseases such as severe acute respiratory syndrome coronavirus 1 (SARS-CoV-1) and middle east respiratory syndrome coronavirus (MERS-CoV) occurred which infected a total of 8,096 people worldwide causing 774 deaths (10% mortality rate) in 26 countries and affected 2,506 people resulting in 866 deaths (35% mortality rate) reported in 27 countries, respectively [6-8]. Currently, multi drug resistant pathogens besides *Staphylococcus aureus,* such as *Klebsiella pneumoniae, Acinetobacter baumannii, Clostridium difficile* and *Pseudomonas aeruginosa* is a serious concern to both nosocomial and community acquired infections [9, 10]. Outbreaks involving the same strain of bacteria are not uncommon and when an antibiotic-resistant strain is involved, the results can be deadly. Moreover, some antibiotic-resistance pathogens in health care facilities also have

become a serious issue due to their possibility of secondary infection and increment of hospital maintenance costs. Methicillin-resistance *Staphylococcus aureus* (MRSA) is a hospital-acquired infection which can be easily transmitted by contact [11]. In the past two decades, methicillin- resistant MRSA infection has increased substantially [12, 13]. MRSA infection is continuously reported even outside of health care facilities and observed among individual with or without known symptoms [14, 15]. A fungal infection caused by *Candida auris* has emerged recently due to its multidrug resistance [16] and has so far proved to be extremely persistent on surfaces. The Centers for Disease Control and Prevents (CDC) showed that 30~60% of patient with *Candida auris* infection have died and the symptoms cannot be easily detected because patients are already sick [17].

The steady increase in nosocomial and community acquired infections in indoor settings and now COVID-19 has brought to the forefront the lack of understanding of the role the indoor environment plays for the health and well-being of the occupants. Improvement on building design has focused on energy efficiency. Buildings account for nearly 40% of the total energy consumption with a significant portion of this going towards heating, ventilation and lighting to ensure, comfort, productivity and health [18]. As buildings are being designed to be air-tight structures to save energy, degradation of indoor air quality is occurring through containment of polluted air (at higher concentrations in dead zones), or introduction of outdoor pollutants indoors or indoor pollutants remaining indoors depending on the ventilation condition [19-21]. Most indoor air pollutant sources are within the buildings and some of the pollutants are introduced through inappropriate ventilation systems [22]. A recent study confirmed that sharing indoor spaces is a major risk factor for SARS-CoV-2 transmission [23]. One person could infect an unusually large

number of people sharing a space through both air and fomite transfer [24]. Viruses could be transferred to up to seven clean surfaces via contaminated fingers [25]. Statistically a contaminated surface could become a vector in spreading infections to at least 14 persons [26]. Relying only on ventilation approaches to ensure 'clean' indoors and one size fit all approach for disinfection has so far proved not to be a feasible approach. Therefore, understanding what indoor environmental factors dominate the spread and persistence of microbes in the air and on surfaces are essential to manage and maintain the 'clean' and 'safe' built environment.

**Motivation**

Microorganisms in built environment reflect indoor characteristics. Numerous studies have found that the indoor microbial communities and their concentrations differ depending on the surrounding conditions, such as human occupancy/activity [27, 28], gender [29, 30], building design [31], or dampness [32]. Studies have been conducted in residences [33-35], offices [36-38], hospitals [39-44], schools [36, 45-48], and public spaces [49-52]. Most airborne microorganisms exist by attaching on the PM. Above 80% of airborne microorganisms in PM are bacteria, followed by fungi, archaea, and virus [53]. *Firmicutes, Bacteroidetes, Actinobacteria,* and *Proteobacteria* are the four major phyla in indoors regardless of the types of buildings [29, 47, 51].

Human activity and occupancy are considered as major sources of the indoor microbial contamination since they result in the increment of airborne microbial concentration in PM [54, 55]. Humans scatter approximately 1.5 million skin cells per hour [56], resuspend settled dust [57], and contribute substantially to the mass of indoor particulate matters during normal activities [58]. Kim and Kim (2007) observed the highest

bacterial and fungal concentration in kindergarten compared to hospitals, elderly welfare facilities, and nurse centers due to differences in the activity rate [39]. A home survey in the United States reported that on average approximately 7,000 taxa of bacteria and 2,000 taxa of fungi existed in house dust [28]. A recent study found that the indoor airborne microbes in most homes were primarily influenced by the outdoor air, and the presence of pets, tap water, and occupancy impacted the microbial diversity [34]. Ratio of living area and occupancy also influenced on the bacterial concentration [33]. Besides the human influence, building type is another factor that impacts on the presence of indoor microorganisms. The presence of *Staphylococcus* sp. in hospital can lead to serious health and facility problems if the strains show methicillin-resistance resulting in MRSA, [59]. Respiratory virus pathogens were detected on multiple surfaces in airport, especially frequently touched surfaces [60].

There is a strong and sufficient evidence to establish relationships between ventilation, airflow pattern and the spread of infectious diseases in buildings [61]. Studies show that ventilation rates of 25 liter/sec per person have the potential to reduce sick building syndrome and sick leave while low ventilation rates at schools can have a negative impact on school absence and respiratory illness. Further investigations into assessing parameters influencing exposure risk between occupants showed that person to person distance of less than 1.1 m in an office increases chances of infection [62]. Although the relationship between microbes and human is symbiosis, some microbes are potentially life-threatening. To minimize the transmission of infectious particles via air and surfaces, the particles' spreading mechanisms from person to another or person to surfaces need to be preceded. Therefore, the main purposes of this study are to determine indoor microbial

characteristics under different occupied conditions and to investigate the fate and transport of indoor microbes in indoor air and surfaces.

**Objective and scope**

The objective of this research is to determine, assess and quantify the mechanisms governing the fate and transport of microbes in indoor spaces. This was done through a combination of field, experimental and laboratory studies combined to inform the existing knowledge gaps required to inform predictive models that can capture the physical and biological mechanisms unique to specific microbe(s), indoor air and surface type combination. The specific objectives are as follows:

**Objective 1**: This study was performed to determine if the presence of specific bacteria indicates the indoor characteristics as a 'bio-fingerprint.' Indoor microbial concentrations and components were reflecting occupants' characteristics such as age and gender and types of building such as hospital, schools, residence, or non-residence. Microbes presenting in the air and surfaces were analyzed. Several bacterial family groups were suggested to describe the indoor spaces.

**Objective 2**: This study was conducted to evaluate the influence of occupant characteristics and built air exchange (BAE) components on the presence and spatial distribution of PM, bacteria, and fungi. Air and surface samples were collected from three educational buildings (elementary school, high school, and university). The effect of occupancy, activity, and gender on PM and microbial concentration and the effect of BAE components

on bacterial spatial distribution were determined. Surface contamination was assessed by the surface type and usage.

**Objective 3**: The investigation identified the gaps in the current literature in the context of determining the adhesion kinetics for the interaction of virus particles on four types of surfaces which are gold, silica, glass, and stainless steel. Vaccinia virus (VACV) was used. Quartz crystal microbalance with dissipation (QCM-D) technique was applied to evaluate the microbial adhesion kinetics in nano scale. Current knowledge on particle attachment, adhesion, and resuspension in indoor spaces and the influence of surface materials were summarized.

**Objective 4**: This study determined and assessed the relationship between unique-microbe surface combination under the influence of varying flow conditions. Organic particles, which included, VACV, measles virus, and *Corynebacterium* sp., and an inorganic particle, BSA, were used. QCM-D were applied to determine the adhesion and detachment kinetics on ideal surfaces, the influence of flow rate on particles adhesion and detachment, and to evaluate the adhered layers' characteristics. Centrifugal experiment was applied to determine interactions between bacteria and real-world surfaces. Particles' behavior near the surface boundary was observed using Particle Image Velocimetry (PIV).

**Intellectual merit and major outcome**: The research was aimed to address the fate and transport of microbes in built environments starting from a wide lens to gaining fundamental insights: Presence of microbes in built environments → microbial

concentration and components under specific occupied conditions → microbial attachment on different types of surfaces → microbial adhesion and detachment kinetics within the boundary layer. The outcomes of the study can provide prior information to predict the type, presence, and transmission of infectious microbes in indoor spaces. Such information is particularly vital for buildings occupied by vulnerable population especially schools or hospitals. The information can also provide guidance in making prior decisions regarding building designs and public policies. The overall research scopes are outlined in **Figure 1.1**.

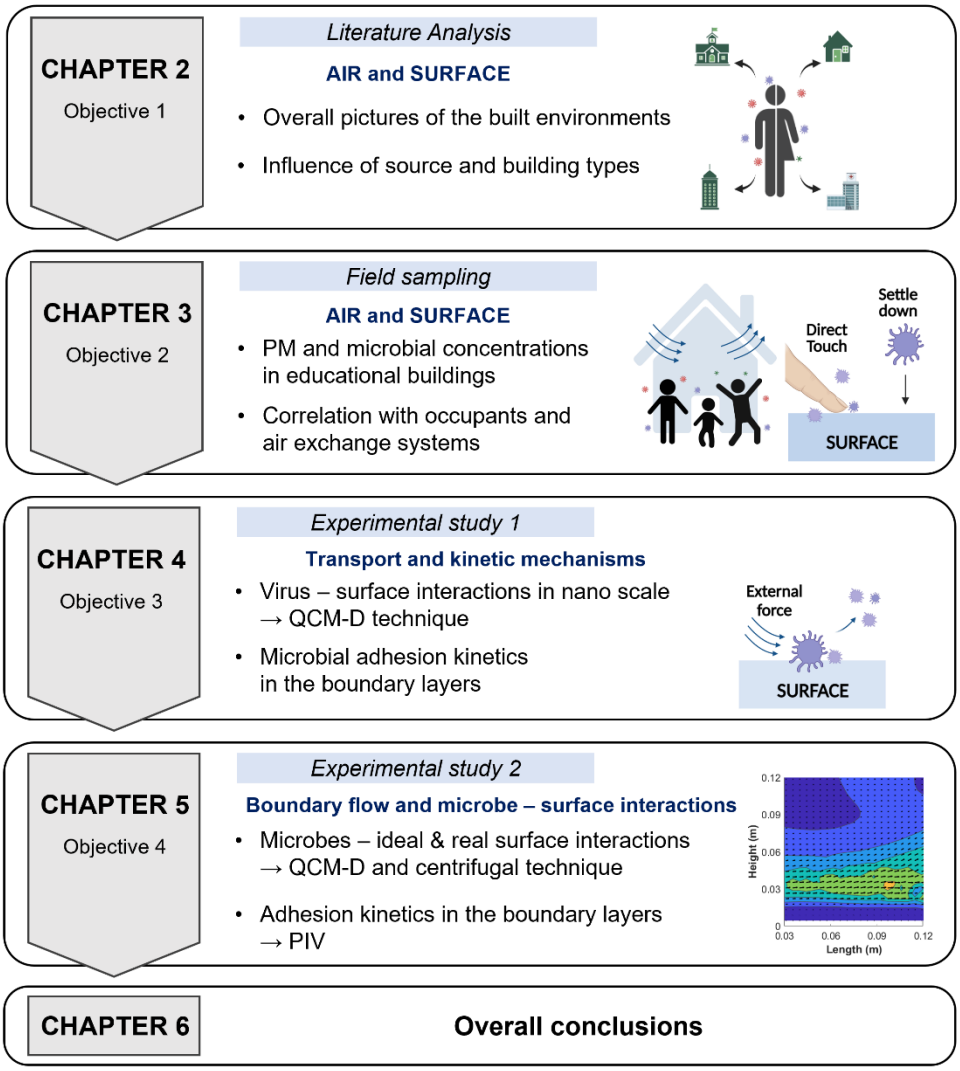


*Created with BioRender.com*

**Figure 1.1.** A diagram of dissertation outline.

# CHAPTER 2. DOES THE PRESENCE OF CERTAIN BACTERIAL FAMILY IN THE MICROBIOME INDICATE SPECIFIC INDOOR ENVIRONMENT CHARACTERISTICS? A FACTORIAL DESIGN APPROACH FOR IDENTIFYING BIO-FINGERPRINTS [1]

## ABSTRACT

The study applies the current knowledge on microbiome in built environments towards identifying microbes, specifically bacteria as bio-fingerprints which can reflect indoor space and occupant characteristics. Data were collected from the literature on the bacterial family and the indoor environment. The factorial design approach was applied to quantify and compare the influence of selected indoor environmental parameters, sampling region (air or surface), sampling locations (residence or non-residence), gender and age and their interactions on the types and concentration of detected bacterial families. Factorial design analysis identified and confirmed *Corynebacteriaceae* and *Lactobacillaceae* as the gender signature for males and females, respectively. The significant bacterial families across all scenarios are: *Corynebacteriaceae, Propionibacteriaceae, Bacillaceae, Staphylococcaceae, Lactobacillaceae, Methylobacteriaceae, Moraxellaceae,*

[1] Results presented in this chapter have appeared in "Seong.D. & Hoque.S., (2020) Indoor and Built Environment, 29(1), 117-131"

*Micrococcaceae*, *Enterobacteriaceae*, *Rhodobacteraceae*, *Streptococcaceae* and *Pseudomonadaceae*. Higher concentrations of *Propionibacteriaceae* indicate that the specific location is an adult-occupied space. *Staphylococcaceae* presence is the bio-fingerprint of contaminated air of hospitals bio-fingerprint and *Moraxellaceae* on hospital surfaces are distinct characteristics. *Streptococcaceae* is a bio-fingerprint of contaminated air of schools and other children-occupied spaces. *Enterobacteriaceae* is a bio-fingerprint of contaminated air of non-residence locations. *Bacillaceae* does not indicate any indoor characteristics.

*Keywords: Built environment, Factorial design, Microbiome, Bio-fingerprint, Microbes, Surface, Indoor air*

## 2.1. INTRODUCTION

The literature on indoor environment and microbes gives a detailed and still evolving picture of the microbiome [56, 63]. Investigations show that the composition of the microbial community reflects outdoor/indoor sources [57, 64, 65] and human occupancy [28, 58]. Different sources could influence the microbial characteristics in the built environment, for instance, gender [29, 30], building location [66], building design [31], or human activity [64, 67]. Prussin and Marr [68] list eight major sources: humans; pets; plants; plumbing systems; heating, ventilation and air conditioning (HVAC) systems; mould; dust resuspension; and the outdoor environment. The studies provide a window into the microbial world in the buildings. However, this field is still far from informing practitioners such as architects or building facilities management or public health officials regarding building design or disinfecting a space or to make any decision pertaining to the

application of the microbial built environment knowledge. To bridge that gap a better understanding is required on the influence or interacting influences of different factors on the microbial 'bio-fingerprint' in an indoor space.

De Wilde and Coley [69] state,

*"Buildings provide an interface between the outdoor environment, which is subject to climate change and the indoor environment, which needs to be maintained within a range that keeps building occupants safe and comfortable, and which is suitable for any key processes that are taking place within the building."*

However, buildings are complex ecosystems. Microbiome investigations are revealing the existing diversity and technological advancements that have allowed for more precise identification of microbial species in the built environment. Cultivation-based studies have been widely used to identify microbial species [36, 37, 70]. Recently DNA-based studies have provided a more detailed picture [34, 48, 57]. Most of the identified bacteria are included in the four major phyla which are *Actinobacteria*, *Bacteroidetes*, *Firmicutes*, and *Proteobacteria* [29, 47, 51]. A home survey in the United States detected that on average approximately 7,000 taxa of bacteria and 2,000 taxa of fungi existed in house dust [28]. Studies have shown that humans scatter approximately 1.5 million skin cells per hour [56], resuspend settled dust [57], and contribute substantially to the mass of indoor particulate matters during normal activities [58]. Previous studies have revealed that higher human density and human activity could result in an increase in indoor microbial levels [1, 57, 71]. Human skin-related bacteria such as *Staphylococcus*, *Streptococcus*, and *Micrococcus* genera are commonly found indoors, and their concentrations change depending on the surrounding conditions [1, 28, 33, 36, 71]. Gender also appears to be a

factor that influences the microbial community. *Lactobacillus* sp. is a bacteria associated with female human subjects which is related to vaginal microorganisms, while *Corynebacterium* sp. and *Dermabacter hominis* have been found in male (human) - occupied rooms or restrooms [30, 72]. In a review by Kelley and Gilbert [56], *Streptococcus* spp., *Corynebacterium* spp., *Flavimonas* spp., *Lactobacillus* spp., *Bacillus* spp., and *Bradyrhizobium* spp. were identified as representatives for an office room. Another study by Bouillard et al. [73] found *Micrococcus* spp., *Staphylococcus* spp., and *Streptococcus* spp. to be most common in indoor air, surfaces and settled dust in a 'healthy' office building. The influence of human population on the adaptability of the microbial community was also shown by Lax et al. [67] where on sampling seven families, the results showed that each family home had its own microbial signature or fingerprint.

Significant associations of microbial species with location, building age, area and floor level were tested through statistical approaches such as Spearman's correlation, Pearson's correlation or bivariate correlation test. The approaches were applied to assess differences between bacterial and fungal load at multiple locations; hospitals, educational facilities, restaurants, offices, dormitories and residences [40, 74]. Schools were observed to have higher bacterial concentrations whereas kitchens and bathrooms had a higher fungal load. By applying Kolmogorov-Smirnov and Kruskal-Wallis test, Wang et al. [66] concluded that the airborne fungi concentration in homes were higher in spring and winter but indoor temperature and humidity had a negligible significance. Niesler et al. [50] reported low correlations between air and surface samples for bacteria and fungi in storerooms of a museum. Indoor microbial compositional similarity/dissimilarity was quantified by the similarity/dissimilarity test such as ANOSIM [34, 47] or Bray-Curtis test

[30, 57, 64]. Several studies used Bayesian source tracking to determine the estimated source of indoor microbiome [29, 75]. Studies continue to identify and determine what is the impact of building and occupant characteristics on indoor microbiome. However, these studies do not identify dominant ‘characteristics' or possible interaction of different characteristics that influence the presence or absence of specific bacteria. Identifying those would help the understanding of the link and would reduce the gap between application and the built environmental microbiome field.

This study focuses on analyzing the existing literature to determine if ‘bio-fingerprints’ can be identified, *i.e.*, if the presence of any bacterial families indicates certain indoor or occupant characteristics. The characteristics assessed are sampling region (air or surface), location (building type, *i.e.*, residences or commercial), age and gender. The factorial design approach [76] is applied to determine the dominant and interacting characteristics (factors).

## 2.2. MATERIALS AND METHODS

### 2.2.1. Data collection and calculation

The data was compiled from thirty-three studies published in different journals from 2005 to 2017. The search words applied are indoor environment, indoor microorganisms, indoor microbes, indoor microbiome, building environment, building microorganisms, building microbes, and building microbiome. For every study, the information collected was: the types of bacteria, the concentration of bacteria, sampling region (e.g. ambient air, surface), sampling location (e.g. residence, hospital, office,

school), gender and age (e.g. children, adult). **Table 2.1** shows the information of the studies classified according to sampling region, sampling location, age and gender.

The table also includes identification procedure and the number of samples from each study. The 'identification procedure' was surveyed to understand the methods applied. It is not included as a 'factor' in the analysis. The study focuses on the final results *i.e.*, bacterial families detected by each study. Except for one study, all studies clearly stated the identification procedures. Most of the air sampling studies used 'culture-based' method to identify microbes, applying the colony morphology approach and biochemical tests such as Gram-staining, oxidase or catalase test. DNA-based identification was generally used for characterizing surface microbes. Due to the sampling design of investigations reported in the literature only microbes identified from surfaces could be classified based on gender. Age was classified between children and adults. Samples collected from early age, *i.e.*, infant to elementary school was organized under children. Samples collected from educational institutions beyond high school was categorized under adults. **Eq. 2.1** was applied to calculate the percentage of each bacterial family, $N_x$, by determining the total number of colonies (CFUs) of each species, $n_{sp}$, belonging to the family divided by the total bacterial count of the specific study. The collected data was sorted based on **Eq. 2.1** and is presented in the supporting information section (**Table A1**).

$$N_x = \frac{\sum_{i=1}^{n_{sp}} (n_1 + n_2 + \cdots + n_{sp}) CFUs \times 100}{Total\ bacterial\ count\ in\ the\ study\ (CFUs)} \qquad \text{Eq. 2.1}$$

**Table 2.1.** The number of samples in each study and their sampling/identification information

| Year | Sampling region | | Sampling location [a] | | Age | | Gender | | Identification procedure | |
|---|---|---|---|---|---|---|---|---|---|---|
| | Air (2811) | Surface (1635) | Res. (773) | Non-Res. (2591) | Children (674) | Adult (717) | Male (312) | Female (334) | Culture based | DNA based |
| 2005 | 180 [45] | 5 [77] | | 180 [45] | 180 [45] | 5 [77] | 2 [77] | 3 [77] | | 5 [77]<br>180 [45] |
| 2007 | 336 [39] | 24 [78] | | 336 [39] | 84 [39] | 24 [78]<br>252 [39] | 12 [78] | 12 [78] | 336 [39] | 24 [78] |
| 2008 | 254 [36] | | | 254 [36] | | 254 [36] | | | 254 [36] | |
| 2009 | 8 [71]<br>208 [40] [b] | | | 8 [71]<br>208 [40] | | | | | | 8 [71] |
| 2010 | 9 [50]<br>25 [41]<br>40 [37] [c]<br>90 [49]<br>192 [46] | 27 [50] | | 25 [41]<br>36 [50]<br>40 [37]<br>90 [49]<br>192 [46] | 192 [46] | | | | 25 [41]<br>36 [50]<br>40 [37]<br>90 [49]<br>192 [46] | |
| 2011 | 32 [79] | 93 [80]<br>120 [29] | | 32 [79] | 93 [80] | 32 [79] | 60 [29] | 60 [29] | 32 [79] | 93 [80]<br>120 [29] |
| 2013 | 72 [70]<br>216 [44] | 34 [81] | | 34 [81]<br>72 [70]<br>216 [44] | | 72 [70] | | | 72 [70]<br>216 [44] | 34 [81] |
| 2014 | 8 [57] [c]<br>66 [52]<br>372 [33] | 32 [82] | 372 [33] | 8 [57]<br>32 [82]<br>66 [52] | | 8 [57] | | | 66 [52] | 8 [57]<br>32 [82]<br>372 [33] |
| 2015 | 25 [47]<br>29 [34]<br>138 [42]<br>318 [43] | 24 [35]<br>205 [83]<br>226 [84]<br>328 [34]<br>497 [85] | 24 [35]<br>337 [34] | 25 [47]<br>138 [42]<br>226 [84]<br>318 [43] | 25 [47]<br>175 [85] | 322 [85] | 238 [85] | 259 [85] | 138 [42]<br>205 [83]<br>318 [43] | 24 [35]<br>25 [47]<br>226 [84]<br>377 [34]<br>497 [85] |
| 2016 | 9 [48]<br>22 [51] | | | 9 [48]<br>22 [51] | 9 [48] | | | | | 9 [48]<br>22 [51] |
| 2017 | 18 [38] | | | 18 [38] | | | | | 18 [38] | |
| Distribution of studies | 23 | 12 | 3 | 24 | 7 | 8 | 4 | 4 | 15 | 17 |

[a] Res.: Residence. Non-Res.: Non-residence. Hospital, office, school, subway station, auditorium, museum, retail store and restaurant are grouped into non-residence. School includes day-care center, kindergarten, elementary school and university. University includes university campus buildings and all kinds of library; [b] Identification procedure is not clearly stated; [c] The number of samples is not clearly stated.

2.2.2. Data analysis

The collected data was arranged to determine the impact of the selected variables: sampling regions, sampling locations, gender and age. Data on viable bacteria, $N_x$ was log transformed to obtain normalized distributions for all datasets. **Figure 2.1** shows the results of *Propionibacteriaceae* percentages (%) from surfaces associated with both genders. The data was log-transformed to ensure normal distribution (based on the Kolmogorov-Smirnov test ($p > 0.05$)).

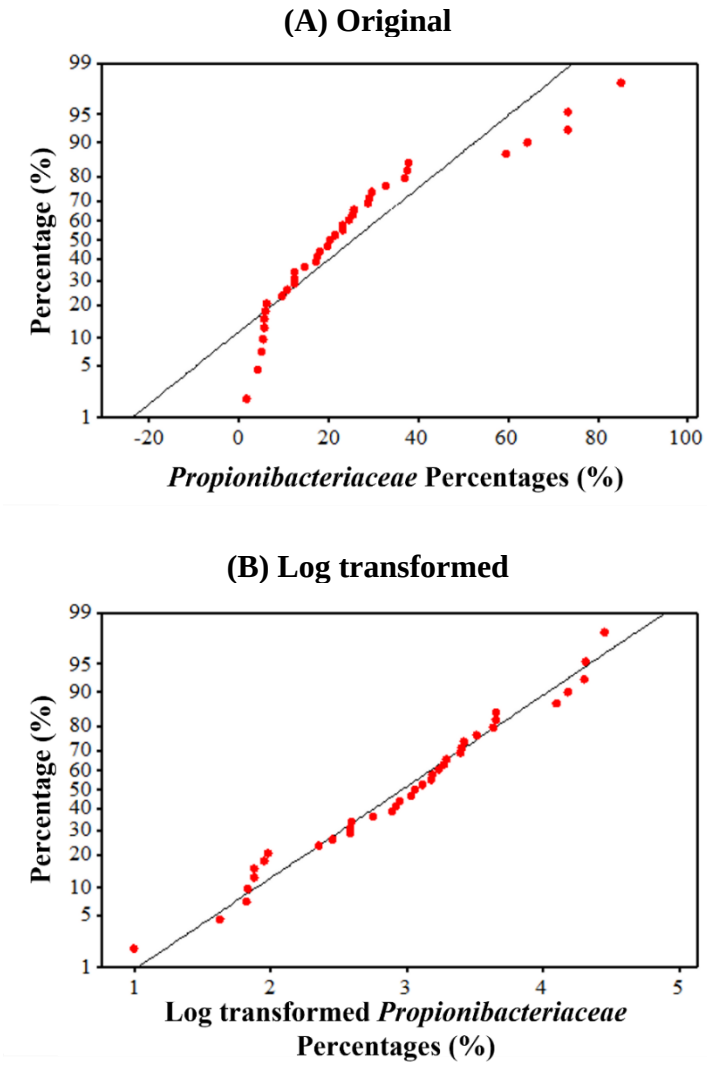


**Figure 2.1.** Distribution of *Propionibacteriaceae* percentages (%) of skin and restroom surfaces of both genders. The normality was evaluated by Kolmogorov-Smirnov test. **(A)** Original ($p < 0.01$) and **(B)** log transformed values ($p > 0.05$).

The factorial design approach was applied to determine if these variables or combination of these variables could influence the type of bacteria detected. Factorial experimental designs are efficient exploratory tools which are applied to assess the impact of selected variables on study objective(s). A two-level factorial design approach was used to determine the main and dominant characteristics (referred to as factors or variables also) which could influence the detected bacteria [76]. The number of experiments required by a full factorial design at two levels is $2^k$ where $k$ is the number of variables or factors. A full factorial design considers the effects of all main factors, *i.e.*, the main effects as well as all possible interactions between the factors. The main effect of a factor measures the average change in the response caused by changing from one level (low setting, -1) to another level (high setting, +1). A two-factor interaction looks at the effect on the response when two factors are simultaneously kept at different levels. The *p*-values indicate whether the effect of the main factor(s) or the interacting effect is significant at a level of 0.05. Analysis of variance (ANOVA) approach was applied to determine the *p*-values.

In the analysis, the sampling location was kept at two levels: residence (-1) and non-residence (+1), for sampling region, air was set as (-1) and any surface was set as (+1), for gender, female was assigned (-1) and male was assigned (+1), and for age the low level (-1) was set for children and the high level for adults (+1). In some scenarios as required, sampling surface was divided into restroom surface (-1) and skin surface (+1). For example, combination of sampling location level (-1) and sampling region level (-1) indicates the samples were collected from ‘air’ in ‘residence’. Combination of age level (+1) and sampling region level (-1) signifies that the ‘air’ samples were collected from ‘adult’ occupied spaces.

Datasets from different studies but at the same combination levels were replicates, the number of which depended on the literature. The number of replications of each combination were as follows: gender and sampling surface have 60 replications for (-1,-1), 274 for (-1,+1), 60 for (+1,-1), and 252 for (+1,+1); sampling location and sampling region have 401 replications for (-1,-1), 372 for (-1,+1), 2098 for (+1,-1), and 524 for (+1,+1) ; age and sampling region have 490 replications for (-1,-1), 268 for (-1,+1), 618 for (+1,-1), and 351 for (+1,+1). A Minitab statistical software (Minitab Inc., State College, PA, USA) was applied for the analysis.

## 2.3. RESULTS

### 2.3.1. Assessing the factorial design approach: Gender and sampling surface

The literature review showed that ambient sampling from indoor air was typically conducted in spaces where both genders occupied or used the space. Gender specific usage was clarified when samples were collected from surfaces. Hence, the analysis of this case focused on surface sampling data obtained from human skin, restrooms and mobile devices. Data from restroom and mobile device surfaces represent a direct transfer from a person to the surface. The only significant difference between one 'touch' to another resulting in the transfer is the age and gender of the person who touched the site. The results of gender influence were applied to assess if the factorial design analysis would identify significant factors, *i.e.*, the factors that could influence the bacterial families detected on the restroom surface.

An overview of the data is shown in **Figure 2.2** which shows the surface bacterial diversity of (A) human skin, (B) restroom, and (C) mobile device. *Propionibacteriaceae* is

the most predominant bacteria of skin (37%) and restroom surfaces (27%), whereas *Staphylococcaceae* is mainly detected on mobile device surfaces (66%). *Propionibacteriaceae* is abundant in places with frequent exposure to human or sebum-producing human skin surface and it is higher in concentration than other skin-related bacteria regardless of gender and age [29, 85-87]. Even though mobile device surfaces are repeatedly touched, *Staphylococcaceae* is present in higher concentrations (66%) than *Propionibacteriaceae* (<1%). Studies concluded that mobile surfaces are exclusively touched by hand where there is a lower concentration of *Propionibacterium* [86] and a higher concentration of *Staphylococcus* [88]. A recent study showed that mobile devices shared 22% of the owner's finger bacteria [89] and higher microbial contamination was observed in younger ages, lower educational levels and male human population groups [83]. There was stronger similarities between the surface microbial communities present

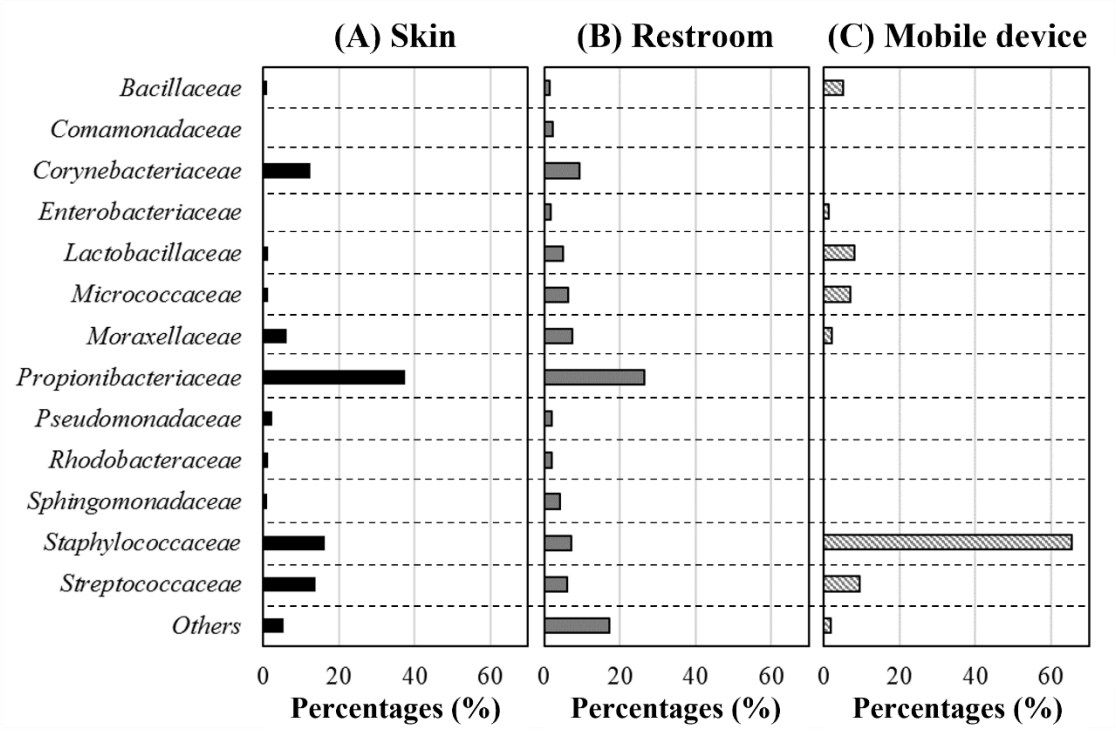


**Figure 2.2.** Surface bacterial diversity and their percentage (%) of **(A)** Skin, **(B)** Restroom and **(C)** Mobile device.

on females' (human) hands and their mobile devices than between the communities on males' hands and their mobile devices [30, 89].

The survey shows that the bacteria on various types of device surfaces reflect characteristics of the user. In case of mobile devices, the data gives information on the correlation between skin bacteria and surfaces touched but information on specific gender influence is limited. Hence, to determine if gender could influence the bacterial characteristics on the touched surface, the data on restrooms was explored exclusively in **Figure 2.3**. The box plots show the percentage range of bacteria which are mainly detected in the samples: *Corynebacteriaceae*, *Micrococcaceae*, *Propionibacteriaceae*, *Bacillaceae*, *Staphylococcaceae*, *Lactobacillaceae*, *Streptococcaceae*, *Methylobacteriaceae*, *Rhodobacteraceae*, *Enterobacteriaceae*, *Moraxellaceae*, and *Pseudomonadaceae*. *Propionibacteriaceae* is the most predominant bacterial family for both genders, ranging from 6 to 74% on female skin and 15 to 85% on male skin.

**Figure 2.3** summarizes the differences in bacterial families present in male and female related samples. The plots indicate that *Corynebacteriaceae* is relatively higher in the male-related samples (median: 14.5% and 7.0%, skin and restroom, respectively) than the female-related samples (median: 7.5% and 3.1%). In contrast, *Lactobacillaceae* is higher in the female-related samples (median: 3.4% and 4.9%) than the male-related samples (median: 1.0% and 0.4%). Relatively higher concentrations of *Lactobacillaceae* was observed in female restroom since it is a vaginal microbiota and abundant on women's palm [30, 90]. Several studies have investigated whether the indoor bacterial environment is different depending on gender. Luongo and her colleagues [30] found that *Corynebacterium* is associated with human skin, but also significantly abundant in the

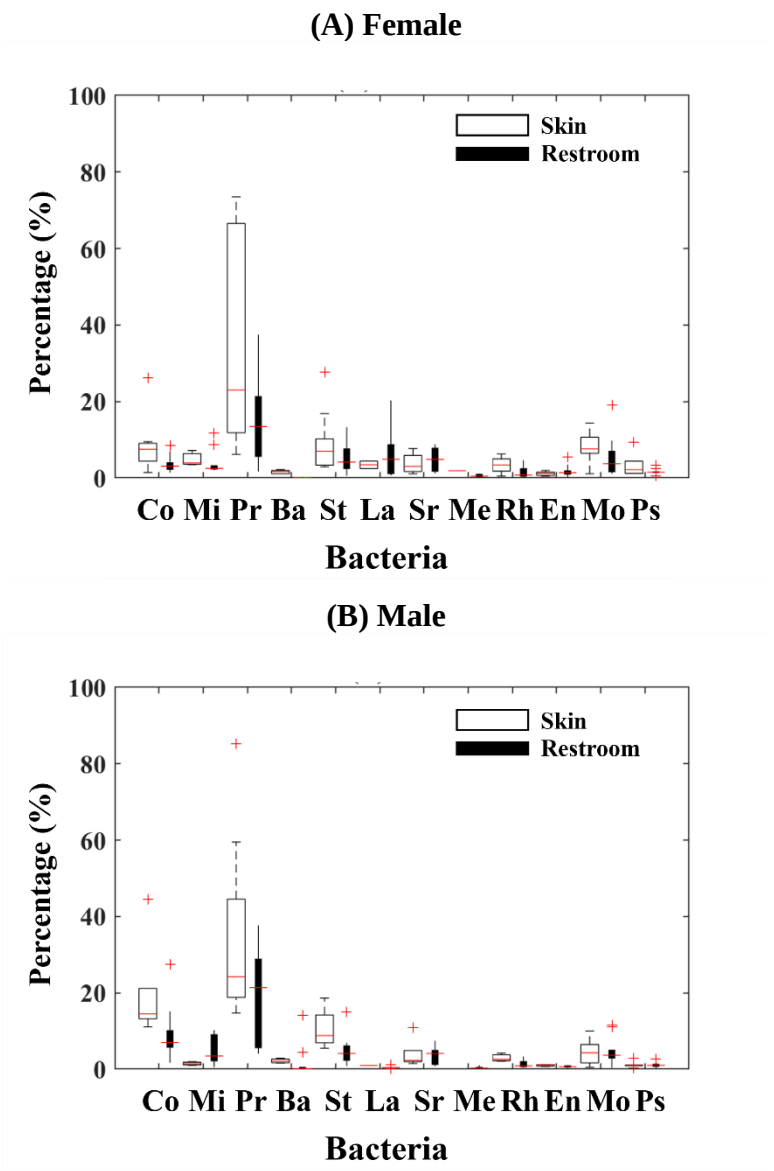


**Figure 2.3.** The bacterial percentage (%) on surfaces related to **(A)** female- and **(B)** male-associated samples.
Co: *Corynebacteriaceae*, Mi: *Micrococcaceae*, Pr: *Propionibacteriaceae*, Ba: *Bacillaceae*, St: *Staphylococcaceae*, La: *Lactobacillaceae*, Sr: *Streptococcaceae*, Me: *Methylobacteriaceae*, Rh: *Rhodobacteraceae*, En: *Enterobacteriaceae*, Mo: *Moraxellaceae*, and Ps: *Pseudomonadaceae*.

male-occupied rooms, while *Lactobacillus* is relatively higher in the female-occupied rooms. In addition, Fierer et al. [90] found 340% and 180% more *Lactobacillaceae* and *Moraxellaceae* on female hands, respectively. *Pseudomonadaceae* was also found to be comparatively more abundant on women's skin [90]. Based on the above discussion and

review of the literature, the presence of *Lactobacillus* and *Moraxellaceae* indicate female associated bacteria, while *Corynebacterium* is associated with males but with a greater uncertainty.

To determine if factorial design analysis can identify the influence of gender and surface sampling location on the bacterial families detected and assess if any can be classified as 'bio-fingerprints' the bacterial families identified in **Figure 2.3** (restroom and human skin surfaces) was tested. The results are given in **Table 2.2**. For the variables, 'G' refers to gender and 'S' refers to sampling surface. The *p*-value refers to the significance of the factor independently or for their interacting effects G×S. If the *p*-value is $< 0.05$, the effect on the bacterial families identified is significant. **Figure 2.4** illustrates the significant effects through the main effects plot with the help of two bacterial families, *Corynebacteriaceae* and *Lactobacillaceae*. **Figure 2.4** is the main effect plot showing the averages of response changes due to changes in the levels of the main factors, gender and sampling surface for the identification of *Corynebacteriaceae* and *Lactobacillaceae*. The comparative steepness of the slopes for each variable indicates which factor is more important. For *Corynebacteriaceae* both gender and sampling surface are equally significant and the *p*-values of 0.03 ($<0.05$) also confirm it (**Table 2.2**). For *Lactobacillaceae,* the slope for the factor gender is steep with the response shifting from female (-1) to male (+1). Hence, gender is significant and the *p*-value of 0.015 ($<0.05$) confirms it. For the second factor, sampling surface the response barely shifts from restroom surface (-1) to skin surface (+1) and is not significant (*p*-value is $0.531 > 0.05$). In the table the variables identified as significant are in bold.

Out of the 12 bacterial families in **Figure 2.3**, significant effect of the variables was seen for eight bacterial families: *Corynebacteriaceae*, *Propionibacteriaceae*, *Bacillaceae*, *Staphylococcaceae, Lactobacillaceae, Methylobacteriaceae, Rhodobacteraceae,* and *Pseudomonadaceae.* Sampling surface and gender are both significant factors for *Corynebacteriaceae*. This leads to the conclusion that both factors could play a significant role in the detection of *Corynebacteriaceae.* Literature data has shown that *Corynebacteriaceae* is present predominantly in locations where the male gender dominates. However, sampling surface is also a significant factor since *Corynebacteriaceae* is skin-related bacteria which is abundant on the human skin [90]. *Propionibacteriaceae*, *Bacillaceae*, *Staphylococcaceae*, and *Rhodobacteraceae* are influenced by where samples are collected ($p < 0.05$). We know that *Propionibacteriaceae* is present on skin and other surfaces regardless of gender. *Bacillaceae* and *Staphylococcaceae* are also not gender specific. *Rhodobacteraceae* is associated with external environmental effects [29]. Hence the identification of these four taxa are only influenced by the sampling surface is supported by evidence from literature. *Lactobacillaceae* and *Pseudomonadaceae* are the bacterial families that are only associated with gender, is significant ($p < 0.05$). This association has also been noted in the literature. *Methylobacteriaceae* shows significant interaction of both gender and sampling surface and their influence cannot be interpreted separately even though, gender as an independent factor is significant. *Enterobacteriaceae*, *Moraxellaceae*, *Streptococcaceae* and *Micrococcaceae* are not identified with a dominant influence ($p > 0.05$) by either variable and are not listed in **Table 2.2** but are in **Figure 2.3**, box plots.

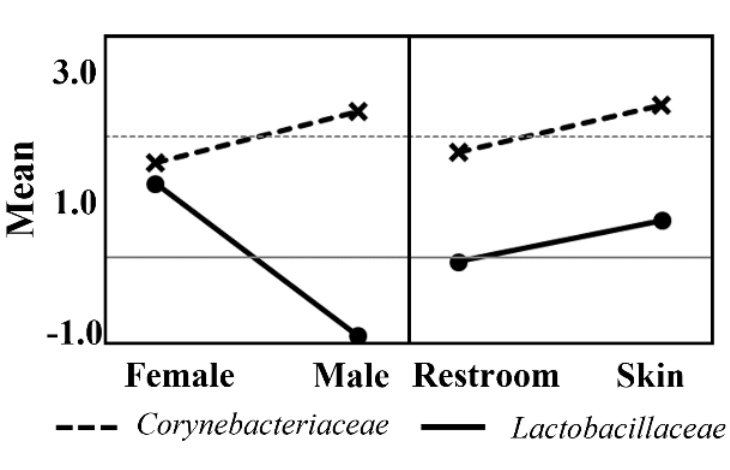


**Figure 2.4.** The main effect plots for *Corynebacteriaceae* and *Lactobacillaceae*.

**Table 2.2.** The influence of gender, G and sampling surface, S (restroom and skin surface)

| Microorganisms | ID | Effect | *p*-value |
|---|---|---|---|
| *Corynebacteriaceae* | G | 0.860 | **0.003** |
| | S | 0.847 | **0.003** |
| | G×S | 0.122 | 0.643 |
| *Propionibacteriaceae* | G | 0.274 | 0.334 |
| | S | 0.685 | **0.022** |
| | G×S | -0.062 | 0.829 |
| *Bacillaceae* | G | 0.631 | 0.268 |
| | S | 2.492 | **0.000** |
| | G×S | -0.312 | 0.580 |
| *Staphylococcaceae* | G | 0.166 | 0.542 |
| | S | 0.836 | **0.004** |
| | G×S | 0.133 | 0.626 |
| *Lactobacillaceae* | G | -1.753 | **0.015** |
| | S | 0.416 | 0.531 |
| | G×S | 0.546 | 0.413 |
| *Methylobacteriaceae* | G | -0.584 | **0.003** |
| | S | 0.158 | 0.372 |
| | G×S | -0.487 | **0.011** |
| *Rhodobacteraceae* | G | 0.190 | 0.662 |
| | S | 1.031 | **0.025** |
| | G×S | -0.033 | 0.940 |
| *Pseudomonadaceae* | G | -0.674 | **0.007** |
| | S | 0.293 | 0.216 |
| | G×S | -0.200 | 0.393 |

A study performed in 2008 found that the concentration of *Enterobacteriaceae* and *Moraxellaceae* are 400% and 180%, higher on women's palm than men's respectively [90] and hence was expected to have a gender signature similar to *Lactobacillaceae.* The factorial design analysis results showing no significant influence due to gender could be because the sampling site of skin had an impact on the results. The current dataset includes forearms, foreheads or back of hands as sample sites, but not the palms of hands. In addition, *Enterobacteriaceae* and *Moraxellaceae* are Gram-negative bacteria which are not able to survive in harsh surrounding environment. Hence, their presence or absence can be influenced by other indoor conditions. The factors gender and sampling surface do not influence the detection of *Streptococcaceae* or *Micrococcaceae* and are influenced by other factors as seen in subsequent analysis. The results demonstrate that factorial design analysis can determine accurately the dominant factors which influence the presence of a specific bacterial families and hence identify bio-fingerprints.

2.3.2. Identification of bio-fingerprint for sampling region and sampling location

(1) Exploring factors sampling region and sampling surface

The two levels for sampling regions were air and surface of the indoor space. Investigators applied different methods/protocols for data collection from the sampling region. The sampling methods from air can be classified under two broad umbrellas: active or passive. Active air sampling methods applied pumps with airflow ranges between 0.004 $m^3$/min to 1 $m^3$/min and a specific liquid medium for the bacteria to grow [91-93]. Representative air samplers used are impingers such as the SKC BioSampler (SKC Inc., PA, USA) and the AGI-30 (Ace Glass Inc., NJ, USA), and impactors such as the Andersen

sampler (Thermo Fisher Scientific Inc., MA, USA) and the Burkard single-stage air sampler (Burkard Manufacturing Co. Ltd., UK) [91]. The passive sampling method used Petri dishes which were either empty or filled with growth medium [32, 38, 45]. Suspended microbes settle onto the plates by gravity. Surface samples were collected using sterile swabs. The number of bacterial families detected from the air is 63 and surface is 48.

**Figure 2.5(A)** shows the indoor bacterial diversity (bacterial order group) for sampling regions: ambient air and surface. Air samples are biased towards two major order groups, Bacillales (41%) and Actinomycetales (31%) whereas surface samples show a more distributed profile: Bacillales (24%), Actinomycetales (22%), Propionibacteriales (17%) and Pseudomonadales (11%). Bacillales and Actinomycetales, which are dominant in both air and surfaces, contain prevalent indoor bacterial genera such as *Micrococcus*, *Bacillus*, *Corynebacterium* and *Staphylococcus*. **Figure 2.5(B)** is a box plot of the percentage of the most detected families in air and surface respectively. **Figure 2.5(B)** shows *Staphylococcaceae* and *Micrococcaceae* are the most abundant bacteria in air samples. *Corynebacteriaceae*, *Moraxellaceae* and *Pseudomonadaceae* are present in proportion ranging between 2~7% of indoor air microbes. In surface samples, *Micrococcaceae, Propionibacteriaceae, Staphylococcaceae, Methylobacteriaceae* and *Enterobacteriaceae* are predominant.

Sampling location was classified into ‘residence’ and ‘non-residence’. Residence refers to apartment and house, and non-residence includes hospital, office, school, auditorium, museum, retail store, subway station and restaurant. The data was further divided into air and surface samples as shown in **Figures 2.6 and 2.7** which show the percentage of bacterial families at different sampling locations. The highest proportion of

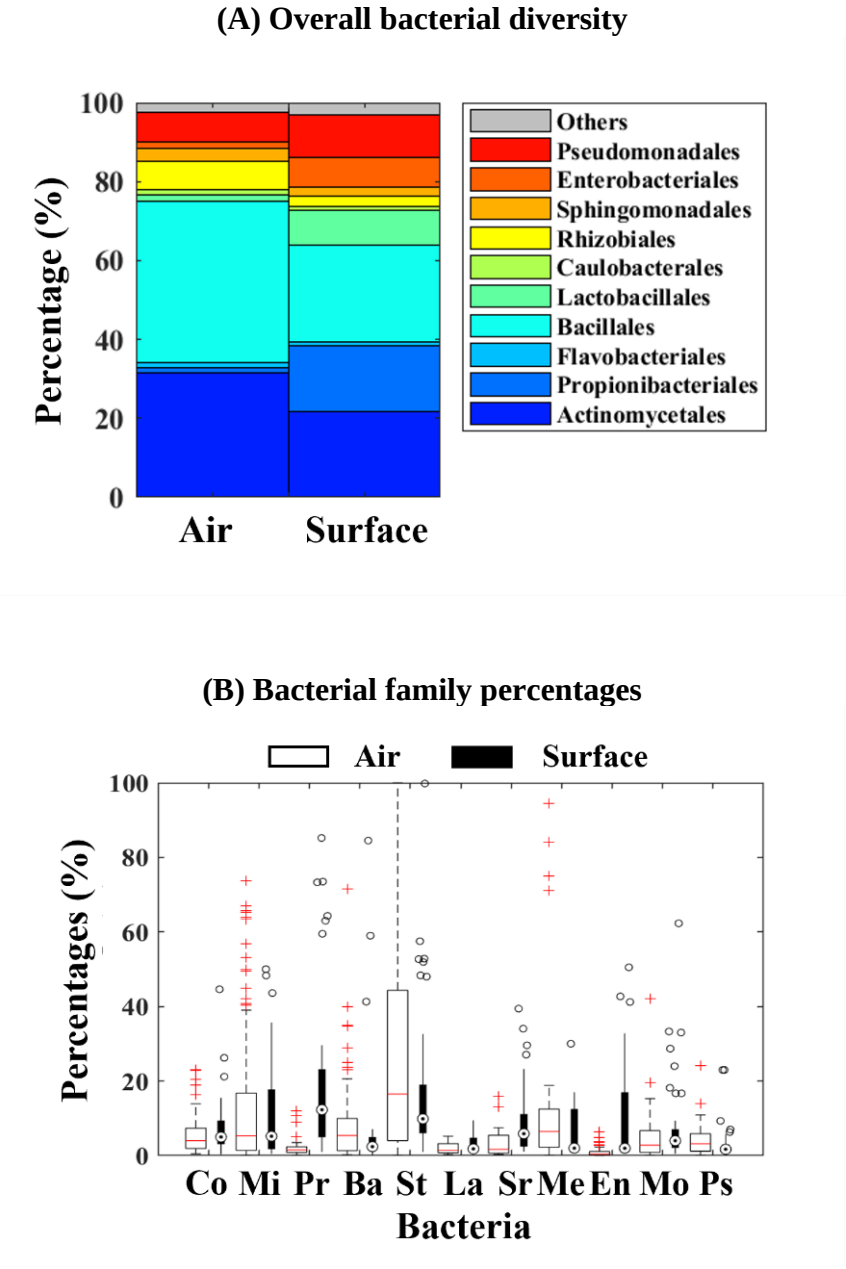


**Figure 2.5. (A)** Bacterial order group diversity of air and surface samples. **(B)** Microbial family percentages in air and surface samples.
Co: *Corynebacteriaceae*, Mi: *Micrococcaceae*, Pr: *Propionibacteriaceae*, Ba: *Bacillaceae*, St: *Staphylococcaceae*, La: *Lactobacillaceae*, Sr: *Streptococcaceae*, Me: *Methylobacteriaceae*, En: *Enterobacteriaceae*, Mo: *Moraxellaceae* and Ps: *Pseudomonadaceae.*

the total bacteria dominating or the predominant bacteria (*Staphylococcaceae*, *Micrococcaceae*, and *Bacillaceae*) is in the air samples of offices (94%), and then hospitals (85%), schools (75%), residences (51%) and public buildings (45%). In surface samples, museum shows the highest proportion (97%), followed by gym (43%), residence (25%) and hospital (4%).

**Figure 2.6** follows the previous findings that the sum of the bacteria mentioned accounts, for approximately 56~77% and 20~66% of total bacterial families in air and surface, respectively. **Figure 2.6** shows that *Staphylococcaceae*, *Micrococcaceae* and *Bacillaceae* are present regardless of sampling location in air. These bacteria are Gram-positive bacteria which are more resistant to harsh environments than Gram-negative bacteria and hence are frequently detected [36, 38]. In surface samples other families identified are *Dermabacteraceae*, *Alicyclobacillaceae* and *Bradyrhizobiaceae* which are not easily detected in the air samples (<1%) except for residence air (1.3%, 4.1% and 0%, respectively). *Methylobacteriaceae* (16%) is detected more in the air of public buildings due to the data from retail stores where it represents over 70% of the identified microbes. This is probably due to water related sources such as sinks and taps [34].

Hospital surfaces showed a different trend with a lower proportion (4%) of the predominant groups (**Figure 2.7(B)**). Instead, *Moraxellaceae* and *Bradyrhizobiaceae* families account for 40% and 22%, respectively. *Staphylococcaceae* presence on the hospital surface was only 3% but was 55%, in the air samples. *Acinetobacter* belonging to *Moraxellaceae* is frequently detected on residence and hospital surfaces [35, 77, 78]. *Bradyrhizobium* is a skin-associated genus that are present in higher concentrations on hospital devices (16%) and other working sites (17%) which are frequently touched by

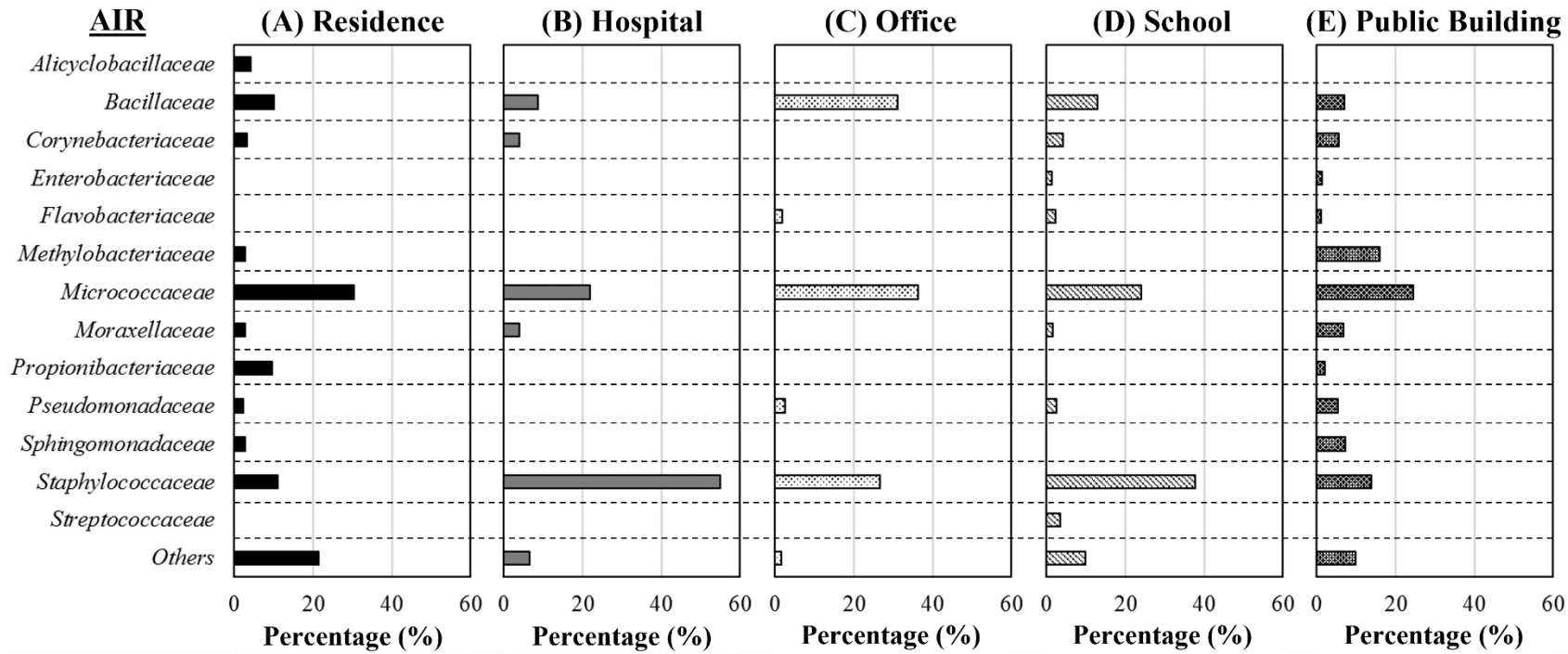


**Figure 2.6.** The bacterial family diversity of the different sampling locations in the **AIR** samples: **(A)** Residence, **(B)** Hospital, **(C)** Office, **(D)** School and **(E)** Public building. Public building includes auditorium, museum, retail store, subway station and restaurant.

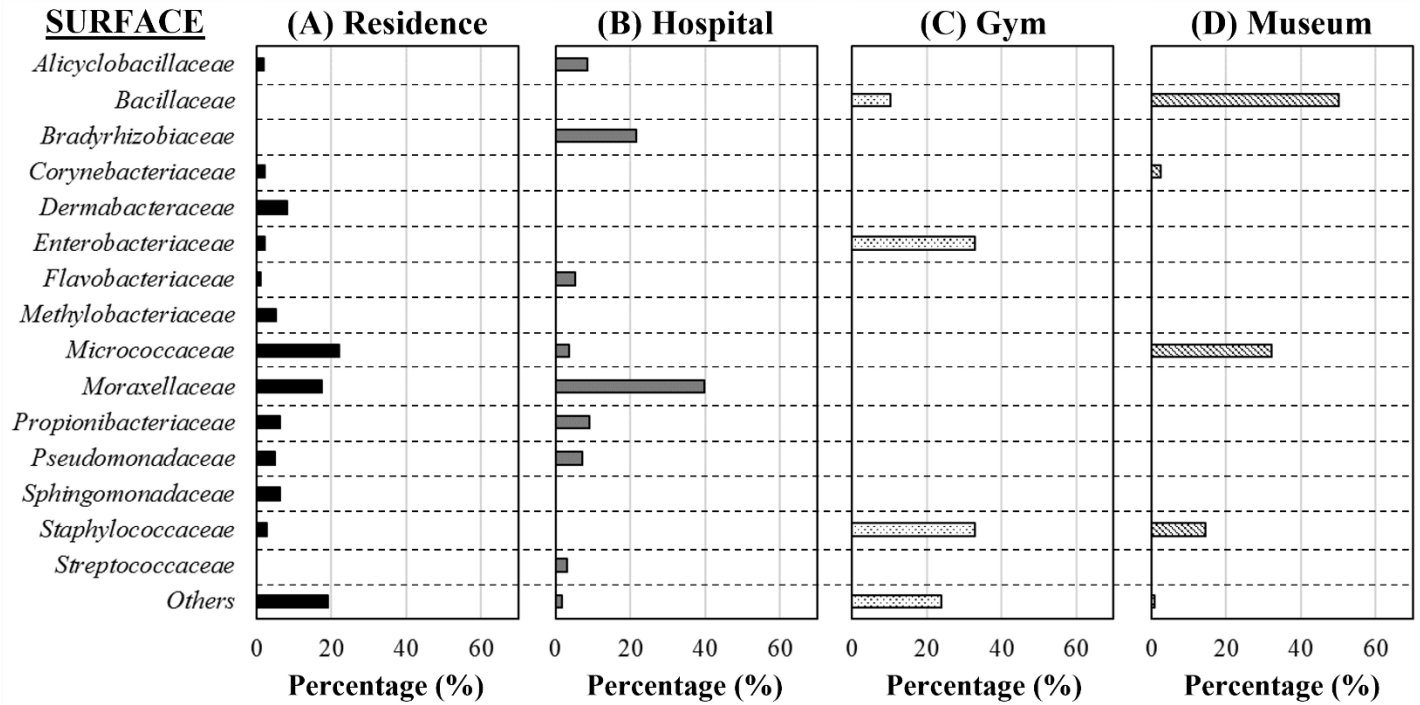


**Figure 2.7.** The bacterial family diversity of the different sampling locations in the **SURFACE** samples: **(A)** Residence, **(B)** Hospital, **(C)** Gym and **(D)** Museum.

staff's hands [81]. *Staphylococcus aureus*, which is included in the *Staphylococcaceae* group, can cause a health problem if the strains show methicillin-resistance (MRSA, Methicillin Resistant Staphylococcus Aureus) [59]. The concentration of *Staphylococcus* species increases with human activities in hospital buildings including lobbies to intensive care units [40-42, 44].

(2) Factorial design analysis

**Table 2.3** summarizes the results of the factorial design analysis. In the table the families for which at least one of the factors (location or region) was significant has been listed. The levels for location are residence and non-residence. The levels for region are air and surface sampling. *Staphylococcaceae* and *Enterobacteriaceae* are significantly influenced by sampling location ($p < 0.05$), which implies that the detection of these families is related to the type or use of a building, *i.e.*, residence/non-residence is significant and the bacterial presence hence detection is not influenced by whether the sampling was conducted in the air or surfaces. *Propionibacteriaceae*, *Enterobacteriaceae* and *Moraxellaceae* are highly influenced by the sampling region (*p-value* < 0.05). The interacting effect of factors is only significant on the presence of *Bacillaceae* (*p-value* < 0.05). None of the main effects are significant for *Bacillaceae* but interacting effects of location and region is significant. This implies that the presence of *Bacillaceae* is not a signature of the location or sampling region but instead if detected its presence is related to a combined influence of these two variables.

**Table 2.3.** The influence of sampling location, L (residence and non-residence) and region, R (air and surface sampling) on the bacterial concentration

| Microorganisms | ID | Effect | *p*-value |
|---|---|---|---|
| *Propionibacteriaceae* | L | -0.904 | **0.000** |
| | R | 0.337 | **0.011** |
| | L×R | -1.391 | 0.126 |
| *Bacillaceae* | L | 0.740 | 0.338 |
| | R | -1.033 | 0.183 |
| | L×R | 1.712 | **0.029** |
| *Staphylococcaceae* | L | 1.149 | **0.031** |
| | R | -0.177 | 0.737 |
| | L×R | 0.622 | 0.240 |
| *Enterobacteriaceae* | L | 0.917 | **0.039** |
| | R | 1.972 | **0.000** |
| | L×R | 0.847 | 0.055 |
| *Moraxellaceae* | L | 0.206 | 0.653 |
| | R | 0.955 | **0.040** |
| | L×R | -0.206 | 0.652 |

2.3.3. Identification of fingerprint for age (children – adult) and sampling region (air – skin surface)

(1) Exploring factors age and sampling region

**Figure 2.8(A)** shows the bacterial diversity in children- and adult-related samples. Children-related samples include day-care centres, kindergartens and elementary schools, and adult samples are those collected from university buildings and libraries. *Staphylococcaceae* (33% in children and 24% in adult) and *Micrococcaceae* (12% and 16% in children and adult respectively) were abundant in both children and adult samples. *Propionibacteriaceae* is higher in adult samples (24%) than in children (6%) while *Streptococcaceae* is higher in children samples (17%) than adult (3%). The average percentage of *Micrococcaceae*, *Staphylococcaceae* and *Streptococcaceae*, which are skin-related bacteria, accounts for up to 62% of the total children microbiome while 43% for

**(A) Bacterial diversity**

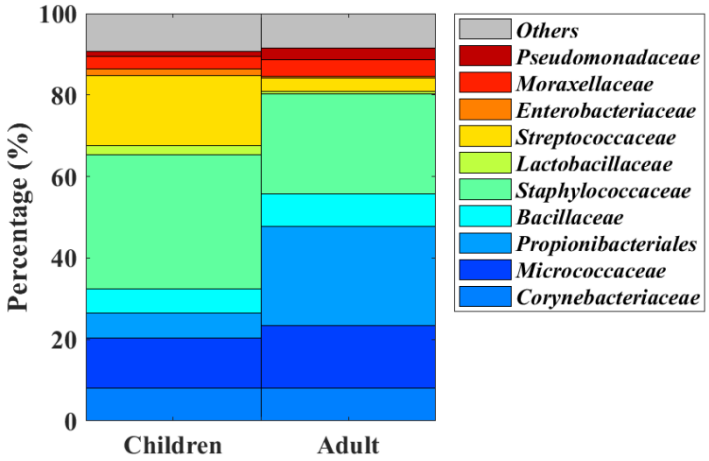


**(B) Bacterial percentages**

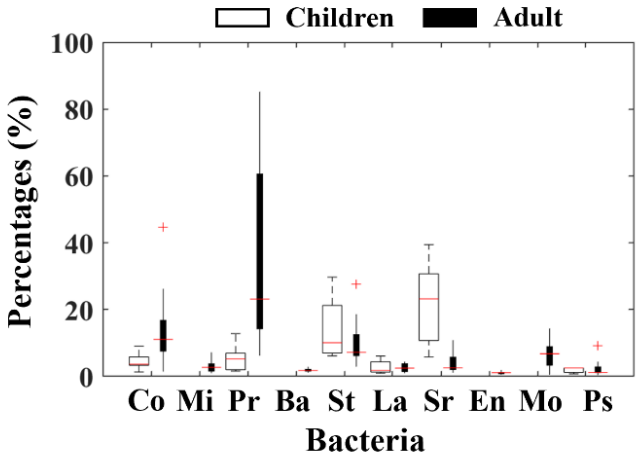


**Figure 2.8. (A)** Bacterial diversity and **(B)** their percentage range (%) in children- and adult-related samples.
Co: *Corynebacteriaceae*, Mi: *Micrococcaceae*, Pr: *Propionibacteriaceae*, Ba: *Bacillaceae*, St: *Staphylococcaceae*, La: *Lactobacillaceae*, Sr: *Streptococcaceae*, En: *Enterobacteriaceae*, Mo: *Moraxellaceae* and Ps: *Pseudomonadaceae*.

adult (**Figure 2.8(A)** and **Table B4**). This may be due to the higher activity levels in children-occupied places compared to adult occupied spaces [33, 46]. Similar results were observed when comparing microbial concentrations between child day-care centres and elderly care centres [94]. As shown in **Figure 2.8(B)**, *Micrococcaceae, Bacillaceae*, *Enterobacteriaceae* and *Moraxellaceae* were not detected on skin surfaces of children. *Corynebacteriaceae* and *Propionibacteriaceae* are higher on the adult-related samples (median: 11% and 23%, respectively), while children-related samples show lower concentration levels (median: 4% and 5%, respectively). *Streptococcaceae* are much higher on children-related surfaces (23% in children and 3% in adult samples).

(2) Factorial design analysis

**Table 2.4** shows the influence of the variables age and sampling region. Age was held at two levels, children and adult. The two levels for sampling region were air and skin surface. Significant influence by the variables was seen in seven bacterial families, *Corynebacteriaceae, Micrococcaceae, Propionibacteriaceae Staphylococcaceae*, *Streptococcaceae, Moraxellaceae* and *Pseudomonadaceae* out of the ten families in **Figure 2.8(B)**. *Bacillaceae, Lactobacillaceae* and *Enterobacteriaceae* were not significantly influenced by any of the factors. Sampling region significantly, *p-value* < 0.05, influences the presence of *Corynebacteriaceae, Micrococcaceae*, *Staphylococcaceae*, and *Moraxellaceae*. This indicates that where sampling was conducted has a determining influence on the detection of these bacterial families. *Pseudomonadaceae* is only significantly influenced by the age (*p-value* < 0.05). *Propionibacteriaceae* and *Streptococcaceae* are the two bacterial families that show up significant interacting effects as well as main effects. In case of *Streptococcaceae* both age

and the interaction effect of age and sampling region is significant. For *Propionibacteriaceae,* the main effect, sampling region is significant as well as the interaction of the two factors – sampling region and age.

**Table 2.4.** The influence of age, A (children and adult) and sampling region, $R_s$ (air and skin surface)

| Microorganisms | ID | Effect | *p*-value |
|---|---|---|---|
| *Corynebacteriaceae* | A | 0.132 | 0.666 |
| | $R_s$ | 0.697 | **0.029** |
| | A×$R_s$ | 0.568 | 0.071 |
| *Micrococcaceae* | A | 0.831 | 0.123 |
| | $R_s$ | -1.809 | **0.002** |
| | A×$R_s$ | 0.482 | 0.365 |
| *Propionibacteriaceae* | A | 0.209 | 0.615 |
| | $R_s$ | 2.276 | **0.000** |
| | A×$R_s$ | 1.047 | **0.017** |
| *Staphylococcacae* | A | 0.066 | 0.772 |
| | $R_s$ | -0.653 | **0.006** |
| | A×$R_s$ | -0.397 | 0.086 |
| *Streptococcaceae* | A | -0.604 | **0.033** |
| | $R_s$ | 0.492 | 0.079 |
| | A×$R_s$ | -0.720 | **0.013** |
| *Moraxellaceae* | A | -0.750 | 0.071 |
| | $R_s$ | 0.940 | **0.032** |
| | A×$R_s$ | 0.300 | 0.456 |
| *Pseudomonadaceae* | A | 0.487 | **0.013** |
| | $R_s$ | -0.188 | 0.313 |
| | A×$R_s$ | -0.325 | 0.087 |

## 2.4. DISCUSSION

### 2.4.1. Influence of indoor air, surfaces, gender and age

The bacterial families across all scenarios identified by the factorial design analysis as being significantly influenced by at least one of the factors are: *Corynebacteriaceae*, *Propionibacteriaceae, Bacillaceae, Staphylococcaceae, Lactobacillaceae,*

*Methylobacteriaceae, Moraxellaceae, Micrococcaceae, Enterobacteriaceae, Rhodobacteraceae, Streptococcaceae* and *Pseudomonadaceae.* They can be separated out into groups that are influenced by any single factor, gender, age, sampling location, region or surface type or any combination of these.

Based on the factorial design analysis, *Propionibacteriaceae* and *Staphylococcaceae* are significantly influenced by one of the factors across all three groups of variables. For gender and sampling surface, surface was significant for *Propionibacteriaceae*, similarly between sampling location and sampling region. The region which identified air or surface sampling as the two levels, was significant. Also, when assessed with the factor age, sampling region (levels are air and skin surface) was significant. The presence of *Propionibacteriaceae* bacterial family is relatively higher in adult and skin surface [87]. However, age as a main effect is not significant but the interaction effect of age and sampling region is significant hence its presence is an indication of adult occupied space and its detection could be dependent on surface type and not occupant characteristics or residency type. *Staphylococcaceae* was significantly influenced by the surface type, sampling region and location but not by gender or age of occupants. *Staphylococcaceae* is seen to dominate in the air of hospitals and while they are present in higher proportion in children occupied spaces it was not significant.

*Corynebacteriaceae, Pseudomonadaceae, Bacillaceae* and *Moraxellaceae* are significantly influenced by factors from two sets of variables out of the three. *Corynebacteriaceae* is significantly influenced by gender (confirmed by literature), region and surface type and not by age or location. Higher concentrations of *Pseudomonadaceae* were observed in adult-occupied spaces and female-related samples (Tables S1 and S4).

The analysis identifies *Pseudomonadaceae* as significantly influenced by both age and gender and coupled with the data sources from the literature, at the locations detected, the occupant characteristics would signify towards being females and adults. *Bacillaceae* detection or presence is dependent on the interacting effects of sampling location and region, though when assessed with gender as the alternative factor, sampling surface is significant. As a result, its presence cannot be attributed to any specific indoor or occupant characteristics. The analysis further picks up *Moraxellaceae* which is significantly influenced by sampling region and not by gender or age. This indicates that the detection of the bacteria may be missed based on where the sampling was conducted. The literature has shown that *Moraxellaceae* is present in higher proportions on hospital surfaces.

*Lactobacillaceae, Methylobacteriaceae, Rhodobacteraceae, Enterobacteriaceae, Streptococcaceae* and *Micrococcaceae* have significant influences by one factor from one set of variables. Gender is a significant factor for *Lactobacillaceae* presence, and it was detected in higher proportions in female related samples. *Methylobacteriaceae* presence also has gender signature but with interacting influence, *i.e.*, other indoor characteristics must be assessed. The factor sampling surface is significant for *Rhodobacteraceae* when assessing gender and sampling surface. This bacterial family is associated with external conditions, hence its detection on an indoor surface is an outdoor signature and is not a bio-fingerprint for indoor characteristics. The factorial design results show that both location and region are significant for *Enterobacteriaceae* which is commonly detected for non-residences. However, there is no interacting effect hence the presence/detection of *Enterobacteriaceae* is equally influenced by location and region, air or surface. *Streptococcaceae* is significantly influenced by age and it is dominant in children occupied

spaces and detection is related to skin samples supported by literature. *Streptococcus* genera is easily transmitted by children [95] and widely distributed in indoors since it is one of the skin-related bacteria [1, 96]. In the current analysis, age was selected as the significant factor indicating that even though the bacterial source is skin related, it is a signature of children's activity or presence. *Micrococcaceae* is identified as significant for sampling surface when assessing age and sampling surface hence, its presence does not indicate any age group.

Based on the data from the literature, air samples mainly consist of Bacillales and Acinomycetales, while surface samples include relatively equal proportions of Bacillales, Actinomycetales, Propionibacteriales and Pseudomonadales. *Propionibacteriaceae*, *Pseudomonadaceae*, *Staphylococcaceae*, *Enterobacteriaceae*, *Micrococcaceae* and *Methylobacteriaceae* are detected at all types of sampling regions and locations such as fitness centres, public restroom [29, 34, 82], residences [33], hospitals [40], offices [37], schools [47] and restaurants [71]. *Enterobacteriaceae* and *Moraxellaceae* are dominant on domestic kitchen sink surfaces [35] showing that surface type influences the presence of these bacterial families. *Streptococcus* species need to be carefully monitored in children-related facilities as it can cause serious health problems such as bacterial pneumonia, for children under 5 years [97]. In addition, the carriage rate of infective *Streptococcus pneumoniae* is much higher in younger children (40~60%) than adults (3~4%) [95]. Several studies have found that *Staphylococcus*, *Corynebacterium* and *Bacillus* genera are measured as the major microorganisms in the air of elementary schools, day-care centres and university buildings [1, 36, 45, 46].

2.4.2. Influence of ventilation systems, temperature, humidity and outdoors

The literature was also surveyed to extract information on ventilation systems, indoor and outdoor conditions such as temperature, humidity and seasons during which sampling was conducted. Less than half the literature reported data on ventilation systems and indoor temperature and humidity. Out of the 15 literatures which had ventilation information, 61% were mechanical systems, 23% were natural and 14% were hybrid. Indoor temperature ranged between 20.0~29.6℃ for mechanical ventilation, 12.2~29.9℃ for hybrid ventilation and 14.8~30.4℃ for natural ventilation. Natural ventilation had higher humidity levels, 38% compared to 29% for mechanical and hybrid ventilation systems for the lower end. At the higher end, humidity levels reached 98% for hybrid ventilation and averaged about 67% for mechanical and natural ventilation.

Although studies have confirmed that ventilation systems could greatly influence the indoor bacterial community [57, 98], what role a system and its components play on the overall bacterial concentration ($CFU/m^3$) and diversity is not understood. Total bacterial concentration ranged from 6 to 1460 $CFU/m^3$ in mechanical ventilation systems, from 10 to 1120 $CFU/m^3$ in hybrid systems, and from 11 to 931 $CFU/m^3$ in natural systems. All bacterial genera which are significantly influenced by one of the factors assessed, were detected in natural and mechanical system, whereas for hybrid ventilation systems *Lactobacillaceae* was not reported. A comparison of the total number of the different types of bacteria present for the three systems was inconclusive. The lowest and highest number was observed in the space with natural ventilation system (3 and 35). In case of hybrid ventilation, the range was 6 to 20 and for mechanical ventilation it was 3 to 34, nearly the same as natural ventilation systems.

Data on outdoor conditions reflecting seasonal effects and geographical location was sparse with four studies, among the 15 literatures which had ventilation data, reporting outdoor temperature and humidity during which sampling was conducted. Seasons when sampling was conducted have been reported in all 15 literatures. However, one study out of 15 literatures showed seasonal variation of predominant bacterial species which are *Staphylococcus*, *Bacillus*, *Corynebacterium* and *Micrococcus*. The study found significantly lower concentrations of predominant bacteria in winter, except for *Staphylococcus* [46].

## 2.5. CONCLUSIONS

The study makes one of the first attempts at applying the current knowledge on bacteria in built environments towards identifying bio-fingerprints which can reflect characteristics and usage of the indoor space. The analysis not only shows that locations such as hospitals and schools have bacterial families distinct from other spaces but also identifies families which are distinct for these environments and have a detrimental effect on health. *Staphylococcaceae* presence in the air of hospitals are bio-fingerprints. *Streptococcaceae* is a bio-fingerprint for schools and other children-occupied spaces. If these bacterial families are detected to dominate in other locations, then it may be an indication of a contaminated indoor space requiring monitoring or intervention. *Moraxellaceae* on hospital surfaces is also a distinct bio-fingerprints for the space. Also, the results show ways of identifying indoor space usage or occupancy characteristics, such as the presence of *Lactobacillaceae* indicates female presence but along with *Pseudomonadaceae* it indicates a higher proportion of space usage by females and adults.

Determining the ‘history’ of a space can be helpful for fields such as environmental forensics but also for making tailored decisions regarding health and safety of occupants, decontamination if required and design decisions.

The results of the study show there is a potential of applying the bacterial characteristics for generating bio-fingerprints which can be associated to or tailored for specific indoor environments. The investigation focuses on select indoor characteristics but with consistent data this can be expanded to determine more rigorously the coupled effects of indoors, outdoors and occupants and ultimately move towards application of this knowledge. However, to achieve that we must close the gaps existing between the bacterial data collected and the information obtained of the associated indoor environmental parameters, outdoor environmental conditions including seasonal variation and impact of geographical location.

# CHAPTER 3. OCCUPANTS, ACTIVITIES, AND DISTANCE FROM VENTS INFLUENCE PRESENCE, QUANTITY AND SPATIAL DISTRIBUTION OF PARTICLES, AND MICROBES FROM INDOOR AND OUTDOOR SOURCES IN SCHOOL BUILDINGS [2]

## ABSTRACT

This study breaks down the effects of occupant characteristics which include number of occupants, activity and age as well as built air exchange components which are vents, doors, and windows on the concentration of particles, bacteria, and fungi. Microbial samples from the ambient and surfaces were collected from multiple sites at an university, high school, and elementary school). Particle levels were monitored, occupant and indoor environment characteristics were recorded. Particle levels and microbial concentrations followed the same trends. Bacterial sources were separated based on whether it was indoors or outdoors. While presence of occupants resulted in an increase in particles and microbes, activity significantly influenced $PM_{10}$ and outdoor signature bacteria. Fungi was not influenced by occupant characteristics. $PM_{10}$ and microbial levels were significant depending on whether the age group of the occupants was averaging under or over the 10-year-old, indicating that policies to improve indoor air quality need to account for the distinct nature of elementary school while high school and universities may have more

[2] Seong.D. Weir.M. & Hoque.S., (2021) Submitted to Environmental Research

similar traits. For surface materials, bacterial levels were lowest on metals and highest on carpets and, tiles but surface usage also dictated the extent of microbial load. Outdoor signature bacterial concentration increased significantly as the distance from the vent increased, but distance from the vent had no influence on levels of indoor signature bacteria. The spatial distribution of indoor signature bacteria significantly varied along the length and height of the room. The trend near the boundaries was different, sometimes reverse to the general trend within the room. The analysis highlighted that within a distance of 20% from the wall bacterial concentration increased along the length indicating possible dominance of wall and boundary effects on bacterial transport before occupants' influence takes over. For height, the trend was upward in the lower half of the room.

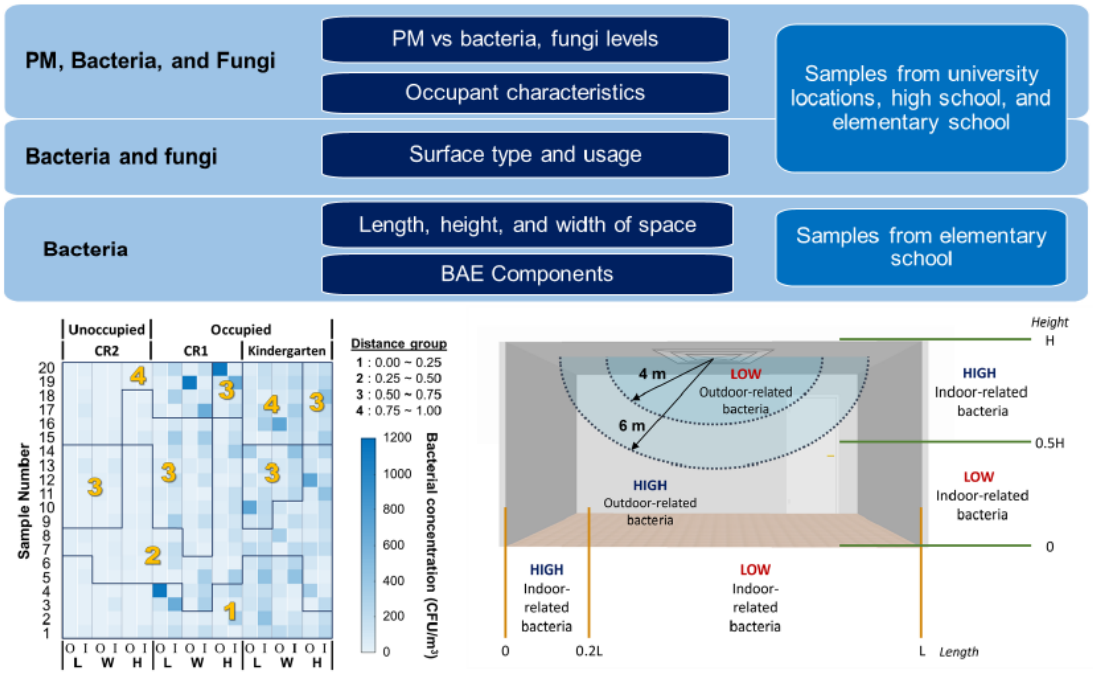


**Figure 3.1.** A graphical abstract of the Chapter 3.

*Keywords: Indoor environment, Microbes, Particles, Ventilation, Occupants, Boundaries*

Highlights

- The overall trend of PM and microbe levels are similar. Hence, monitoring PM levels could provide baseline data on the indoor air quality. However, occupant characteristics dictate if the influence is significant for $PM_{2.5}$ or $PM_{10}$ and if the microbial changes are due to indoor or outdoor signature bacteria or fungi.
- Metal surfaces had the lowest level of microbial load. Frequently touched surfaces contain higher level of microbial contaminants for the same surface type. This highlights that choosing materials for indoor spaces should incorporate understanding usage, location where the material will be placed, and properties.
- Among the built air exchange elements, vents, doors, and windows; vents play a significant role on the concentration levels of outdoor signature bacteria found indoors but does not influence bacteria generated by indoor sources.
- The spatial distribution of indoor signature bacteria varies along the length and height of the space. The trend reverses near the walls indicating air flow pattern and boundary effects influences the concentration levels up to a certain distance and then the effect of occupants' take over.

## 3.1. INTRODUCTION

Buildings and the microbial world influence occupants' health [99, 100] just as building design and the built environment play a significant role in ensuring health and safety of the occupants [21, 101-103]. The ubiquitous and interacting role of microbes, indoor air, and hygiene was suggested by Pettenkofer in 1858, [104] and the role of ventilation to ensure healthy conditions was also researched by others in that era [105].

COVID-19 has now forced an evaluation of the influence of buildings, and indoor spaces on air flow and infection transmission [23, 106] and it has become urgent that we must understand how to design our built environment such that it plays a more active role in maintaining health and wellness.

To understand what influences the microbial characteristics in the indoor environment, studies have focused on assessing influence of the microbial source and occupancy. We know that indoor and outdoor sources and human presence influence the diversity of the microbes detected in an indoor space [27, 56, 57, 68]. Occupant characteristics tend to homogenize the diversity of indoor bacterial bioaerosols [28, 65]. However, utilizing the knowledge to inform building design not only for comfort but for health is yet to be realized [103, 107-109].

Most airborne microorganisms exist by attaching on particulate matter (PM) and more than 80% of it are bacteria followed by fungi, archaea, and virus [53]. Recent studies revealed a positive relationship between $PM_{2.5}$ concentration and the number of people infected with viruses such as influenza and coronaviruses [110-113]. Occupancy resulted in an increase of airborne bacterial concentration and PM [54, 55]. Higher concentrations of gram positive cocci was observed in child daycare centers as a result of activity and transmission from children's body [46]. *Staphylococcus*, *Micrococcus*, *Bacillus* and *Propionibacterium* are also frequently detected indoor microbes since their source is human-related [28, 33, 36, 109]. Differences in the PM and bacterial composition have been reported based on ventilation type, where hybrid and natural ventilation resulted in indoor conditions nearly similar to outdoor conditions [114, 115]. On the other hand, mechanical ventilation resulted in PM and $CO_2$ reduction [116-118] and several studies

observed lower bacterial concentration (CFU/$m^3$) in mechanically ventilated buildings than naturally ventilated ones [38, 39]. Predominant bacteria such as *Staphylococcus*, *Micrococcus*, and *Bacillus* are detected regardless of the type of ventilation [44, 45, 71].

A search through the literature highlights that indoor environment conditions influence the presence and characteristics of PM and microbes. But the investigations do not explore whether or how specific indoor environment elements can influence their dispersion and hence transmission. Few studies correlate the information on aerosols with indoor design to predict the concentration in the space which can help provide guidelines for interior designers, architects, or public health decision makers leading to improved health and wellness for occupants. Wu et al. [119] noted that fungi levels positively correlate with indoor temperature, indoor relative humidity, and number of open windows in libraries sampled using a linear regression model. Utilizing indoor microbiome datasets, a diversity-time-area relationship model was developed by Ma et al. [120] to estimate diversity. Adequate usage of indoor air exchange components such as windows, and HVAC returns/vents is associated with indoor air quality, students' performance, and health [121-124], particularly for children [125]. A study by Bennett et al. [126] at an urban primary school classrooms demonstrated the significant influence of the infiltration of outdoor pollutants on $PM_{2.5}$ levels while crustal elements drove $PM_{10}$ levels possibly introduced by foot traffic and re-entrained due to resuspension. Ventilation levels were below ASHRAE guidelines for most of the day.

The research reported here assessed the influence of occupant characteristics and built air exchange (BAE) components on the presence and spatial distribution of PM, bacteria, and fungi based on data collected from multiple education facilities. This study

designated BAE components as the elements in the indoor space that facilitate air flow. They include windows, doors, and HVAC entry/exit points. Occupant characteristics refer to number of occupants, age, gender, and activity level. This paper: (a) assesses the extent of influence of occupant characteristics on PM, bacteria, and fungal levels, and determines if there is any significant correlation between PM and microbial levels, (b) assesses the influence of surface type and usage on bacteria and fungi levels and, (c) evaluates the influence of BAE components on the ambient spatial distribution of bacteria for fixed occupant characteristics.

## 3.2. MATERIAL AND METHODS

The analysis is based on data from the following locations: 1) university – three offices, two classrooms, and a laboratory; 2) two high schools – classrooms, locker rooms, and a library, 3) an elementary school – three classrooms and a library. Overall, 268 air samples and 134 surface samples were collected from October 2018 to February 2019.

***Location of BAE components:*** Interior orientation or décor such as placement of tables, chairs, or shelves were noted. Room dimensions and distance of BAE locations - vent, door, and window from a reference point in the room was measured. Indoor temperature, humidity, and airflow at the vents were recorded. All indoor spaces were mechanically ventilated, and windows were sealed or closed during sampling. Indoor environmental conditions were measured using ABM-200 (Airflow and Environmental Meter, CPS Products, Inc., USA). Indoor temperature was 22.4±0.2℃ at the elementary school and 21.1±1.9℃ at the high school, respectively. Humidity ranged between 40% and

50% in elementary school and was between 35% and 40% in high school. Air changes per hour (ACH) ranged from 3 to 6 overall.

***Occupant characteristics:*** Occupancy and activity were noted by the respective instructor, librarian or attending coach/instructor. The instructors were asked about the number of students who were present in class and to rate the activity level. Activity was rated at two levels: 0 (normal activity: sitting, talking, studying, or walking) and +1 (high activity: running or moving around continuously). Minimum occupancy was 0 (unoccupied) and maximum was 40. Based on the type and use of the buildings, the space was assigned as specific dominant age groups: elementary school (children), high school (adolescents), and university (adults). An IRB exempt for the study is in **Appendix C**.

3.2.1. Sampling approach

Indoor PM, bacteria and fungi were sampled from the ambient air. Particle size distribution was monitored using Optical Particle Sizer 3330 (TSI Inc., USA) at an airflow rate of 0.001 $m^3$/min with 1-minute intervals over 30 or 60 minutes depending on the sampling condition. Airborne microbes were sampled simultaneously applying passive air sampling method due to cost-efficiency and easy operation [127]. Opened Petri dishes filled with tryptic soy agar (TSA) media, MilliporeSigma™ M Air T™ Agar Cassettes (EMD Millipore Corp., USA) were placed in selected rooms for 60 minutes. The location and height of Petri dishes varied in order to investigate the influence of BAE components. 49 of PM samples were collected (31, 11, and 7 samples at the university, high school, and elementary school, respectively) and 209 of microbial samples were collected (37, 102, and 70 samples, respectively). Samples were collected in duplicates and incubated at room temperature for 5 days. After 5 days of incubation, shape, texture, and color of dominant

colonies were recorded and microbial identification was done using MALDI-TOF analysis at an accredited laboratory. Based on the results from the labs and colony morphology, the bacteria and fungi were identified. Microbial concentration was quantified using colony-forming units per cubic meter of air (CFU/$m^3$) [128].

Duplicate surface samples were collected from each surface tested, using sterile swabs, Puritan™ EnviroMax® Sterile Environmental Sampling Swabs (Puritan Medical Products Company LCC, USA). The swabs were rubbed horizontally, vertically and diagonally across the sampling area of 100 $cm^2$ [84]. Sampled swabs were immediately placed back into the tube filled with 15 mL of phosphate buffered saline at pH 7.2 (Gibco™, USA). In the laboratory, aliquots of swabbed sample were spread on tryptic soy agar plates and the plates were incubated. Microbial identification proceeded the same way as described for air sampling. All samples were stored at 4°C before analysis.

Detected bacterial species were classified into two groups – indoor and outdoor related [109]. Bacterial species such as *Corynebacterium* sp., *Micrococcus* sp., and *Staphylococcus* sp. were classified as indoor related [45, 71] and *Bacillus* sp. and *Aerococcus* sp. detections were attributed to outdoor signature [128, 129]. Fungal species were not separated out as indoor or outdoor related since detected fungi species were abundant both indoors and outdoors such as *Alternaria* spp., *Aspergillus* spp., *Penicillium* sp., and *Pithomyces* spp. [130-132].

### 3.2.2. Analysis

**Figure 3.2** is a schematic representation of the distances measured from the sampling location to the BAE elements and the boundaries of the indoor space *i.e.*, the length, height, and width. Raw distance values between BAE components and sample

locations were used in the analysis. Distance to the boundaries were rescaled values to lie within 0 and 1. Height was measured from the floor. Length and width were measured from the walls with the origins as shown in the figure, the corner on the same side but opposite to the exit door. Length increased as sampling location moved towards the door edge while width increased as distance of the sampling location moved towards the windows.

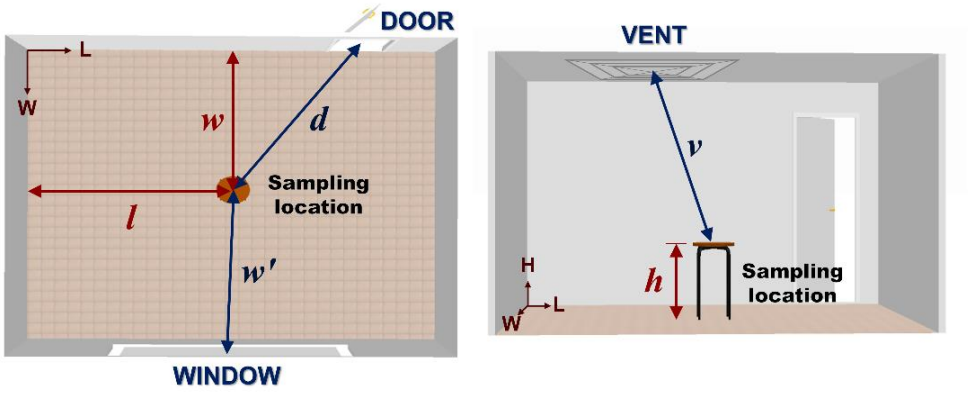


**Figure 3.2.** Distances from sampling location to BAE components and boundaries, length (L), width (W), and height (H).

R 3.6.2 and MATLAB were used for analysis. Data normality was tested using Shapiro-Wilk test. One-way analysis of variance (ANOVA) test was applied to evaluate whether the environmental conditions, such as occupancy, activity, and age, significantly influenced the log-transformed PM concentrations. Mann-Whitney-Wilcoxon test was applied on the raw microbial concentrations ($CFU/m^3$) to determine any significant difference depending on the environmental conditions because the normality was not satisfied [133]. Spearman correlation was performed to identify the strength and association between PM and microbial concentrations. Data significance was tested at a *p-value* of 0.05. To gain insight into how the boundaries of the indoor spaces (walls, floor, and ceiling) and the BAE elements (vents, doors, and windows) influence the spatial distribution of microbes' concentration, the significance of distance was assessed.

Furthermore, *k*-means clustering analysis was applied to assess if microbial concentrations formed distinguishable clusters in accordance with the distances from the space boundaries (*l*, *w*, and *h*) or the BAE components (*v*, *d*, and *w'*). The k-means method is popular due to ease of interpretation, speed of convergence and adaptability [134]. The elbow method was used to determine that two clusters were optimum for the analysis.

## 3.3. RESULTS AND DISCUSSIONS

### 3.3.1. Occupant characteristics, particulate matter, and microbial concentrations

**Table 3.1** summarizes the occupant characteristics (activity rate, age, gender, and number of occupants), PM mass concentration ($\mu g/m^3$) and microbial concentration ($CFU/m^3$) at each location. At the university, there were no occupants in the laboratory during the sampling period and one to four occupants in the offices. For occupied classrooms at the university, there were on an average eight students. All sampling locations for the elementary school had up to 16 occupants including one or two adults. In the high school locker rooms, classrooms and the library were sampled. Locker rooms were designated male and female and averaged five occupants each, in the classroom there were 10 students on an average and seven students in the library. Samples in the elementary school were collected from both occupied and unoccupied classrooms. Activities were rated as normal (0) and high activities (+1).

Hourly mass concentration of $PM_{2.5}$ and $PM_{10}$ across all locations ranged from 27 to 286 $\mu g/m^3$ and 48 to 4554 $\mu g/m^3$, respectively. The highest $PM_{2.5}$ and $PM_{10}$ concentrations were measured at the kindergarten as well as the highest total microbial concentration (345 $CFU/m^3$) was detected in kindergarten. The least amount of total

microbial concentration was observed at a university laboratory location (4 CFU/$m^3$). Fungi was rarely detected in the university. The microbial level at the high school library was less than other high school locations, with fungal and bacterial concentrations of 9 CFU/$m^3$ and 27 CFU/$m^3$, respectively. Particle levels were negligible as well. Compared to the high school library the particle levels and microbial concentration were higher at the elementary school library. The bacterial and fungi concentrations were 231 CFU/$m^3$ and 81 CFU/$m^3$. Indoor-related signature bacterial concentrations were higher than outdoor-related signature bacteria regardless of sampling locations. At the university, occupied classroom had the highest indoor related bacteria with outdoor related bacteria levels relatively low for all spaces.

**Figure 3.3** shows the PM mass concentration (µg/$m^3$) and the corresponding airborne microbial concentration (CFU/$m^3$). The PM levels showed positive relations with the bacterial concentrations. The positive relation can be attributed overall to the influence of occupant characteristics and the BAE components. Occupancy and activity resulted in an equivalent increase in PM and microbial levels. When air exchange was working, both PM and microbial levels decreased. Spearman rank correlations between $PM_{2.5}$ and indoor, outdoor bacterial and fungal concentrations were 0.5 (*p-value* > 0.05), 0.3 (*p-value* > 0.05), and -0.1 (*p-value* > 0.05), respectively indicating indoor signature bacteria had a somewhat stronger positive correlation with $PM_{2.5}$. For $PM_{10}$ and indoor, outdoor bacterial and fungal concentrations the rank correlations were 0.6 (*p-value* < 0.05), 0.5 (*p-value* < 0.05), and 0.3 (*p-value* > 0.5), respectively. In this case as well, indoor signature bacteria had a strong significant correlation with $PM_{10}$. Hence, while slightly strong positive correlations were noted between PM and indoor signature bacterial concentrations for both < 2.5 µm and <

10 μm particles, a weak correlation existed between PM levels and outdoor signature bacterial concentration. This would imply differing factors influence outdoor, indoor signature bacteria and PM levels.

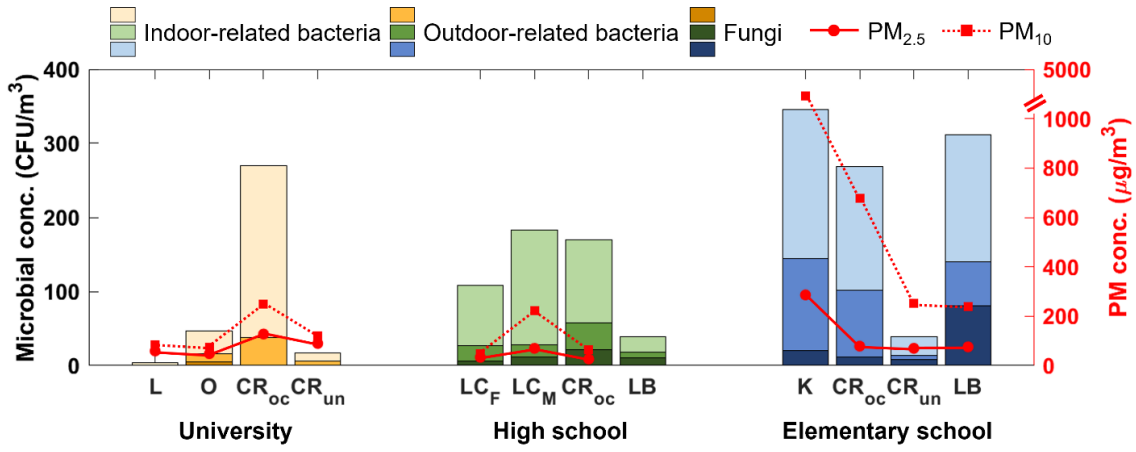


**Figure 3.3.** Microbial concentration (CFU/$m^3$) and relative PM concentration (μg/$m^3$) of the university, high school, and elementary school in average.
L: Laboratory, O: Office room, $CR_{oc}$: Occupied classroom, $CR_{un}$: Unoccupied classroom, $LC_F$: Female locker room, $LC_M$: Male locker room, LB: Library, and K: Kindergarten.

**Figure 3.4** is a box plot of the microbial concentration against gender, occupancy (activity), and age. Samples that were collected from university offices and high school locker rooms used by self-identified male or female occupant or reserved for specific genders were placed in male or female groups accordingly. Male-related locations had higher concentration of bacteria and fungi compared to spaces exclusively used by females. Regardless of whether the space was designed for a specific gender group or not, occupied classrooms had much higher total microbial concentration than unoccupied ones. Data from university, high school, and elementary school were classified based on age - adult, adolescence, and child, respectively. Samples from elementary school classrooms showed the highest total microbial concentration compared to other age groups.

**Table 3.1.** Activity rate, age, gender, number of occupants, and hourly PM mass concentration and microbial concentration of sampling location

| Location | Activity [a] | Occupant | $PM_{2.5}$ [b] ($\mu g/m^3$) | $PM_{10}$ [b] ($\mu g/m^3$) | Concentration [b, c] ($CFU/m^3$) | | | | |
|---|---|---|---|---|---|---|---|---|---|
| | | | | | Out | In | Bac | Fun | Tot |
| **All locations** | | | **67 ± 59** | **305 ± 925** | **36 ± 100** | **98 ± 127** | **133 ± 174** | **16 ± 30** | **149 ± 182** |
| **University** | | | **63 ± 40** | **96 ± 76** | **14 ± 22** | **67 ± 126** | **81 ± 133** | **2 ± 7** | **84 ± 133** |
| Laboratory | | 0 | 59 ± 32 | 86 ± 54 | n.d.[d] | 4 ± 7 | 4 ± 7 | n.d. | 4 ± 7 |
| Office | 0 | 1 ~ 4 | 48 ± 37 | 75 ± 67 | 11 ± 16 | 34 ± 45 | 45 ± 45 | 6 ± 11 | 52 ± 47 |
| Classroom | 0 | 0 ~ 8 | 105 ± 52 | 173 ± 118 | 21 ± 29 | 122 ± 174 | 143 ± 181 | n.d. | 143 ± 181 |
| *Occupied* | 0 | ~ 8 | 128 ± 59 | 250 ± 163 | 30 ± 32 | 189 ± 193 | 219 ± 193 | n.d. | 219 ± 193 |
| *Unoccupied* | | 0 | 90 ± 52 | 123 ± 67 | 7 ± 16 | 11 ± 17 | 17 ± 32 | n.d. | 17 ± 32 |
| **High school** | | | **93 ± 73** | **168 ± 188** | **19 ± 28** | **81 ± 114** | **100 ± 125** | **16 ± 21** | **116 ± 127** |
| Locker room | , 0 | ~ 5 | 52 ± 24 | 135 ± 110 | 20 ± 28 | 130 ± 148 | 150 ± 164 | 10 ± 11 | 160 ± 168 |
| *Female* | 0 | ~ 5 | 34 ± 11 | 48 ± 16 | 24 ± 33 | 92 ± 134 | 115 ± 157 | 7 ± 10 | 122 ± 162 |
| *Male* | 0 | ~ 5 | 70 ± 18 | 222 ± 76 | 17 ± 23 | 164 ± 156 | 180 ± 169 | 12 ± 12 | 193 ± 170 |
| Classroom *Occupied* | 0, +1 | ~ 10 | 27 ± 14 | 63 ± 75 | 21 ± 32 | 70 ± 90 | 92 ± 97 | 23 ± 27 | 115 ± 99 |
| Library | 0 | ~ 7 | - | - | 8 ± 10 | 19 ± 24 | 27 ± 32 | 9 ± 11 | 36 ± 34 |
| **Elementary school** | | | **135 ± 109** | **1601 ± 2159** | **71 ± 163** | **137 ± 137** | **208 ± 222** | **23 ± 42** | **231 ± 237** |
| Kindergarten | +1 | ~ 15 | 286 ± 36 | 4554 ± 1771 | 124 ± 152 | 200 ± 115 | 325 ± 180 | 20 ± 28 | 345 ± 178 |
| Classroom | 0 | ~ 16 | 74 ± 45 | 465 ±351 | 48 ± 179 | 96 ± 130 | 144 ± 222 | 10 ± 16 | 154 ± 225 |
| *Occupied (CR1)* | 0 | ~ 16 | 79 ± 50 | 677 ±420 | 91 ± 249 | 167 ± 153 | 258 ± 270 | 11 ± 18 | 269 ± 273 |
| *Unoccupied (CR2)* | | 0 | 70 ± 59 | 253 ± 115 | 5 ± 9 | 25 ± 25 | 30 ± 27 | 9 ± 14 | 39 ± 36 |
| Library | 0 | ~ 15 | 76 | 240 | 59 ± 78 | 172 ± 156 | 231 ± 219 | 81 ± 80 | 312 ± 284 |

[a] 0 (normal activity: sitting, talking, studying, or walking) and +1 (high activity: running or moving around). When unoccupied it was assumed there was no activity or minimal activity for example occasional momentary entrance of someone.
[b] Averaged concentration ± Standard deviation
[c] Out: Outdoor-related bacteria, In: Indoor-related bacteria, Bac: Bacteria, Fun: Fungi, and Tot: Total microorganisms
[d] n.d.: Not detected

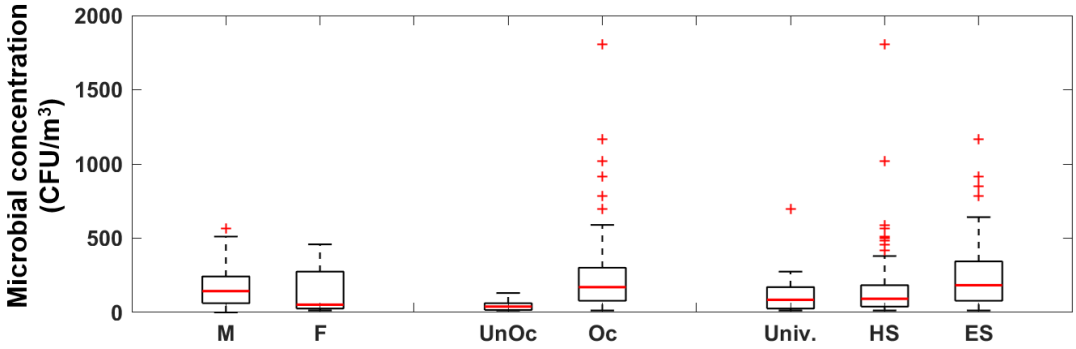


**Figure 3.4.** Distribution of averaged airborne microbial concentrations in terms of gender (male and female), occupancy (unoccupied and occupied), and age (university, high school, and elementary school).
M: Male-related samples, F: Female-related samples, UnOc: Unoccupied classroom (no activity), Oc: Occupied classroom (normal to high activity), Univ.: University samples (adult), HS: High school samples (adolescence), and ES: Elementary school samples (children).

**Table 3.2** summarizes the results of ANOVA and Mann-Whitney-Wilcoxon test to determine the significance of occupancy. activity, and age on log-transformed PM and microbial concentrations, respectively. Activities at the high school and elementary school had a significant impact on $PM_{10}$ levels (*p-value* < 0.05). In the elementary school, students' activity influenced $PM_{2.5}$ concentrations. Occupancy was significant for PM levels in the high school. ANOVA test confirmed that $PM_{10}$ levels were significant depending on whether the age group of the occupants was averaging under or over the 10-year-old mark *i.e.*, elementary school was distinct from high school and university locations. Occupancy significantly influenced both outdoor- and indoor-related bacterial concentrations at the university and elementary school (*p-value* < 0.05) whereas fungi levels were not (*p-value* > 0.05). Outdoor bacterial concentration levels were significantly influenced by activities at the elementary school and age was significant for all microbes.

**Table 3.2.** Significance of occupant characteristics on the log-transformed number of PM [ANOVA] and microbial concentrations [Mann-Whitney-Wilcoxon test]

| Sampling location | Occupant characteristics | ANOVA | | Mann-Whitney-Wilcoxon | | | | |
|---|---|---|---|---|---|---|---|---|
| | | Log $PM_{2.5}$ | Log $PM_{10}$ | Outdoor bacteria | Indoor bacteria | Bacteria | Fungi | Total microbes |
| University | Occupancy | 0.912 | 0.521 | **0.013** | **0.009** | **0.001** | 0.157 | **0.001** |
| | Activity | n.a. | n.a. | n.a. | n.a. | n.a. | n.a. | n.a. |
| High school | Occupancy | **0.023** | **0.007** | 0.175 | 0.826 | 0.736 | 0.178 | 0.442 |
| | Activity | 0.198 | **0.009** | 0.922 | 0.458 | 0.557 | 0.715 | 0.779 |
| Elementary school | Occupancy | 0.169 | 0.128 | **0.000** | **0.000** | **0.000** | 0.079 | **0.000** |
| | Activity | **0.032** | **0.028** | **0.002** | 0.137 | **0.018** | 0.779 | **0.024** |
| All locations | Age | 0.058 | **0.000** | **0.014** | **0.004** | **0.002** | **0.000** | **0.000** |

n.a.: Not applicable because all activity rates at the university were recorded 0.

With regards to PM, the presence of occupants influenced the extent of indoor PM levels [126, 135-138] as this study also saw for high school but not for elementary school and the university. This could be due to the associated activity. When occupied, activity levels were significant for $PM_{10}$ in the high school. Studies have shown that coarse particles ($PM_{10}$) in schools tend to be related to outside sources such as soil, resuspension, and physical activity [126, 137, 139, 140] which explains the significance for $PM_{10}$ for both occupancy and activity at the high school which includes locker rooms as sampling locations. Occupancy showed a relationship with both outdoor and indoor signature bacteria at the university and elementary school but not the high school. When assessing activity, the influence due to it at the elementary school was significant for particles and for outdoor signature bacteria. While higher activity levels showed significant changes to bacterial concentrations, as noted in previous studies, this appeared to be driven by the outdoor signature bacteria. For fungi, occupant characteristics and activity had no

significant impact, emphasizing that indoor environmental conditions [70, 141] probably played a more important role.

3.3.2. Surface materials and sites on microbial concentration on surfaces

Indoor surface samples were collected from eight different surface sites: tables, doors, chairs, bookshelves, computers, lockers, floors, and vents from the elementary school and high schools. Associated surface materials were wood, metal, plastic, carpet, and tile. The extent of surface contamination with relation to site and material type due to bacterial concentration and fungal detection have been summarized in **Figure 3.5**.

The number of samples and their percentages are shown in **Figure 3.5(A)**. 64 surfaces were sampled in total. Wood (36%) was the most abundant surface type followed by plastic (29%), metal (25%), carpet (5%) and tile (5%). **Figures 3.5(B)** and **(C)** plot the bacterial concentrations versus surface materials and sites. The range of bacterial load on computers excluding the screen was $0.7\times10^5$ to $75.3\times10^5$ CFU/100cm$^2$. Higher microbial contamination was observed on carpet surfaces averaging $27.3\times10^5$ CFU/100cm$^2$. Samples collected from back of the chair had a mean concentration of $11.0\times10^5$ CFU/100cm$^2$ bacteria which was approximately two times higher than the average bacterial load sampled from table surfaces ($5.1\times10^5$ CFU/100cm$^2$). Metal had the lowest mean microbial contamination ($2.3\times10^5$ CFU/100cm$^2$) followed by wood ($6.8\times10^5$ CFU/100cm$^2$), tile ($8.4\times10^5$ CFU/100cm$^2$), plastic ($10.7\times10^5$ CFU/100cm$^2$), and carpet ($27.3\times10^5$ CFU/100cm$^2$). Relatively higher concentrations ($10.7\times10^5$ CFU/100cm$^2$) were detected on surfaces made of plastic. The high levels were driven by the samples from computer surfaces. Both chair and table surfaces were made of the same materials, wood and plastic.

Carpet surfaces showed the highest contamination (over $27.3\times10^5$ CFU/100cm$^2$) which was three times higher than bacteria on tiles.

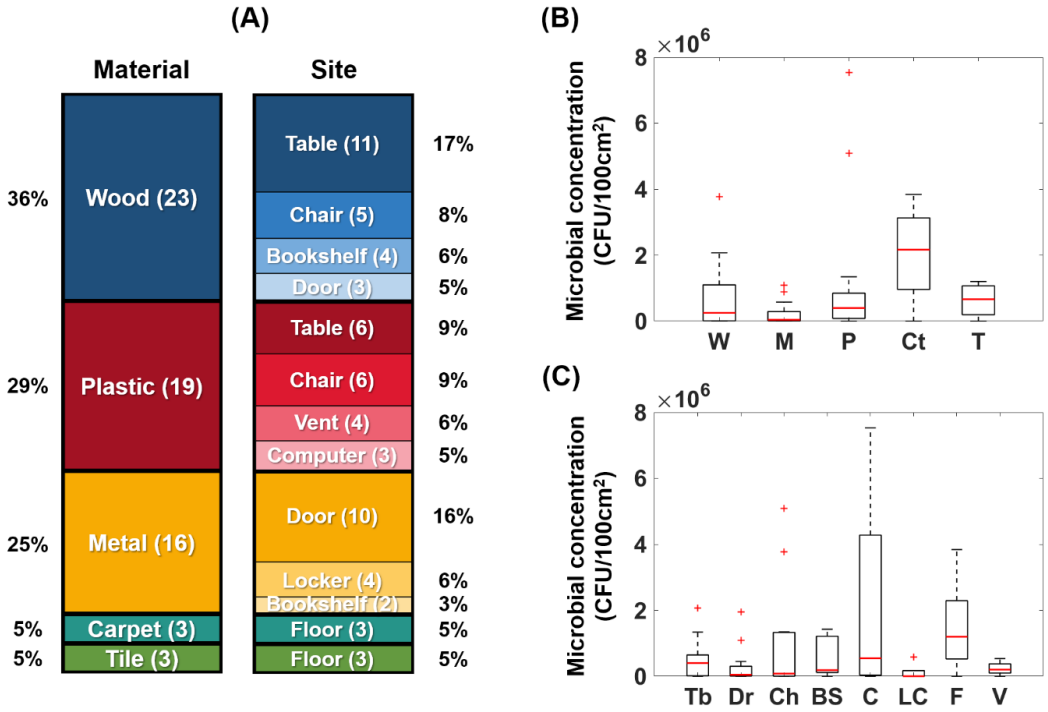


**Figure 3.5. (A)** The number of surface materials and sites. Numbers are represented in parenthesis. Surface microbial contamination (CFU/100cm$^2$) on **(B)** different surface materials and **(C)** sites.
W: Wood, M: Metal, P: Plastic, Ct: Carpet, T: Tile, Tb: Table, Dr: Door, Ch: Chair, BS: Bookshelf, C: Computer, LC: Locker, F: Floor, and V: Vent.

**Table 3.3** summarizes the results of one-way ANOVA and Mann-Whitney-Wilcoxon tests to determine if difference of bacterial concentration between pairs of surface materials was significant. Due to lack of sufficient fungal data, the tests were confined to bacterial concentration only. The tests identified the concentrations on metal surfaces to be significantly different from plastic, carpet, and tile surfaces (*p-value* < 0.05), however, the difference of bacterial concentration levels between wood and metal surfaces were not significant. Carpet surfaces was found to have significantly different bacterial concentration compared to all the other surfaces materials (*p-value* < 0.05). Mann-

Whitney-Wilcoxon test was also conducted to determine the significance between sampling sites. Whether the surface was frequently exposed to touch via hands *i.e.*, tables, chairs, computer surfaces etc. or was walked upon *i.e.*, floor was significant (*p-value* = 0.009). Fungi was detected on all surface materials except carpets. 90% of plastic surfaces (17 surfaces out of 19) were contaminated by fungi. 57% of metal and wood surfaces also showed positive fungi detection.

**Table 3.3.** Significance of bacterial concentration on different surface materials evaluated by one-way ANOVA and Mann-Whitney-Wilcoxon test

| **Material** | Metal | Wood | Plastic | Carpet |
|---|---|---|---|---|
| Wood | 0.092 | | | |
| Plastic | **0.016** | 0.471 | | |
| Carpet | **0.008** | **0.016** | **0.030** | |
| Tile | **0.038** | 0.335 | 0.408 | **0.039** [a] |

[a] One-way ANOVA test was applied

Studies have looked into why or what surface properties enhance or reduces microbial attachment and growth, for example, hydrophilic, negatively charged, and oxide coated surfaces have been found to be favorable for bacterial attachment [142] while another investigation confirmed that very low bacteria attachment occurred on hydrophilic surfaces [143]. The impact of surface roughness was inconclusive based on a survey of the literature with opposing conclusions [144-146]. Adhesion kinetics have been shown to change the levels of attachment of viruses for a range of surfaces [147]. Fungi growth has been found to be favorable on plastic surfaces while ceiling tiles required more time to be covered by fungi [141]. In this study, fungi were detected on one tile surface. Understanding the fundamental governing mechanisms of surface and microbial attachment is vital but the information has to be coupled with insight into surface exposure and usage to ensure the right materials are chosen based on characteristics, location, and function.

3.3.3. Spatial distribution of microbes

**Figure 3.6** shows the average microbial concentration (CFU/m$^3$) at each sampling site for kindergarten and classrooms at the elementary school. The size of each dark blue, green, and red circles represents outdoor- and indoor-related bacterial and fungal proportions, respectively. The center of the circle indicates the sampling site. There were ten sampling sites at each room. Samples were collected twice at each sampling site. The asterisk mark (*) next to the specific circle indicates that the fungi concentration was below a limit of detection. In classrooms 1 and 2 (CR1 and CR2), there were four vents (*v1*, *v2*, *v3*, and *v4*), one door (*d1*) and one window (*w'1*). Kindergarten had five vents (*v1*, *v2*, *v3*, *v4* and *v5*), two doors (*d1* and *d2*) and two windows (*w'1* and *w'2*). CR2 was unoccupied, while CR1 and kindergarten were occupied. The figure summarizes the concentration of outdoor, indoor bacteria and fungi at the sampling locations relative to BAE components

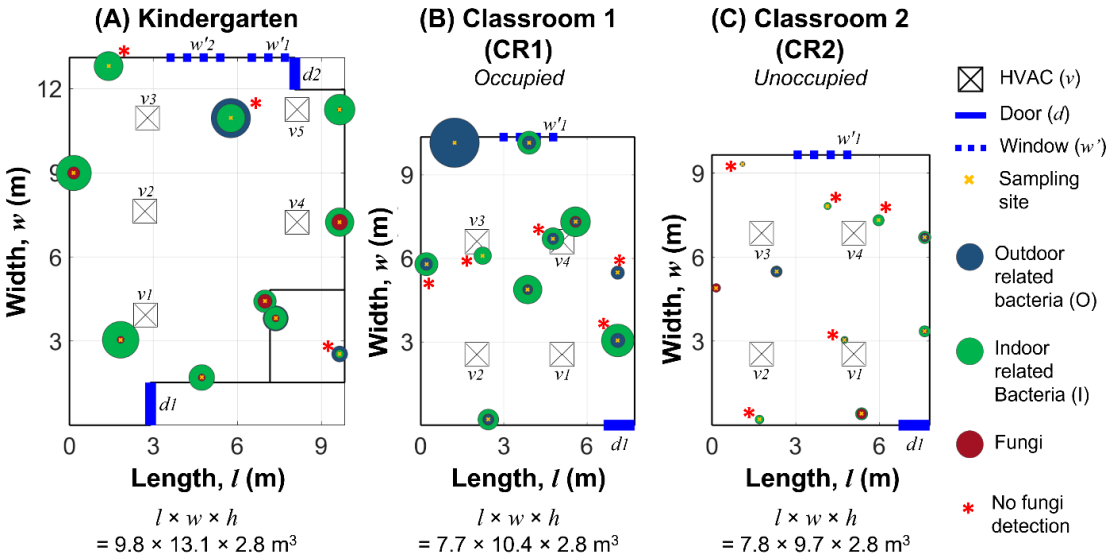


**Figure 3.6.** Average microbial concentration at each location. **(A)** Kindergarten, **(B)** Classroom 1 (CR1), and **(C)** Classroom 2 (CR2) at the elementary school. The size of the dark blue, green, and red circles represents outdoor- and indoor-related bacterial and fungal proportions, respectively. The center of the circle indicates the sampling site. The asterisk mark (*) indicates that the fungi concentration was below a limit of detection.

and across the length, width, and height. It highlights the variability of the concentration of the microbes across the classrooms. To gain further insight on the influence, if any, of the BAE components, an in-depth look is taken at the bacterial concentrations. Fungi is not considered due to insufficient data.

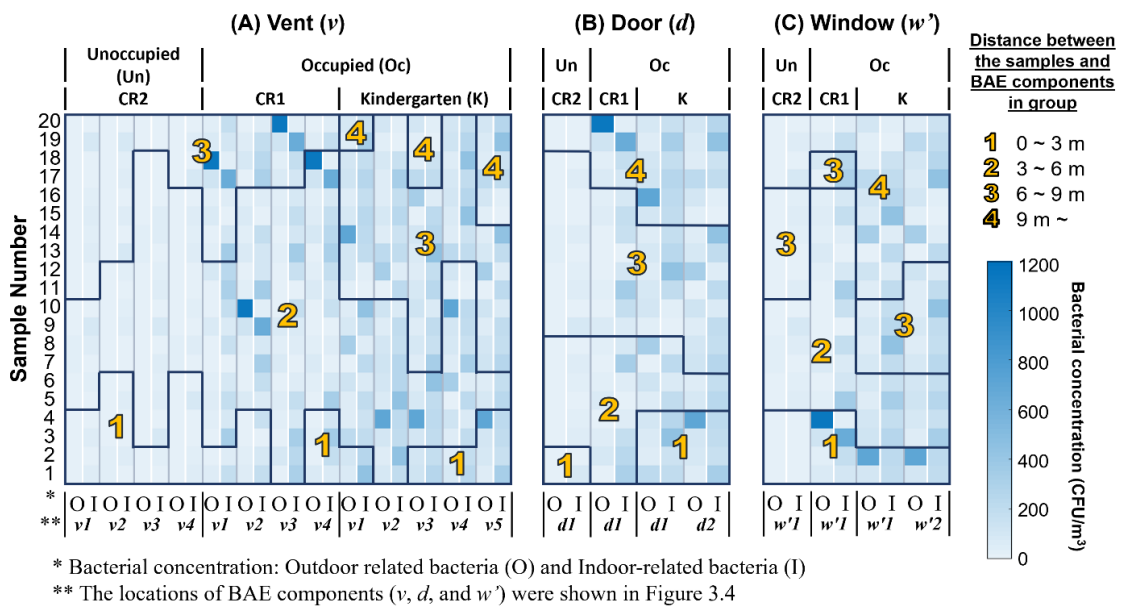


**Figure 3.7.** Outdoor- and indoor-related bacterial concentrations by distance from **(A)** Vent, **(B)** Door, and **(C)** Window. O and I indicate the outdoor- and indoor-related bacteria, respectively.

**Figure 3.7** visualizes the bacterial concentration with respect to the distance from each BAE component. The distances have been grouped into four ranges: 0 ~ 3 m (group 1), 3 ~ 6 m (group 2), 6 ~ 9 m (group 3) and > 9 m (group 4) for kindergarten, CR1 and CR2. Bacterial concentrations were lower in CR2 and more uniformly distributed regardless of BAE distance. In CR1, relatively higher outdoor-related bacterial concentrations were observed further away from the vent and door. Bacterial load in the kindergarten did not appear to show much variation with respect to distances from the vent and doors. The occupied rooms (CR1 and kindergarten) had higher outdoor-related

bacterial concentrations near the window locations while the concentration appears to be uniformly distributed for CR2 regardless of the distance from the window.

Across all sampling locations, indoor-related bacteria appeared to be well mixed. **Figure 3.8** describes the bacterial concentrations with respect to the distance to the boundaries of the indoor space. Normalized length and width were categorized into four groups: 0 ~ 3 m (group 1), 3 ~ 6 m (group 2), 6 ~ 9 m (group 3) and > 9 m (group 4) while for height the categories were: 0 ~ 1 m (group 1), 1~ 2 m (group 2), and 2 ~ 3 m (group 3). In CR1, higher bacterial concentrations were observed near the walls (length in distance group 1 and width in distance group 4) and ceiling (height in distance group 3). Kindergarten showed well-mixed indoor-related bacterial levels across the length, width, and height. Relatively higher outdoor-related bacteria were detected around the middle of the room.

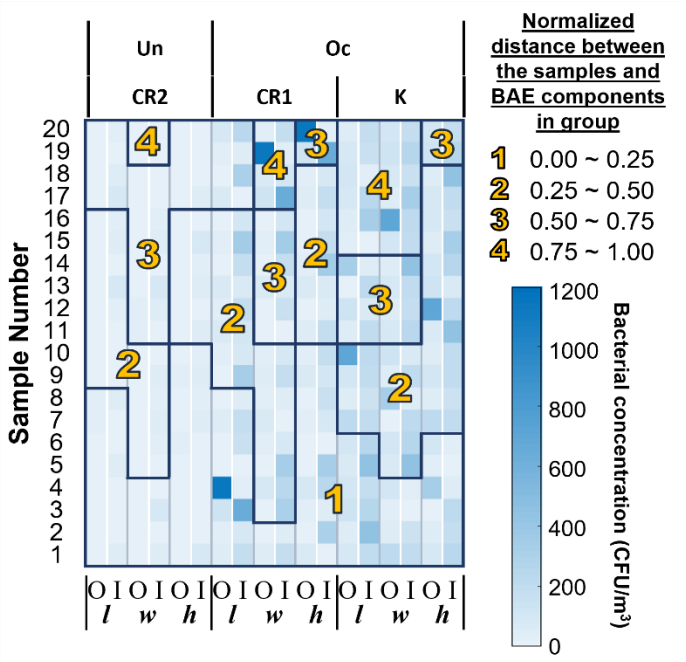


**Figure 3.8.** Outdoor- and indoor-related bacterial concentration against normalized length (L), width (W), and height (H) of the room. O and I represent outdoor- and indoor-related bacteria, respectively.

Based on **Table 3.2**, occupancy and activity were significant factors for the elementary school and then **Figures 3.7** and **3.8** highlighted the uniformity of bacterial concentration, outdoor and indoor signature, for unoccupied rooms. Hence, additional clustering analysis was conducted focusing on the occupied classrooms to assess how the BAE components influenced the spatial distribution patterns of the bacteria in presence of occupants as well as across the length, height, and width of the classrooms as shown in **Figure 3.9**. Cluster 1 in **Figure 3.9(A)** contains the distance ranges of 6 to 9 m from the vent to the sampling location while cluster 2 consists of the range 3 to 6 m. For distance from the door, cluster 1 in **Figure 3.9(B)** has the ranges between 3 to 6 m and, 6 to 9 m, and cluster 2 includes distances greater than 9 m. **Figure 3.9(C)** which classifies the distances from the window, distances greater than 6 m is in cluster 1 while cluster 2 mainly includes the distance less than 6 m. Hence, cluster 1 represents sampling locations far away

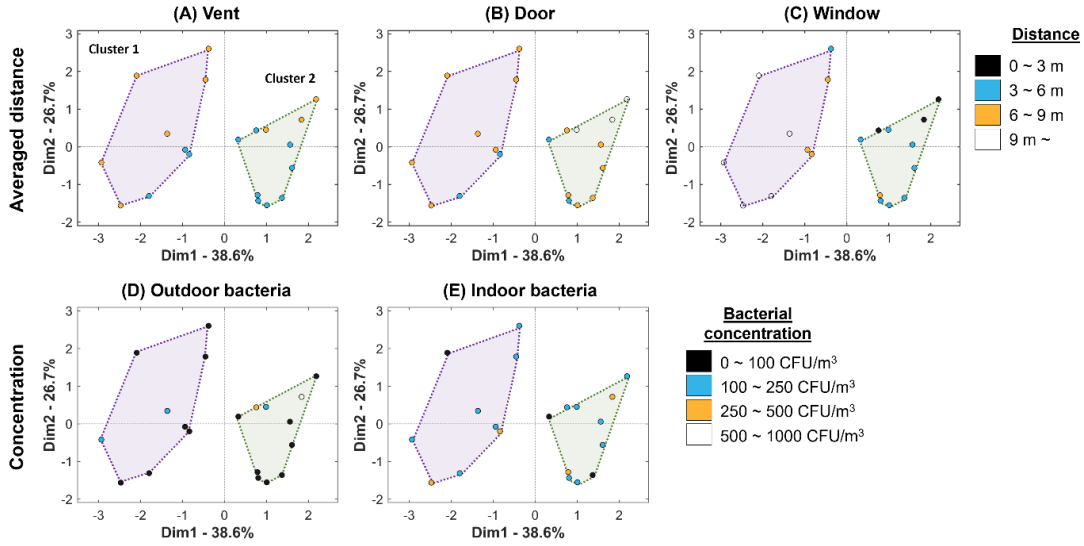


**Figure 3.9.** Clustering analysis of the averaged distance to BAE components in the occupied rooms in elementary school. BAE distance of **(A)** vent, **(B)** door, and **(C)** window and corresponding bacterial concentrations, **(D)** outdoor- and **(E)** indoor-related bacteria, respectively.

from the vent and window but near the door, while cluster 2 indicates samples near the vent and window but far from the door. Corresponding bacterial concentration for outdoor signature bacteria shows that sampling locations of concentrations more than 250 CFU/m$^3$ are in cluster 2 as shown in **Figure 3.9(D)**. The data in cluster 1 is within the range of 0-250 CFU/m$^3$. The distribution of indoor-related bacteria does not appear to be different in the two clusters. Comparing the **Figures 3.8 and 3.9**, lower concentrations of outdoor signature bacteria are further from the vent, window but nearer to the door and vice versa. In case of indoor signature bacteria, no trend is noticeable.

Similar analysis with respect to the length, width, and height (**Figure 3.10**) revealed an exclusive cluster along the normalized distance range of 0 to 3 for length with respect to concentrations between 100-500 CFU/m$^3$ for indoor signature bacteria. There were no other distinct groups.

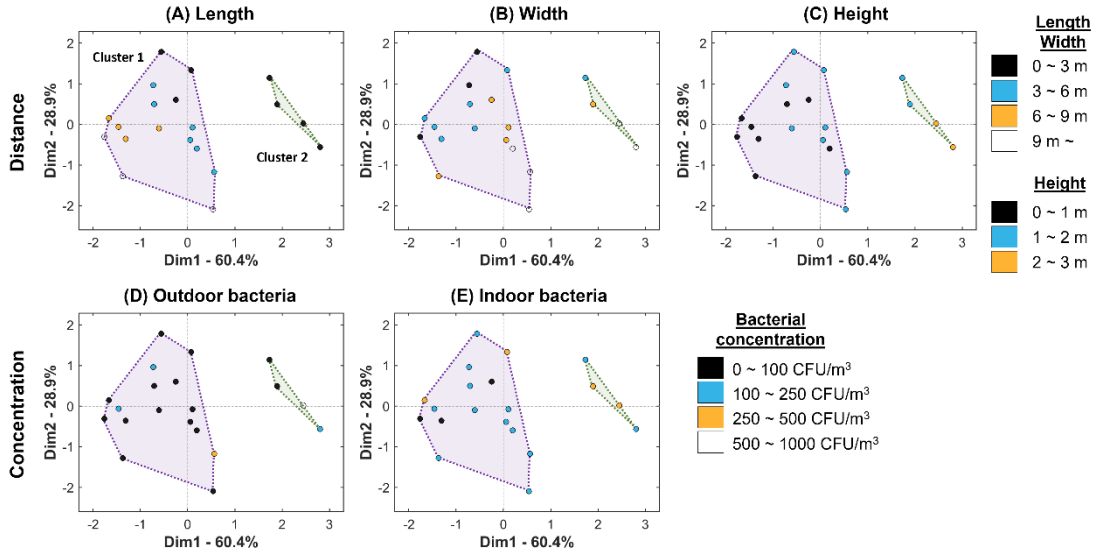


**Figure 3.10.** Clustering analysis of the distance to the boundaries in the occupied rooms in elementary school. The distance of **(A)** length, **(B)** width, and **(C)** height and corresponding bacterial concentrations, **(D)** outdoor- and **(E)** indoor-related bacteria, respectively.

To identify the range or distance at which the spatial distribution transitions the statistical significance of the influence of distance on bacterial concentration was tested. **Table 3.4** summarizes the significances of indoor- and outdoor-related bacterial concentrations with respect to the distance of BAE components and building elements. The distance to the BAE components was not a significant factor for indoor-related bacteria (*p-value* > 0.05). For outdoor related bacteria distance from the vent was only significant. **Figure 3.11** the vent distance against the concentration of outdoor signature bacteria and a linear trend can be seen, R= 0.78 (black line). The plot also highlights the change in the slope at a distance less than 0.4 m determined to be significant as shown in **Table 3.4**. The upward trend, increasing outdoor bacterial concentration with increasing distance, exists across all distances from the vent, but the slope is slightly less steep initially indicating the effects of the vent drops off more sharply as the distance from the vent increases.

**Table 3.4.** Significance of bacterial concentration with respect to the distance of BAE components and building elements evaluated by Mann-Whitney-Wilcoxon test

| **BAE components** | **Bac**[1] | **Distance** | | | | | | | | |
|---|---|---|---|---|---|---|---|---|---|---|
| | | ≤ 1 m | ≤ 2 m | ≤ 3 m | ≤ 4 m | ≤ 5 m | ≤ 6 m | ≤ 7 m | ≤ 8 m | ≤ 9 m |
| Vent | Out | | | | **0.017** | **0.017** | **0.020** | 0.344 | 0.862 | |
| | In | | | | 0.290 | 0.512 | 0.362 | 0.231 | 0.118 | |
| Door | Out | | | | 0.862 | 0.344 | 0.080 | 0.671 | 0.364 | 0.223 |
| | In | | | | 0.298 | 1.000 | 0.603 | 0.939 | 0.741 | 0.397 |
| Window | Out | 0.664 | 0.664 | 0.125 | 0.930 | 0.908 | 0.196 | 0.196 | 0.173 | 0.295 |
| | In | 0.603 | 0.603 | 0.560 | 0.694 | 0.643 | 0.939 | 0.939 | 0.283 | 0.458 |
| **Building elements** | **Bac** | **Normalized distance** | | | | | | | | |
| | | ≤ 0.1 | ≤ 0.2 | ≤ 0.3 | ≤ 0.4 | ≤ 0.5 | ≤ 0.6 | ≤ 0.7 | ≤ 0.8 | ≤ 0.9 |
| Length | Out | 0.850 | 0.162 | 0.592 | 1.000 | 0.616 | 0.761 | 0.969 | 0.827 | 0.827 |
| | In | 0.528 | **0.021** | 0.117 | 0.322 | 0.354 | 0.362 | 0.616 | 0.694 | 0.694 |
| Width | Out | 0.298 | 0.916 | 0.386 | 0.234 | 0.589 | 0.463 | 0.302 | 0.073 | 0.223 |
| | In | 0.298 | 0.090 | 0.869 | 0.606 | 0.757 | 0.105 | 0.117 | 0.205 | 0.367 |
| Height | Out | | | 0.165 | 0.217 | 0.256 | 0.290 | 0.068 | | |
| | In | | | 0.383 | 0.114 | **0.049** | 0.314 | 0.147 | | |

[1] Out: outdoor-related bacteria and In: indoor-related bacteria

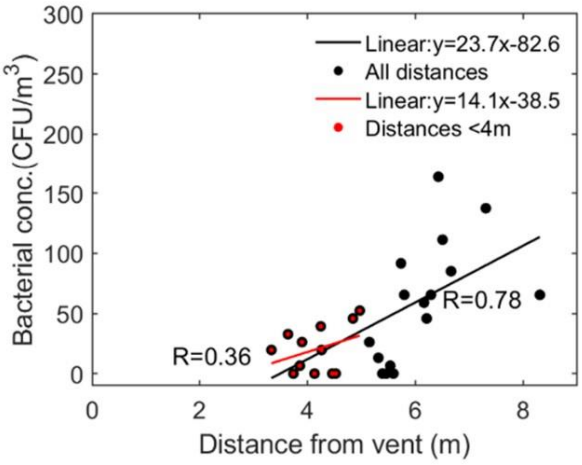


**Figure 3.11.** Scatter plots of distance of the vent versus outdoor bacterial concentration.

**Figures 3.12 (A) and (B)** show the trends across the length and height (black line) as well as the trend to the point (red line) at which a transition is noted in **Table 3.4**. The length of the room originates from the opposite end of the door entrance. Across the length there is a decrease in the indoor bacterial concentration but initially (less than 20% from the wall and more than 80% away from the door) there is an upward trend of the concentration. Overall, the concentration of indoor signature bacteria falls as the distance to the door decreases. The initial increase can be attributed to the effect of the wall on the air flow transporting the aerosols. Afterwards there appears to be a homogenizing effect on the spatial distribution of the indoor signature bacteria probably due to the proximity of the occupants. For height, originating from the floor to the top of the room, overall, the concentration of indoor bacteria decreases as the sample location moves towards the ceiling. There is also an opposing trend, though slight, near the bottom half of the space. The different trends nearer the walls can be due to the impact of the wall on the airflow pattern. Also, in case of height, the occupants' activities and breathing may have more

impact near the floor. Across the height, the highest sampling location was on top of the tallest shelf.

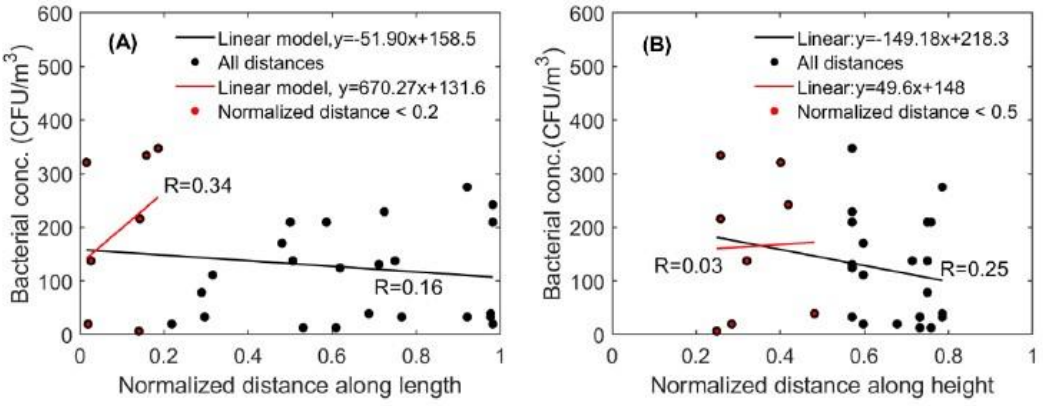


**Figure 3.12.** Scatter plots of **(A)** normalized length, and **(B)** normalized height versus indoor bacterial concentrations.

**Figure 3.13** summarizes the bacterial concentrations with respect to the BAE components and building elements. Vents influenced the spatial distribution of outdoor related bacteria and relatively lower levels were detected near the vent. As distance increased from the vent, concentration levels increased and at distance range of 4 m to 6 m from the vent, significant changes in outdoor-related bacteria were observed. The spatial distribution of indoor signature bacteria was significant along the length and height with transitions occurring at a distance of 80% from the side of the door and halfway from the floor. Computational fluid dynamics (CFD) simulation of the kindergarten location replicating the same airflow conditions was conducted to gain more insight on how the particles are distributed. In the simulation particles released from two sources around the center of the room were tracked for 15 minutes. Most of the particles moved towards the side of the space where the origin of the length of the room is. Increasing trend of the number of particles was observed within a distance of 20% from the side wall. Flow at the

boundaries and by the side walls had an effect on the particles' spatial distribution. The CFD simulation also demonstrated higher airflow velocities when closer to the walls. Similar behavior of the flow pattern near the walls have also been reported in the literature [148].

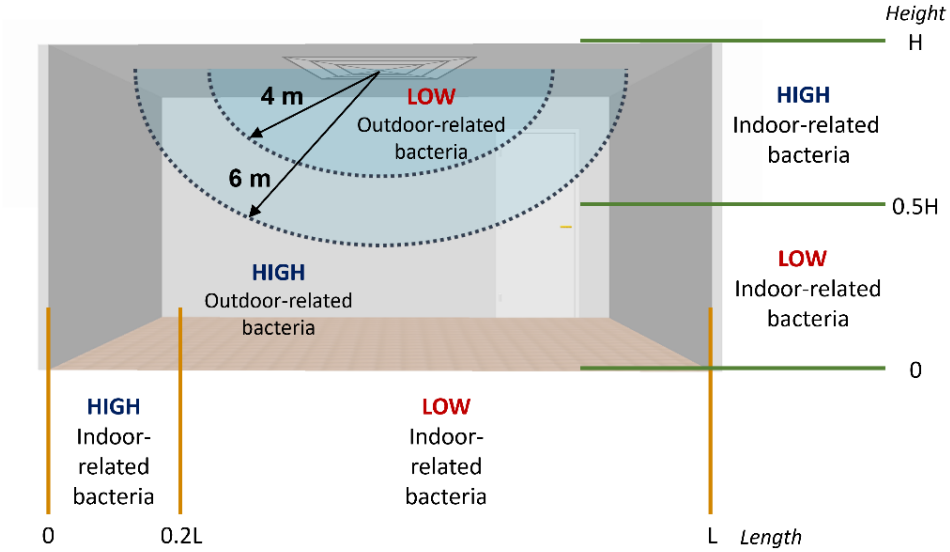


**Figure 3.13.** Schematic diagram of the bacterial concentrations in the indoor space.

## 3.4. CONCLUSIONS

This work investigated the significance of occupant characteristics (number of occupants, activity, and age) on the presence of PM, bacteria, and fungi at multiple school buildings. While PM levels (high school) and bacterial concentration (university and elementary school) were significantly influenced by occupancy, the activity level of the occupants further dictated the type of PM and bacteria that was influenced. Hence, monitoring PM levels could provide baseline data on the extent of the effects of air changes. But to ensure a space is adequately ventilated and maintains air quality, information on the occupants and planned activities need to be incorporated for optimizing the indoor environment. Furthermore, $PM_{10}$ and microbial levels were significant depending on

whether the age group of the occupants was averaging under or over the 10-year-old, highlighting that policies to improve indoor air quality have to account for the distinct nature of elementary school while high school and universities may have more similar traits.

Indoor surface materials such as wood, metal, plastic, carpet, and tiles which dominated the sites sampled, were assessed. Computer and carpet surfaces showed the highest microbial concentration while metal surfaces had the lowest. This could be due to properties of the materials but also may be influenced by what the surface was used for or exposed to. Surfaces that where frequently touched had relatively higher bacterial contamination even they were made of the same materials. This has been noted in other investigations as well [149].

The analysis highlighted that the influence of vents diminishes with distance with respect to outdoor bacteria. The decreasing effect of the vents was shown by the increase of the concentration level of outdoor bacteria. It also showed the limited influence vents have when the microbial source was indoors. Presence of occupants and activity effected the spatial distribution of the indoor signature bacteria. However, air flow near the walls dictated concentration levels at the proximity of the boundaries as seen in the trends shown in the scatter plots. Therefore, overall, bacteria from outdoor sources were more closely related to the vent location while indoor signature bacteria, *i.e.* bacteria originating due to the occupants were more influenced by the indoor space dimensions. This highlights the need for filtration of inlet air that will lead to the prevention of the colonization of the indoor space with outdoor bacteria and maintain ventilation conditions that will control the microbial population generated by the occupants.

Understanding what factors control or influence indoor biological contaminants is critical, if building design is to incorporate criteria for maintaining health and reduce infection transmission, especially after the lessons of the ongoing pandemic. By identifying crucial zones where the ventilation performance may not be up to the design specifications or identifying how occupant behavior may enhance or minimize the 'health' of a space, steps can be taken to make the indoor areas being used safer. This study provides a different approach towards sampling and analyzing for microbes in the built environment by focusing on identifying ways to associate the information to spatial details. More extensive data can be utilized to generate 'design equations' that can correlate the significant variables describing occupant characteristics and BAE components to spatial and temporal distribution of microbes.

# CHAPTER 4. FATE AND TRANSPORT OF ENVELOPED VIRUSES IN INDOOR BUILT SPACES – THROUGH UNDERSTANDING VACCINIA VIRUS AND SURFACE INTERACTIONS [3]

## ABSTRACT

The current coronavirus disease 2019 (COVID-19) pandemic has reinforced the necessity of understanding and establishing baseline information on the fate and transport mechanisms of viruses under indoor environmental conditions. Mechanisms governing virus interactions in built spaces have thus far been established based on our knowledge on the interaction of inorganic particles in indoor spaces and do not include characteristics specific to viruses. Studies have explored the biological and kinetic processes of microbes' attachments on surfaces in other fields but not in the built environment. There is also extensive literature on the influence of indoor architecture on air flow, temperature profiles, and forces influencing aerosol transport. Bridging the gap between these fields will lead to the generation of novel frameworks, methodologies and know-how that can identify undiscovered pathways taken by viruses and other microbes in the built environment. Our study summarizes the assessment of the influence of surface properties on the adhesion kinetics of vaccinia virus on gold, silica, glass, and stainless-steel surfaces. We found that

[3] Results presented in this chapter have appeared in "Seong,D., Kingsak,M., Lin,Y., Wang,Q., & Hoque.S., (2021) Biomaterials Translational, 2(1), 50"

on gold the virus layer was more viscoelastic compared to stainless steel. There was results further highlight the importance of converging different fields of research to assess the fate and transport of microbes in indoor built spaces.

*GRAPHICAL ABSTRACT*

To limit transmission due to infectious droplets we must understand, "What factors control the transport, deposition, adhesion, and persistence of pathogens indoors?" The pandemic has reinforced the necessity of establishing baseline information on how viruses under indoor environmental conditions optimize survivability and transmission. Virus-surface interactions investigations using vaccinia virus sheds light on part of the picture.

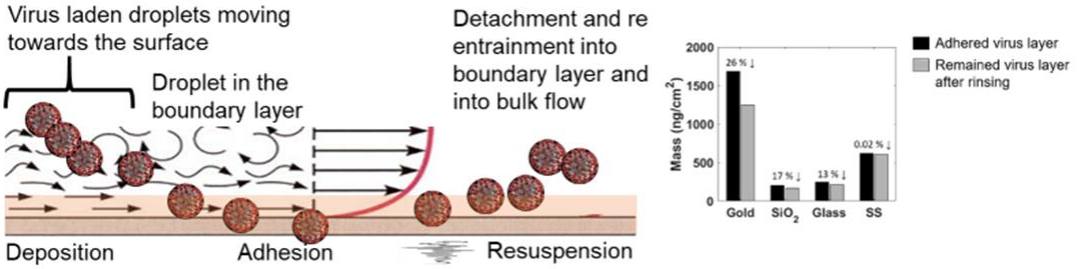


**Figure 4.1**. A graphical abstract of the Chapter 4.

*Keywords: Adhesion kinetics, Aerosols, Built environments, Resuspension, Surface properties, Ventilation*

## 4.1. INTRODUCTION

The significance of the built environment and the materials that construct it has become critical during the ongoing pandemic. How long does the severe acute respiratory syndrome coronavirus 2 (SARS-CoV-2) survive in the air and on surfaces? Since the pandemic hit this has been a perpetual question with the answer still being investigated. It

is well known that contaminated surfaces are significant vectors in the transmission of infection both in hospitals and in the community [150, 151]. Recent investigations [152] into determining stability of the virus on different surfaces and in the aerosolized form revealed that the SARS-CoV-2 virus can survive for 3 hours in the aerosolized form and 72 hours on plastic and stainless steel [153] with survivability varying based on indoor and outdoor conditions [154, 155]. The transmission forms for both SARS-CoV-1 and SARS-CoV-2 are similar [152, 156]. Studies on transmission routes for influenza virus have documented the dominant influence of airborne transmission via suspended and settled droplets [157-159] resulting in guidelines of social distancing (~6 feet, about 1.83 m) to prevent person to person transmission [160].

The studies all focus on obtaining data on either the influence of air circulation such as sampling in an aerosolized environment or via inoculating different types of surfaces. The investigations do not account for the fact that the two events are not isolated. Aerosolized virus laden droplets must be transported to the boundaries near the surfaces, deposit from the boundary layer on to the surface and subsequently adhere. Recent events have also shown the high probability of aerosolized transmission [161-163]. The question that needs to be answered to successfully limit transmission is, “What conditions control the transport, deposition, adhesion, and persistence of airborne SARS-CoV-2 in air and on surfaces?” The interface of the boundary layer and the surface influences the transport and deposition of particles including virus laden droplets. **Figure 4.2** illustrates the concept. The fluid mechanical boundary layer is the flow region (air) very near the surface where viscous forces dominate and transitions to a region of high velocity of air [164]. Air flow in indoor spaces is often treated as well mixed but, investigations have shown the

significant influence of near surface air motion on particle deposition [165] and resuspension [166]. There is however a lack of information on the relationship between the magnitude of shear forces and boundary flow velocity characteristics on the transport mechanism of viruses particularly near surfaces. Released virus droplets or aerosolized viruses will over time reach the boundary layers near the surface where they will subsequently 'attach' to the surface and adhere to it. Investigations in aqueous suspensions have shown the wide ranging and variable influence of wall shear rates on the deposition, adhesion and detachment of particles and microbes [167-169]. The attachment process is influenced by the surface characteristics which include surface roughness (RH), porosity or morphology, or microbial characteristics which are mobility, flexibility, or hydrophilicity [170, 171].

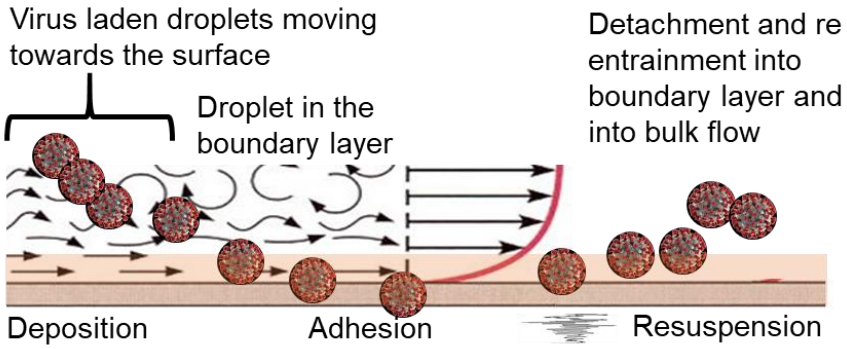


**Figure 4.2**. Schematic illustration of the fate and transport of virus particles at the intersection of bulk and boundary layer flow.

To gain insight on these processes and their influence on the fate and transport of microbes in the indoor space, the authors assessed the adhesion behavior of model enveloped viruses, vaccinia virus (VACV) and measles virus (MV), bacteria (*Corynebacterium* sp.), and bovine serum albumin (BSA) on various types of surfaces seen in the built environment under flow conditions. The investigation is a prelude to further

studies on how the complex interaction of the multiple variables of an indoor space can influence the fate and transport of microbes in the bulk flow and boundary layer. This article also summarizes the current knowledge on particle deposition, attachment and re-entrainment in indoor spaces and the influence of properties of materials on the particle transport behavior. The paper concludes by discussing the results of the authors' work in context of past investigations and future directions.

## 4.2. MATERIALS AND METHODS

### 4.2.1. VACV culturing and purification

Vero cells (CDC, Atlanta, GA, USA) were cultured in Dulbecco's modified Eagle's medium (Corning, Manassas, VA, USA) supplemented with 10% fetal bovine serum (Atlanta Biologicals, Flowery Branch, GA, USA), 2 mM L-glutamine, 1 mM sodium pyruvate, and 100 U/mL penicillin-streptomycin (HyClone, Marlborough, MA, USA). Cell cultures were maintained at 37℃ in a $CO_2$ incubator with 5% $CO_2$ and 95% air. VACV was propagated in Vero cells with the presence of 2% fetal bovine serum Dulbecco's modified Eagle's medium. The infected cells were incubated at 37℃ for 2 to 4 days until the microscopic cytopathic effect was complete.

The virus purification method was modified from Hruby *et. al.* [172]. In brief, the infected cells were harvested and subjected to homogenization. Cell debris was removed by centrifugation at 12,296 × g for 15 minutes at 4℃ (Sorvall® RC5C plus, Newtown, CT, USA). The virus pellets were precipitated by centrifugation at 81,799 × g for 3 hours at 4℃ (Beckman L8-70M, Palo Alto, CA, USA) and resuspended in 1 mM Tris buffer (pH 8) overnight. Purified virus was obtained through a side-band-pull from a gradient of

sucrose centrifuged at 22,504 ×g for 40 minutes at 4℃. Vero cells were plated in 6-well plates at a density of $6 \times 10^5$ cells per well one day prior experiment. Ten-fold serial dilutions of purified virus were made in phosphate buffered saline. The virus samples of each dilution were placed onto the prepared 6-well plate cultured with Vero cells, then incubated at room temperature in a laminar flow hood for 30 minutes. After infection, unbound virus was removed and replaced with 1% agarose (VWR Life Science, Radnor, PA, USA) in 2% fetal bovine serum Dulbecco's modified Eagle's medium. The plates were incubated at 37℃ and 5% $CO_2$ for 2 to 4 days until able to visualize plaques. The virus titer was calculated using an average number of plaques, dilution factor, and the inoculum volume as described elsewhere [173].

4.2.2. Quartz crystal microbalance with dissipation analysis

The quartz crystal microbalance with dissipation (QCM-D) approach was applied to investigate virus adhesion and detachment on four types of sensor surfaces [174, 175]. QCM-D technique was performed using Q-sense E4 (Biolin Scientific, Gothenburg, Sweden). Polished AT-cut 5-MHz quartz crystals coated with four materials were selected: gold (QSX 301) with RH < 1 nm, $SiO_2$ (QSX 303) with RH < 1 nm, sodalime-glass (QSX 337) with RH < 20 nm, and stainless-steel (QSX 304) with RH < 1 nm. Temperature in the modules was controlled at 23℃. Three flow rates were assessed: $8.33 \times 10^{-6}$ $m^3/s$ (50 µL/min), $1.67 \times 10^{-6}$ $m^3/s$ (100 µL/min), and $3.33 \times 10^{-6}$ $m^3/s$ (200 µL/min). Before the experiment, all sensors were pre-cleaned with ultraviolet/ozone light for 10 minutes to remove organic contaminants on the surface. MilliQ water was first injected into the modules to provide a baseline measurement. Then, virus suspension suspended in 1 mM Tris buffer was injected at a selected flow rate. Experiments were initiated at four initial

concentrations, $6.45 \times 10^4$ PFU/mL, $2.00 \times 10^5$ PFU/mL, $2.25 \times 10^5$ PFU/mL and $2.68 \times 10^5$ PFU/mL. Virus attachment resulted in the decrease of frequency and increase of dissipation. Once both frequency and dissipation attained a constant value, the modules were rinsed with the baseline solution. Changes of frequency ($\Delta f$) and dissipation ($\Delta D$) on the sensor crystal were recorded using QSoft401 and the data were analyzed using QSense Dfind software (Biolin Scientific, Gothenburg, Sweden). Before the start of any experiment and in between each experiment, QCM-D modules and sensors were thoroughly cleaned using a 2% sodium dodecyl sulfate solution (Fisher Scientific, Waltham, MA, USA) and ultraviolet/ozone treatment and dried with $N_2$ gas.

The QCMD detects mass and dissipation change through the excitation of the sensor crystal which oscillates at a specific frequency due to the application of a certain voltage across the electrodes because of piezoelectric properties [176, 177]. Mass change ($\Delta m$) on the sensor crystal causes frequency change ($\Delta f$) and is defined by Sauerbrey relation as shown in **Eq. 4.1** where $c$ is 17.7 ng/Hz/cm$^2$ for a 5-MHz crystal, and $n$ is the overtone.

$$\Delta m = -\frac{\Delta f \times c}{n} \qquad \text{Eq. 4.1}$$

Dissipation ($D$) is caused by the adsorption of the viscoelastic film and is described as the ratio of dissipated and stored energy [178, 179]. Energy lost during crystal oscillation is calculated using the measured dissipation based on **Eq. 4.2** where, $E_{diss}$ is the energy dissipated during one oscillatory cycle and $E_{strd}$ is the energy stored in the oscillation system [180, 181].

$$D = -\frac{E_{diss}}{2\pi E_{strd}} \quad \text{Eq. 4.2}$$

4.2.3. Measurement of virus characteristics

(1) Atomic force microscopy

Glass slides were cleaned by Piranha solution (30% hydrogen peroxide and concentrated sulfuric acid with 3:7 ratio from Fisher) at 75°C for 2 hours following by washed and sonicated in MilliQ water. The cleaned glass slides were then immerged in 1 mg/mL poly(diallyl dimethylammonium chloride) (PDDA) solution overnight, rinsed with MilliQ water (Millipore, Burlington, MA, USA) and dried with $N_2$ gas. PDDA (molecular weight 100,000 to 200,000) was purchased from Sigma-Aldrich (St. Louis, MO, USA). The PDDA glass substrate was then immerged in VACV solution at the concentration of 1 × $10^4$ plaque-forming unit/mL for 1 hour, gently rinsed with water and dried with $N_2$ gas. Atomic force microscopy images of VACV on glass slides and surface roughness were obtained by SPA 300 instrument (Veeco, Santa Barbara, CA, USA) in ambient conditions under tapping mode at a scan rate of 1 Hz and scan size of 10 × 10 $\mu m^2$.

(2) Fluorescence microscopy

A recombinant VACV expressing green fluorescence protein was placed onto a glass slide and evaporated to dryness in a laminar flow hood. The excessive green fluorescence protein tagged viruses were gently washed out by phosphate buffered saline solution. The fluorescence images were acquired using a fluorescent microscope (Olympus IX81, Shinjuku-ku, Tokyo, Japan) with disk scanning unit confocal mode.

(3) Zeta potential measurement

The purified virions were incubated for 5 minutes and overnight in 1 mM Tris buffer pH 8 and pH 4.5. The virus samples were then transferred to a DTS1070 disposable capillary cell (Malvern, Malvern, Worcestershire, UK) for zeta potential measurements. The measurements were performed at 25°C with a Zetasizer Nano-ZS (Malvern).

(4) Transmission electron microscopy imaging

The virus was dropped onto a carbon coated copper grid for 30 minutes, and the excess virus solution was blotted off. The grid was washed with several drops of MilliQ water and dried by slow evaporation in air at room temperature. After the adsorption, 2% uranyl acetate was applied to the grid for negative staining. The morphology of the purified VACV was characterized by Transmission electron microscopy (Hitachi HT7800, Chiyoda-ku, Tokyo, Japan).

## 4.3. RESULTS

### 4.3.1. VACV characteristics

VACV, a member of the poxvirus family, is an enveloped virus [182]. It consists of a large double-stranded DNA genome approximately 190 kb in length, a protein layer known as the palisade, and the envelope composed of surface tubules, enveloped proteins, and lipid membranes, as illustrated in **Figure 4.3(A)** [183-186]. VACV has an oval to brick-shaped architecture with the dimensions of 270 nm in diameter and 350 nm in length [184, 185]. The purified VACV using in this study expresses green fluorescence protein and can be observed under a fluorescent microscope as shown in **Figure 4.3(B)**. Surface

charge of the virus is one of the important factors that play an essential role in numerous sorption processes, for example adsorption and adhesion, which are governed by electrostatic interactions [187]. To investigate the physical and charge characteristics of the purified virions, atomic force microscopy and dynamic light scattering were performed. In **Figure 4.3(C)**, VACV shows a negative surface charge with a zeta potential of approximately -30 mV in pH 8 Tris buffer solution and -20 mV in pH 4.5 Tris buffer solution, incubated in the buffers for 5 minutes and overnight, using Zetaseizer. In addition, atomic force microscopy revealed that a good deposition of negatively charged virions on a positively charged PDDA-glass substrate was found (**Figure 4.3(D)**). The average size of VACV is ~200-350 nm in different directions as observed under transmission electron microscope (**Figure 4.3(E)**), which is consistent with literature report [188-190].

4.3.2. Virus adhesion kinetics via QCM-D

**Table 4.1** shows the details of the frequency and dissipation shifts for both adhesion and detachment, and **Figures 4.4(A)-(D)** display the frequency ($\Delta f$), and dissipation ($\Delta D$) shifts of the third overtone. Four types of sensors were applied to investigate the relation between the types of sensor material and virus adhesion, gold, silica, glass, and stainless-steel (SS).

**Table 4.1.** Frequency ($\Delta f$) and dissipation ($\Delta D$) shift due to VACV adhesion and mass ($\Delta m$) of adhered VACV on the sensor surface calculated by Sauerbrey relation

| Sensor | VACV adhesion | | VACV detachment | |
|---|---|---|---|---|
| | $\Delta f$ (Hz) | $\Delta D$ ($\times 10^{-6}$) | $\Delta f$ (Hz) | $\Delta D$ ($\times 10^{-6}$) |
| Gold | -5.77 | 1.90 | -5.37 | 1.39 |
| $SiO_2$ | -31.70 | 1.85 | -27.60 | 0.98 |
| Glass | -29.81 | 2.52 | -27.22 | 1.72 |
| Stainless-steel | -22.16 | 2.40 | -21.23 | 2.11 |

Note: VACV: vaccinia virus. This is representative of an experiment started at $2.00 \times 10^5$ PFU/mL

MilliQ water was first entered for a baseline. A stable baseline was observed prior to VACV injection regardless of the type of sensor material. The black arrows indicated the injection of VACV ($2.0\times10^5$ plaque-forming unit/mL). At 4 minutes, sensors were exposed to the virus suspension, thus, rapid decrease in frequency was observed due to sensor – virus bindings. Rapid increase in dissipation was observed corresponding to the virus adhesion to the sensor surface. The frequency and energy dissipation were monitored in real time while the virus adhesion resulted in the built up of multilayers on the sensor crystals. When no more significant changes in frequency and dissipation were observed, MilliQ water (blue arrows in **Figures 4.4(A)-(D)**) flow was started to rinse the sensor surface and to measure the virus detachment, concurrently. Gold sensor resulted in the smallest change of frequency, $\Delta f$ = -5.77 Hz while silica had the maximum frequency shifts of -31.70 Hz. Glass had a frequency shift of -29.81 Hz while SS exhibited a frequency shift between silica and glass, -22.16 Hz. $\Delta D$ for all sensors ranged from $1.85\times10^{-6}$ to $2.52\times10^{-6}$. Increase in frequency and decrease in dissipation were observed due to virus detachment and is an indicator of virus – surface adhesion characteristics *i.e.*, whether the film layers formed is soft or rigid or became rigid due to multi-layer formation. Even though increase in frequency and decrease in dissipation were measured after rinsing, the values did not return to baseline levels. This indicates that the cleaning step washed away soft layers, but remaining layers on the sensor crystals had become rigid and could not be 'cleaned' thoroughly to negligible values. **Figure 4.4(E)** shows the calculated mass of virus layers after adhesion and then after rinsing *i.e.*, extent of detachment applying the Sauerbrey relation. For $SiO_2$, 13% of mass was removed after rinsing (189.1 ng/cm$^2$ of adsorbed virus layer and 164.6 ng/cm$^2$ of remained virus layer), followed by glass, 9%

(177.8 and 162.4 ng/cm$^2$), gold, 7% (34.4 and 32.0 ng/cm$^2$). The lowest removal occurred for stainless-steel after rinsing (132.2 and 126.7 ng/cm$^2$).

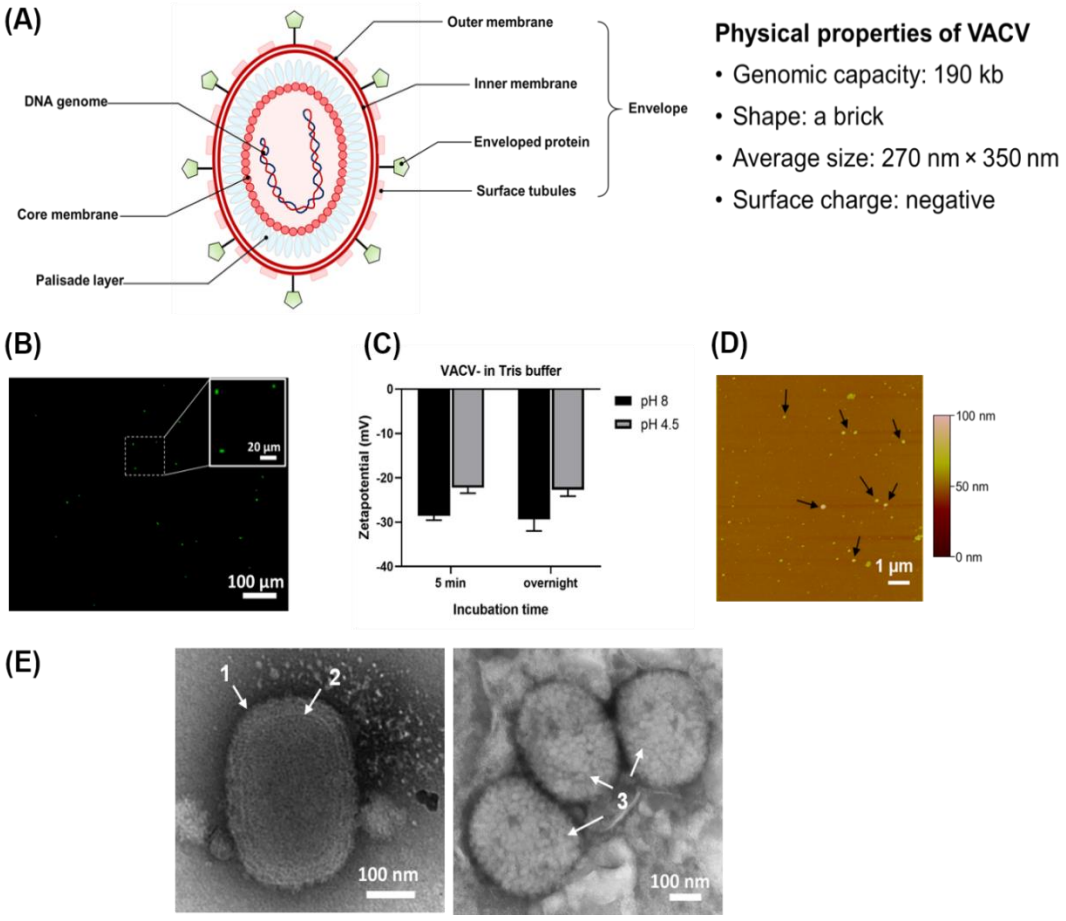


**Figure 4.3**. VACV structural and physical properties. **(A)** Schematic illustration of the VACV structure, genomic capacity, shape, average size, and surface charge. **(B)** Fluorescence imaging of green fluorescence protein-tagged VACV (green). **(C)** Zeta potentials of VACV over the pH 8 and 4.5 in 1 mM Tris buffer. Data are expressed as mean ± SD. **(D)** Atomic force microscopy image of VACV deposited on PDDA-glass substrate. The black arrows point to VACV particles. **(E)** Representative transmission electron microscopic images of VACV. The white arrows point to (1) outer membrane, (2) core membrane, and (3) surface tubules. Scale bars: 100 µm in B, 1 µm in D and 100 nm in E. PDDA: poly(diallyl dimethylammonium chloride); VACV: vaccinia virus. The duplicate samples were measured, and two experiments were repeated to acquire the data.

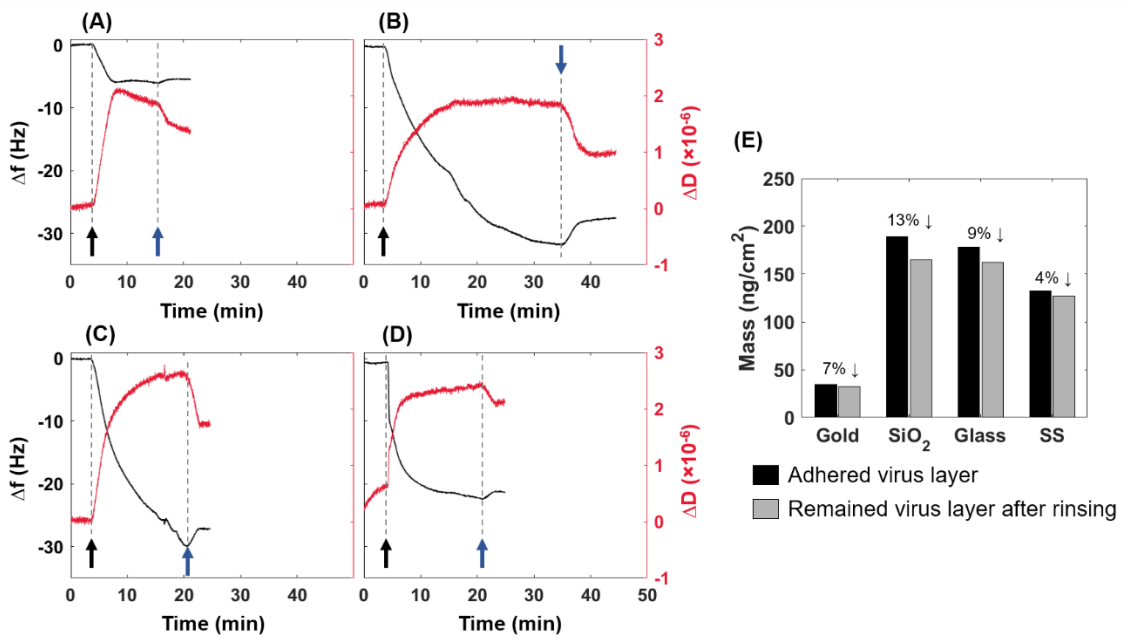


**Figure 4.4**. Quartz crystal microbalance with dissipation analysis of the frequency (Δf, black line) and dissipation (ΔD, red line) ($\times 10^{-6}$) shifts of VACV on **(A)** gold, **(B)** $SiO_2$, **(C)** glass, and **(D)** stainless-steel. Black arrow: VACV injection; blue arrow: rinsing with MilliQ. VACV: vaccinia virus. **(E)** Mass of adhered and remained virus layer on the sensor surfaces calculated by Sauerbrey relation. VACV: vaccinia virus. SS: stainless-steel. This is representative of an experiment started at 2.00 × 105 PFU/mL.

**Figure 4.5** displays the *f-D* plots to assess the structural conformation of the adhered VACV layers. The slope (K, $\Delta D/\Delta f$) represents the adsorption kinetic process on the sensor crystal. Higher K indicates the structural conformation of the layer on the sensor surface is soft and flexible whereas lower K represents that the layer is thin and rigid. Initially a soft layer ($K_1$) is formed while as it adheres to the sensor surface and then the layer becomes firm ($K_2$). After the rinsing step, part of the adhered layer has been removed from the sensor (increase in frequency) and the remaining layer is more rigid ($K_3$). **Figure 4.5(A)** shows the adsorption process for VACV-gold. In comparison to **Figures 4.5(B)-(D)** which represents the adhesion process of VACV for silica, glass, and SS respectively, $K_1$ and $K_2$ is the steepest for gold sensor indicating the layer attached is more viscoelastic compared to the others. The sensor also has the lowest $K_3$ value which indicates that the

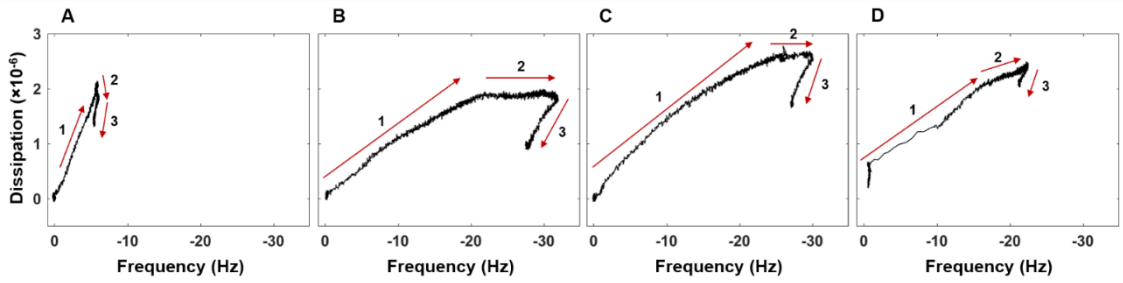


**Figure 4.5**. Frequency-dissipation plots for VACV for **(A)** gold, **(B)** $SiO_2$, **(C)** glass, and **(D)** stainless-steel. '1', '2', and '3' show the steps of the adhesion process, '1' adhesion, '2' reaching saturation and '3' detachment due to the wash cycle. The numbers correspond to the slope represented by K1, K2 and K3. VACV: vaccinia virus. This is representative of an experiment started at 2.00 × 105 PFU/mL.

layer remaining is thin, and rigid as opposed to its counterparts. **Figure 4.5(B)** and **(C)** show similar characteristics of the layer formed initially at the beginning of adherence of VACV to silica and glass. $K_2$ and $K_3$ values for silica are less than glass. VACV-SS interaction based on $K_1$, $K_2$ and $K_3$ is very similar in magnitude to glass. SS surface is positively charged [191] and the extent of detachment of negatively charged VACV is significantly less compared to the other sensors.

## 4.4. DISCUSSION

The results focus on one aspect of the multi-faceted problem – influence of surface type on attachment and detachment of VACV. The significance of understanding how surface properties control the adhesion kinetics is highlighted. During the initial adhesion process the viscoelastic nature of the virus layer was dependent on the surface type. After the first phase of attachment, there is a plateau indicating saturation has been reached and the layer is becoming rigid. Rinse cycle is started immediately, and the extent washed off differs based on the properties of the layer formed and for these surface types, surface

charge. Gold behaves very differently from the other surfaces, in that while mass attached is lower than SS, it remains attached. Glass and silica appear to be the 'cleanest' surfaces since adhered viruses were easily cleaned compared to other surfaces. The effect of 'flow' on the behavior of VACV-surface interactions remains to be investigated and correlated. In the sections below the factors that can influence fate and transport of aerosols including microbes are discussed.

4.4.1. Phenomena influencing deposition

Extensive investigation in the factors influencing deposition of inorganic particles has been done because of the significant role it plays on human health and exposure. The deposition phenomena are influenced by multiple factors which include particle characteristics, air flow, interior design, and surface coverings [192-195]. The interacting effect of ventilation, location of furniture and air changes have shown that while higher air changes removed particles faster, localized exposure and deposition is influenced by a combination of multiple factors [196]. Experimental and modeling studies determined a lumped parameter: deposition velocity or loss rate coefficient for a range of particle sizes to distinguish the effects of the multi-dimensional design space which describe the indoor environment [197, 198]. Deposition velocities and loss rate coefficients provide a bulk perspective of the transport and removal of particles from the air [199]. The rate at which deposition occurred is represented by deposition velocity, $v_d$ as shown in $v_d = \frac{M}{tCA_s}$ where $M$ is the mass of particle on a sample surface, $t$ is time of exposure, $C$ is time-weighted average mass concentration of particles in air and $A_s$ is the surface sample area.

Studies in small scale chambers and real houses have shown that particle removal by deposition is significantly correlated to diameter, surface to air temperature difference,

surface orientation, spatial location, and RH [192, 195, 198]. Deposition constants have been shown to be related to building wall textures, orientation and particle size [200]. Among surface properties, the influence of RH has been assessed. Lai and Nazaroff [201] observed that particle deposition increased for most particle sizes onto smooth and rough vertical surfaces, with roughness simulated using smooth glass plates and sandpaper. While deposition clearly increased with near wall airflow velocity the influence of surface roughness became less evident [197] probably due to the dominance of the fluid momentum boundary layer.

Deposition velocities in relation to microbe carrying particles or for microbes have not been investigated extensively. Typically, the studies incorporate properties or stay within the range of parameters accepted for inorganic particles. For example a computational fluid dynamic (CFD) model based on Eulerian-Lagrangian framework simulated the deposition of *Staphylococcus* and *Micrococcus*, the conclusions identified that mixing and ventilation conditions influenced deposition of the bacterial species [202]. The spherical species have a diameter ~ 1μm and were selected because of the proximity of the physical characteristics for the application of stokes' law and lack of information for microbes. Studies cannot account for the characteristics of the different types of microbes, bacteria, viruses, and fungi which can influence transport and deposition. Whyte and Eaton [203] calculated deposition velocities as a function of concentration of airborne particles carrying microbes by collecting samples from clean rooms and operation theatres. Seong and Hoque [109] assessed the influence of sampling region and sampling location on bacterial species detected.

4.4.2. Adhesion forces governing surface interaction

The forces encountered in adhesion of solid particles on solid surfaces either in air (at different humidity levels) or in water or other media are molecular interactions defined by Van der Waals' forces, electrostatic interaction, liquid bridges, double layer interaction and polar and/or metallic bonds [204-207]. Dust and activated carbon appear to preferentially adhere to insulated surfaces such as PVC or glass compared to aluminum and copper [208]. Physics-based model such as the Hamaker model depending exclusively on Van der Waals forces was not successful in interpreting the adhesion mechanism and results indicated the significance of considering polar contributions [208, 209]. Other investigations have looked into particle shape and size pointing out the limitation that most studies tend to focus on spherical particles [210, 211].

Deryaguin–Muller–Toporov (DMT), Johnson–Kendall–Roberts (JKR) and Maugis–Pollock (MP) models [212-214] have been applied to describe molecular attraction forces and the influence of contact areas between particles and surfaces. Surface roughness and contact angle have a high impact on the magnitude of the van der Waals forces. Higher humidity levels, beyond 50% tend to enhance adhesion [204, 209]; however, the hydrophilic/hydrophobic nature of particles and surfaces impacts the degree of influence [215]. For example, adhesion force of glass on glass or glass on silica surfaces for diameters ~20 to 60 μm treated to be hydrophobic remained constant for all humidity levels while for hydrophilic conditions, at 50~60% humidity adhesion force increases or resuspension decreased [216]. The anomaly observed for hydrophobic surfaces and the increasing deviation from classical theoretical predictions for larger size particles have been attributed to the water film formed between particles and surfaces and/or the

electrostatic forces. Adhesion force magnitudes decreasing with particle size [204]. Particles of size in the range >1μm to ~5μm adherence to surfaces is determined by the nature of the contact and are harder to resuspend but larger size particles are easier to resuspend and the adhesion mechanism is influenced by contact points, and geometry [205, 217].

This literature survey on adhesion of microbiological particles to surfaces target bacteria and viruses. Studies focusing on bacteria are dominated by areas such as biocorrosion [218], biomaterial implants [219, 220], environmental microbiology [221], food industry [222], and microbial fuel cells [223]. The adhesion mechanism is modeled typically using the Derjaguin, Landau, Verwey, Overbeek (DLVO) approach, or the thermodynamic approach or the extended DLVO or XDLVO model [224-227]. The DLVO theory is based on the non-specific interaction energies between the van der Waals forces and the electrostatic double layer forces which can be attractive or repulsive contingent on the bacteria-surface combination. Thermodynamic theory on the other hand is based on the concept of surface free energies which would account for the various types of interactions including van der Waals, electrostatic and dipole moments. Since the DLVO theory assumed inert chemical surfaces, a modification was added to the theory by adding a short-range Lewis acid-base term which will account for the hydrophobicity / hydrophilicity in an extended XDLVO theory [228].

The XDLVO theory has been applied to shed light on the mechanisms governing the adhesion of viruses to certain surfaces. For example a study by Chrysikopoulos and Syngouna [229] looked at the interaction of bacteriophages, MS2 and ΦX174 with clay colloids. The virus attachment was described by the Freundlich isotherm and the Lewis

acid-base term in the XDLVO model was critical in explaining the hydrophobic interaction mediated attachment. XDLVO approach was utilized to model the attachment of human adenoviruses and two bacteriophages, P22 and MS2 [230] to lip balms. The study showed that drying of the lip balms resulted in the drop of surface free energy which made the surfaces highly hydrophobic. XDLVO model results predicted that attachment was favored due to short range strong hydrophobic interaction. Hydrophobic and electrostatic interactions were also shown to govern the attachment of MS2 bacteriophage to surfaces treated with polyelectrolyte multilayers [231].

Recent investigations have tried to unravel the implications of virus adhesion kinetics with regard to health effects, infection transmission and SARS-CoV-2 [153, 232-234] by utilizing representative surrogates such as a lentivirus [233] or through conducting a theoretical analysis utilizing existing data to assess the influence of different surfaces and environmental conditions including temperature, humidity, and pH [155, 232, 235]. Experimental methods for determining the adhesion force and kinetic mechanisms include using the centrifuge approach [236, 237] or the QCM-D [230, 231, 238] and AFM [239, 240]. Liu et al. [241] used floor dust as surrogates for fungal spore and high-speed imaging to capture the effect of velocity on resuspension. For microbes and surfaces of the built environment, investigation has focused on antimicrobial properties of metal alloys such as copper – zinc, copper – silver on surfaces and their application [141, 242-244]. The studies highlight the significant differences that exist between the adhesion mechanisms for inorganic particles versus microbes [245].

4.4.3. The mechanism of resuspension

Measurements of resuspension have been expressed as resuspension factors or resuspension rates [246]. Resuspension factor is the ratio of air borne contaminant concentration per unit air volume to the contaminant surface concentration per unit area on the ground and resuspension rate is defined as the fraction of a surface species removed in unit time [246].

Experimental results showed that smaller particles required larger flow velocity to achieve the same amount of detachment as the larger particles. The detachment fraction was also dependent on the surface adhesion energy of the particles ranging between ~32 μm and ~76 μm with higher velocities required for higher adhesion energy [247]. Punjrath and Heldman [248] studied particle entrainment in a wind tunnel and theorized that two mechanisms: a) initiation of particle movement when shear stresses on the particles exceed friction forces acting on the particles and b) transfer of momentum from other moving particles dominated resuspension.

Modeling studies comprised of two approaches – statistical and/or force balance. Theoretical models have simulated the mechanisms at a micro scale [166, 249-251], whereas CFD models have focused on capturing the movement of a specific activity such as foot tapping [210] and analytical models [252] have applied multiple fundamental concepts such as dimensional analysis to model the effects. The Eulerian method, in which particles are treated as a continuum, has been traditionally applied to the cases of heavy particle deposits while Lagrangian methods have been applied to individually track relatively light particles in monolayer or few multi-layer systems [253, 254]. In Lagrangian-based models, particle transport is generally modeled through the addition of

gravitational, drag, added mass, Saffman's lift, bed impact forces and Bassett forces [255]. Among these forces, Bassett forces (force due to acceleration of the particle) have been considered negligible and bed impact forces are more dominant than lift forces. Braaten et al. [249] assumed that fluid forces are applied at the surface in discrete 'bursts' following a probability distribution. Saffman's lift force [256] has been used in the literature to describe the particle motion when studying particle deposition mainly. Mollinger and Nieuwstadt [257] and Leighton and Acrivos [258] also developed expressions for the lift force for particles touching the wall. Shi and Bayless [259] developed a CFD model of a gas-particle flow in cyclones. The authors incorporated a balance of adhesion and lift-off forces to account for particle detachment from the surfaces.

Due to the inherent random nature of particle behavior, statistical approaches for predicting resuspension such as Monte Carlo simulations [260] and Lagrangian stochastic models have been proposed [261]. The stochastic models showed that resuspension can be captured numerically but appropriate attention needs to be given to fluctuations created due to turbulent flow or bursts created due to surface impacts [166, 250]. Loosmore et al. [246] developed empirical models to calculate resuspension rate, using five parameters: friction velocity, time since the wind flow begin, particle diameter, particle density, and roughness height and identified friction velocity and time of exposure as the most important factors. In an indoor space particle resuspension magnitude could vary by two to three orders of magnitude. Resuspension rates between $3\times10^{-7}$ and $6\times10^{-6}$ $min^{-1}$ were found for super micron particles of density 1000 $kg/m^3$. Substantial resuspension of particles of diameter 2.5 μm and 5 μm occurred with source strengths ranging from 0.03 mg/min to 0.5 mg/min, a range estimated for human activities [192, 193, 262].

Few studies have explored the effects of resuspension of microbes. Krauter and Biermann [263] examined the re-aerosolization of dry spores (0.6~1.1 μm) in a ventilation duct. Resuspension rates of fungal spores on both steep and plastic duct materials were between $6\times10^{-2}$ and $6\times10^{-4}$ $min^{-1}$, which decreased to 10 times less than the initial rates within 30 minutes. In depth analysis of the influence of friction, surface roughness, exposure time and forces which have been assessed to an extent for particles have not been quantified regarding bacteria, viruses, or fungi.

## 4.5. CONCLUSIONS

The current pandemic has reinforced the necessity of establishing baseline information on how viruses under indoor environmental conditions optimize survivability and transmission. Based on the discussions above, investigations into understanding this phenomenon can be separated into three main categories. One category investigates the effects of indoor environmental factors and surface properties on boundary flow characteristics. The second group of studies assess the influence of the same variables on various phenomena such as drag force, electrostatic force or thermophoretic force which effects aerosol fate and transport. The last category is the effect of physical and biological properties on the deposition, attachment, and persistence of microbes on surfaces. Typically, the three categories discussed are investigated independent of each other with some overlap occurring in categories 1 and 2. But, an indoor environment with a range of bacteria, viruses and fungal species and an evolving microbial world encompasses all three categories as shown in **Figure 4.6**. To successfully understand, assess and predict how the

indoor environment perpetuates transmission from air to surfaces and vice versa, we must bridge the gaps between these fields.

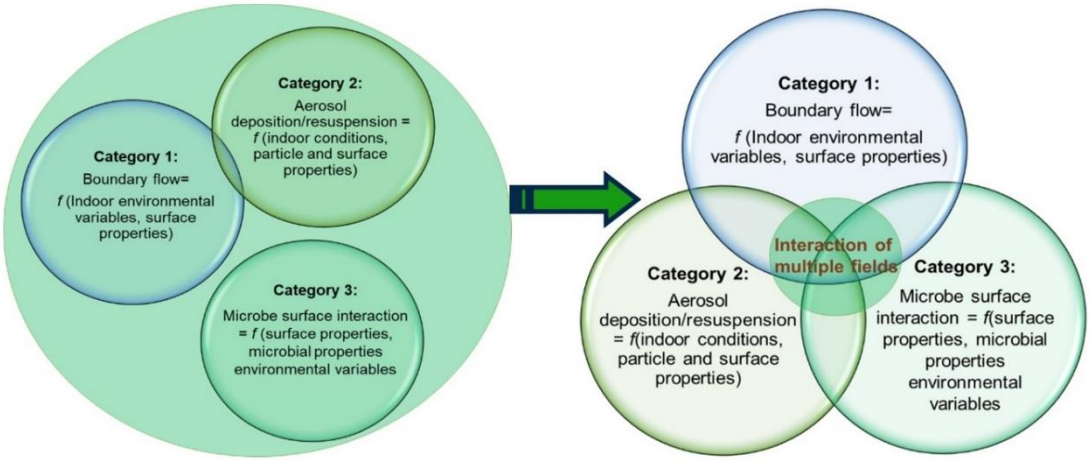


**Figure 4.6**. A schematic representation of the current state and future research directions. *f*: function.

# CHAPTER 5. CHARACTERIZATION AND QUANTIFICATION OF MICROBES – SURFACE – FLOW INTERACTIONS: COMPARSION AMONG ENVELOPED VIRUSES, BACTERIA, AND PROTEIN


## ABSTRACT

The study investigated the influence of surface properties, types of particles, and boundary flow on inorganic and organic particles' attachment and detachment. The experiments processed in two scopes. Attachment and detachment of particles in the flow system using QCM-D experiment (the first scope) and in the static system using centrifugal assay (the second scope). Four particles were selected, vaccinia virus (VACV), measles virus (MV), *Corynebacterium* sp., and bovine serum albumin (BSA). Four sensor surfaces, gold, $SiO_2$, glass, and stainless-steel, and three indoor surfaces, hickory, stainless-steel, and glass were tested. The adhesion and detachment of organic particles were related to the types of surfaces, types of particles, and the flow rate, but major effect varied. All organic particles formed soft and viscoelastic layers, while inorganic particles formed a very rigid and thin film. The size of particles influenced initial adhesion. During detachment phase, the maximum removal rate was observed at the first stage of detachment phase. Detachment rates increased with increasing flow rate, but particles were not completely removed from surfaces. The layers were more easily removed at low flow rates (Re of the flow was 72.26) if surface shear stress ($\tau_s$) was lower (0.02~0.12 kg/m/s$^2$). If the surface shear stress was

higher than the shear stress ($\tau_s \gg \tau_f$) generated due to flow, removal of the particles from the surface did not occur. The boundary flow conditions on the QCMD mimic the conditions on near surfaces in indoor spaces. The results show that some combinations of microbes and surfaces enhance attachment and persist under undisturbed 'flow' conditions.

## 5.1. INTRODUCTION

Spreading infectious microbes in indoors has threaten people sharing the spaces. A recent outbreak of severe acute respiratory syndrome coronavirus 2 (SARS-CoV-2), *i.e.*, COVID-19, has brought out the significance of understanding indoor environments. Before COVID-19, there were global infectious virus problems, severe acute respiratory disease coronavirus 1 (SARS-CoV-1) and middle east respiratory syndrome (MERS). In addition, methicillin-resistance *Staphylococcus aureus* (MRSA) has been reported as a global serious hospital-acquired infection due to their possibility of secondary infection and ease of transmission by contact [11]. A fungal infection caused by *Candida auris* has emerged recently due to its multidrug resistance [16] and has so far proved to be extremely persistent on surfaces.

A recent study confirmed that the sharing the indoor spaces is a major risk factor for SARS-CoV-2 transmission [23]. Once small droplets containing viral particles released, these viral particles could be transmitted via air and surface contact and survive for 3 hours [264]. One person could infect unusually large number of people sharing a space through both air and fomite transfer [24]. One contaminated finger could become a vehicle of virus spreading up to seven clean surfaces and one contaminated surface could infect at least 14 persons by direct contact [25, 26]. Viral particles remained infectious for

8 to 48 hours on household surfaces, such as wood, stainless-steel, plastic, and cloth [265]. Although transmission of infectious microorganisms in indoor spaces have been reported, subsequent microbial fate and transport is not understood. Few studies have explored the influence of indoor conditions and built components on the spatio-temporal distribution of the indoor microbiome [120, 266]. Current findings cannot fully interpret, quantify, and predict microbes – surface interactions particularly in the context of building surfaces and indoor spaces. Based on previous findings in other fields such as the food production or the microchip industry, it is known that microbial adhesion is influenced by microbial characteristics and surface properties. Microbial characteristics include microbial shape, mobility, flexibility, or hydrophilicity [170, 171] and surface properties considered are surface roughness, porosity or contact angle [143, 267, 268]. Studies also do not couple the influence of external forces generated due to boundary flow on the deposition, attachment of microbes to surfaces and subsequently possible detachment. Incorporating diffusive movement of *Bacillus subtilis* into the surface-advective-diffusive mathematical model resulted in a decrease of the concentration of the bacteria by 20% on the surface [269].

This study combines centrifugal assay, Quartz Crystal Microbalance with Dissipation monitoring (QCM-D), and Particle Image Velocimetry (PIV) approaches to assess and compare the influence of boundary flows and surface properties on the interaction of a specific microorganism with selected surfaces. The adhesion behavior of model enveloped viruses, vaccinia virus (VACV) and measles virus (MV) were used as a surrogate of SARS-CoV-2. *Corynebacterium* sp. was selected due to abundance in indoors [109], and bovine serum albumin (BSA) was applied as a control. The objectives are characterization and quantification of microbes – surface interactions and assessment of

the impact of surface properties. Centrifugal experiment was applied to determine interactions between bacteria and indoor surfaces. Impact of surface properties were assessed. QCM-D were applied to determine the adhesion and detachment kinetics on ideal surfaces, the influence of flow rate (external force) on particles adhesion and detachment, and to evaluate the adhered layers' characteristics. Particles' behavior near the surface boundary was observed using Particle Image Velocimetry (PIV).

## 5.2. MATERIALS AND METHODS

### 5.2.1. Surface property measurements

Hickory, stainless-steel, and glass were selected as real indoor surfaces. Three surface properties were measured: surface roughness, contact angle, and porosity. Surface roughness was measured using Scanning Electron Microscope (SEM), TESCAN Vega-3 (TESCAN, CZ). Roughness parameter was calculated by root mean square roughness (RMS), $R_q$ (μm), based on the two-dimensional SEM micrographs [270]. Contact angle was measured to characterize the surface hydrophobicity/hydrophilicity using VCA Optima (AST Prod., Inc., USA). Hydrophilic surface was determined if contact angle was less than 90˚ while contact angle more than 90° was regarded as hydrophobic [271]. Porosity was evaluated using mercury intrusion porosimetry, POREMASTER (Quantachrome Inst., Co., USA).

### 5.2.2. Bacterial and virus preparation

*Corynebacterium* sp. (ATCC 15927) was grown on tryptic soy agar and broth (TSA and TSB). Aliquots of *Corynebacterium* sp. were spread on the TSA plates and incubated

at 37℃ for 16 hours. A single colony was inoculated into the liquid medium (TSB) and incubated overnight at 37℃. The bacterial concentration was quantified using colony-forming units per mL of sample (CFU/mL). *Corynebacterium* sp. in stationary phase was used. Bacterial pellets were precipitated by centrifugation at 4,500 rpm for 10 minutes (Beckman L8-70M) and resuspended in phosphate buffered saline (pH 7.2). The precipitation procedure was performed three times to remove TSB residue [272]. Bacterial suspension was stored at 4℃.

Vero cells were cultured in Dulbecco's Modified Eagle's Medium (DMEM, Corning) supplemented with 10% fetal bovine serum (FBS), 2 mM L-glutamine, 1 mM sodium pyruvate, and 100 U/mL penicillin-streptomycin (HyClone). To prepare a vaccinia virus (VACV) and measles virus (MV) stock, Vero cells were plated in cell culture dishes the day before infection and incubated in a humidified, 5% $CO_2$ incubator at 37℃. When the cells were approximately 80% confluent monolayer, the 10% FBS supplemented medium was changed into 2% FBS supplemented medium, and the cells were then infected with the virus. After several days, the infected cells were harvested and purified. In brief, cell debris was removed by centrifugation at 9,000 rpm for 15 minutes at 4℃ (Sorvall® RC5C plus). The virus pellets were precipitated by centrifugation at 30,000 rpm for 3 hours at 4℃ (Beckman L8-70M) over a 20% sucrose cushion. VACV and MV solution were resuspended in 1 mM Tris buffer (pH 8) and 20 mM citrate-phosphate buffer (pH 7), respectively. Purified virus was obtained through a side-band-pull from a gradient of sucrose centrifuged at 13,500 rpm for 40 minutes at 4℃. The viral infectivity was determined by plaque assay. VACV at the concentration of $2.5\times10^5$ PFU/mL and MV at

$1.0\times10^3$ PFU/mL were obtained. To prepare the bovine serum albumin (BSA) solution, BSA was dissolved in MilliQ water with the concentration of 2 mg/mL.

5.2.3. Bacterial adhesion and resuspension: Centrifugal assay

Centrifugal assay was assessed to investigate the bacterial adhesion and resuspension. *Corynebacterium* sp. was used as a target bacterium due to its presence in indoors [273]. *Corynebacterium* sp. at stationary phase was used. Hickory, stainless-steel, and glass were cut into 10 mm by 10 mm size coupons and soaked in 70% ethanol for sterilization. All experiments were performed in a laminar flow hood. The number of bacteria was measured using Beckman Coulter Multisizer 4 (Beckman Coulter, Inc., USA). Centrifugal assay was conducted in two steps. Surface coupons were submerged under *Corynebacterium* sp. suspension for attachment (STEP 1). After a certain adhesion time, they were centrifuged for causing detachment (STEP 2) for 1 min.

5.2.4. Quartz crystal microbalance with dissipation (QCM-D) technique

Quartz crystal microbalance with dissipation (QCM-D) was applied to quantify microbial adhesion and detachment on the specific sensor surfaces. Microbial attachment and detachment test was performed under controlled and closed flow system using a QCM-D device, Q-sense E4 (Biolin Scientific, Sweden). A MasterFlex peristaltic pump (Cole-Parmer, USA) was connected to each QCM-D module. Polished AT-cut 5-MHz quartz crystals coated with four different materials were selected; gold (QSX 301) with surface roughness (RH) < 1 nm, $SiO_2$ (QSX 303) with RH < 1 nm, sodalime-glass (QSX 337) with RH < 20 nm, and stainless-steel (QSX 304) with RH < 1 nm. Each sensor had a diameter of 14 mm and was mounted on each QCM-D module. Sensors were exposed to the particle

suspension at the same time through the peristaltic pump. Temperature in the modules was controlled at 23°C. Before the experiment, all sensors were pre-cleaned with UV/Ozone lights for 10 minutes to remove organic contaminants on the surface. **Figure 5.2** shows a schematic diagram of the QCM-D experimental procedure. Two tests were performed. **Test 1** was conducted to investigate the particle adhesion and detachment at the fixed flow rate. **Test 2** was performed to determine the particle detachment with increasing flow rate. Experimental cycles of the particle adhesion and detachment were proceeded in following steps. (1) MilliQ water was first injected to provide a baseline; (2) Then, particle suspension was injected for adhesion of microbes onto the sensor surfaces at the selected flow rate; (3) in test 1, MilliQ water was entered again to induce detachment of adhered particles on the sensor surfaces. In case of test 2, (3) the flow rate was increased from 100 to 1000 µL/min ($1.7\times10^{-6}$ to $1.7\times10^{-5}$ $m^3/s$), gradually. Three attachment flow rates were assessed in test 1: 50 µL/min ($8.3\times10^{-6}$ $m^3/s$), 100 µL/min ($1.7\times10^{-6}$ $m^3/s$), and 200 µL/min

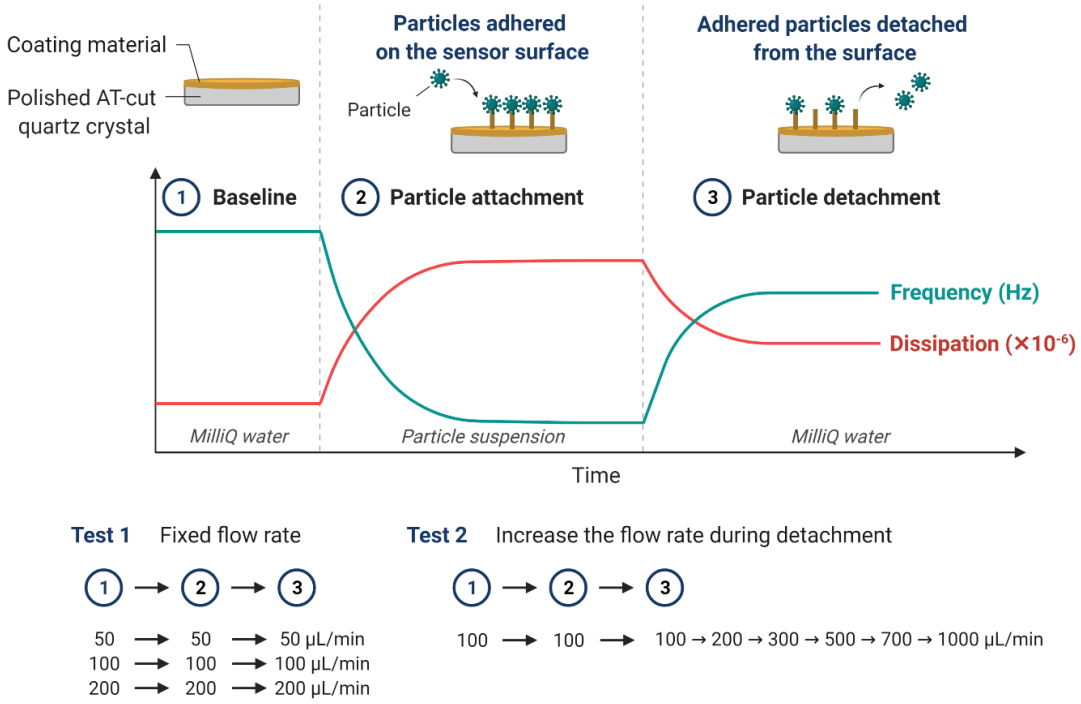


**Figure 5.1.** A schematic diagram of the QCM-D procedure. *Created with BioRender.com*

($3.3\times10^{-6}$ $m^3/s$). For the test 2, attachment flow rate was fixed at 100 µL/min. Transition to the next phase was decided when frequency and dissipation reached and maintained the stabilized status at least 10 minutes. Changes of frequency ($\Delta f$) and dissipation ($\Delta D$) on the sensor crystals were recorded in real-time by QSoft401 software. Obtained data were analyzed using QSense Dfind software (Biolin Scientific, Sweden). The fluid density was estimated to be same as water, 1,000 $kg/m^3$. Each experiment was carried out in triplicate. After and between each experiment QCM-D modules and sensors were cleaned following the cleaning protocols. Modules were sonicated in a 2% (v/v) sodium dodecyl sulfate (SDS) solution for 30 minutes, rinsed with MilliQ water, and dried with $N_2$ gas. Sensor crystals were sonicated in the 2% SDS solution for 20 minutes.

Microbes and BSA adhered on the sensor crystals and form a rigid or viscoelastic film on the sensor surface. Mass change ($\Delta m$) on the sensor crystal causes frequency change ($\Delta f$) and is defined by Sauerbrey relation as follows:

$$\Delta m = -\frac{\Delta f \times c}{n} \qquad \text{Eq. 5.1}$$

where $c$ is 17.7 $ng/Hz/cm^2$ at a resonance frequency (5-MHz), and $n$ is the overtone numbers. The change of dissipation parameter ($D$) is caused due to viscoelastic film adsorption and described as the ratio of dissipated and stored energy [178, 179]. Energy lost during crystal oscillation is calculated using the measured dissipation as follows:

$$D = \frac{E_{diss}}{2\pi E_{strd}} \qquad \text{Eq. 5.2}$$

where $E_{diss}$ is the energy dissipated during one oscillatory cycle and $E_{strd}$ is the energy stored in the oscillation system [180, 181]. Sauerbrey equation shows a linear relationship between mass and frequency changes and is valid for a thin and rigid surface. As overlayers

on the sensor crystal become thick and soft, the relationship is no longer linear, therefore, viscoelastic model needs to be applied [274-277]. The change of dissipation values ($\Delta D$) bigger than $1.0\times10^{-6}$ per 10 Hz indicated that viscoelastic layers were formed on the sensor surface [278, 279]. The film characteristics such as thickness, viscosity and elastic modulus were defined using the Voigt model [280, 281]. The viscoelastic film formation on a sensor crystal is described in **Figure 5.2**. The Voigt model expressed a strong relation between changes of frequency and dissipation and viscoelasticity of the films in a bulk liquid as follows:

$$\Delta f \approx -\frac{1}{2\pi\rho_0 h_0}\left\{\frac{\eta_3}{\delta_3} + h_1\rho_1\omega' - 2h_1\left(\frac{\eta_3}{\delta_3}\right)^2 \frac{\eta_1\omega'^2}{{\mu_1}^2 + \omega'^2{\eta_1}^2}\right\} \qquad \text{Eq. 5.3}$$

$$\Delta D \approx -\frac{1}{\pi f\rho_0 h_0}\left\{\frac{\eta_3}{\delta_3} + 2h_1\left(\frac{\eta_3}{\delta_3}\right)^2 \frac{\eta_1\omega'}{{\mu_1}^2 + \omega'^2{\eta_1}^2}\right\} \qquad \text{Eq. 5.4}$$

where $\rho$ is the density, $h$ is the thickness, $\eta$ is the shear viscosity, $\delta$ is the viscous penetration depth, $\omega'$ is the angular frequency of the oscillation, $\mu$ is the elastic shear modulus, and subscripted numbers indicate the layers' number. The surface shear stress ($\tau_s$) and flow shear stress ($\tau_f$) were defined by the shear rate ($\gamma$) and the shear viscosity ($\eta_2$) and liquid viscosity ($\eta_3$) as follows:

$$\tau_s = \gamma\eta_2 \qquad \text{Eq. 5.5}$$

$$\tau_f = \gamma\eta_3 \qquad \text{Eq. 5.6}$$

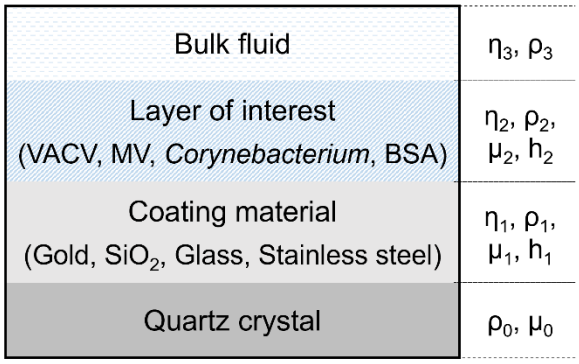


**Figure 5.2.** A schematic diagram of viscoelastic layer on the QCM-D sensor crystal in a bulk liquid.

5.2.5. Particle Image Velocimetry experiments

PIV was applied to investigate the influence of the surface types and ventilation conditions on boundary flow characteristics and microbial deposition. Bacterial deposition characteristics near the carpet, wood, and glass surfaces were investigated. Charge-couple device (CCD) cameras recorded the 2-dimensional spatio-temporal change of microbes. The CCD cameras captured 0.15×0.15 $m^2$ of area of interest. The airflow was seeded with oil droplets (1 μm in diameter). Microbes were sprayed into the chamber (1.2×0.9×0.9 $m^3$) using a collision nebulizer. The plane of interest was illuminated with a Nd:YAG laser (LaVision, Inc., USA). The frictional shear stress ($\tau_{fric}$, kg/m/$s^2$) near the boundary surface was calculated using **Eq. 5.7** [282]. The frictional shear stress near the boundary surface was calculated. These experiments were conducted with bacteria only because the nano-size of the viral particles lead to higher uncertainty in detection and counting using a particle counter.

$$\tau_{fric} = \frac{0.332\rho {u_f}^2}{\sqrt{Re}} \quad \text{Eq. 5.7}$$

where $u_f$ is the velocity of the fluid (m/s) and Re is the Reynolds number.

5.2.6. Statistical analysis

R 3.6.2 and Minitab (Minitab. Inc., USA) were applied. The 2-level factorial design approach was applied to analyze the experiment [283]. All experiments were done in triplicates. Data significance was evaluated at *p*-level of 0.05 using one-way ANOVA.

## 5.3. RESULTS AND DISCUSSIONS

5.3.1. Quantifying microbe-surface adhesion and detachment mechanism using QCM-D

(1) Inorganic and organic particles' characteristics

**Table 5.1** summarized the characteristics of QCM-D sensor crystals and virus, bacteria, and BSA. Surface roughness values of sensor crystals were provided from manufacturer and size of particles, water contact angle ($\theta_w$) and zeta potential were averaged from literature reports. All sensor crystal surfaces were hydrophilic ($\theta_w < 90°$) [284-290]. $SiO_2$ sensor was the most hydrophilic. Gold and stainless-steel (SS) were considered as relatively hydrophobic among the sensors. All sensors and particles were negatively charged at the pH ranges of 7 to 9 [291-294]. Glass was highly negative charged surface while gold surface was weakly negative charged. All particles were also negatively charged, and the values ranged from -16 mV to -36 mV [295-300]. The size of viruses was between 120 to 350 nm. A single elliptical shaped VACV particle had dimensions of 270 nm by 350 nm and a single MV particle, which was spherical shaped, was with diameter

120~250 nm [184, 185, 301]. BSA has the smallest size (7.1 nm) whereas *Corynebacterium* sp. was the largest particle presented in rod-shaped with size ranged from 300 nm to 8000 nm [302, 303].

**Table 5.1.** Surface characteristics of QCM-D sensor crystals and particles, mean±std.

| **Sensor** | **Surface roughness** [a] | **Water contact angle ($\theta_w$)** | **Zeta potential** [b] |
|---|---|---|---|
| Gold | < 1 nm | 67.5±7.5° [284-287] | -29.5±0.7 mV [291, 292] |
| $SiO_2$ | < 1 nm | 15.3±8.7° [284-286] | -51.0 mV [291] |
| Glass | < 20 nm | 27.0±4.2° [288, 289] | -87.0 mV [294] |
| SS | < 1 nm | 56.7±11.4° [286, 288, 290] | -64.8 mV [293] |
| **Particle** | **Size** [c] | **Water contact angle ($\theta_w$)** | **Zeta potential** |
| VACV | 270 nm in D<br>350 nm in L<br>[184, 185] | n.d. [d] | -30 mV [e] |
| MV | 120~250 nm in D [301] | n.d. | -16.0±1.4 mV [295] |
| *Corynebacterium* sp. | 300~800 nm in D<br>1500~8000 nm in L<br>[303] | 87.3±16.6° [299, 304] | -36.5±15.6 mV [296-299] |
| BSA | 7.1 nm [302] | 56.9±21.0° [305, 306] | -20.3±2.1 mV [300] |

[a] provided from manufacturer; [b] measured at pH 7~9 in 1 mM solution; [c] D is diameter and L is length; [d] indicated no data; and [e] measured by the author

5.3.2. Determination of particle adhesion and detachment kinetics via QCM-D

**Figure 5.3** displays the representative plots of $\Delta f$ and $\Delta D$ at the fifth overtone number during adhesion and detachment process with the flow rate of 50 µL/min. All $\Delta f$ and $\Delta D$ values at steady state are detailed in **Table 5.2.** Arrows 1 and 2 indicate the injection of particle suspension and MilliQ water, respectively. The influences of buffer solutions were negligible. When $\Delta f$ and $\Delta D$ stabilized, it was considered that the particle adhesion process reached equilibrium. After that, MilliQ water flow was started to induce

detachment. The inorganic particle, BSA, showed rapid shifts of Δ*f* and Δ*D* for all types of sensor surfaces. Once BSA suspension was exposed to the sensor crystals, both Δ*f* and Δ*D* quickly reached steady states. These rapid changes indicated the rapid adhesion of BSA particles onto surfaces. Previous studies also presented rapid BSA adsorptions on various surfaces [307, 308]. Large shifts in Δ*D* were observed on the organic particles. MV showed the largest shifts in Δ*f* and Δ*D* on all sensor surfaces. Bacteria shows minimum Δ*f*. Unlike BSA adhesion, the organic particles showed slower shifts in Δ*f* and Δ*D* as reported in

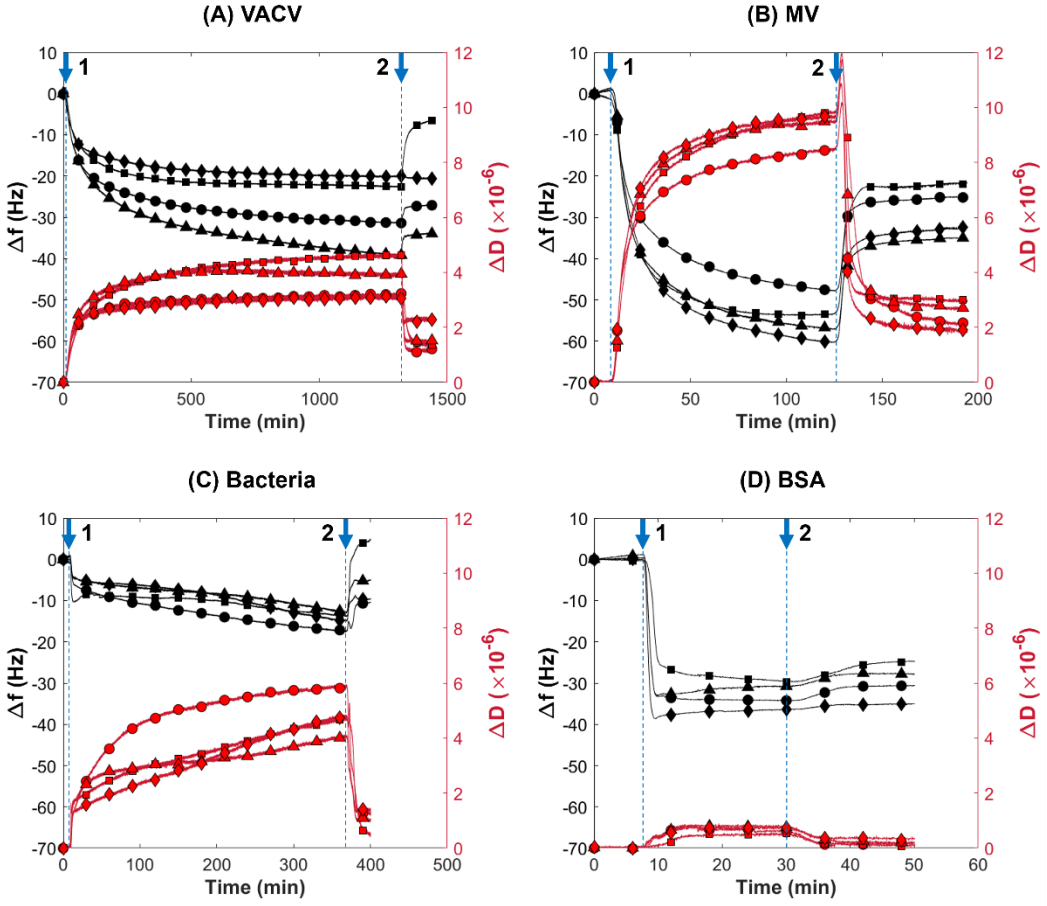


**Figure 5.3.** Frequency (Δ*f*, black, left y-axis) (Hz) and dissipation (Δ*D*, red, right y-axis) ($\times 10^{-6}$) shifts of **(A)** VACV, **(B)** MV, **(C)** bacteria, and **(D)** BSA on four different sensor crystals, gold (●), $SiO_2$ (■), glass (▲), and stainless-steel (♦) at the fixed flow rate of 50 µL/min. The 5$^{th}$ overtones are shown. Blue arrows 1 and 2 indicate injecting suspension (start of attachment phase) and MilliQ water (start of detachment phase), respectively.

organic and inorganic particles behaved differently on the surfaces. After MilliQ water was injected to induce detachment, initial increase in $\Delta f$ and subsequent decrease were observed, however, $\Delta f$ and $\Delta D$ values did not return to zero which indicated that the particles remained on the sensor crystals and the layers were transformed to be thin and rigid.

(1) Initial adhesion duration

As shown in **Figure 5.3**, adhesion duration was dependent on the type of particle. VACV required the longest exposure time (approximately 22 hours) followed by bacteria (6 hours), MV (2 hours) and BSA (0.3 hours). The longest exposure time was observed on the VACV layers on gold and glass surface, while $SiO_2$ and SS surfaces showed 8 hours of exposure time. To investigate the time for the first stage of attachment, adhesion duration was assessed. Adhesion duration in **Figure 5.4** was determined by the ratio of $\Delta D$ and $\Delta f$. The $\Delta D/\Delta f$ values express the structural conformation of layers and the values continuously change as particles are attached, rearranged, and detached. The time taken to adhere during the first stage of attachment was determined by the first $\Delta D/\Delta f$ value. The detailed interpretation of the $\Delta D/\Delta f$ value (slope, K) has been described in the **section 5.3.2(4)** and the $\Delta D/\Delta f$ values used in the current section were $K_{a,1}$. According to the **Figure 5.4**, the first stage of adhesion of VACV and MV was longer than bacteria and BSA. Adhesion durations of MV and BSA were not influenced by the flow rate. Attachment to gold sensors took longer duration for most cases while other surfaces required a similar magnitude of time except for VACV. Hence, the first step of adhesion of bacteria and BSA required a shorter time than that of VACV and MV. These differences could be due to their size differences (**Table 5.1**). Bacteria, which have the largest diameter, easily adhered on the surface probably due to their higher surface area. BSA quickly adhered initially because

they had a higher diffusion rate associated with their much smaller radius [309]. VACV and MV sizes fall in the mid-range and neither factors dominate. MV and BSA appeared to maintain consistent adhesion kinetics regardless of the flow rate.

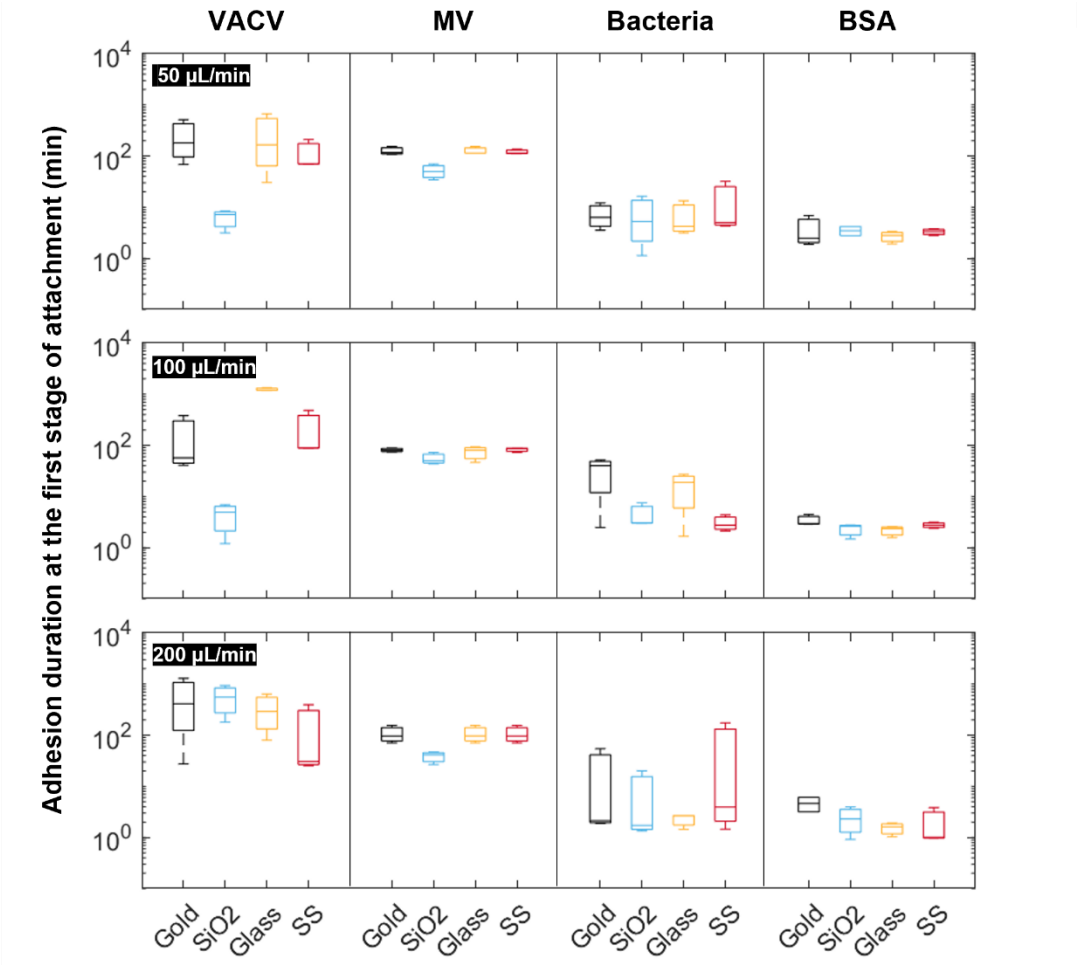


**Figure 5.4.** Adhesion duration (min) at the first stage of attachment shown in log-scaled y-axis.

(2) Test 1: Particle adhesion and detachment at the fixed flow rates

Based on the $\Delta f$ and $\Delta D$ measurements, mass changes on the sensor crystals were calculated using Sauerbrey relation and viscoelastic model. $\Delta D$ of VACV, MV and bacteria (**Figure 5.3)** indicated that these particles formed soft and thick layers on all types of

sensors ($\Delta D$ > $1.0\times10^{-6}$ per 10 Hz), therefore, the viscoelastic model was applied to calculate mass changes ($\Delta m_v$). On the other hand, since $\Delta D$ values of BSA layers were below $1.0\times10^{-6}$ per 10 Hz, Sauerbrey relation was applied ($\Delta m_s$). **Figure 5.5** shows the mass ($\Delta m$) on each sensor crystal and $\Delta m$ values at the steady state have been presented in **Table 5.2**. BSA formed thin and light layers on all types of surfaces (< 150 ng/cm$^2$) as reported in previous studies [308, 310]. BSA formed a thin layer on both hydrophobic and hydrophilic surfaces, however, higher surface coverage and strong adhesion were observed on the hydrophilic surfaces [308, 310]. ANOVA further confirmed that the type of surface did not significantly impact on the BSA mass (*p-value* > 0.05), which could be because all sensor surfaces were hydrophilic ($\theta_w$ < 90°, **Table 5.1**). On the other hand, ANOVA confirmed that the flow rate was significant for BSA attachment (*p-value* < 0.05). Hence, flow rate governed the BSA adhesion regardless of surface type. During the rinsing phase, changes in the BSA mass were small on all sensor crystals. This was probably because BSA formed a firm bond with the sensor surfaces. Most BSA particles' attachment were irreversible and did not resuspend at the tested flow rates, also seen in other investigations [308]. Several researchers also showed difficulties in BSA removal from QCM-D sensors even at the higher temperature (~200°C), higher SDS concentrations or long rinsing time [278, 311]. The mass changes of organic particles ranged from 300 to 4000 ng/cm$^2$. Since higher $\Delta D$ values were observed, it is considered that the organic particles formed soft and viscoelastic multilayers on the sensors (**Figure 5.3**). As described in **Figure 5.5** and **Table 5.2,** VACV formed lighter layers compared to MV and bacteria. The mass of VACV on glass and SS sensors was higher than that on gold and $SiO_2$. The sensor types significantly influenced the VACV mass (*p-value* < 0.05) attached, while the flow rate was a non-

significant variable (*p-value* > 0.05). The highest MV mass (4067.9 ng/cm$^2$) was observed on the gold surface at the flow rate of 50 µL/min. Glass and SS also showed higher MV adhesion. Bacteria showed similar tendencies as MV. Gold, glass, and SS sensor surfaces were covered with thick bacteria layers (> 1985.3 ng/cm$^2$) while bacteria on the $SiO_2$ surface was less than 899.1 ng/cm$^2$. However, the type of sensor and the flow rate were not statistically significant for the MV and bacteria adhesion (*p-value* > 0.05). During the detachment phase, increase in frequency and decrease in dissipation were observed within a short period of time (**Figure 5.3**). Large decreases in $\Delta D$ values on VACV, MV, and bacteria layers demonstrated that loosely attached organic particles were removed and the layers became thin and rigid. However, even when sensor crystals were rinsed with MilliQ water, $\Delta f$ and $\Delta D$ values did not return to zero which indicated that the particles still remained and formed thin layers on the sensor crystals. The highest removal rate was observed for VACV and bacteria layers on $SiO_2$ sensors (0.8±0.1 and 0.8±0.1, respectively)

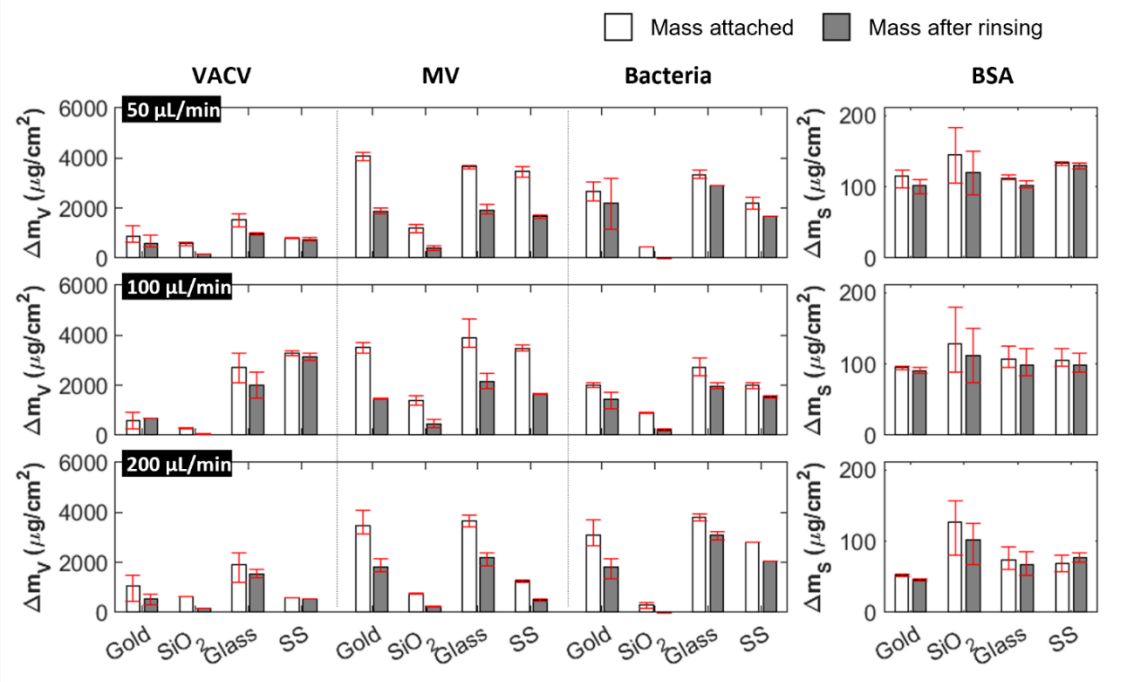


**Figure 5.5.** Mass changes calculated by viscoelastic model ($\Delta m_v$) and Sauerbrey relation ($\Delta m_s$) on each sensor crystal.

**Table 5.2.** Frequency and dissipation shifts and mass change on sensor surfaces

| Flow rate | Particle | VACV | | | | MV | | | |
|---|---|---|---|---|---|---|---|---|---|
| | Sensor | Gold | $SiO_2$ | Glass | SS | Gold | $SiO_2$ | Glass | SS |
| 50 µL/min | $\Delta f$ (Hz) | -28.1±2.8 | -21.9±3.4 | -40.4±7.4 | -24.6±4.4 | -44.8±2.8 | -45.7±7.2 | -56.2±2.2 | -59.8±0.7 |
| | $\Delta D$ ($\times 10^{-6}$) | 3.0±0.2 | 3.8±0.8 | 4.1±0.4 | 4.1±1.5 | 8.0±0.4 | 9.1±0.7 | 9.1±0.3 | 9.2±0.4 |
| | $\Delta m$ [a] ($ng/cm^2$) | 886.8±366.5 | 570.4±92.1 | 1523.9±373.6 | 797.1±52.1 | 4067.9±179.8 | 1184.1±250.4 | 3643.9±89.4 | 3452.2±201.5 |
| | Att rate [b] ($ng/cm^2/min$) | 0.7±0.3 | 1.5±1.4 | 1.1±0.4 | 0.6±0.0 | 31.8±5.3 | 9.0±3.7 | 28.6±5.2 | 27.0±4.7 |
| | Removal rate | 0.3±0.0 | 0.7±0.0 | 0.4±0.1 | 0.1±0.2 | 0.5±0.0 | 0.7±0.0 | 0.5±0.1 | 0.5±0.0 |
| 100 µL/min | $\Delta f$ (Hz) | -22.7±6.6 | -12.7±3.4 | -36.5±2.8 | -30.7±3.6 | -60.7±6.1 | -58.5±9.2 | -64.4±10.7 | -64.7±1.9 |
| | $\Delta D$ ($\times 10^{-6}$) | 3.3±1.6 | 2.0±0.2 | 4.0±0.6 | 5.7±0.7 | 10.1±1.0 | 10.1±0.7 | 10.3±0.5 | 9.8±0.1 |
| | $\Delta m$ [a] ($ng/cm^2$) | 601.1±482.8 | 295.9±28.3 | 2706.7±836.2 | 3268.1±122.7 | 3498.5±292.2 | 1382.4±256.6 | 3909.3±651.4 | 3475.7±168.7 |
| | Att rate ($ng/cm^2/min$) | 0.5±0.4 | 1.8±0.2 | 2.2±0.7 | 2.7±0.1 | 38.7±4.6 | 16.2±4.7 | 45.4±11.2 | 38.3±0.5 |
| | Removal rate | 0.3 | 0.8±0.1 | 0.3±0.0 | 0.0±0.0 | 0.6±0.0 | 0.7±0.1 | 0.4±0.0 | 0.5±0.0 |
| 200 µL/min | $\Delta f$ (Hz) | -26.2±2.7 | -21.7±1.7 | -40.1±5.1 | -23.7±2.8 | -39.1±7.3 | -30.0±7.6 | -47.5±6.8 | -39.1±4.9 |
| | $\Delta D$ ($\times 10^{-6}$) | 2.9±0.1 | 4.4±0.1 | 4.7±0.8 | 2.4±0.1 | 6.9±0.5 | 7.8±0.7 | 8.0±0.6 | 8.1±0.4 |
| | $\Delta m$ [a] ($ng/cm^2$) | 1079.1±549.5 | 614.4 | 1919.7±610.6 | 574.3 | 3496.1±503.2 | 753.5±22.7 | 3665.6±247.3 | 1257.4±65.0 |
| | Att rate ($ng/cm^2/min$) | 0.8±0.4 | 0.4 | 1.4±0.4 | 0.4 | 35.3±17.2 | 7.4±2.8 | 35.4±10.2 | 12.6±6.8 |
| | Removal rate | 0.4±0.1 | 0.7 | 0.3±0.1 | 0.1 | 0.5±0.0 | 0.7±0.1 | 0.4±0.0 | 0.6±0.0 |

[a] Viscoelastic model was applied for VACV, MV, and bacteria; Sauerbrey relation was applied for BSA; [b] attachment rate at the earlier phase of attachment ($K_1$)

**Table 5.2.** Frequency and dissipation shifts and mass change on sensor surfaces (continued)

| Flow rate | Particle | Bacteria | | | | BSA | | | |
|---|---|---|---|---|---|---|---|---|---|
| | Sensor | Gold | $SiO_2$ | Glass | SS | Gold | $SiO_2$ | Glass | SS |
| 50 µL/min | $\Delta f$ (Hz) | -13.6±3.3 | -9.2±3.9 | -14.1±4.0 | -11.8±4.9 | -31.9±4.0 | -40.4±15.3 | -31.4±0.8 | -37.2±0.7 |
| | $\Delta D$ ($\times 10^{-6}$) | 4.3±1.7 | 4.1±1.2 | 3.9±1.0 | 4.1±1.2 | 0.7±0.2 | 0.7±0.2 | 0.7±0.0 | 0.8±0.1 |
| | $\Delta m$ [a] ($ng/cm^2$) | 2666.1±592.6 | 429 | 3313.9±179.2 | 2205.7±313.5 | 114.1±14.2 | 144.5±54.9 | 112.4±3.0 | 133.1±2.5 |
| | Att rate ($ng/cm^2/min$) | 8.1±0.6 | 1.2 | 8.3±3.5 | 6.8±1.8 | 5.3±1.5 | 5.8±1.7 | 5.1±0.8 | 6.1±1.2 |
| | Removal rate | 0.2±0.4 | 0.1 | 0.0±0.2 | 0.1 | 0.1±0.0 | 0.2±0.0 | 0.1±0.0 | 0.0±0.0 |
| 100 µL/min | $\Delta f$ (Hz) | -27.1±0.7 | -37.0±12 | -42.3±3.7 | -26.6±2.0 | -26.4±0.8 | -35.9±13.1 | -29.6±4.6 | -29.4±4.0 |
| | $\Delta D$ ($\times 10^{-6}$) | 5.6±0.7 | 5.8±0.5 | 5.5±0.3 | 5.5±0.0 | 0.5±0.0 | 0.6±0.2 | 0.6±0.0 | 0.6±0.1 |
| | $\Delta m$ [a] ($ng/cm^2$) | 2001.2±107.5 | 899.1±29.0 | 2715.7±354.4 | 1985.3±144.9 | 94.5±2.8 | 128.3±47.0 | 106.0±16.4 | 105.1±14.2 |
| | Att rate ($ng/cm^2/min$) | 5.7±1.2 | 2.7±0.4 | 7.8±2.2 | 5.1±0.3 | 3.3±0.7 | 4.4±1.4 | 3.7±0.8 | 3.7±0.8 |
| | Removal rate | 0.3±0.1 | 0.8±0.1 | 0.3±0.0 | 0.2±0.0 | 0.0±0.0 | 0.1±0.1 | 0.1±0.0 | 0.1±0.0 |
| 200 µL/min | $\Delta f$ (Hz) | -15.3±4.2 | -4.8±1.3 | -17.6±12.7 | -12.2±7.0 | -14.4±0.5 | -35.3±11.4 | -20.7±4.5 | -19.2±4.8 |
| | $\Delta D$ ($\times 10^{-6}$) | 3.5±1.7 | 3.9±2.7 | 3.8±2.4 | 3.9±2.6 | 0.4±0.0 | 0.5±0.2 | 0.4±0.1 | 0.3±0.0 |
| | $\Delta m$ [a] ($ng/cm^2$) | 3105.6±530.3 | 296.3±163.2 | 3804.2±211.6 | 2804.8 | 51.6±1.9 | 126.2±40.9 | 74.1±16.0 | 68.7±17.1 |
| | Att rate ($ng/cm^2/min$) | 105.4±166.4 | 10.0±11.5 | 10.5±9.5 | 12.2 | 2.5±0.8 | 7.8±4.2 | 4.4±1.8 | 3.5±1.9 |
| | Removal rate | 0.4±0.1 | 0 | 0.2±0.0 | 0.3 | 0.1±0.0 | 0.2±0.0 | 0.1±0.0 | -0.1±0.1 |

[a] Viscoelastic model was applied for VACV, MV, and bacteria; Sauerbrey relation was applied for BSA; [b] attachment rate at the earlier phase of attachment ($K_1$)

at the flow rate of 100 µL/min, while VACV mass which adhered on SS sensor did not change significantly at higher flow rates (< 0.1). At least 40% of MV was removed during the detachment phase regardless of the type of sensor and the flow rate.

Virus adhesion on different types of surfaces have been reported in various fields and these studies highlighted the hydrophobic/hydrophilic and electrostatic interactions between virus particles and surfaces. A study found that hydrophobic and electrostatic interactions were major effects of MS2 bacteriophage virus adhesion [312]. Dang *et al*. [231] demonstrated MS2 adhesion process using QCM-D. The virus particles directly interacted with the surface at the earlier stage, and then virus-virus interactions controlled the adhesion kinetics. The authors also showed that negatively charged particles were rapidly and strongly adhered on the oppositely charged surface, while slower and weaker adhesion rates were observed when both particles and surface were negatively charged [231]. Besides virus particles, the characteristics of bacterial cell surface and bacterial adhesion are also related. Hydrophilic bacterial cell surface of *Corynebacterium* sp. ($\theta_w$ = 70.0±3.0°) resulted in the higher mass adhesion on the sensor crystals except for $SiO_2$ surface [304]. Presence of pili or fimbriae on bacterial cell surfaces could prevent a direct interaction between bacteria and surface [313]. According to Ott *et al*. [314], pili formation was not directly associated with the adhesion process. Bacterial motility also impacted on the bacterial adhesion if surface and bacterial species have a similar hydrophobicity and hydrophilicity [315]. *Corynebacterium* sp. has been reported as a non-motile bacterium [316]. Therefore, the effect of the pili presence and motility of *Corynebacterium* sp. could be negligible.

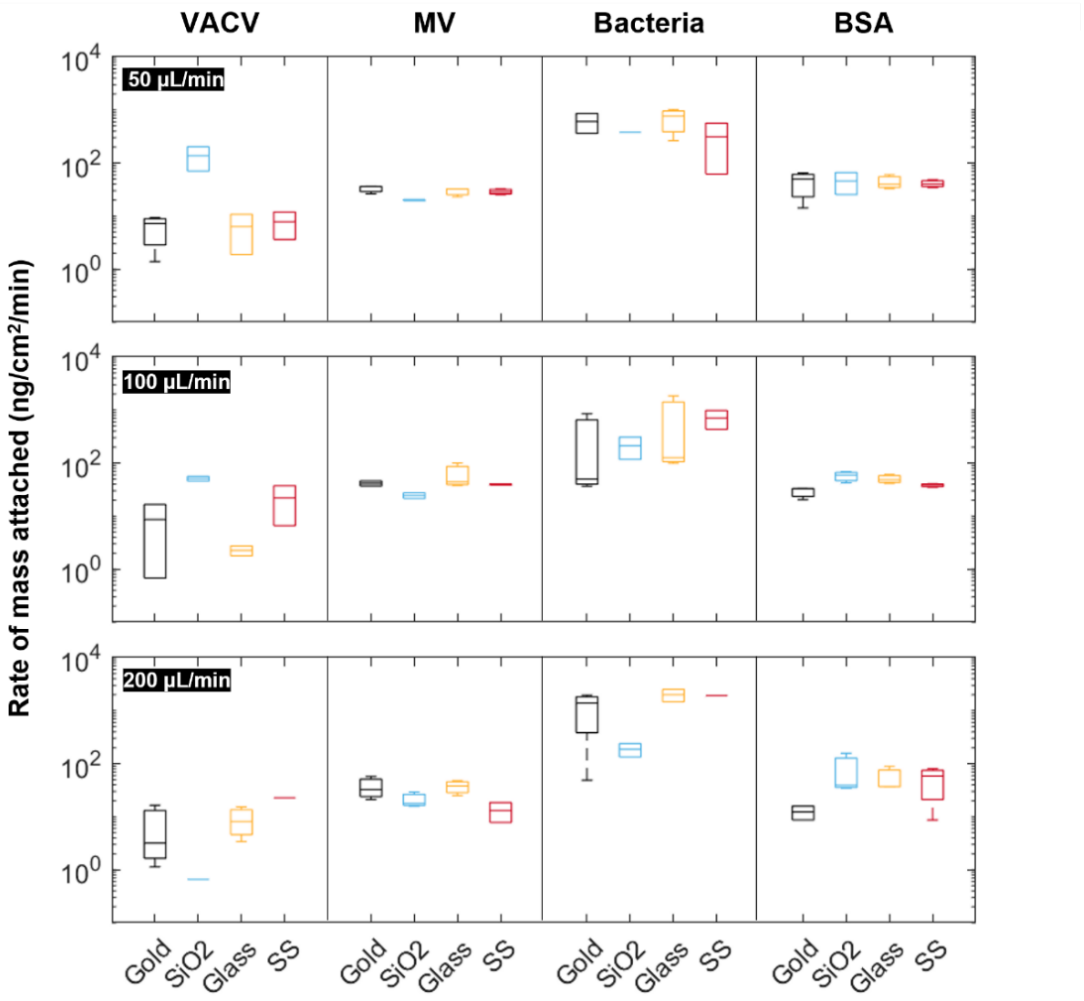


**Figure 5.6.** Rate of mass attached (ng/cm$^2$/min) at the first stage of attachment shown in log-scaled y-axis.

To compare the particle-surface interactions at the earlier attachment stage, the rates of mass attached on each surface are plotted **Figure 5.6**. **Figure 5.6** represents the rate of adhesion (ng/cm$^2$/min) corresponding to the **Figure 5.4**. Bacteria showed the highest attachment rate for the same time period. In accordance with the **Figure 5.4**, MV and BSA had similar attachment rates regardless of the flow rate. VACV rapidly adhered on the $SiO_2$ surface at the lower flow rate while a slower adhesion was observed at higher flow rates. Although some studies reported that the electrostatic interactions between

particles and surfaces highly affected the initial adhesion kinetics [231, 317], this study assessed adhesion mechanism on negatively charged surfaces only, hence effect of electrostatic interactions is neutralized. Indeed, the rate of adhesion during the earlier stages was mostly determined by the type of particle rather than the surface charges.

(3) Test 2: Particle detachment from the surfaces – Effect of the external shear stress

The rinsing flow rates were increased to determine the effect of external forces, *i.e.*, shear stress due to flow, on detachment. Two shear stresses were calculated using **Eqs. 5.5** and **5.6**. Surface shear stress ($\tau_s$) is the interaction between sensor surface and film in direct contact with and flow shear stress ($\tau_f$) indicates the interaction between film and bulk fluid as illustrated in **Figure 5.7**. **Figure 5.8** represents the mass removal rates and the changes of shear stresses during detachment process. The highest decrease in mass was observed on the MV layers during the detachment process. At least 40% of adhered MV were removed from the surface at the first detachment flow rate (100 µL/min). According to Kao *et al.*, round cells weakly interacted with the surface due to a 'point contact' [317]. Therefore, because spherical-shape MV formed a weak bond with the surfaces, MV layers

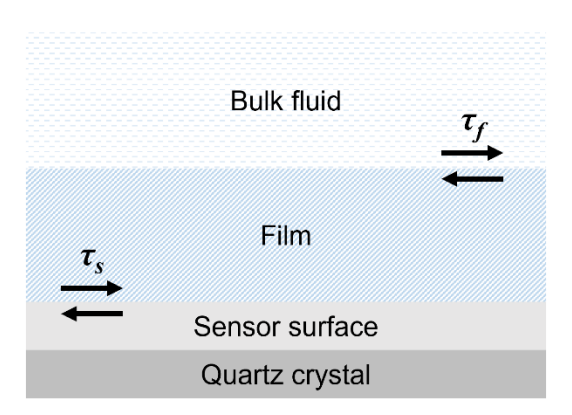


**Figure 5.7.** A schematic diagram of surface ($\tau_s$) and flow shear stress ($\tau_f$).

were easily removed. On the other hand, lower removal rate (less than 40%) of VACV and bacteria could be also attributed to the shape of particles. Rod-shape bacteria and elliptical-shape VACV could provide larger surface contact area, so that stronger bonds between particle and surface could be formed. BSA showed the smallest removal because BSA formed very firm bonds with the surfaces [308].

Initially at the first stage (at a flow rate of 100 μL/min), maximum removal occurred from the sensor surface. Subsequently, slight removal of both organic and inorganic particles occurred from the surface with increasing flow rates. Highest removal rates were seen from $SiO_2$ surface. Most organic particles that adhered on the $SiO_2$ surface were rinsed out due to lower surface shear stress ($\tau_s$) between organic particles and $SiO_2$ surface, as seen in **Figure 5.8(B)**. Higher surface shear stresses were observed on VACV – gold surface, MV – gold surface, and bacteria – SS surface, and removal rate slightly decreased accordingly. It is hypothesized that the layers became relatively static even at the highest flow rates because of the higher surface shear stress ($\tau_s > \tau_f$). Due to the steadiness of the layer, the viscoelastic layers could be reoriented or rearranged by interacting with the bulk fluid, therefore a small increase of mass on the surface could be observed. Unlike the viscoelastic layers, rigid BSA films on $SiO_2$ surface did not respond to the bulk flow and the surface shear stress ($\tau_s$) surpassed the flow shear stress ($\tau_f$). Although the increasing flow rates improved the particle removal from the surfaces, the applied forces created due to only flow were not enough to cause complete detachment and microbes – surface interaction mechanisms dominated.

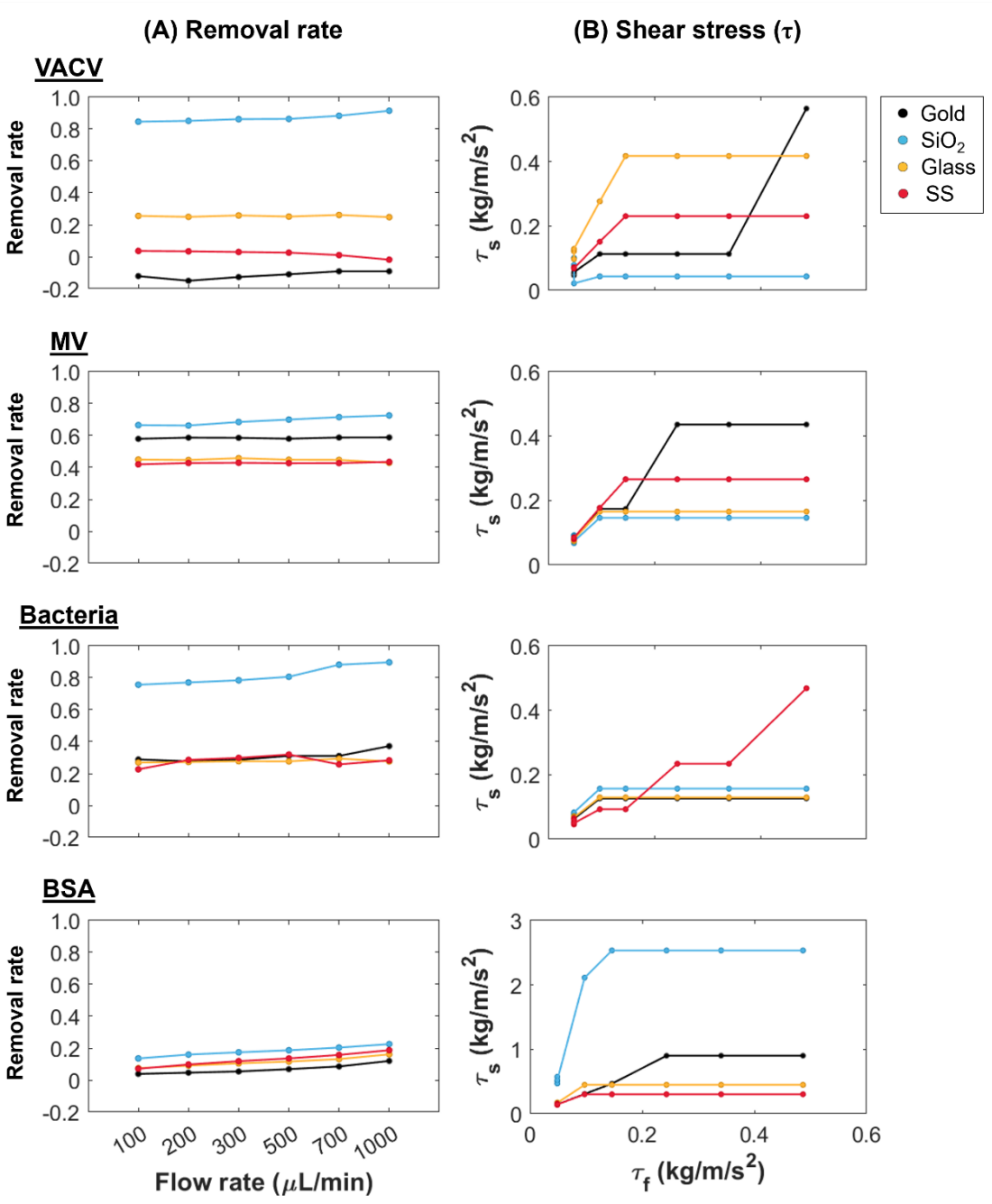


**Figure 5.8. (A)** Removal rates and **(B)** relation between surface ($\tau_s$) and flow shear stress ($\tau_f$).

(4) Structural conformation of the layers

The structural conformation of the organic and inorganic particles on four different sensors was investigated using the Δ*f* against Δ*D* plots. Changes in slope (K-value, ΔD/Δ*f*) represents conformational changes on the surface. Changes from high to low K-values indicate that the layers on the sensor crystals changed from flexible and soft to rigid layers, while the opposite changes demonstrate the increase of layers' viscoelasticity. **Figure 5.9** shows a representative Δ*f*-ΔD plot of VACV on gold sensor. During the attachment phase, two K-values were observed, $K_{a,1}$ and $K_{a,2}$. These values indicated that the VACV structural conformation on the gold surface changed from a soft to rigid layer during attachment. Slope changes during detachment can be interpreted in the same way. During the attachment or detachment, the slopes changed up to four times.

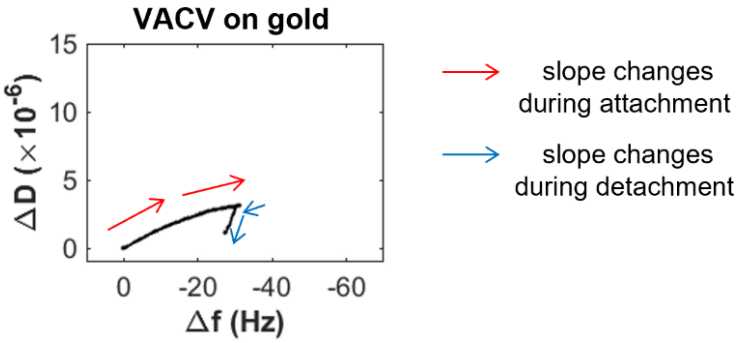


**Figure 5.9.** Slope changes of VACV on gold sensor during attachment and detachment phase. Red and blue lines indicate attachment and detachment, respectively.

K-values at the attachment and detachment phase on different sensors and particles are visualized in **Figure 5.10** and the values are presented in **Table 5.3**. VACV, bacteria and BSA had two or three slope changes ($K_{a,1}$, $K_{a,2}$, and $K_{a,3}$), while MV had one K-value

($K_{a,1}$) during attachment. This indicated MV adhesion was a single adsorption mechanism on the sensor crystals, while others needed two or three adhesion steps. BSA showed the largest decrease in slope, therefore, BSA layers was soft at the initial adhesion process, and then the layers became very rigid. Soft layer formation at the initial process was also observed for VACV and bacteria. While VACV layer was formed, the formation process was different depending on the types of surfaces at the low flow rate, but with increasing flow rate the influence of surface type decreased. MV and bacteria, however, showed similar trends regardless of the flow rates. In detachment process, two to four K-values were calculated ($K_{d,1}$, $K_{d,2}$, $K_{d,3}$, and $K_{d,4}$) in detachment process. The layers were reformed from soft to rigid layers in most of the cases. Slopes kept changing until the layer reached steady state. Same as the attachment process, BSA showed a single detachment process, while the viruses and bacteria needed three changes. Once detachment process started, MV, bacteria and BSA layers shifted from soft to rigid, while VACV layers became flexible at the first K-value change, and then the $K_d$ values decreased.

(5) Principal Component Analysis (PCA)

PCA was applied to gain a better understanding of correlations between variables such as the type of particle, type of sensor, flow rate, and QCM-D outputs including $\Delta f$, $\Delta D$, $\Delta m$, surface viscosity, shear stress, elasticity, and Reynolds number. PCA represents the most relevant information of the data by reducing the number of variables to two principal components. In **Figure 5.11(A)**, two distinct groups were observed, organic particles (VACV, MV, bacteria) and inorganic particles (BSA) which demonstrated differences between the organic and inorganic particles on the sensor surface. It is considered that layers' characteristics of each particle resulted in the formation of these

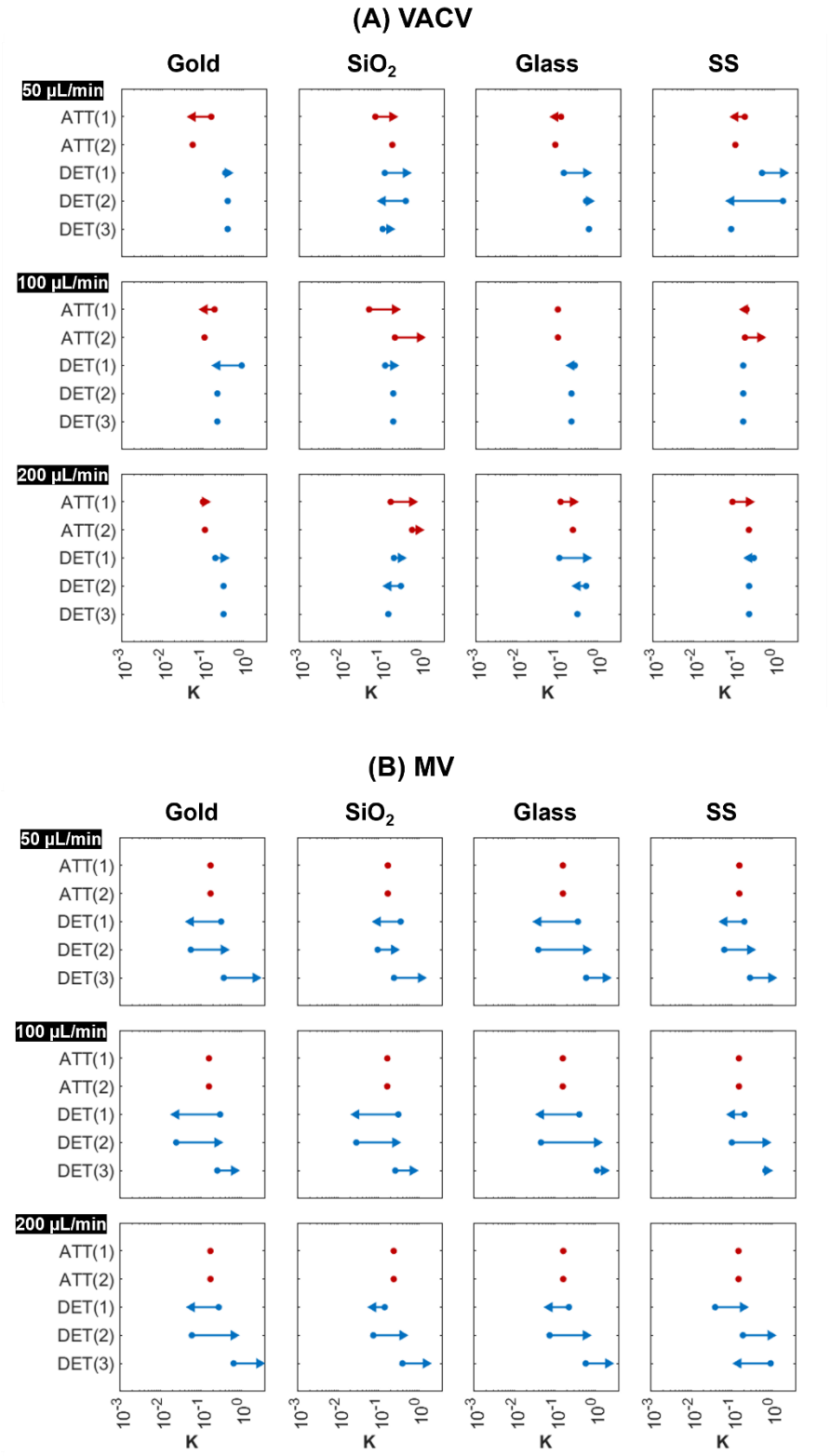


**Figure 5.10.** Visualized slope changes during attachment and detachment. **(A)** VACV, **(B)** MV, **(C)** Bacteria, and **(D)** BSA. Red and blue allows represent the attachment and detachment phase, respectively. The dots indicate there are no more changes.

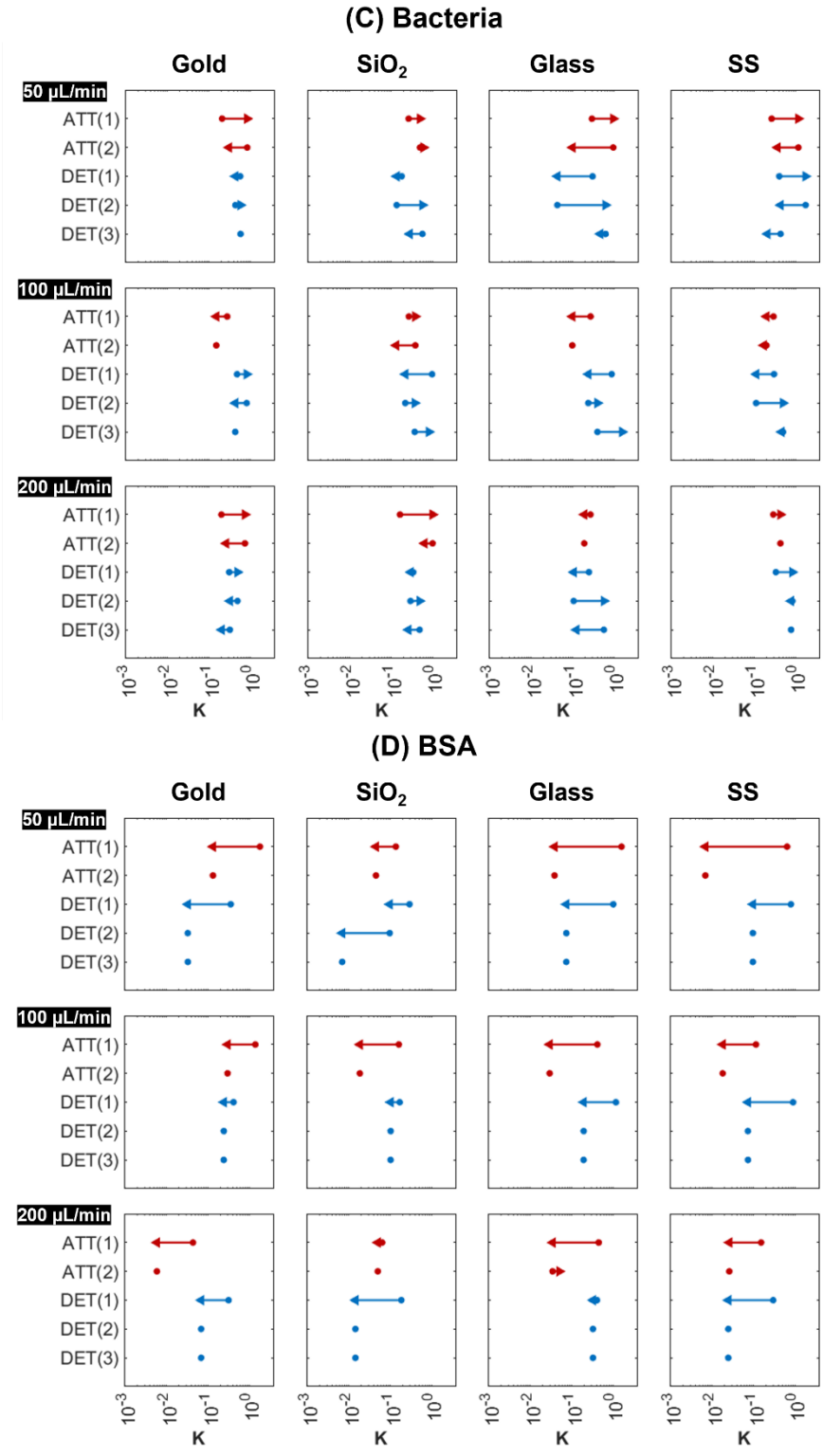


**Figure 5.10.** (continued) Visualized slope changes during attachment and detachment. **(A)** VACV, **(B)** MV, **(C)** Bacteria, and **(D)** BSA. Red and blue allows represent the attachment and detachment phase, respectively. The dots indicate there are no more changes.

**Table 5.3.** Slopes of Δ*f*-Δ*D* plots

| Flow rate | Particle | Sensor | $K_{a,1}$* | $K_{a,2}$ | $K_{a,3}$ | $K_{d,1}$ | $K_{d,2}$ | $K_{d,3}$ | $K_{d,4}$ |
|---|---|---|---|---|---|---|---|---|---|
| 50 µL/min | VACV | Gold | 0.16 | 0.06 | | 0.36 | 0.41 | | |
| | | $SiO_2$ | 0.08 | 0.20 | | 0.13 | 0.43 | 0.12 | 0.17 |
| | | Glass | 0.13 | 0.09 | | 0.15 | 0.53 | 0.62 | |
| | | SS | 0.19 | 0.11 | | 0.50 | 1.65 | 0.09 | |
| | MV | Gold | 0.17 | | | 0.32 | 0.06 | 0.37 | 2.27 |
| | | $SiO_2$ | 0.17 | | | 0.36 | 0.10 | 0.24 | 1.13 |
| | | Glass | 0.16 | | | 0.37 | 0.04 | 0.60 | 1.82 |
| | | SS | 0.15 | | | 0.20 | 0.07 | 0.28 | 0.96 |
| | Bacteria | Gold | 0.21 | 0.84 | 0.31 | 0.57 | 0.44 | 0.58 | |
| | | $SiO_2$ | 0.27 | 0.50 | 0.60 | 0.18 | 0.14 | 0.57 | 0.28 |
| | | Glass | 0.29 | 0.96 | 0.10 | 0.30 | 0.04 | 0.63 | 0.46 |
| | | SS | 0.27 | 1.17 | 0.37 | 0.40 | 1.75 | 0.44 | 0.21 |
| | BSA | Gold | 1.80 | 0.13 | | 0.36 | 0.03 | | 1.80 |
| | | $SiO_2$ | 0.14 | 0.05 | | 0.29 | 0.10 | 0.01 | 0.14 |
| | | Glass | 1.59 | 0.04 | | 1.01 | 0.07 | | 1.59 |
| | | SS | 0.64 | 0.01 | | 0.80 | 0.10 | | 0.64 |
| 100 µL/min | VACV | Gold | 0.20 | 0.11 | | 0.92 | 0.23 | | |
| | | $SiO_2$ | 0.05 | 0.23 | 0.96 | 0.13 | 0.21 | | |
| | | Glass | 0.11 | | | 0.28 | 0.23 | | |
| | | SS | 0.21 | 0.19 | 0.45 | 0.17 | | | |
| | MV | Gold | 0.16 | | | 0.30 | 0.02 | 0.26 | 0.66 |
| | | $SiO_2$ | 0.17 | | | 0.31 | 0.03 | 0.26 | 0.71 |
| | | Glass | 0.16 | | | 0.40 | 0.05 | 1.11 | 1.64 |
| | | SS | 0.15 | | | 0.21 | 0.10 | 0.69 | 0.75 |

**Table 5.3.** Slopes of Δ*f*-Δ*D* plots (continued)

| Flow rate | Particle | Sensor | $K_{a,1}$* | $K_{a,2}$ | $K_{a,3}$ | $K_{d,1}$ | $K_{d,2}$ | $K_{d,3}$ | $K_{d,4}$ |
|---|---|---|---|---|---|---|---|---|---|
| | Bacteria | Gold | 0.28 | 0.15 | | 0.48 | 0.82 | 0.44 | |
| | | $SiO_2$ | 0.27 | 0.38 | 0.13 | 0.97 | 0.22 | 0.37 | 0.82 |
| | | Glass | 0.27 | 0.10 | | 0.88 | 0.24 | 0.40 | 1.57 |
| | | SS | 0.29 | 0.20 | 0.17 | 0.30 | 0.11 | 0.50 | 0.46 |
| | BSA | Gold | 1.39 | 0.30 | | 0.41 | 0.24 | | |
| | | $SiO_2$ | 0.16 | 0.02 | | 0.17 | 0.10 | | |
| | | Glass | 0.42 | 0.03 | | 1.17 | 0.19 | | |
| | | SS | 0.11 | 0.02 | | 0.90 | 0.07 | | |
| 200 µL/min | VACV | Gold | 0.10 | 0.11 | | 0.21 | 0.33 | | 0.10 |
| | | $SiO_2$ | 0.18 | 0.61 | 0.89 | 0.22 | 0.32 | 0.16 | 0.18 |
| | | Glass | 0.12 | 0.25 | | 0.12 | 0.53 | 0.32 | 0.12 |
| | | SS | 0.09 | 0.24 | | 0.31 | 0.24 | | 0.09 |
| | MV | Gold | 0.17 | | | 0.28 | 0.06 | 0.65 | 2.79 |
| | | $SiO_2$ | 0.24 | | | 0.14 | 0.07 | 0.39 | 1.49 |
| | | Glass | 0.16 | | | 0.22 | 0.07 | 0.58 | 2.09 |
| | | SS | 0.15 | | | 0.04 | 0.19 | 0.92 | 0.15 |
| | Bacteria | Gold | 0.20 | 0.75 | 0.26 | 0.31 | 0.49 | 0.32 | 0.20 |
| | | $SiO_2$ | 0.16 | 1.00 | 0.64 | 0.34 | 0.29 | 0.49 | 0.26 |
| | | Glass | 0.27 | 0.19 | | 0.25 | 0.11 | 0.57 | 0.12 |
| | | SS | 0.29 | 0.43 | | 0.34 | 0.84 | 0.78 | |
| | BSA | Gold | 0.04 | 0.01 | | 0.31 | 0.07 | 0.04 | 0.01 |
| | | $SiO_2$ | 0.06 | 0.05 | | 0.19 | 0.01 | 0.06 | 0.05 |
| | | Glass | 0.45 | 0.03 | 0.05 | 0.41 | 0.33 | 0.45 | 0.03 |
| | | SS | 0.15 | 0.03 | | 0.30 | 0.02 | 0.15 | 0.03 |

* $K_{a,i}$: the $i^{th}$ slope during attachment; $K_{d,i}$: the $i^{th}$ slope during detachment

distinct clusters. Organic particles formed soft and thick layers while inorganic particles formed rigid and thin layers. Inorganic particles have the positive effect on PC1 while organic particles have the negative effect on PC1. No distinct separation was observed in terms of PC2. The first principal component accounts for 59.4% and the second principal components accounts for 20.6% of the variation in the data, therefore, the two components represent a cumulative variation of 80.0%. In **Figure 5.11(B),** the two principal components account for 77.7% of the variation in the data. The flow rate showed distinct clusters (shaded in **figure 5.12(C)**) and the flow rate of 200 µL/min has the positive effect of the PC2 while the flow rate less than 100 µL/min have the negative effect of the PC2.

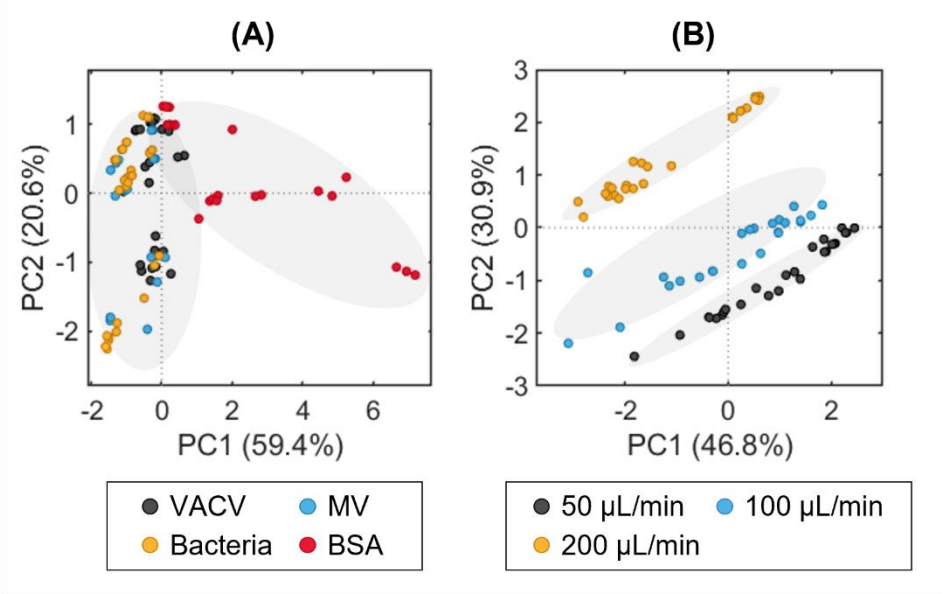


**Figure 5.11.** Principal component analysis (PCA) plots of factor scores on the first and the second principal component (PC1 and PC2). **(A)** organic and inorganic particles (VACV, MV, bacteria, and BSA) and **(B)** flow rates.

5.3.3. Bacterial interaction with ‘real-world’ surface types

**Figure 5.12(A)** shows the change of attachment fraction ($N_{Att}/N_0$). Attachment fractions of *Corynebacterium* sp. for all surfaces were stable after 5 hours of exposure time. Stainless-steel had the highest attachment fraction (0.58) followed by hickory (0.47) and glass (0.35). One-way ANOVA showed that types of surfaces significantly influenced the bacterial attachment (*p-value* < 0.05). *Corynebacterium* sp. attachment greatly varied with contact angle (*p-value* < 0.05) while surface roughness and porosity did not impact the bacterial attachment (*p-value* > 0.05). **Figure 5.12(B)** shows the bacterial detachment fraction corresponding to the attachment. 15% detachment of the bacterial suspension form the stainless-steel surface occurred after centrifuging for 1 minute, which had been exposed to the bacterial suspension for 30 minutes. This is in concordance with the bacterial removal rate (0.15) at the flow rate of 50 µL/min from the QCM-D study. At 2 hours the species had adhered to the surface strongly enough that no detachment was detected. For wood, detachment was negligible after 5 hours. Glass surface behaved differently, with detachment occurring after exposure of the surface to the suspension for more than 8 hours. This could be because that bacterial attachment occurred in layers over time as noticed in the QCM-D studies.

Surface roughness, contact angle, and porosity were measured to quantify the surface properties. Three surface properties were measured: surface roughness, contact angle, and porosity. Hickory had the highest surface roughness, $R_q$, (46.36 µm) followed by stainless-steel (12.04 µm) and glass (6.15 µm). Porosity showed a similar pattern, hickory (63.54%), stainless-steel (35.70%), and glass (13.26%), respectively. The stainless-steel surface was hydrophobic (103.05˚) while hickory (63.02˚) and glass (22.75˚)

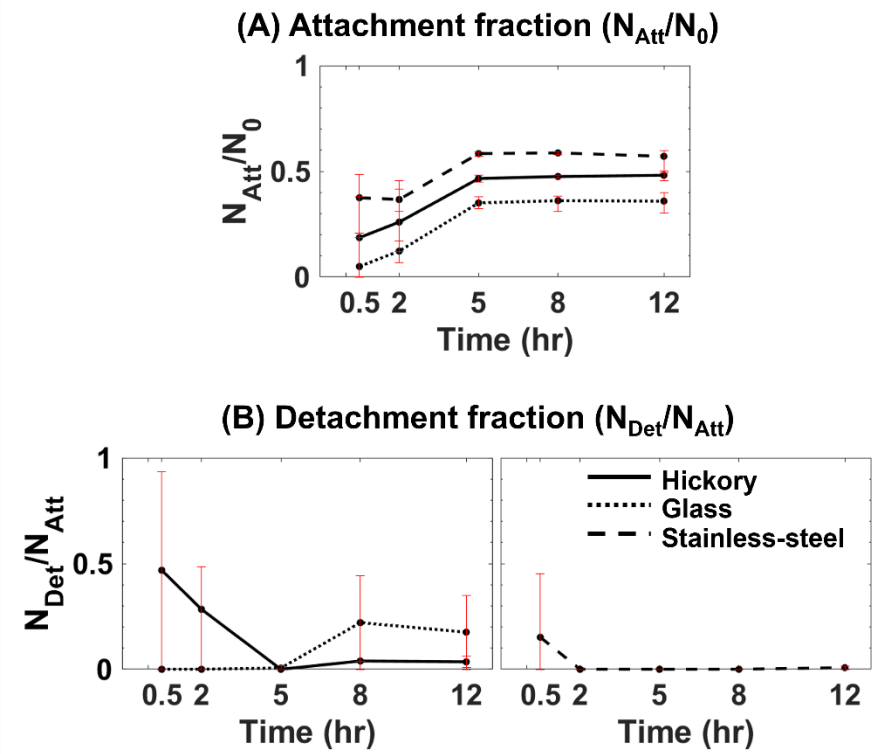


**Figure 5.12. (A)** Change of attachment fraction ($N_{Att}/N_0$) over exposure time and **(B)** Detachment fraction ($N_{Det}/N_{Att}$) of hickory, glass and stainless-steel centrifuged at 1 min.

were hydrophilic. The study showed that surface roughness and porosity did not affect the *Corynebacterium* sp. attachment, while contact angle was significant. Other studies have had similar results where surface roughness did not impact the bacterial adhesion [144, 145]. On the other hand, several researchers have demonstrated the significance of surface roughness [170, 267, 318]. However, these studies focused on the very small range of roughness (0.01~3.30 µm) compared to the current study (6.15~46.36 µm). Higher surface roughness has not been considered in bacterial attachment and detachment studies yet. Unlike previous findings that hydrophilic or lower porosity surfaces (e.g. glass) resulted in more bacterial attachment than hydrophobic or higher porosity surfaces, the current result

showed higher bacterial attachment on hydrophobic surface (e.g. stainless-steel) that porosity was not noticeable [142, 319]. Although studies have been conducted on cell surface properties such as surface hydrophobicity, surface energy or resistance to disinfectants [320, 321], more investigation is required to quantify microbial attachment and detachment as a function of built surface properties.

(2) Particle behaviors near surface boundary

The velocities and bacterial movement near the different surfaces were captured using PIV. The test surfaces were placed in a test chamber where inlet air velocity of 3.6 m/s was maintained. **Figures 5.13** and **5.14(A)** show the velocity magnitude vector plots and the corresponding velocity profiles. The velocity profile represents the u-velocities at a length of 0.067 m in **Figure 5.13**. The change of the number of suspended bacteria was simultaneously monitored (**Figure 5.14(B)**). The number of particles decreased over time due to particle deposition. **Table 5.4** summarized the calculated velocity, Reynolds number, and frictional shear stress ($\tau_{fric}$) from the PIV and QCM-D experiment. In PIV

**Table 5.4.** Physical parameters of PIV and QCM-D

| | **Surface** | **Velocity (m/s)** | **Re** | $\boldsymbol{\tau_{fric}}$ **(kg/m/s$^2$)** |
|---|---|---|---|---|
| PIV | Carpet | 0.009 | 89.06 | $3.43\times10^{-6}$ |
| | Glass | 0.007 | 69.27 | $2.35\times10^{-6}$ |
| | Wood | 0.023 | 227.61 | $1.40\times10^{-5}$ |
| | **Flow rate** | **Velocity (m/s)** | **Re** | $\boldsymbol{\tau_{fric}}$ **(kg/m/s$^2$)** |
| QCM-D | 100 µL/min | 0.005 | 72.26 | $4.89\times10^{-3}$ |
| | 200 µL/min | 0.010 | 144.51 | $1.38\times10^{-2}$ |
| | 300 µL/min | 0.016 | 216.77 | $2.54\times10^{-2}$ |
| | 500 µL/min | 0.026 | 361.29 | $5.47\times10^{-2}$ |
| | 700 µL/min | 0.036 | 505.80 | $9.06\times10^{-2}$ |
| | 1000 µL/min | 0.052 | 722.57 | $1.55\times10^{-1}$ |

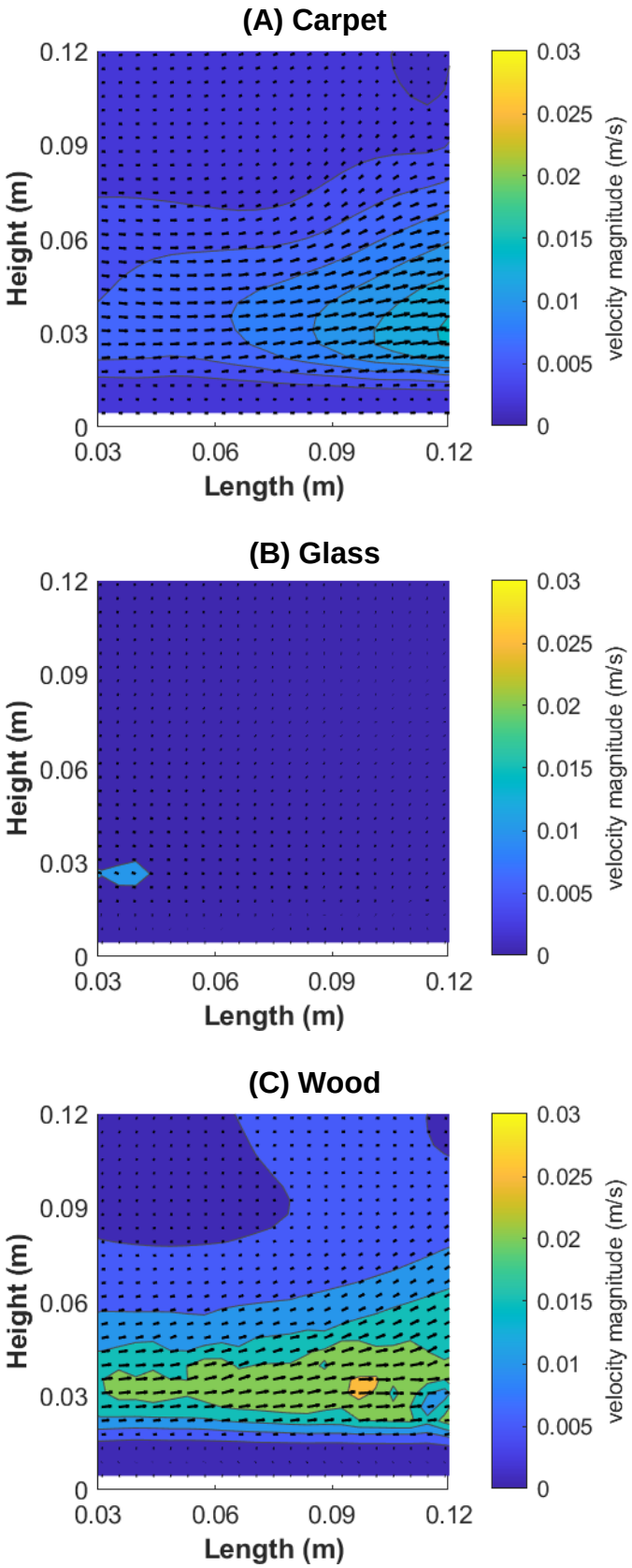


**Figure 5.13.** Velocity magnitude near the **(A)** carpet, **(B)** glass, and **(C)** wood surfaces.

test, lower velocities were measured near the glass surface ($0.7\times10^{-3}$ m/s) compared to the carpet ($0.9\times10^{-3}$ m/s) and wood ($2.3\times10^{-3}$ m/s) surfaces. Reynolds numbers near the surfaces based on PIV measurements were within the ranges of QCM-D tests, while $\tau_{fric}$ near boundary surface were much lower than QMC-D ones. This large differences in $\tau_{fric}$ was observed due to the fluid properties. QCM-D was operated under liquid fluid system with water density of 1,000 kg/m$^3$, while PIV was conducted under gaseous fluid system with air density of 1.204 kg/m$^3$. Higher number of suspending bacteria near the wood surface in **Figure 5.14(B)** indicated that the higher Reynolds number near the surface prevents bacterial deposition and subsequent attachment.

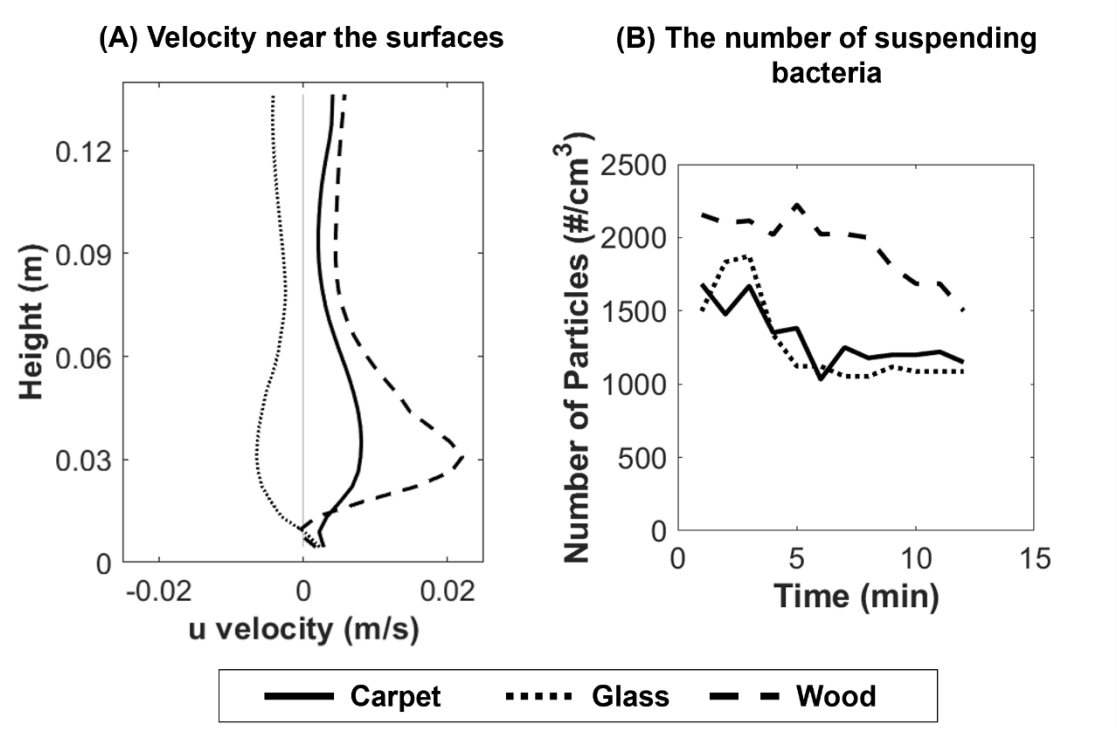


**Figure 5.14. (A)** u-velocity (m/s) near the surfaces and **(B)** the number of suspending bacteria simultaneously monitored during the velocity measurement.

## 5.4. CONCLUSIONS

The study was conducted to assess the adhesion and detachment behavior of model enveloped viruses, VACV and MV, bacteria, and BSA on various types of surfaces using QCM-D. VACV required the longest time to reach an equilibrium status (22 hours) while other particles required less than 6 hours. All organic particles formed soft and flexible layers. The adhesion and detachment of organic particles were related to the type of surface, type of particle, and the flow rate but major effects varied depending on each particle – surface combination. The initial adhesion duration and rates were related to the characteristics of particles rather than surface (substrate) properties and the flow rates. During the adhesion phase, the layers were continuously rearranged and reoriented until steady conditions were reached. These adhesion steps were determined by the type of particles. During the detachment phase, most of the weakly adhered particles were removed from the surface. Increase in removal rate was observed with increasing flow rates. Maximum removal rate was observed at the first stage of detachment process for all sensors and particles. Higher surface shear stress indicated difficulties of particles resuspension. BSA, which forms a very thin layer, had much higher surface shear stress ($\tau_s \gg \tau_f$), so that only 20% of layers were removed. Organic particles on $SiO_2$ surfaces showed very higher removal rate due to lower surface shear stress ($\tau_s$). If surface shear stress of a viscoelastic layer is higher than the flow shear stress ($\tau_s > \tau_f$), the layers could interact with the bulk fluid resulting in a slight increase of mass of layer. Although the increase of flow rates resulted in increased particle removal from the surfaces, the applied forces were not enough to cause complete detachment of microbes.

# CHAPTER 6. CONCLUSIONS AND FUTURE RESEARCH

## 6.1. CONCLUSIONS

The overall objective of this research is characterization of the fate and transport of indoor microbial behavior in air and on surfaces. To understand indoor microbial fate and transport mechanism, the study was conducted in three parts: (1) Determination of relation between microbial characteristics and indoor surrounding conditions, (2) Determination of the impact of occupant characteristic and built air change component on microbial concentration and spatial distribution, and (3) Determination of flow – surface – microbial interactions. This research was the combination of extensive literature review, field sampling, and experimental approaches to inform predictive model development. Specific conclusions of each part are summarized below:

**Part 1.** Determination of relation between microbial characteristics and indoor surrounding conditions

- Presence of specific bacterial family can determine the indoor occupied characteristics. These bacterial family reflects a history of the space, therefore, they could be considered as a bio-fingerprint of the related space.
    - Gender signature: *Coryebacteriaceae* was dominant in male-occupied spaces and *Lactobacillaceae* and *Pseudomonadaceae* indicated female presence.

- Age signature: *Propionibacteriaceae* and *Streptococcaceae* indicated the space was occupied with adult and kid, respectively.
- Building signature: Higher concentrations of *Staphylococcaceae* in air and *Moraxellaceae* on surfaces were related to the hospital buildings. *Enterobacteriaceae* presence indicated non-residence buildings.

- These knowledge on bacteria in built environments could be used as *a priori* information to design, control and manage a healthy and clean environment.

**Part 2.** Determination of the impact of occupant characteristics and built air change components on microbial concentration and spatial distribution.

- PM levels and bacterial concentrations were highly influenced by occupancy.
- There were no relations between fungi concentration and occupant characteristics.
- The occupants' age levels, under or over 10-year-old, were significant on $PM_{10}$ levels and microbial concentrations.
    - Policies to improve indoor air quality need to consider the distinct nature of elementary school.
- Surface contamination varied depending on the types of materials and touch frequency.
    - Higher contamination level was observed on carpet and computer surface, while lower level was observed on metal surfaces.
    - Surface usage dictated the extent of microbial load.
- Distance from the ventilation system, side walls, and floor impacted on bacterial concentration and spatial distribution.

- Outdoor-related bacteria were increased as the distance from the vent increased while indoor-related bacteria were related to the presence of occupant and activity.
- Bacterial concentrations were influenced by the air flow near the walls.

- The study highlighted the significance of identifying occupant characteristics and crucial zones within the indoor space, where the influence of ventilation was limited.

**Part 3.** Determination of flow – surface – microbial interactions.

- This part investigated the adhesion and detachment behavior of VACV, MV, *Corynebacterium* sp., and BSA on different types of surfaces under varying flowrates.
- Microbial attachment kinetics
  - Organic particles formed soft and viscoelastic layers while inorganic particles formed thin and rigid layer.
  - Very small particles or large particles quickly adhered on the surface.
  - Types of surfaces were significant for VACV adhesion.
  - Flow rates were not significant for overall mass attachment of organic particles.
- Microbial detachment kinetics
  - Maximum removal rate was observed at the first stage of detachment. After then, the removal rate was slightly increased with increasing flow rates.
  - Surface shear stress ($\tau_s$) was highly related to the particles' detachment.

- Thin layers showed the minimum removal rate due to much higher surface shear stress than flow shear stress ($\tau_s \gg \tau_f$).
- If viscoelastic layers had higher surface shear stress than the flow shear stress, the layers could be reoriented or rearranged by interacting with the bulk fluid, therefore, a small increase of mass on the surface could be observed.

## 6.2. FUTURE RECOMMENDATIONS

The investigation the current study can be extended to a predictive mathematical model development with following recommendations.

- Determine the influence of airflow on the decay/deposition/transport on bacteria and viruses in indoor spaces as a function of properties describing each microbe.
- Incorporate the data describing adhesion kinetics of pairings of microbe-surface into models.
- Through sensitivity analysis identify dominating characteristics of microbes and surfaces under indoor flow conditions that influence transport, deposition, adhesion and detachment.
- Determine microbial attachment and detachment kinetics in air.

# REFERENCES


[1] S. F. Hayleeyesus and A. M. Manaye, "Microbiological quality of indoor air in university libraries," *Asian Pac. J. Trop. Biomed.*, vol. 4, pp. S312-S317, 2014.

[2] Y. Lv *et al.*, "The influence of ventilation mode and personnel walking behavior on distribution characteristics of indoor particles," *Building and Environment,* vol. 149, pp. 582-591, 2019.

[3] J. Liu *et al.*, "Indoor air quality and occupants' ventilation habits in China: Seasonal measurement and long-term monitoring," *Building and Environment,* 2018.

[4] EPA. "Indoor Air Quality (IAQ)." https://www.epa.gov/indoor-air-quality-iaq (accessed February, 2017).

[5] WHO. "WHO Coronavirus (COVID-19) Dashboard." World Health Organization. https://covid19.who.int/ (accessed November, 2021).

[6] WHO. "Middle East respiratory syndrome coronavirus (MERS-CoV)." https://www.who.int/news-room/fact-sheets/detail/middle-east-respiratory-syndrome-coronavirus-(mers-cov) (accessed November, 2021).

[7] J. Xiao, M. Fang, Q. Chen, and B. He, "SARS, MERS and COVID-19 among healthcare workers: A narrative review," *Journal of Infection and Public Health,* vol. 13, no. 6, pp. 843-848, 2020, doi: 10.1016/j.jiph.2020.05.019.

[8] Y. Liang *et al.*, "Highlight of immune pathogenic response and hematopathologic effect in SARS-CoV, MERS-CoV, and SARS-Cov-2 infection," *Front. Immunol.*, vol. 11, p. 1022, 2020.

[9] "Antibiotic resistance threats in the United States," U.S. Department of Health and Human Services, Centers for Disease Control and Prevention, 2019.

[10] J. L. Zimmermann, T. Shimizu, H. U. Schmidt, Y. F. Li, G. E. Morfill, and G. Isbary, "Test for bacterial resistance build-up against plasma treatment," (in English), *New J. Phys.*, Article vol. 14, p. 16, Jul 2012, Art no. 073037, doi: 10.1088/1367-2630/14/7/073037.

[11] H. Lei, R. M. Jones, and Y. Li, "Exploring surface cleaning strategies in hospital to prevent contact transmission of methicillin-resistant Staphylococcus aureus," *BMC Infect. Dis.*, vol. 17, no. 1, p. 85, 2017.

[12] D. M. Sievert, M. L. Wilson, M. J. Wilkins, B. W. Gillespie, and M. L. Boulton, "Public Health Surveillance for Methicillin-Resistant Staphylococcus aureus: Comparison of Methods for Classifying Health Care- and Community-Associated Infections," (in English), *Am. J. Public Health,* Article vol. 100, no. 9, pp. 1777-1783, Sep 2010, doi: 10.2105/ajph.2009.181958.

[13] R. P. Wenzel, "THE EMERGENCE OF METHICILLIN-RESISTANT STAPHYLOCOCCUS-AUREUS," (in English), *Ann. Intern. Med.,* Editorial Material vol. 97, no. 3, pp. 440-442, 1982, doi: 10.7326/0003-4819-97-3-440.

[14] H. R. Perez, R. Johnson, P. L. Gurian, S. G. Gibbs, J. Taylor, and I. Burstyn, "Isolation of airborne oxacillin-resistant Staphylococcus aureus from culturable air samples of urban residences," *Journal of occupational and environmental hygiene,* vol. 8, no. 2, pp. 80-85, 2011.

[15] A. Gandara, L. C. Mota, C. Flores, H. R. Perez, C. F. Green, and S. G. Gibbs, "Isolation of Staphylococcus aureus and antibiotic-resistant Staphylococcus aureus from residential indoor bioaerosols," *Environmental health perspectives,* vol. 114, no. 12, pp. 1859-1864, 2006.

[16] E. S. Spivak and K. E. Hanson, "Candida auris: an emerging fungal pathogen," *Journal of clinical microbiology,* vol. 56, no. 2, pp. e01588-17, 2018.

[17] CDC. "Candida auris." https://www.cdc.gov/fungal/candida-auris/index.html (accessed 2019).

[18] A. Persily, "Challenges in developing ventilation and indoor air quality standards: The story of ASHRAE Standard 62," *Building and Environment,* vol. 91, pp. 61-69, 2015, doi: 10.1016/j.buildenv.2015.02.026.

[19] P. Spiru and P. L. Simona, "A review on interactions between energy performance of the buildings, outdoor air pollution and the indoor air quality," *Energy Procedia,* vol. 128, pp. 179-186, 2017.

[20] G. Cao *et al.*, "A review of the performance of different ventilation and airflow distribution systems in buildings," *Building and Environment,* vol. 73, pp. 171-186, 2014.

[21] S. Hoque and F. B. Omar, "Coupling Computational Fluid Dynamics Simulations and Statistical Moments for Designing Healthy Indoor Spaces," *International Journal of Environmental Research and Public Health*, vol. 16, no. 5, p. 800, 2019. [Online]. Available: https://www.mdpi.com/1660-4601/16/5/800.

[22] S. Suryawanshi, A. S. Chauhan, R. Verma, and T. Gupta, "Identification and quantification of indoor air pollutant sources within a residential academic campus," *Science of the Total Environment*, vol. 569, pp. 46-52, 2016.

[23] J. G. Allen and L. C. Marr, "Recognizing and controlling airborne transmission of SARS-CoV-2 in indoor environments," *Indoor Air*, vol. 30, no. 4, p. 557, 2020.

[24] J. A. Al-Tawfiq and A. J. Rodriguez-Morales, "Super-spreading events and contribution to transmission of MERS, SARS, and SARS-CoV-2 (COVID-19)," *J. Hosp. Infect.*, vol. 105, no. 2, pp. 111-112, 2020.

[25] J. Barker, I. Vipond, and S. F. Bloomfield, "Effects of cleaning and disinfection in reducing the spread of Norovirus contamination via environmental surfaces," *J. Hosp. Infect.*, vol. 58, no. 1, pp. 42-49, 2004.

[26] F. Rheinbaben, S. Schünemann, T. Gross, and M. Wolff, "Transmission of viruses via contact in ahousehold setting: experiments using bacteriophage φX174 as a model virus," *J. Hosp. Infect.*, vol. 46, no. 1, pp. 61-66, 2000.

[27] S. Lax *et al.*, "Longitudinal analysis of microbial interaction between humans and the indoor environment," (in English), *Science*, Article vol. 345, no. 6200, pp. 1048-1052, Aug 2014, doi: 10.1126/science.1254529.

[28] A. Barberan *et al.*, "The ecology of microscopic life in household dust," (in eng), *Proc. Biol. Sci.*, Research Support, Non-U.S. Gov't

Research Support, U.S. Gov't, Non-P.H.S. vol. 282, no. 1814, Sep 7 2015, doi: 10.1098/rspb.2015.1139.

[29] G. E. Flores *et al.*, "Microbial biogeography of public restroom surfaces," *PLoS One*, vol. 6, no. 11, p. e28132, 2011.

[30] J. C. Luongo, A. Barberán, R. Hacker-Cary, E. E. Morgan, S. L. Miller, and N. Fierer, "Microbial analyses of airborne dust collected from dormitory rooms predict the sex of occupants," *Indoor Air*, vol. 27, no. 2, pp. 338-344, 2017.

[31] S. W. Kembel *et al.*, "Architectural design influences the diversity and structure of the built environment microbiome," *The ISME journal*, vol. 6, no. 8, pp. 1469-1479, 2012.

[32] J. B. Emerson *et al.*, "Impacts of flood damage on airborne bacteria and fungi in homes after the 2013 Colorado Front Range flood," *Environmental science & technology,* vol. 49, no. 5, pp. 2675-2684, 2015.

[33] Z. Fang, C. Gong, Z. Ouyang, P. Liu, L. Sun, and X. Wang, "Characteristic and concentration distribution of culturable airborne bacteria in residential environments in Beijing, China," *Aerosol Air Qual Res,* vol. 14, no. 3, pp. 943-53, 2014.

[34] M. Miletto and S. E. Lindow, "Relative and contextual contribution of different sources to the composition and abundance of indoor air bacteria in residences," *Microbiome,* vol. 3, no. 1, p. 61, 2015.

[35] B. Moen, E. Røssvoll, I. Måge, T. Møretrø, and S. Langsrud, "Microbiota formed on attached stainless steel coupons correlates with the natural biofilm of the sink surface in domestic kitchens," *Canadian Journal of Microbiology,* vol. 62, no. 2, pp. 148-160, 2015.

[36] D. W. Chan, P. H. Leung, C. S. Tam, and A. Jones, "Survey of airborne bacterial genus at a University Campus," *Indoor Built Environ.,* vol. 17, no. 5, pp. 460-466, 2008.

[37] M. Gołofit-Szymczak and R. L. Górny, "Bacterial and fungal aerosols in air-conditioned office buildings in Warsaw, Poland—The winter season," *Int. J. Occup. Saf. Ergonomics,* vol. 16, no. 4, pp. 465-476, 2010.

[38] R. V. C. Rendon, B. C. B. Garcia, and P. G. Vital, "Assessment of airborne bacteria in selected occupational environments in Quezon City, Philippines," *Arch. Environ. Occup. Health,* vol. 72, no. 3, pp. 178-183, 2017.

[39] K. Y. Kim and C. N. Kim, "Airborne microbiological characteristics in public buildings of Korea," *Building and Environment,* vol. 42, no. 5, pp. 2188-2196, 2007.

[40] C. S. Tang, F. F. Chung, M. C. Lin, and G. H. Wan, "Impact of patient visiting activities on indoor climate in a medical intensive care unit: a 1-year longitudinal study," *Am. J. Infect. Control,* vol. 37, no. 3, pp. 183-188, 2009.

[41] K. Y. Kim, Y. S. Kim, and D. Kim, "Distribution characteristics of airborne bacteria and fungi in the general hospitals of Korea," *Ind. Health,* vol. 48, no. 2, pp. 236-243, 2010.

[42] S. C. Verde *et al.*, "Microbiological assessment of indoor air quality at different hospital sites," *Research in Microbiology*, vol. 166, no. 7, pp. 557-563, 2015.

[43] P. Luksamijarulkul and S. Pipitsangjan, "Microbial air quality and bacterial surface contamination in ambulances during patient services," *Oman Med. J.*, vol. 30, no. 2, p. 104, 2015.

[44] E. Hoseinzadeh, M. R. Samarghandie, S. A. Ghiasian, M. Y. Alikhani, and G. Roshanaie, "Evaluation of bioaerosols in five educational hospitals wards air in Hamedan, During 2011-2012," *Jundishapur Journal of Microbiology,* vol. 6, no. 6, 2013.

[45] H. Aydogdu, A. Asan, M. T. Otkun, and M. Ture, "Monitoring of fungi and bacteria in the indoor air of primary schools in Edirne city, Turkey," *Indoor Built Environ.*, vol. 14, no. 5, pp. 411-425, 2005.

[46] H. Aydogdu, A. Asan, and M. T. Otkun, "Indoor and outdoor airborne bacteria in child day-care centers in Edirne City (Turkey), seasonal distribution and influence of meteorological factors," *Environmental Monitoring and Assessment*, vol. 164, no. 1-4, pp. 53-66, 2010.

[47] S.-K. Shin *et al.*, "Metagenomic insights into the bioaerosols in the indoor and outdoor environments of childcare facilities," *PLoS One*, vol. 10, no. 5, p. e0126960, 2015.

[48] W. Deng *et al.*, "Distribution of bacteria in inhalable particles and its implications for health risks in kindergarten children in Hong Kong," *Atmospheric Environment*, vol. 128, pp. 268-275, 2016.

[49] Y.-P. Chen, Y. Cui, and J.-G. Dong, "Variation of airborne bacteria and fungi at Emperor Qin's Terra-Cotta Museum, Xi'an, China, during the “Oct. 1” gold week period of 2006," *Environmental Science and Pollution Research*, vol. 17, no. 2, pp. 478-485, 2010.

[50] A. Niesler *et al.*, "Microbial contamination of storerooms at the Auschwitz-Birkenau Museum," *Aerobiologia*, vol. 26, no. 2, pp. 125-133, 2010.

[51] A. Hoisington, J. Maestre, K. Kinney, and J. A. Siegel, "Characterizing the bacterial communities in retail stores in the United States," *Indoor Air*, vol. 26, no. 6, pp. 857-868, 2016.

[52] S. H. Hwang and J. B. Park, "Comparison of culturable airborne bacteria and related environmental factors at underground subway stations between 2006 and 2013," *Atmospheric Environment,* vol. 84, pp. 289-293, 2014.

[53] Y. Zhai, X. Li, T. Wang, B. Wang, C. Li, and G. Zeng, "A review on airborne microorganisms in particulate matters: composition, characteristics and influence factors," *Environment international,* vol. 113, pp. 74-90, 2018.

[54] D. Hospodsky *et al.*, "Human occupancy as a source of indoor airborne bacteria," *PLoS One,* vol. 7, no. 4, p. e34867, 2012.

[55] R. I. Adams *et al.*, "Chamber bioaerosol study: outdoor air and human occupants as sources of indoor airborne microbes," *PLoS One,* vol. 10, no. 5, p. e0128022, 2015.

[56] S. T. Kelley and J. A. Gilbert, "Studying the microbiology of the indoor environment," *Genome biology,* vol. 14, no. 2, p. 1, 2013.

[57] J. F. Meadow *et al.*, "Indoor airborne bacterial communities are influenced by ventilation, occupancy, and outdoor air source," *Indoor Air,* vol. 24, no. 1, pp. 41-48, 2014.

[58] J. Qian, D. Hospodsky, N. Yamamoto, W. W. Nazaroff, and J. Peccia, "Size-resolved emission rates of airborne bacteria and fungi in an occupied classroom," *Indoor Air,* vol. 22, no. 4, pp. 339-351, 2012.

[59] F. B. Solomon, F. W. Wadilo, A. A. Arota, and Y. L. Abraham, "Antibiotic resistant airborne bacteria and their multidrug resistance pattern at University teaching referral Hospital in South Ethiopia," *Ann. Clin. Microbiol. Antimicrob.,* vol. 16, no. 1, p. 29, 2017.

[60] N. Ikonen *et al.*, "Deposition of respiratory virus pathogens on frequently touched surfaces at airports," *BMC Infect. Dis.*, vol. 18, no. 1, pp. 1-7, 2018.

[61] Y. Li *et al.*, "Role of ventilation in airborne transmission of infectious agents in the built environment–a multidisciplinary systematic review," *Indoor Air,* vol. 17, no. 1, pp. 2-18, 2007.

[62] Z. T. Ai and A. K. Melikov, "Airborne spread of expiratory droplet nuclei between the occupants of indoor environments: A review," (in eng), *Indoor Air,* vol. 28, no. 4, pp. 500-524, Jul 2018, doi: 10.1111/ina.12465.

[63] J. L. Green, "Can bioinformed design promote healthy indoor ecosystems?," *Indoor Air*, vol. 24, no. 2, pp. 113-115, 2014, doi: 10.1111/ina.12090.

[64] F. Weikl *et al.*, "Fungal and bacterial communities in indoor dust follow different environmental determinants," *PLoS One*, vol. 11, no. 4, p. e0154131, 2016.

[65] R. Adams, I., M. Miletto, S. Lindow, E., J. Taylor, W., and T. Bruns, D., "Airborne Bacterial Communities in Residences: Similarities and Differences with Fungi," *PLOSone*, vol. 9, no. 3, pp. e91283 (1-7), 2014.

[66] X. Wang *et al.*, "Associations of dwelling characteristics, home dampness, and lifestyle behaviors with indoor airborne culturable fungi: On-site inspection in 454 Shanghai residences," *Building and Environment*, vol. 102, pp. 159-166, 2016.

[67] S. Lax *et al.*, "Longitudinal analysis of microbial interaction between humans and the indoor environment," *Science*, vol. 345, no. 6200, p. 1048, 2014.

[68] A. J. Prussin and L. C. Marr, "Sources of airborne microorganisms in the built environment," *Microbiome*, vol. 3, no. 1, p. 78, 2015.

[69] P. De Wilde and D. Coley, "The implications of a changing climate for buildings," ed: Elsevier, 2012.

[70] B. Ghosh, H. Lal, R. Kushwaha, N. Hazarika, A. Srivastava, and V. Jain, "Estimation of bioaerosol in indoor environment in the university library of Delhi," *Sustainable Environmental Research*, vol. 23, pp. 199-207, 2013.

[71] P. Chan, P. Yu, Y. Cheng, C. Chan, and P. Wong, "Comprehensive characterization of indoor airborne bacterial profile," *JEnvS*, vol. 21, no. 8, pp. 1148-1152, 2009.

[72] J. F. Meadow *et al.*, "Humans differ in their personal microbial cloud," *PeerJ*, vol. 3, p. e1258, 2015.

[73] L. Bouillard, O. Michel, M. Dramaix, and M. Devleeschouwer, "Bacterial contamination of indoor air, surfaces, and settled dust, and related dust endotoxin concentrations in healthy office buildings," *Annals of Agricultural and Environmental Medicine*, vol. 12, no. 2, pp. 187-192, 2005.

[74] S. Mentese, M. Arisoy, A. Y. Rad, and G. Güllü, "Bacteria and fungi levels in various indoor and outdoor environments in Ankara, Turkey," *Clean–Soil, Air, Water*, vol. 37, no. 6, pp. 487-493, 2009.

[75] E. M. Hartmann *et al.*, "Antimicrobial chemicals are associated with elevated antibiotic resistance genes in the indoor dust microbiome," *Environmental Science & Technology,* vol. 50, no. 18, pp. 9807-9815, 2016.

[76] G. E. Box, W. G. Hunter, and J. S. Hunter, *Statistics for experimenters: an introduction to design, data analysis, and model building*. JSTOR, 1978.

[77] I. Dekio *et al.*, "Detection of potentially novel bacterial components of the human skin microbiota using culture-independent molecular profiling," *Journal of medical microbiology,* vol. 54, no. 12, pp. 1231-1238, 2005.

[78] Z. Gao, C.-h. Tseng, Z. Pei, and M. J. Blaser, "Molecular analysis of human forearm superficial skin bacterial biota," *Proceedings of the National Academy of Sciences*, vol. 104, no. 8, pp. 2927-2932, 2007.

[79] J. Karbowska-Berent, R. L. Górny, A. B. Strzelczyk, and A. Wlazło, "Airborne and dust borne microorganisms in selected Polish libraries and archives," *Building and Environment,* vol. 46, no. 10, pp. 1872-1879, 2011.

[80] K. A. Capone, S. E. Dowd, G. N. Stamatas, and J. Nikolovski, "Diversity of the human skin microbiome early in life," *J. Invest. Dermatol.,* vol. 131, no. 10, pp. 2026-2032, 2011.

[81] L. Oberauner, C. Zachow, S. Lackner, C. Högenauer, K.-H. Smolle, and G. Berg, "The ignored diversity: complex bacterial communities in intensive care units revealed by 16S pyrosequencing," *Sci. Rep.,* vol. 3, p. srep01413, 2013.

[82] N. Mukherjee, S. E. Dowd, A. Wise, S. Kedia, V. Vohra, and P. Banerjee, "Diversity of bacterial communities of fitness center surfaces in a US metropolitan area," *International journal of environmental research and public health,* vol. 11, no. 12, pp. 12544-12561, 2014.

[83] M. Koroglu, S. Gunal, F. Yildiz, M. Savas, A. Ozer, and M. Altindis, "Comparison of keypads and touch-screen mobile phones/devices as potential risk for microbial contamination," *The Journal of Infection in Developing Countries,* vol. 9, no. 12, pp. 1308-1314, 2015.

[84] G. Stellato, A. La Storia, T. Cirillo, and D. Ercolini, "Bacterial biogeographical patterns in a cooking center for hospital foodservice," *Int. J. Food Microbiol.,* vol. 193, pp. 99-108, 2015.

[85] S. Ying *et al.*, "The influence of age and gender on skin-associated microbial communities in urban and rural human populations," *PLoS One,* vol. 10, no. 10, p. e0141842, 2015.

[86] E. K. Costello, C. L. Lauber, M. Hamady, N. Fierer, J. I. Gordon, and R. Knight, "Bacterial community variation in human body habitats across space and time," *Science,* vol. 326, no. 5960, pp. 1694-1697, 2009.

[87] A. C. Jahns and O. A. Alexeyev, "Microbial colonization of normal skin: Direct visualization of 194 skin biopsies," *Anaerobe,* vol. 38, pp. 47-49, 2016.

[88] H. Ayçiçek, H. Aydoğan, A. Küçükkaraaslan, M. Baysallar, and A. C. Başustaoğlu, "Assessment of the bacterial contamination on hands of hospital food handlers," *Food control,* vol. 15, no. 4, pp. 253-259, 2004.

[89] J. F. Meadow, A. E. Altrichter, and J. L. Green, "Mobile phones carry the personal microbiome of their owners," *PeerJ,* vol. 2, p. e447, 2014.

[90] N. Fierer, M. Hamady, C. L. Lauber, and R. Knight, "The influence of sex, handedness, and washing on the diversity of hand surface bacteria," *Proceedings of the National Academy of Sciences,* vol. 105, no. 46, pp. 17994-17999, 2008.

[91] R. I. Adams *et al.*, "Ten questions concerning the microbiomes of buildings," *Building and Environment,* vol. 109, pp. 224-234, 2016.

[92] H. Yuan *et al.*, "Cell concentration, viability and culture composition of airborne bacteria during a dust event in Beijing," *JEnvS,* 2016.

[93] D. Nesa *et al.*, "Comparative performance of impactor air samplers for quantification of fungal contamination," *Journal of Hospital Infection,* vol. 47, no. 2, pp. 149-155, 2001.

[94] J. Madureira, I. Paciência, J. C. Rufo, C. Pereira, J. P. Teixeira, and E. de Oliveira Fernandes, "Assessment and determinants of airborne bacterial and fungal concentrations in different indoor environments: Homes, child day-care centres, primary schools and elderly care centres," *Atmospheric Environment,* vol. 109, pp. 139-146, 2015.

[95] S. Mehr and N. Wood, "Streptococcus pneumoniae–a review of carriage, infection, serotype replacement and vaccination," *Paediatr. Respir. Rev.,* vol. 13, no. 4, pp. 258-264, 2012.

[96] R. R. Dunn, N. Fierer, J. B. Henley, J. W. Leff, and H. L. Menninger, "Home life: factors structuring the bacterial diversity found within and between homes," *PLoS One,* vol. 8, no. 5, p. e64133, 2013.

[97] K. L. O'Brien *et al.*, "Burden of disease caused by Streptococcus pneumoniae in children younger than 5 years: global estimates," *The Lancet,* vol. 374, no. 9693, pp. 893-902, 2009.

[98] D. Miller, D. Hospodsky, S. Gorthala, W. Nazaroff, and J. Peccia, "Seasonal variation of indoor bacterial aerosols in naturally ventilated urban classrooms with high outdoor particulate matter concentrations," 2014.

[99] W. W. Nazaroff, "Embracing microbes in exposure science," (in English), *Journal of Exposure Science and Environmental Epidemiology,* Article vol. 29, no. 1, pp. 1-10, Jan 2019, doi: 10.1038/s41370-018-0075-4.

[100] J. Peccia and S. E. Kwan, "Buildings, Beneficial Microbes, and Health," *Trends Microbiol.,* vol. 24, no. 8, pp. 595-597, Aug 2016, doi: 10.1016/j.tim.2016.04.007.

[101] S. Wilkie, T. Townshend, E. Thompson, and J. Ling, "Restructuring the built environment to change adult health behaviors: a scoping review integrated with behavior change frameworks," *Cities & Health,* vol. 2, no. 2, pp. 198-211, 2018/11/30 2018, doi: 10.1080/23748834.2019.1574954.

[102] A. Singh, M. Syal, S. C. Grady, and S. Korkmaz, "Effects of green buildings on employee health and productivity," (in eng), *Am. J. Public Health,* vol. 100, no. 9, pp. 1665-8, Sep 2010, doi: 10.2105/ajph.2009.180687.

[103] S. W. Kembel *et al.*, "Architectural Design Drives the Biogeography of Indoor Bacterial Communities," *PLoS One,* vol. 9, no. 1, p. e87093, 2014, doi: 10.1371/journal.pone.0087093.

[104] M. Pettenkofer, "XXIX.—Volumetric estimation of atmospheric carbonic acid," *Quarterly Journal of the Chemical Society of London,* 10.1039/QJ8581000292 vol. 10, no. 4, pp. 292-297, 1858, doi: 10.1039/QJ8581000292.

[105] J. Sundell, "On the history of indoor air quality and health," *Indoor air,* vol. 14, no. Suppl 7, pp. 51-58, 2004.

[106] H. Qian, T. Miao, L. Liu, X. Zheng, D. Luo, and Y. Li, "Indoor transmission of SARS-CoV-2," *Indoor Air,* 2020.

[107] G. Z. Brown, J. Kline, G. Mhuireach, D. Northcutt, and J. Stenson, "Making microbiology of the built environment relevant to design," *Microbiome,* vol. 4, no. 1, p. 6, 2016/02/16 2016, doi: 10.1186/s40168-016-0152-7.

[108] P. F. Horve *et al.,* "Building upon current knowledge and techniques of indoor microbiology to construct the next era of theory into microorganisms, health, and the built environment," *J. Expo. Sci. Environ. Epidemiol.,* vol. 30, no. 2, pp. 219-235, 2020/03/01 2020, doi: 10.1038/s41370-019-0157-y.

[109] D. Seong and S. Hoque, "Does the presence of certain bacterial family in the microbiome indicate specific indoor environment characteristics? A factorial design approach for identifying bio-fingerprints," *Indoor Built Environ.,* vol. 29, no. 1, p. 1420326X19853865, 2020, doi: 10.1177/1420326x19853865.

[110] X. Wu, R. C. Nethery, B. M. Sabath, D. Braun, and F. Dominici, "Exposure to air pollution and COVID-19 mortality in the United States," *MedRxiv,* 2020.

[111] K. Mehmood, M. I. Saifullah, and M. M. Abrar, "Can exposure to PM2. 5 particles increase the incidence of coronavirus disease 2019 (COVID-19)?," *The Science of the Total Environment,* 2020.

[112] N. T. Tung *et al.,* "Particulate matter and SARS-CoV-2: a possible model of COVID-19 transmission," *Science of The Total Environment,* vol. 750, p. 141532, 2021.

[113] G. Chen *et al.,* "The impact of ambient fine particles on influenza transmission and the modification effects of temperature in China: a multi-city study," *Environment international,* vol. 98, pp. 82-88, 2017.

[114] H. Chang, S. Kato, and T. Chikamoto, "Effects of outdoor air conditions on hybrid air conditioning based on task/ambient strategy with natural and mechanical ventilation in office buildings," *Building and environment,* vol. 39, no. 2, pp. 153-164, 2004.

[115] J. F. Meadow *et al.,* "Bacterial communities on classroom surfaces vary with human contact," *Microbiome,* vol. 2, no. 1, p. 7, 2014.

[116] J. S. Park, N. Y. Jee, and J. W. Jeong, "Effects of types of ventilation system on indoor particle concentrations in residential buildings," *Indoor Air,* vol. 24, no. 6, pp. 629-638, 2014.

[117] T. Ben-David and M. S. Waring, "Impact of natural versus mechanical ventilation on simulated indoor air quality and energy consumption in offices in fourteen US cities," *Building and Environment,* vol. 104, pp. 320-336, 2016.

[118] Y. Zhao, H. Sun, and D. Tu, "Effect of mechanical ventilation and natural ventilation on indoor climates in Urumqi residential buildings," *Building and Environment,* vol. 144, pp. 108-118, 2018.

[119] D. Wu *et al.*, "On-site investigation of the concentration and size distribution characteristics of airborne fungi in a university library," (in eng), *Environ Pollut,* vol. 261, p. 114138, Jun 2020, doi: 10.1016/j.envpol.2020.114138.

[120] Z. Ma, "A new DTAR (diversity–time–area relationship) model demonstrated with the indoor microbiome," *Journal of Biogeography,* vol. 46, no. 9, pp. 2024-2041, 2019, doi: 10.1111/jbi.13636.

[121] Z. Bakó-Biró, D. J. Clements-Croome, N. Kochhar, H. B. Awbi, and M. J. Williams, "Ventilation rates in schools and pupils' performance," *Building and environment,* vol. 48, pp. 215-223, 2012.

[122] P. Wargocki and D. P. Wyon, "Ten questions concerning thermal and indoor air quality effects on the performance of office work and schoolwork," *Building and Environment,* vol. 112, pp. 359-366, 2017.

[123] M. Turunen, O. Toyinbo, T. Putus, A. Nevalainen, R. Shaughnessy, and U. Haverinen-Shaughnessy, "Indoor environmental quality in school buildings, and the health and wellbeing of students," *International journal of hygiene and environmental health,* vol. 217, no. 7, pp. 733-739, 2014.

[124] U. Haverinen-Shaughnessy, R. J. Shaughnessy, E. C. Cole, O. Toyinbo, and D. J. Moschandreas, "An assessment of indoor environmental quality in schools and its association with health and performance," *Building and Environment,* vol. 93, pp. 35-40, 2015.

[125] R. Kishi *et al.*, "Indoor environmental pollutants and their association with sick house syndrome among adults and children in elementary school," *Building and Environment,* vol. 136, pp. 293-301, 2018.

[126] J. Bennett *et al.*, "Sources of indoor air pollution at a New Zealand urban primary school; a case study," *Atmospheric Pollution Research,* vol. 10, no. 2, pp. 435-444, 2019.

[127] C. Pasquarella, O. Pitzurra, and A. Savino, "The index of microbial air contamination," *J. Hosp. Infect.,* vol. 46, no. 4, pp. 241-256, 2000.

[128] D. Seong, R. S. Norman, and S. Hoque, "Influence of indoor conditions on microbial diversity and quantity in schools," in *E3S Web of Conferences,* 2019, vol. 111: EDP Sciences.

[129] S. Bonetta, S. Bonetta, S. Mosso, S. Sampò, and E. Carraro, "Assessment of microbiological indoor air quality in an Italian office building equipped with an HVAC system," *Environmental monitoring and assessment,* vol. 161, no. 1, pp. 473-483, 2010.

[130] J. P. Cabral, "Can we use indoor fungi as bioindicators of indoor air quality? Historical perspectives and open questions," *Science of the total environment,* vol. 408, no. 20, pp. 4285-4295, 2010.

[131] N. H. M. Hussin, L. M. Sann, M. N. Shamsudin, and Z. Hashim, "Characterization of bacteria and fungi bioaerosol in the indoor air of selected primary schools in Malaysia," *Indoor Built Environ.,* vol. 20, no. 6, pp. 607-617, 2011.

[132] H. Salonen *et al.*, "Airborne viable fungi in school environments in different climatic regions–A review," *Atmospheric Environment,* vol. 104, pp. 186-194, 2015.

[133] E. McCrum-Gardner, "Which is the correct statistical test to use?," *British Journal of Oral and Maxillofacial Surgery,* vol. 46, no. 1, pp. 38-41, 2008.

[134] J. Han, M. Kamber, and J. Pei, "Data mining concepts and techniques third edition," *The Morgan Kaufmann Series in Data Management Systems,* vol. 5, no. 4, pp. 83-124, 2011.

[135] R. Shaughnessy and H. Vu, "Particle loadings and resuspension related to floor coverings in chamber and in occupied school environments," *Atmospheric environment,* vol. 55, pp. 515-524, 2012.

[136] K. Slezakova, E. de Oliveira Fernandes, and M. do Carmo Pereira, "Assessment of ultrafine particles in primary schools: Emphasis on different indoor microenvironments," *Environmental pollution,* vol. 246, pp. 885-895, 2019.

[137] P. Pegas *et al.*, "Indoor and outdoor characterisation of organic and inorganic compounds in city centre and suburban elementary schools of Aveiro, Portugal," *Atmospheric Environment,* vol. 55, pp. 80-89, 2012.

[138] F. Amato *et al.*, "Sources of indoor and outdoor PM2.5 concentrations in primary schools," *Science of the Total Environment,* vol. 490, pp. 757-765, 2014.

[139] G. S. Ajmani *et al.*, "Fine particulate matter exposure and olfactory dysfunction among urban-dwelling older US adults," *Environmental research,* vol. 151, pp. 797-803, 2016.

[140] D. Ekmekcioglu and S. S. Keskin, "Characterization of indoor air particulate matter in selected elementary schools in Istanbul, Turkey," *Indoor Built Environ.,* vol. 16, no. 2, pp. 169-176, 2007.

[141] C. P. Hoang, K. A. Kinney, R. L. Corsi, and P. J. Szaniszlo, "Resistance of green building materials to fungal growth," *International Biodeterioration & Biodegradation,* vol. 64, no. 2, pp. 104-113, 2010.

[142] S. Flint, J. Brooks, and P. Bremer, "Properties of the stainless steel substrate, influencing the adhesion of thermo-resistant streptococci," *J. Food Eng.,* vol. 43, no. 4, pp. 235-242, 2000.

[143] M. Fletcher and G. Loeb, "Influence of substratum characteristics on the attachment of a marine pseudomonad to solid surfaces," *Applied and Environmental Microbiology,* vol. 37, no. 1, pp. 67-72, 1979.

[144] L. R. Hilbert, D. Bagge-Ravn, J. Kold, and L. Gram, "Influence of surface roughness of stainless steel on microbial adhesion and corrosion resistance," *International biodeterioration & biodegradation,* vol. 52, no. 3, pp. 175-185, 2003.

[145] F. Riedewald, "Bacterial adhesion to surfaces: the influence of surface roughness," *PDA J. Pharm. Sci. Technol.,* vol. 60, no. 3, pp. 164-171, 2006.

[146] M. D'Orazio *et al.*, "Effects of water absorption and surface roughness on the bioreceptivity of ETICS compared to clay bricks," *Building and environment,* vol. 77, pp. 20-28, 2014.

[147] D. Seong, M. Kingsak, Y. Lin, Q. Wang, and S. Hoque, "Fate and transport of enveloped viruses in indoor built spaces – through understanding vaccinia virus and surface interactions," *Biomaterials Translational,* vol. 2, no. 1, pp. 50-59. doi: 10.3877/cma.j.issn.2096-112X.2021.01.007, 2021, doi: 10.3877/cma.j.issn.2096-112X.2021.01.007.

[148] M. Wang, C.-H. Lin, and Q. Chen, "Advanced turbulence models for predicting particle transport in enclosed environments," *Building and Environment,* vol. 47, pp. 40-49, 2012.

[149] M. H. Weir, T. Shibata, Y. Masago, D. L. Cologgi, and J. B. Rose, "Effect of Surface Sampling and Recovery of Viruses and Non-Spore-Forming Bacteria on a Quantitative Microbial Risk Assessment Model for Fomites," *Environmental Science & Technology,* vol. 50, no. 11, pp. 5945-5952, 2016/06/07 2016, doi: 10.1021/acs.est.5b06275.

[150] C. B. Hall, R. G. Douglas, Jr., and J. M. Geiman, "Possible Transmission by Fomites of Respiratory Syncytial Virus," *The Journal of Infectious Diseases,* vol. 141, no. 1, pp. 98-102, 1980, doi: 10.1093/infdis/141.1.98.

[151] K. H. Chan, J. S. M. Peiris, S. Y. Lam, L. L. M. Poon, K. Y. Yuen, and W. H. Seto, "The Effects of Temperature and Relative Humidity on the Viability of the SARS Coronavirus," (in eng), *Adv. Virol.,* vol. 2011, pp. 734690-734690, 2011, doi: 10.1155/2011/734690.

[152] N. van Doremalen *et al.*, "Aerosol and Surface Stability of SARS-CoV-2 as Compared with SARS-CoV-1," *New England Journal of Medicine,* 2020, doi: 10.1056/NEJMc2004973.

[153] A. W. H. Chin *et al.*, "Stability of SARS-CoV-2 in different environmental conditions," *The Lancet Microbe,* vol. 1, no. 1, p. e10, 2020, doi: 10.1016/S2666-5247(20)30003-3.

[154] K. Azuma, U. Yanagi, N. Kagi, H. Kim, M. Ogata, and M. Hayashi, "Environmental factors involved in SARS-CoV-2 transmission: effect and role of indoor environmental quality in the strategy for COVID-19 infection control," *Environmental Health and Preventive Medicine,* vol. 25, no. 1, p. 66, 2020/11/03 2020, doi: 10.1186/s12199-020-00904-2.

[155] J. Biryukov *et al.*, "Increasing Temperature and Relative Humidity Accelerates Inactivation of SARS-CoV-2 on Surfaces," *mSphere,* vol. 5, no. 4, pp. e00441-20, 2020, doi: 10.1128/mSphere.00441-20.

[156] Y.-C. Chen *et al.*, "SARS in hospital emergency room," (in eng), *Emerging infectious diseases,* vol. 10, no. 5, pp. 782-788, 2004, doi: 10.3201/eid1005.030579.

[157] N. I. Stilianakis and Y. Drossinos, "Dynamics of infectious disease transmission by inhalable respiratory droplets," (in eng), *Journal of the Royal Society, Interface,* vol. 7, no. 50, pp. 1355-1366, 2010, doi: 10.1098/rsif.2010.0026.

[158] J. Wei and Y. Li, "Airborne spread of infectious agents in the indoor environment," (in eng), *Am. J. Infect. Control,* vol. 44, no. 9 Suppl, pp. S102-8, Sep 2 2016, doi: 10.1016/j.ajic.2016.06.003.

[159] L. Liu, Y. Li, P. V. Nielsen, J. Wei, and R. L. Jensen, "Short-range airborne transmission of expiratory droplets between two people," (in eng), *Indoor Air,* vol. 27, no. 2, pp. 452-462, Mar 2017, doi: 10.1111/ina.12314.

[160] "Public Health Recommendations after Travel from Areas with Potential Risk of Exposure to Coronavirus Disease 2019 (COVID-19)." https://www.cdc.gov/coronavirus/2019-ncov/php/risk-assessment.html (accessed March 30, 2020).

[161] S. B. Omer, P. Malani, and C. del Rio, "The COVID-19 Pandemic in the US: A Clinical Update," *JAMA,* 2020, doi: 10.1001/jama.2020.5788.

[162] R. Read, "A choir decided to go ahead with rehearsal. Now dozens of members have COVID-19 and two are dead," in *Los Angeles Times*, *https://www.latimes.com/world-nation/story/2020-03-29/coronavirus-choir-outbreak*, ed, 2020.

[163] G. Correia, L. Rodrigues, M. Gameiro da Silva, and T. Gonçalves, "Airborne route and bad use of ventilation systems as non-negligible factors in SARS-CoV-2 transmission," (in eng), *Med. Hypotheses,* vol. 141, p. 109781, Aug 2020, doi: 10.1016/j.mehy.2020.109781.

[164] G. Morrison, P. S. J. Lakey, J. Abbatt, and M. Shiraiwa, "Indoor boundary layer chemistry modeling," *Indoor Air,* vol. 29, no. 6, pp. 956-967, Nov 2019, doi: 10.1111/ina.12601.

[165] A. C. K. Lai and W. W. Nazaroff, "Modeling indoor particle deposition from turbulent flow onto smooth surfaces," (in English), *Journal of Aerosol Science*, Article vol. 31, no. 4, pp. 463-476, Apr 2000. [Online]. Available: <Go to ISI>://WOS:000085829800006.

[166] G. Ziskind, M. Fichman, and C. Gutfinger, "Effects of shear on particle motion near a surface- application to resuspension," *Journal of Aerosol Science,* vol. 29, no. 3, pp. 323-338, 1998. [Online]. Available: .

[167] A. Goransson and C. Tragardh, "Mechanisms responsible for sub-micron particle deposition in a laminar wall jet," (in English), *Colloid Surf. A-Physicochem. Eng. Asp.*, Article vol. 211, no. 2-3, pp. 133-144, Dec 2002, Art no. Pii s0927-7757(02)00259-5, doi: 10.1016/s0927-7757(02)00259-5.

[168] J. Sjollema, H. J. Busscher, and A. H. Weerkamp, "Deposition of oral streptococci and polystyrene latices onto glass in a parallel plate flow cell," *Biofouling,* vol. 1, no. 2, pp. 101-112, 1988/06/01 1988, doi: 10.1080/08927018809378100.

[169] H. J. Busscher and H. C. van der Mei, "Microbial adhesion in flow displacement systems," (in eng), *Clinical microbiology reviews,* vol. 19, no. 1, pp. 127-41, Jan 2006, doi: 10.1128/cmr.19.1.127-141.2006.

[170] N. Mitik-Dineva *et al.*, "Escherichia coli, Pseudomonas aeruginosa, and Staphylococcus aureus attachment patterns on glass surfaces with nanoscale roughness," *Curr. Microbiol.,* vol. 58, no. 3, pp. 268-273, 2009.

[171] J. S. Kesavan, P. D. Humphreys, J. R. Bottiger, E. R. Valdes, V. K. Rastogi, and C. K. Knox, "Deposition Method, Relative Humidity and Surface Property Effects of Bacterial Spore Reaerosolization via Pulsed Air Jet," *Aerosol Sci. Technol.,* vol. 51, no. 9, pp. 1027-1034, 2017.

[172] D. E. Hruby, L. A. Guarino, and J. R. Kates, "Vaccinia virus replication I. Requirement for the host-cell nucleus," *J. Virol.,* vol. 29, no. 2, pp. 705-715, 1979.

[173] E. J. Mendoza, K. Manguiat, H. Wood, and M. Drebot, "Two Detailed Plaque Assay Protocols for the Quantification of Infectious SARS-CoV-2," *Current Protocols in Microbiology,* vol. 57, no. 1, p. cpmc105, 2020.

[174] J. Lee, J. Jang, D. Akin, C. A. Savran, and R. Bashir, "Real-time detection of airborne viruses on a mass-sensitive device," *Applied Physics Letters,* vol. 93, no. 1, p. 013901, 2008.

[175] T. M. P. Hewa, G. A. Tannock, D. E. Mainwaring, S. Harrison, and J. V. Fecondo, "The detection of influenza A and B viruses in clinical specimens using a quartz crystal microbalance," *J. Virol. Methods,* vol. 162, no. 1-2, pp. 14-21, 2009.

[176] A. Jaiswal, S. Smoukov, M. Poggi, and B. Grzybowski, "Quartz Crystal Microbalance with Dissipation Monitoring (QCM-D): Real-Time Characterization of Nano-Scale Interactions at Surfaces," *Nsti Nanotech 2008,* vol. 1, pp. 855-858, 2008.

[177] F. Höök, M. Rodahl, P. Brzezinski, and B. Kasemo, "Energy dissipation kinetics for protein and antibody− antigen adsorption under shear oscillation on a quartz crystal microbalance," *Langmuir,* vol. 14, no. 4, pp. 729-734, 1998.

[178] J. L. Jordan and E. J. Fernandez, "QCM-D sensitivity to protein adsorption reversibility," *Biotechnology and bioengineering,* vol. 101, no. 4, pp. 837-842, 2008.

[179] M. C. Dixon, "Quartz crystal microbalance with dissipation monitoring: enabling real-time characterization of biological materials and their interactions," *Journal of biomolecular techniques: JBT,* vol. 19, no. 3, p. 151, 2008.

[180] G. Dunér, E. Thormann, and A. Dėdinaitė, "Quartz Crystal Microbalance with Dissipation (QCM-D) studies of the viscoelastic response from a continuously growing grafted polyelectrolyte layer," *Journal of colloid and interface science,* vol. 408, pp. 229-234, 2013.

[181] A. Doliška, V. Ribitsch, K. S. Kleinschek, and S. Strnad, "Viscoelastic properties of fibrinogen adsorbed onto poly (ethylene terephthalate) surfaces by QCM-D," *Carbohydr. Polym.*, vol. 93, no. 1, pp. 246-255, 2013.

[182] K. L. Roberts and G. L. J. T. i. m. Smith, "Vaccinia virus morphogenesis and dissemination," vol. 16, no. 10, pp. 472-479, 2008.

[183] H. L. Kaufman, F. J. Kohlhapp, and A. J. N. r. D. d. Zloza, "Oncolytic viruses: a new class of immunotherapy drugs," vol. 14, no. 9, pp. 642-662, 2015.

[184] Z. S. Guo *et al.*, "Vaccinia virus-mediated cancer immunotherapy: cancer vaccines and oncolytics," vol. 7, no. 1, p. 6, 2019.

[185] J. Dubochet, M. Adrian, K. Richter, J. Garces, and R. J. J. o. v. Wittek, "Structure of intracellular mature vaccinia virus observed by cryoelectron microscopy," vol. 68, no. 3, pp. 1935-1941, 1994.

[186] R. C. Condit, N. Moussatche, and P. J. A. i. v. r. Traktman, "In a nutshell: structure and assembly of the vaccinia virion," vol. 66, pp. 31-124, 2006.

[187] B. Michen and T. J. J. o. a. m. Graule, "Isoelectric points of viruses," vol. 109, no. 2, pp. 388-397, 2010.

[188] P. Roberts, "Efficient removal of viruses by a novel polyvinylidene fluoride membrane filter," *J. Virol. Methods,* vol. 65, no. 1, pp. 27-31, 1997.

[189] M. Cyrklaff *et al.*, "Cryo-electron tomography of vaccinia virus," *Proceedings of the National Academy of Sciences,* vol. 102, no. 8, pp. 2772-2777, 2005.

[190] R. M. Martin *et al.*, "Contact transmission of vaccinia to an infant diagnosed by viral culture and metagenomic sequencing," in *Open forum infectious diseases*, 2020, vol. 7, no. 4: Oxford University Press US, p. ofaa111.

[191] K. Takahashi and S. Fukuzaki, "Cleanability of titanium and stainless steel particles in relation to surface charge aspects," (in English), *Biocontrol Sci.*, Article vol. 13, no. 1, pp. 9-16, Mar 2008, doi: 10.4265/bio.13.9.

[192] T. L. Thatcher, W. A. Fairchild, and W. W. Nazaroff, "Particle Deposition from Natural Convection Enclosure Flow Onto Smooth Surfaces," *Aerosol Sci. Technol.*, vol. 25, no. 4, pp. 359-374, 1996/01/01 1996, doi: 10.1080/02786829608965402.

[193] T. L. Thatcher and D. W. Layton, "Deposition, resuspension, and penetration of particles within a residence," *Atmos. Environ.*, vol. 29, no. 13, p. 1487, 1995.

[194] A. C. Lai, "Particle deposition indoors: a review," (in eng), *Indoor Air*, vol. 12, no. 4, pp. 211-4, Dec 2002, doi: 10.1034/j.1600-0668.2002.01159.x.

[195] B. Zhao and J. Wu, "Particle deposition in indoor environments: Analysis of influencing factors," *J. Hazard. Mater.*, vol. 147, no. 1, pp. 439-448, 2007/08/17/ 2007, doi: https://doi.org/10.1016/j.jhazmat.2007.01.032.

[196] S. Hoque and F. B. Omar, "Coupling Computational Fluid Dynamics Simulations and Statistical Moments for Designing Healthy Indoor Spaces," (in English), *International Journal of Environmental Research and Public Health*, Article vol. 16, no. 5, p. 16, Mar 2019, Art no. 800, doi: 10.3390/ijerph16050800.

[197] S. El Hamdani, K. Limam, M. O. Abadie, and A. Bendou, "Deposition of fine particles on building internal surfaces," *Atmospheric Environment*, vol. 42, no. 39, pp. 8893-8901, 2008/12/01/ 2008, doi: https://doi.org/10.1016/j.atmosenv.2008.09.005.

[198] Y. Wang, A. G. Li, X. W. Fan, S. Y. Lu, and L. Y. Shang, "Effects of Surface Properties of Vertical Textiles Indoors on Particle Deposition: A Small-scale Chamber Study," (in English), *Aerosol Air Qual. Res.*, Article vol. 19, no. 4, pp. 885-895, Apr 2019, doi: 10.4209/aaqr.2018.08.0321.

[199] W. W. Nazaroff, A. J. Gadgil, and C. J. Weschler, *Critique of the use of deposition velocity in modeling indoor air quality*. United States: American Society for Testing and Materials, 1993.

[200] M. Abadie, K. Limam, and F. Allard, "Indoor particle pollution: Effect of wall textures on particle deposition," *Building and Environment*, vol. 36, pp. 821-827, 2001.

[201] A. Lai, C.K. and W. Nazaroff, "Supermicron particle deposition from turbulent chamber flow onto smooth and rough vertical surfaces," *Atmospheric Environment*, vol. 39, pp. 4893-4900, 2005. [Online]. Available: .

[202] L. T. Wong, W. Y. Chan, K. W. Mui, and A. C. K. Lai, "An Experimental and Numerical Study on Deposition of Bioaerosols in a Scaled Chamber," *Aerosol Sci. Technol.*, vol. 44, no. 2, pp. 117-128, 2010/02/01 2010, doi: 10.1080/02786820903426226.

[203] W. M. Whyte and T. Eaton, "Deposition velocities of airborne microbe-carrying particles," 2016.

[204] M. B. Ranade, "Adhesion and Removal of Fine Particles on Surfaces," *Aerosol Sci. Technol.*, vol. 7, no. 2, pp. 161-176, 1987/01/01 1987, doi: 10.1080/02786828708959155.

[205] M. Corn, "The adhesion of solid particles to solid surfaces, I. A review," *J. Air Pollut. Control Assoc.*, vol. 11, no. 11, pp. 523-528, 1961.

[206] M. Corn, "The Adhesion of Solid Particles to Solid Surfaces II," *J. Air Pollut. Control Assoc.*, vol. 11, no. 12, pp. 566-584, 1961/12/01 1961, doi: 10.1080/00022470.1961.10468039.

[207] J. Visser, "PARTICLE ADHESION AND REMOVAL: A REVIEW," *Particulate Science and Technology*, vol. 13, no. 3-4, pp. 169-196, 1995/07/01 1995, doi: 10.1080/02726359508906677.

[208] C. L. C. Tan, S. Gao, B. S. Wee, A. Asa-Awuku, and B. J. R. Thio, "Adhesion of Dust Particles to Common Indoor Surfaces in an Air-Conditioned Environment," *Aerosol Sci. Technol.*, vol. 48, no. 5, pp. 541-551, 2014/05/04 2014, doi: 10.1080/02786826.2014.898835.

[209] H. K. Christenson, "Adhesion and surface energy of mica in air and water," *The Journal of Physical Chemistry*, vol. 97, no. 46, pp. 12034-12041, 1993/11/01 1993, doi: 10.1021/j100148a032.

[210] I. Goldasteh, Y. L. Tian, G. Ahmadi, and A. R. Ferro, "Human induced flow field and resultant particle resuspension and transport during gait cycle," *Building and Environment*, vol. 77, pp. 101-109, Jul 2014, doi: 10.1016/j.buildenv.2014.03.016.

[211] M. E. Mullins, L. P. Michaels, V. Menon, B. Locke, and M. B. Ranade, "Effect of Geometry on Particle Adhesion," *Aerosol Sci. Technol.*, vol. 17, no. 2, pp. 105-118, 1992/01/01 1992, doi: 10.1080/02786829208959564.

[212] M. C. Audry, S. Ramos, and E. Charlaix, "Adhesion between highly rough alumina surfaces: an atomic force microscope study," (in eng), *Journal of colloid and interface science,* vol. 331, no. 2, pp. 371-8, Mar 15 2009, doi: 10.1016/j.jcis.2008.11.050.

[213] B. V. Derhaguin, V. M. Muller, and Y. P. Toporov, "Effect of Contact Deformations on the Adhesion of Particles," *Journal of colloid and interface science,* vol. 53, no. 2, pp. 314-326, 1975.

[214] B. Nasr, G. Ahmadi, A. R. Ferro, and S. Dhaniyala, "A model for particle removal from surfaces with large-scale roughness in turbulent flows," (in English), *Aerosol Sci. Technol.,* Article vol. 54, no. 3, pp. 291-303, Mar 2020, doi: 10.1080/02786826.2019.1692126.

[215] Y. Kim *et al.,* "Effects of relative humidity and particle and surface properties on particle resuspension rates," *Aerosol Sci. Technol.,* vol. 50, no. 4, pp. 339-352, 2016/04/02 2016, doi: 10.1080/02786826.2016.1152350.

[216] R. Jones, H. M. Pollock, J. A. S. Cleaver, and C. S. Hodges, "Adhesion Forces between Glass and Silicon Surfaces in Air Studied by AFM: Effects of Relative Humidity, Particle Size, Roughness, and Surface Treatment," *Langmuir,* vol. 18, no. 21, pp. 8045-8055, 2002/10/01 2002, doi: 10.1021/la0259196.

[217] J. Katainen, M. Paajanen, E. Ahtola, V. Pore, and J. Lahtinen, "Adhesion as an interplay between particle size and surface roughness," *Journal of colloid and interface science,* vol. 304, no. 2, pp. 524-529, 2006/12/15/ 2006, doi: https://doi.org/10.1016/j.jcis.2006.09.015.

[218] K. Bohinc *et al.,* "Metal surface characteristics dictate bacterial adhesion capacity," *Int. J. Adhes. Adhes.,* vol. 68, pp. 39-46, 2016.

[219] Y. H. An and R. J. Friedman, "Concise review of mechanisms of bacterial adhesion to biomaterial surfaces," *J. Biomed. Mater. Res.,* vol. 43, no. 3, pp. 338-348, 1998, doi: 10.1002/(sici)1097-4636(199823)43:3<338::aid-jbm16>3.0.co;2-b.

[220] Y. W. Ji *et al.,* "Comparison of surface roughness and bacterial adhesion between cosmetic contact lenses and conventional contact lenses," (in eng), *Eye & contact lens,* vol. 41, no. 1, pp. 25-33, Jan 2015, doi: 10.1097/icl.0000000000000054.

[221] C. Berne, C. K. Ellison, A. Ducret, and Y. V. Brun, "Bacterial adhesion at the single-cell level," *Nature Reviews Microbiology,* vol. 16, no. 10, pp. 616-627, 2018/10/01 2018, doi: 10.1038/s41579-018-0057-5.

[222] C. K. Bower, J. McGuire, and M. A. Daeschel, "The adhesion and detachment of bacteria and spores on food-contact surfaces," *Trends Food Sci. Technol.,* vol. 7, no. 5, pp. 152-157, 1996/05/01/ 1996, doi: https://doi.org/10.1016/0924-2244(96)81255-6.

[223] B. E. Logan and J. M. Regan, "Microbial fuel cells--challenges and applications," (in eng), *Environ Sci Technol,* vol. 40, no. 17, pp. 5172-80, Sep 1 2006.

[224] R. Jasevicius, R. Baronas, R. Kacianauskas, and R. Simkus, "Numerical modeling of bacterium-surface interaction by applying DEM," in *New Paradigm of Particle Science and Technology, Proceedings of the 7th World Congress on Particle Technology*, vol. 102, W. Ge *et al.* Eds., (Procedia Engineering, 2015, pp. 1408-1414.

[225] M. Katsikogianni and Y. F. Missirlis, "Concise review of mechanisms of bacterial adhesion to biomaterials and of techniques used in estimating bacteria-material interactions," (in eng), *Eur Cell Mater,* vol. 8, pp. 37-57, Dec 7 2004, doi: 10.22203/ecm.v008a05.

[226] X. Zhang, Q. Zhang, T. Yan, Z. Jiang, X. Zhang, and Y. Y. Zuo, "Quantitatively Predicting Bacterial Adhesion Using Surface Free Energy Determined with a Spectrophotometric Method," *Environmental Science & Technology,* vol. 49, no. 10, pp. 6164-6171, 2015/05/19 2015, doi: 10.1021/es5050425.

[227] S. Bayoudh, A. Othmane, L. Mora, and H. Ben Ouada, "Assessing bacterial adhesion using DLVO and XDLVO theories and the jet impingement technique," *Colloids Surf. B. Biointerfaces,* vol. 73, no. 1, pp. 1-9, 2009/10/01/ 2009, doi: https://doi.org/10.1016/j.colsurfb.2009.04.030.

[228] C. J. van Oss, "Hydrophobicity of biosurfaces — Origin, quantitative determination and interaction energies," *Colloids Surf. B. Biointerfaces,* vol. 5, no. 3, pp. 91-110, 1995/11/10/ 1995, doi: https://doi.org/10.1016/0927-7765(95)01217-7.

[229] C. V. Chrysikopoulos and V. I. Syngouna, "Attachment of bacteriophages MS2 and ΦX174 onto kaolinite and montmorillonite: Extended-DLVO interactions," *Colloids Surf. B. Biointerfaces,* vol. 92, pp. 74-83, 2012/04/01/ 2012, doi: https://doi.org/10.1016/j.colsurfb.2011.11.028.

[230] X. Wang, R. Şengür-Taşdemir, İ. Koyuncu, and V. V. Tarabara, "Lip balm drying promotes virus attachment: Characterization of lip balm coatings and XDLVO modeling," *Journal of colloid and interface science,* vol. 581, pp. 884-894, 2021/01/01/ 2021, doi: https://doi.org/10.1016/j.jcis.2020.07.143.

[231] H. T. T. Dang and V. V. Tarabara, "Virus deposition onto polyelectrolyte-coated surfaces: A study with bacteriophage MS2," *Journal of colloid and interface science,* vol. 540, pp. 155-166, 2019/03/22/ 2019, doi: https://doi.org/10.1016/j.jcis.2018.12.107.

[232] E. Joonaki, A. Hassanpouryouzband, C. L. Heldt, and O. Areo, "Surface Chemistry Can Unlock Drivers of Surface Stability of SARS-CoV-2 in a Variety of Environmental Conditions," *Chem,* vol. 6, no. 9, pp. 2135-2146, 2020/09/10/ 2020, doi: https://doi.org/10.1016/j.chempr.2020.08.001.

[233] I. Katoh *et al.*, "Potential Risk of Virus Carryover by Fabrics of Personal Protective Gowns," (in English), *Frontiers in Public Health,* Perspective vol. 7, no. 121, 2019-May-22 2019, doi: 10.3389/fpubh.2019.00121.

[234] S. J. Smither, L. S. Eastaugh, J. S. Findlay, and M. S. Lever, "Experimental aerosol survival of SARS-CoV-2 in artificial saliva and tissue culture media at medium and high humidity," (in eng), *Emerg Microbes Infect,* vol. 9, no. 1, pp. 1415-1417, Dec 2020, doi: 10.1080/22221751.2020.1777906.

[235] S. M. Duan *et al.*, "Stability of SARS coronavirus in human specimens and environment and its sensitivity to heating and UV irradiation," (in eng), *Biomed Environ Sci,* vol. 16, no. 3, pp. 246-55, Sep 2003.

[236] J. Knoll, W. R. Darnmert, and H. Nirschl, "Integration of a microscope into a centrifuge for adhesion force measurement of particles," *Powder Technol.,* vol. 305, pp. 147-155, Jan 2017, doi: 10.1016/j.powtec.2016.09.065.

[237] P. Kulvanich and P. J. Stewart, "Fundamental considerations in the measurement of adhesional forces between particles using the centrifuge method," *Int. J. Pharm.,* vol. 35, no. 1-2, pp. 111-120, Feb 1987, doi: 10.1016/0378-5173(87)90079-2.

[238] R. X. Huang, P. Yi, and Y. Z. Tang, "Probing the interactions of organic molecules, nanomaterials, and microbes with solid surfaces using quartz crystal microbalances: methodology, advantages, and limitations," *Environmental Science-Processes & Impacts,* vol. 19, no. 6, pp. 793-811, Jun 2017, doi: 10.1039/c6em00628k.

[239] K. Page, M. Wilson, N. J. Mordan, W. Chrzanowski, J. Knowles, and I. P. Parkin, "Study of the adhesion of Staphylococcus aureus to coated glass substrates," *JMatS,* vol. 46, no. 19, pp. 6355-6363, 2011, doi: 10.1007/s10853-011-5582-9.

[240] I. Yakub and W. O. Soboyejo, "Adhesion of E. coli to silver- or copper-coated porous clay ceramic surfaces," *Journal of Applied Physics,* vol. 111, no. 12, p. 124324, 2012, doi: 10.1063/1.4722326.

[241] Z. J. Liu, H. T. Niu, R. Rong, G. Q. Cao, B. J. He, and Q. H. Deng, "An experiment and numerical study of resuspension of fungal spore particles from HVAC ducts," (in English), *Science of the Total Environment,* Article vol. 708, p. 11, Mar 2020, Art no. 134742, doi: 10.1016/j.scitotenv.2019.134742.

[242] C. Feigley *et al.*, "Experimental tests of copper components in ventilation systems for microbial control," *HVAC&R Research,* vol. 19, pp. 53-62, 2013, doi: 10.1080/10789669.2012.735150.

[243] E. Tamburini, V. Donega, M. G. Marchetti, P. Pedrini, C. Monticelli, and A. Balbo, "Study on Microbial Deposition and Contamination onto Six Surfaces Commonly Used in Chemical and Microbiological Laboratories," *International Journal of Environmental Research and Public Health,* vol. 12, no. 7, pp. 8295-8311, Jul 2015, doi: 10.3390/ijerph120708295.

[244] V. Villapún, L. Dover, A. Cross, and S. González, "Antibacterial Metallic Touch Surfaces," *Materials,* vol. 9, no. 9, p. 736, 2016, doi: 10.3390/ma9090736.

[245] H. Straub *et al.*, "Bacterial Adhesion on Soft Materials: Passive Physicochemical Interactions or Active Bacterial Mechanosensing?," *Advanced Healthcare Materials,* vol. 8, no. 8, p. 1801323, 2019, doi: 10.1002/adhm.201801323.

[246] G. Loosmore, A.,, "Evaluation and development of models for resuspension of aerosols at short times after deposition," *Atmospheric Environment,* vol. 37, pp. 639-647, 2003. [Online]. Available: .

[247] A. H. Ibrahim, P. F. Dunn, and R. M. Brach, "Microparticle detachment from surfaces exposed to turbulent air flow: controlled experiments and modeling," *Aerosol Science,* vol. 34, pp. 765-782, 2003. [Online]. Available: .

[248] J. S. Punjrath and D. R. Heldman, "Mechanisms of small particle re-entrainment from flat surfaces," *Aerosol Science,* vol. 3, pp. 429-440, 1972. [Online]. Available: .

[249] D. A. Braaten, K. T. Paw U, and R. H. Shaw, "Particle resuspension in a turbulent boundary layer-observed and modeled," *Journal of Aerosol Science,* vol. 5, pp. 613-628, 1990. [Online]. Available: .

[250] G. Ziskind, "Particle resuspension from surfaces: revisited and re-evaluated," *Rev. Chem. Eng.,* vol. 22, no. 1-2, pp. 1-123, 2006.

[251] G. Ziskind, M. Fichman, and C. Gutfinger, "Resuspension of particulates from surfaces to turbulent flows-review and analysis," *Journal of Aerosol Science,* vol. 26, no. 4, pp. 613-644, 1995. [Online]. Available: .

[252] Y. Kim, A. Gidwani, B. E. Wyslouzil, and C. W. Sohn, "Source term models for fine particle resuspension from indoor surfaces," (in English), *Building and Environment,* Article vol. 45, no. 8, pp. 1854-1865, Aug 2010, doi: 10.1016/j.buildenv.2010.02.016.

[253] Z. Cheng, X. Yu, T.-J. Hsu, and S. Balachandar, "A numerical investigation of fine sediment resuspension in the wave boundary layer—Uncertainties in particle inertia and hindered settling," *Comput Geosci,* vol. 83, pp. 176-192, 2015, doi: 10.1016/j.cageo.2015.07.009.

[254] S. Ji, A. Ouahsine, H. Smaoui, and P. Sergent, "3D Numerical Modeling of Sediment Resuspension Induced by the Compounding Effects of Ship-Generated Waves and the Ship Propeller," *J. Eng. Mech.,* vol. 140, no. 6, 2014, doi: 10.1061/(ASCE)EM.1943-7889.0000739.©2014.

[255] R.-Q. Wang, "Large - Eddy Simulation (LES) of settling particle cloud dynamics," *International Journal of Multiphase Flow,* vol. 67, pp. 65-75, 2014.

[256] P. G. Saffman, "The lift on a small sphere in a slow shear flow," *Fluid Mechanics,* vol. 22, p. 25, 1964.

[257] A. M. Mollinger and F. T. M. Nieuwstadt, "Measurement of the lift force on a particle fixed to the wall in the viscous sublayer of a fully developed turbulent boundary layer," *Journal of Fluid Mechanics,* vol. 316, pp. 285-306, 1996.

[258] D. Leighton and A. Acrivos, "The lift on a small sphere touching a plane in the presence of a simple shear flow," *Journal of Applied Mathematics and Physics,* vol. 36, pp. 174-178, 1985.

[259] L. Shi and D. Bayless, J.,, "Comparison of boundary conditions for predicting the collection efficiency of cyclones," *Powder Technol.,* vol. 173, pp. 29-37, 2007.

[260] J. G. Benito, K. A. V. Aracena, R. O. Uñac, A. M. Vidales, and I. Ippolito, "Monte Carlo modelling of particle resuspension on a flat surface," *Journal of Aerosol Science,* vol. 79, pp. 126-139, 2015, doi: 10.1016/j.jaerosci.2014.10.006.

[261] C. Henry and J.-P. Minier, "A stochastic approach for the simulation of particle resuspension from rough substrates: Model and numerical implementation,"

*Journal of Aerosol Science,* vol. 77, pp. 168-192, 2014, doi: 10.1016/j.jaerosci.2014.08.005.

[262] A. Ferro, R., R. Kopperpaud, J., and L. Hildemann, M., "Source strengths for indoor Human Activities that resuspend particulate matter," *Environ. Sci. Technol.,* vol. 38, pp. 1759-1764, 2004.

[263] P. Krauter and A. Biermann, "Reaersolization of fluidized spores in ventilation systems," *Applied and Environmental Microbiology,* vol. 73, no. 7, pp. 2165-2172, 2007. [Online]. Available: .

[264] G. A. Somsen, C. van Rijn, S. Kooij, R. A. Bem, and D. Bonn, "Small droplet aerosols in poorly ventilated spaces and SARS-CoV-2 transmission," *The Lancet Respiratory Medicine,* vol. 8, no. 7, pp. 658-659, 2020.

[265] J. Oxford *et al.*, "The survival of influenza A (H1N1) pdm09 virus on 4 household surfaces," *Am. J. Infect. Control,* vol. 42, no. 4, pp. 423-425, 2014.

[266] D. Seong and S. Hoque, "Influence of indoor conditions on microbial diversity and quantity in schools," presented at the Clima 2019, REHVA 13th HVAC World Congress, Bucharest, Romania, 2019.

[267] D.-H. Kang, H. Choi, Y.-J. Yoo, J.-H. Kim, Y.-B. Park, and H.-S. Moon, "Effect of polishing method on surface roughness and bacterial adhesion of zirconia-porcelain veneer," *Ceram. Int.,* vol. 43, no. 7, pp. 5382-5387, 2017.

[268] K. Bohinc *et al.*, "Available surface dictates microbial adhesion capacity," *Int. J. Adhes. Adhes.,* vol. 50, pp. 265-272, 2014.

[269] D. Seong and S. Hoque, "Mathematical model simulating fungal and bacterial growth on surfaces in indoor spaces," in *Indoor Air*, Philadelphia, PA, 2018.

[270] E. Gadelmawla, M. Koura, T. Maksoud, I. Elewa, and H. Soliman, "Roughness parameters," *J. Mater. Process. Technol.,* vol. 123, no. 1, pp. 133-145, 2002.

[271] C. Piao, J. E. Winandy, and T. F. Shupe, "From hydrophilicity to hydrophobicity: A critical review: Part I. Wettability and surface behavior," *Wood and Fiber Science,* vol. 42, no. 4, pp. 490-510, 2010.

[272] A. L. Olsson, A. Wargenau, and N. Tufenkji, "Optimizing bacteriophage surface densities for bacterial capture and sensing in quartz crystal microbalance with dissipation monitoring," *ACS applied materials & interfaces,* vol. 8, no. 22, pp. 13698-13706, 2016.

[273] D. Seong and S. Hoque, "Does the presence of certain bacterial family in the microbiome indicate specific indoor environment characteristics? A factorial design approach for identifying bio-fingerprints," *Indoor and Built Environment,* vol. 29, no. 1, pp. 117-131, 2020, doi: 10.1177/1420326x19853865.

[274] K. K. Kanazawa and J. G. Gordon, "Frequency of a quartz microbalance in contact with liquid," *Analytical Chemistry,* vol. 57, no. 8, pp. 1770-1771, 1985.

[275] S. Slavin *et al.*, "Adsorption behaviour of sulfur containing polymers to gold surfaces using QCM-D," *Soft Matter,* vol. 8, no. 1, pp. 118-128, 2012.

[276] T. Feng and H. Xian-He, "Relations between mass change and frequency shift of a QCM sensor in contact with viscoelastic medium," *Chinese Physics Letters,* vol. 30, no. 5, p. 050701, 2013.

[277] S. K. Solongo *et al.*, "Cationic collector conformations on an oxide mineral interface: Roles of pH, ionic strength, and ion valence," *Miner. Eng.*, vol. 150, p. 106277, 2020.

[278] G. Dong, L. He, D. Pang, L. Wei, and C. Deng, "An in situ study of the deposition of a calcium phosphate mineralized layer on a silicon-substituted hydroxyapatite sensor modulated by bovine serum albumin using QCM-D technology," *Ceram. Int.,* vol. 42, no. 16, pp. 18648-18656, 2016.

[279] S. V. Vaidya, M. Yuan, A. R. Narváez, D. Daghfal, J. Mattzela, and D. Smith, "Protein-resistant properties of a chemical vapor deposited alkyl-functional carboxysilane coating characterized using quartz crystal microbalance," *Applied Surface Science,* vol. 364, pp. 896-908, 2016.

[280] S. X. Liu and J.-T. Kim, "Application of Kevin—Voigt model in quantifying whey protein adsorption on polyethersulfone using QCM-D," *JALA: Journal of the Association for Laboratory Automation,* vol. 14, no. 4, pp. 213-220, 2009.

[281] M. V. Voinova, M. Rodahl, M. Jonson, and B. Kasemo, "Viscoelastic acoustic response of layered polymer films at fluid-solid interfaces: continuum mechanics approach," *Physica Scripta,* vol. 59, no. 5, p. 391, 1999.

[282] R. Groh, "On Boundary Layers: Laminar, Turbulent and Skin Friction," in *AEROSPACE ENGINEERING*, ed, 2016.

[283] R. L. Ott and M. T. Longnecker, *An introduction to statistical methods and data analysis*. Nelson Education, 2015.

[284] D. Yongabi *et al.*, "Ionic strength controls long-term cell-surface interactions–A QCM-D study of S. cerevisiae adhesion, retention and detachment," *Journal of colloid and interface science,* vol. 585, pp. 583-595, 2021.

[285] D. Yongabi *et al.*, "QCM-D study of time-resolved cell adhesion and detachment: Effect of surface free energy on eukaryotes and prokaryotes," *ACS applied materials & interfaces,* vol. 12, no. 16, pp. 18258-18272, 2020.

[286] S. Maity, S. Nir, T. Zada, and M. Reches, "Self-assembly of a tripeptide into a functional coating that resists fouling," *Chem. Commun.*, vol. 50, no. 76, pp. 11154-11157, 2014, doi: 10.1039/c4cc03578j.

[287] D. Pang, L. He, L. Wei, H. Zheng, and C. Deng, "Preparation of a beta-tricalcium phosphate nanocoating and its protein adsorption behaviour by quartz crystal microbalance with dissipation technique," *Colloids Surf. B. Biointerfaces,* vol. 162, pp. 1-7, 2018, doi: 10.1016/j.colsurfb.2017.11.020.

[288] K. R. De Aguiar, K. Rischka, L. Gätjen, P.-L. M. Noeske, W. L. Cavalcanti, and U. P. Rodrigues-Filho, "Biomimetic PDMS-hydroxyurethane terminated with catecholic moieties for chemical grafting on transition metal oxide-based surfaces," *Applied Surface Science,* vol. 427, pp. 166-175, 2018, doi: 10.1016/j.apsusc.2017.08.142.

[289] G. Kaleli-Can, H. F. Özgüzar, and M. Mutlu, "Development of mass sensitive sensor platform based on plasma polymerization technique: Quartz tuning fork as transducer," *Applied Surface Science,* vol. 540, p. 148360, 2021, doi: 10.1016/j.apsusc.2020.148360.

[290] N. Weber, A. Pesnell, D. Bolikal, J. Zeltinger, and J. Kohn, "Viscoelastic Properties of Fibrinogen Adsorbed to the Surface of Biomaterials Used in Blood-Contacting Medical Devices," *Langmuir,* vol. 23, no. 6, pp. 3298-3304, 2007, doi: 10.1021/la060500r.

[291] T. Kojima, "Combined reflectometric interference spectroscopy and quartz crystal microbalance detect differential adsorption of lipid vesicles with different phase transition temperatures on SiO2, TiO2, and Au surfaces," *Analytical chemistry,* vol. 89, no. 24, pp. 13596-13602, 2017.

[292] B. Jachimska, S. Świątek, J. Loch, K. Lewiński, and T. Luxbacher, "Adsorption effectiveness of β-lactoglobulin onto gold surface determined by quartz crystal microbalance," *Bioelectrochemistry,* vol. 121, pp. 95-104, 2018.

[293] E. Yoshida and T. Hayakawa, "Adsorption Analysis of Lactoferrin to Titanium, Stainless Steel, Zirconia, and Polymethyl Methacrylate Using the Quartz Crystal

Microbalance Method," *BioMed Research International*, vol. 2016, pp. 1-7, 2016, doi: 10.1155/2016/3961286.

[294] A. Sze, D. Erickson, L. Ren, and D. Li, "Zeta-potential measurement using the Smoluchowski equation and the slope of the current–time relationship in electroosmotic flow," *Journal of colloid and interface science*, vol. 261, no. 2, pp. 402-410, 2003, doi: 10.1016/s0021-9797(03)00142-5.

[295] T. N. Figueira *et al.*, "Structure–Stability–Function Mechanistic Links in the Anti-Measles Virus Action of Tocopherol-Derivatized Peptide Nanoparticles," *ACS Nano*, vol. 12, no. 10, pp. 9855-9865, 2018, doi: 10.1021/acsnano.8b01422.

[296] S. R. Haas, F. R. Nascimento, I. A. H. Schneider, and C. Gaylarde, "Flocculation of fine fluorite particles with Corynebacterium xerosis," *Revista de Microbiologia*, vol. 30, no. 3, pp. 225-230, 1999, doi: 10.1590/s0001-37141999000300007.

[297] A. M. Elmahdy, S. E. El-Mofty, N. A. Abdel-Khalek, and A. A. El-Midany, "Impact of the Adsorption of Corynebacterium Diphtheriae Intermedius Bacteria on Enhancing the Separation Selectivity of Dolomite and Apatite," *Adsorption Science & Technology*, vol. 29, no. 1, pp. 47-58, 2011, doi: 10.1260/0263-6174.29.1.47.

[298] A. van der Wal, M. Minor, W. Norde, A. J. Zehnder, and J. Lyklema, "Conductivity and dielectric dispersion of gram-positive bacterial cells," *Journal of colloid and interface science*, vol. 186, no. 1, pp. 71-79, 1997.

[299] H. H. Rijnaarts, W. Norde, J. Lyklema, and A. J. Zehnder, "DLVO and steric contributions to bacterial deposition in media of different ionic strengths," *Colloids Surf. B. Biointerfaces*, vol. 14, no. 1-4, pp. 179-195, 1999.

[300] R. Li, Z. Wu, Y. Wangb, L. Ding, and Y. Wang, "Role of pH-induced structural change in protein aggregation in foam fractionation of bovine serum albumin," *Biotechnology Reports*, vol. 9, pp. 46-52, 2016, doi: 10.1016/j.btre.2016.01.002.

[301] P. Gastanaduy, P. Haber, P. A. Rota, and M. Patel. "Measles Virus." CDC. https://www.cdc.gov/vaccines/pubs/pinkbook/meas.html (accessed November, 2021).

[302] Y. M. Serebrennikova, A. Roth, D. E. Huffman, J. M. Smith, J. N. Lindon, and L. H. García-Rubio, "Multiwavelength Transmission Spectroscopy Revisited for the Characterization of the Protein and Polystyrene Nanoparticle Mixtures," *Applied Spectroscopy*, vol. 67, no. 2, pp. 196-203, 2013, doi: 10.1366/12-06701.

[303] G. Betts, "Other spoilage bacteria," *Food spoilage microorganisms,* pp. 668-693, 2006.

[304] M. Van Loosdrecht, J. Lyklema, W. Norde, G. Schraa, and A. Zehnder, "The role of bacterial cell wall hydrophobicity in adhesion," *Applied and environmental microbiology,* vol. 53, no. 8, pp. 1893-1897, 1987.

[305] S. Kruss, T. Wolfram, R. Martin, S. Neubauer, H. Kessler, and J. P. Spatz, "Stimulation of Cell Adhesion at Nanostructured Teflon Interfaces," *Adv. Mater.,* vol. 22, no. 48, pp. 5499-5506, 2010, doi: 10.1002/adma.201003055.

[306] P. R. Waghmare and S. K. Mitra, "Contact angle hysteresis of bovine serum albumin (BSA) solution/metal (Au-Cr) coated glass substrate," *Colloid. Polym. Sci.,* vol. 291, no. 2, pp. 375-381, 2013, doi: 10.1007/s00396-012-2756-1.

[307] A. Dolatshahi-Pirouz, K. Rechendorff, M. Hovgaard, M. Foss, J. Chevallier, and F. Besenbacher, "Bovine serum albumin adsorption on nano-rough platinum surfaces studied by QCM-D," *Colloids Surf. B. Biointerfaces,* vol. 66, no. 1, pp. 53-59, 2008.

[308] H. Juvonen, A. Määttänen, P. Ihalainen, T. Viitala, J. Sarfraz, and J. Peltonen, "Enhanced protein adsorption and patterning on nanostructured latex-coated paper," *Colloids Surf. B. Biointerfaces,* vol. 118, pp. 261-269, 2014.

[309] A. A. Feiler, A. Sahlholm, T. Sandberg, and K. D. Caldwell, "Adsorption and viscoelastic properties of fractionated mucin (BSM) and bovine serum albumin (BSA) studied with quartz crystal microbalance (QCM-D)," *Journal of colloid and interface science,* vol. 315, no. 2, pp. 475-481, 2007.

[310] Y. Jeyachandran, E. Mielczarski, B. Rai, and J. Mielczarski, "Quantitative and qualitative evaluation of adsorption/desorption of bovine serum albumin on hydrophilic and hydrophobic surfaces," *Langmuir,* vol. 25, no. 19, pp. 11614-11620, 2009.

[311] Y. S. Hedberg, M. S. Killian, E. Blomberg, S. Virtanen, P. Schmuki, and I. Odnevall Wallinder, "Interaction of bovine serum albumin and lysozyme with stainless steel studied by time-of-flight secondary ion mass spectrometry and X-ray photoelectron spectroscopy," *Langmuir,* vol. 28, no. 47, pp. 16306-16317, 2012.

[312] A. Armanious *et al.*, "Viruses at Solid–Water Interfaces: A Systematic Assessment of Interactions Driving Adsorption," *Environmental Science & Technology,* vol. 50, no. 2, pp. 732-743, 2016, doi: 10.1021/acs.est.5b04644.

[313] A. L. J. Olsson, H. C. Van Der Mei, H. J. Busscher, and P. K. Sharma, "Influence of Cell Surface Appendages on the Bacterium−Substratum Interface Measured Real-Time Using QCM-D," *Langmuir,* vol. 25, no. 3, pp. 1627-1632, 2009, doi: 10.1021/la803301q.

[314] L. Ott, M. Höller, J. Rheinlaender, T. E. Schäffer, M. Hensel, and A. Burkovski, "Strain-specific differences in pili formation and the interaction of Corynebacterium diphtheriae with host cells," *BMC Microbiol.,* vol. 10, no. 1, p. 257, 2010, doi: 10.1186/1471-2180-10-257.

[315] J. Gutman, S. L. Walker, V. Freger, and M. Herzberg, "Bacterial attachment and viscoelasticity: physicochemical and motility effects analyzed using quartz crystal microbalance with dissipation (QCM-D)," *Environmental science & technology,* vol. 47, no. 1, pp. 398-404, 2013.

[316] T. Brabb, D. Newsome, A. Burich, and M. Hanes, "Infectious Diseases," Elsevier, 2012, pp. 637-683.

[317] W.-L. Kao, H.-Y. Chang, K.-Y. Lin, Y.-W. Lee, and J.-J. Shyue, "Effect of surface potential on the adhesion behavior of NIH3T3 cells revealed by quartz crystal microbalance with dissipation monitoring (QCM-D)," *The Journal of Physical Chemistry C,* vol. 121, no. 1, pp. 533-541, 2017.

[318] A. Han, J. K. Tsoi, F. P. Rodrigues, J. G. Leprince, and W. M. Palin, "Bacterial adhesion mechanisms on dental implant surfaces and the influencing factors," *Int. J. Adhes. Adhes.,* vol. 69, pp. 58-71, 2016.

[319] G. Feng, Y. Cheng, S.-Y. Wang, D. A. Borca-Tasciuc, R. W. Worobo, and C. I. Moraru, "Bacterial attachment and biofilm formation on surfaces are reduced by small-diameter nanoscale pores: how small is small enough?," *NPJ biofilms and microbiomes,* vol. 1, no. 1, pp. 1-9, 2015.

[320] A. M. Gallardo-Moreno, M. L. Navarro-Pérez, V. Vadillo-Rodríguez, J. M. Bruque, and M. L. González-Martín, "Insights into bacterial contact angles: difficulties in defining hydrophobicity and surface Gibbs energy," *Colloids Surf. B. Biointerfaces,* vol. 88, no. 1, pp. 373-380, 2011.

[321] H. Wang, L. Cai, Y. Li, X. Xu, and G. Zhou, "Biofilm formation by meat-borne Pseudomonas fluorescens on stainless steel and its resistance to disinfectants," *Food Control,* vol. 91, pp. 397-403, 2018.

[322] C.-C. Jung, P.-C. Wu, C.-H. Tseng, and H.-J. Su, "Indoor air quality varies with ventilation types and working areas in hospitals," *Building and Environment,* vol. 85, pp. 190-195, 2015.

[323] H. Lal, T. Punia, B. Ghosh, A. Srivastava, and V. Jain, "Comparative study of bioaerosol during monsoon and post-monsoon seasons at four sensitive sites in Delhi region," *International Journal of Advancement in Earth and Environmental Sciences,* vol. 1, no. 2, pp. 1-7, 2013.

[324] K. J. Heo and B. U. Lee, "Seasonal variation in the concentrations of culturable bacterial and fungal aerosols in underground subway systems," *Journal of Aerosol Science,* vol. 92, pp. 122-129, 2016.

[325] A. Rajasekar and R. Balasubramanian, "Assessment of airborne bacteria and fungi in food courts," *Building and Environment,* vol. 46, no. 10, pp. 2081-2087, 2011.

[326] J. S. Pastuszka, U. K. T. Paw, D. O. Lis, A. Wlazło, and K. Ulfig, "Bacterial and fungal aerosol in indoor environment in Upper Silesia, Poland," *Atmospheric Environment,* vol. 34, no. 22, pp. 3833-3842, 2000.

[327] D. Guan, C. Guo, Y. Li, H. Lv, and X. Yu, "Study on the Concentration and Distribution of the Airborne Bacteria in Indoor Air in the Lecture Theatres at Tianjin Chengjian University, China," *Procedia Engineering,* vol. 121, pp. 33-36, 2015.

[328] A. Alum and G. Z. Isaacs, "Aerobiology of the built environment: Synergy between Legionella and fungi," *Am. J. Infect. Control,* vol. 44, no. 9, pp. S138-S143, 2016.

[329] Y. Li, H. Fu, W. Wang, J. Liu, Q. Meng, and W. Wang, "Characteristics of bacterial and fungal aerosols during the autumn haze days in Xi'an, China," *Atmospheric Environment,* vol. 122, pp. 439-447, 2015.

[330] N. Y. Hsu, P. Y. Chen, H. W. Chang, and H. J. Su, "Changes in profiles of airborne fungi in flooded homes in southern Taiwan after Typhoon Morakot," *Science of the total environment,* vol. 409, no. 9, pp. 1677-1682, 2011.

[331] G. Marchand, C. Duchaine, J. Lavoie, M. Veillette, and Y. Cloutier, "Bacteria emitted in ambient air during bronchoscopy—a risk to health care workers?," *Am. J. Infect. Control,* 2016.

[332] B. Li and B. E. Logan, "Bacterial adhesion to glass and metal-oxide surfaces," *Colloids Surf. B. Biointerfaces,* vol. 36, no. 2, pp. 81-90, 2004.

[333] M. N. Momba and P. Kaleni, "Regrowth and survival of indicator microorganisms on the surfaces of household containers used for the storage of drinking water in rural communities of South Africa," *Water Research,* vol. 36, no. 12, pp. 3023-3028, 2002.

[334] P. Di Ciccio *et al.*, "Biofilm formation by Staphylococcus aureus on food contact surfaces: Relationship with temperature and cell surface hydrophobicity," *Food Control,* vol. 50, pp. 930-936, 2015.

[335] P. Krauter and A. Biermann, "Reaerosolization of fluidized spores in ventilation systems," *Applied and environmental microbiology,* vol. 73, no. 7, pp. 2165-2172, 2007.

[336] W. Liu, C. Huang, Y. Hu, Z. Zou, L. Shen, and J. Sundell, "Associations of building characteristics and lifestyle behaviors with home dampness-related exposures in Shanghai dwellings," *Building and Environment,* vol. 88, pp. 106-115, 2015.

[337] M. Riggs, "Resident cleanup activities, characteristics of flood-damaged homes and airborne microbial concentrations in New Orleans, Louisiana, October 2005," *Environmental Research,* vol. 106, no. 3, pp. 401-409, 2008, doi: 10.1016/j.envres.2007.11.004.

[338] N.-Y. Hsu, P.-Y. Chen, H.-W. Chang, and H.-J. Su, "Changes in profiles of airborne fungi in flooded homes in southern Taiwan after Typhoon Morakot," *Science of The Total Environment,* vol. 409, no. 9, pp. 1677-1682, 2011, doi: 10.1016/j.scitotenv.2011.01.042.

[339] D. Seong and S. Hoque, "Bacterial Diversiy in the Indoor Environment: A Factorial Design Approach for Isolating the Impact of Environmental Conditions and Sampling Methods," presented at the The American Association for Aerosol Research, Raleigh, North Carolina, Oct 16-20, 2017.

[340] F. El Moustaid, A. Eladdadi, and L. Uys, "Modeling bacterial attachment to surfaces as an early stage of biofilm development," *Math. Biosci. Eng,* vol. 10, no. 3, pp. 821-842, 2013.

[341] D. Schwarcz, H. Levine, E. Ben-Jacob, and G. Ariel, "Uniform modeling of bacterial colony patterns with varying nutrient and substrate," *Physica D: Nonlinear Phenomena,* vol. 318, pp. 91-99, 2016.

[342] K. Ito, "Numerical prediction model for fungal growth coupled with hygrothermal transfer in building materials," *Indoor Built Environ.,* vol. 21, no. 6, pp. 845-856, 2012.

[343] J. G. Schumacher, *Survival, transport, and sources of fecal bacteria in streams and survival in land-applied poultry litter in the upper Shoal Creek basin, southwestern Missouri, 2001-2002*. US Department of the Interior, US Geological Survey, 2003.

[344] R. Lindqvist and G. Barmark, "Specific growth rate determines the sensitivity of Escherichia coli to lactic acid stress: implications for predictive microbiology," *BioMed research international,* vol. 2014, 2014.

[345] R. Lindqvist, "Estimation of Staphylococcus aureus growth parameters from turbidity data: characterization of strain variation and comparison of methods," *Applied and environmental microbiology,* vol. 72, no. 7, pp. 4862-4870, 2006.

[346] H. Diagnostics. "Micrococcus." https://catalog.hardydiagnostics.com/cp_prod/Content/hugo/Micrococcus.htm (accessed November, 2017).

[347] K. Davey, "Modelling the combined effect of temperature and pH on the rate coefficient for bacterial growth," *Int. J. Food Microbiol.,* vol. 23, no. 3-4, pp. 295-303, 1994.

[348] I. Burdett, T. Kirkwood, and J. Whalley, "Growth kinetics of individual Bacillus subtilis cells and correlation with nucleoid extension," *Journal of bacteriology,* vol. 167, no. 1, pp. 219-230, 1986.

[349] J. P. Wood *et al.,* "Environmental persistence of Bacillus anthracis and Bacillus subtilis spores," *PLoS One,* vol. 10, no. 9, p. e0138083, 2015.

[350] A. Trinci, "A kinetic study of the growth of Aspergillus nidulans and other fungi," *Microbiology,* vol. 57, no. 1, pp. 11-24, 1969.

[351] J. Clarke, C. Johnstone, N. Kelly, R. McLean, N. Rowan, and J. Smith, "A technique for the prediction of the conditions leading to mould growth in buildings," *Building and Environment,* vol. 34, no. 4, pp. 515-521, 1999.

[352] N. J. Rowan, C. M. Johnstone, R. C. McLean, J. G. Anderson, and J. A. Clarke, "Prediction of toxigenic fungal growth in buildings by using a novel modelling system," *Applied and Environmental Microbiology,* vol. 65, no. 11, pp. 4814-4821, 1999.

[353] K. Sedlbauer, "Prediction of mould growth by hygrothermal calculation," *Journal of Thermal Envelope and Building Science,* vol. 25, no. 4, pp. 321-336, 2002.

[354] A. Mendes *et al.,* "Indoor air quality and thermal comfort in elderly care centers," *Urban Climate,* vol. 14, pp. 486-501, 2015.

[355] Y. Al horr, M. Arif, M. Katafygiotou, A. Mazroei, A. Kaushik, and E. Elsarrag, "Impact of indoor environmental quality on occupant well-being and comfort: A

review of the literature," *International Journal of Sustainable Built Environment*, vol. 5, no. 1, pp. 1-11, 2016/06/01/ 2016, doi: https://doi.org/10.1016/j.ijsbe.2016.03.006.

[356] M. Lee, K. Mui, L. Wong, W. Chan, E. Lee, and C. Cheung, "Student learning performance and indoor environmental quality (IEQ) in air-conditioned university teaching rooms," *Building and Environment*, vol. 49, pp. 238-244, 2012.

[357] EIA, "Total electricity consumption and expenditure intensities," 2012.

[358] M. Vadney, B. Fox, M. Mosser, S. Fraser, and B. Bernstein, "Benchmarking K-12 Schools: How the Building Energy Performance System Continues to Track and Compare Energy Data in the Northeast and Mid-Atlantic," presented at the ACEEE Summer Study on Energy Efficiency in Buildings, CA, USA, 2012.

[359] L. D. Pereira, D. Raimondo, S. P. Corgnati, and M. G. Da Silva, "Energy consumption in schools–A review paper," *Renewable and Sustainable Energy Reviews*, vol. 40, pp. 911-922, 2014.

[360] A. Allouhi, Y. El Fouih, T. Kousksou, A. Jamil, Y. Zeraouli, and Y. Mourad, "Energy consumption and efficiency in buildings: current status and future trends," *Journal of Cleaner production*, vol. 109, pp. 118-130, 2015.

[361] L. Pérez-Lombard, J. Ortiz, and C. Pout, "A review on buildings energy consumption information," *Energy and buildings*, vol. 40, no. 3, pp. 394-398, 2008.

[362] H.-J. Oh, I.-S. Nam, H. Yun, J. Kim, J. Yang, and J.-R. Sohn, "Characterization of indoor air quality and efficiency of air purifier in childcare centers, Korea," *Building and Environment*, vol. 82, pp. 203-214, 2014.

[363] A. Barberán *et al.*, "The ecology of microscopic life in household dust," in *Proc. R. Soc. B*, 2015, vol. 282, no. 1814: The Royal Society, p. 20151139.

[364] EPA, "Typical Indoor Air Pollutants," 2014. [Online]. Available: https://www.epa.gov/sites/production/files/2014-08/documents/refguide_appendix_e.pdf.

[365] J. F. Meadow *et al.*, "Indoor airborne bacterial communities are influenced by ventilation, occupancy, and outdoor air source," (in eng), *Indoor Air*, Research Support, Non-U.S. Gov't vol. 24, no. 1, pp. 41-8, Feb 2014, doi: 10.1111/ina.12047.

[366] M. Stryjakowska-Sekulska, A. Piotraszewska-Pajak, A. Szyszka, M. Nowicki, and M. Filipiak, "Microbiological quality of indoor air in university rooms," *Pol J Environ Stud,* vol. 16, no. 4, p. 623, 2007.

[367] C. J. Ter Braak and P. F. Verdonschot, "Canonical correspondence analysis and related multivariate methods in aquatic ecology," *Aquatic sciences,* vol. 57, no. 3, pp. 255-289, 1995.

[368] K. C. Dannemiller, J. F. Gent, B. P. Leaderer, and J. Peccia, "Indoor microbial communities: influence on asthma severity in atopic and nonatopic children," *Journal of Allergy and Clinical Immunology,* vol. 138, no. 1, pp. 76-83. e1, 2016.

[369] R. I. Adams, M. Miletto, J. W. Taylor, and T. D. Bruns, "Dispersal in microbes: fungi in indoor air are dominated by outdoor air and show dispersal limitation at short distances," *The ISME journal,* vol. 7, no. 7, p. 1262, 2013.

# APPENDIX A: SUPPLEMENTARY INFORMATION OF CHAPTER 1

**Table A1.** Bacteria and fungi concentration and dominant species in different sampling conditions

| Country | Sampling site | Methods | Bacteria | | | | Fungi | | | | Ref. |
|---|---|---|---|---|---|---|---|---|---|---|---|
| | | | CFU/m³ | Temp. [a] (℃) | Hum. [b] (%) | Dominant species | CFU/m³ | Temp. (℃) | Hum. (%) | Dominant species | |
| Ethiopia | University library | Settled plate | 367<br>~ 2595 | - | - | *Micrococcus*<br>*Staphylococcus*<br>*Streptococcus* | 524<br>~ 1992 | - | - | filamentous species | [1] |
| Taiwan | Hospital | Burkard sampler | 197<br>~ 1341 | | | | 320<br>~ 1172 | | | | [322] |
| India | University | BIO-PUMP with Air-O-Cell Cassette | 1860<br>~ 9333 | 12.6<br>~ 19.6 | 47.8<br>~ 59 | - | 200<br>~ 9733 | 16.3<br>~ 29.5 | 74.1<br>~ 80 | *Fusarium*<br>*Penicillium*<br>*Aspergillus*<br>*Alternaria* | [323] |
| China | Restaurant | SKC Bio-Sampler | 37<br>~ 137 | 22±2 | 60±10 | *Pseudomonas* spp.<br>*Micrococcus* sp.<br>*Bacillus* sp. | - | - | - | - | [71] |
| Korea | Subway station | Bio-Culture device | 167±84<br>~ 323±78 | 22±0.1 | 32±0.2<br>~ 42±0.4 | - | 13±6<br>~ 137±21 | 22±0.1 | 32±0.2<br>~ 42±0.4 | - | [324] |
| Singapore | University food courts | Andersen 6-stage Cascade Impactor | 226±10<br>~ 621±10 | 26±1<br>~ 28±1 | 63±2<br>~ 68±2 | *Clostridium*<br>*Corynebacterium*<br>*Micrococcus*<br>*Pseudomonas*<br>*Alcaligens*<br>*Salmonella*<br>*Mycobacterium*<br>*Staphylococcus*<br>*Acinetobacter* | 240±25<br>~ 551±15 | 27±1<br>~ 28±2 | 58±4<br>~ 63±5 | *Acrmonium*<br>*Aspergillus*<br>*Bipolaris*<br>*Cladosporium*<br>*Geotrichum*<br>*Mortierella*<br>*Pencillium*<br>*Rhizopus*<br>*Sporothrix*<br>*Trichoderma* | [325] |

## Table A1. (continued)

| Country | Sampling site | Methods | Bacteria | | | | Fungi | | | Ref. |
|---|---|---|---|---|---|---|---|---|---|---|
| | | | CFU/m$^3$ | Temp. [a] (℃) | Hum. [b] (%) | Dominant species | CFU/m$^3$ | Temp. (℃) | | |
| Poland | Office rooms | 6-stage Andersen impactor | 13 ~ 4344 | Summer & Winter | *Micrococcus* spp. *Staphylococcus* sp. *Bacillus sphaericus* | 18 ~ 1689 | Summer | *Candida* sp. *Cladosporium herbarum* *Cladosporium sphaerospermum* *Myrothecium* sp. *Rhodotrula* sp. *Cladosporium cladosporioides* *Penicillium aurantiogriseum* | | [326] |
| | Healthy homes | 6-stage Andersen impactor | 182 ~ 7745 | | | 34 ~ 2924 | | | | |
| | Moldy homes | 6-stage Andersen impactor | 178 ~ 4751 | | | 49 ~ 16968 | | | | |
| China | University classrooms | Natural sedimentation method | 209 ~ 838 | 22±1.5 | 34±2 | - | - | - | - | [327] |
| | | Andersen sampler | 353 ~ 1932 | 22±1.5 | 34±2 | - | - | - | - | |
| USA | Office rooms | PBI SAS-Super ISO Air Sampler & Settled plates | 12 ~ 202 | Summer & Winter | Total mesophilic Legionella | 12 ~ 252 | Summer & Winter | | - | [328] |
| | Residential | | 8 ~ 298 | Summer | | 9 ~ 198 | Summer & Winter | | | |
| China | Roof of the university building | 6-stage Andersen Impactor | 498 ~ 1737 | Haze days & Non-haze days | *Staphylococcus* *Micrococcus* *Neisseria* | 247.6 ~ 1703.9 | Haze days & Non-haze days | | | [329] |
| Korea | Underground subway | 17G9 GilAir Sampler | 7 ~ 5583 | 27.9 ~ 29.6 | 46.5 ~ 53.3 | *Staphylococcus* spp. *Micrococcus* spp. | - | - | - | [52] |
| Taiwan | Flooded home | Burkard portable air sampler | - | - | - | - | 2841 ~ 41286 | - | *Aspergillus* spp. | [330] |

**Table A1.** (continued)

| Country | Sampling site | Methods | Bacteria | | | | Fungi | | | Ref. |
|---|---|---|---|---|---|---|---|---|---|---|
| | | | CFU/m³ | Temp. [a] (℃) | Hum. [b] (%) | Dominant species | CFU/m³ | Temp. (℃) | | |
| Taiwan | Patient room | 6-stage Andersen impactor | 2964 ~ 7236 | June & December | | *Bacillus cereus* *Micrococcus luteus* *Staphylococcus epidermidis* *Acinetobacter baumannii* | 5954 ~ 11654 | October & December | | [40] |
| Canada | Hospital | Cyclonic sampler<br>Andersen impactor | 40 ~ 580 | - | - | *Staphylococcus* spp. *Bacillus* *Micrococcus* *Corynebacterium* spp. | - | - | - | [331] |
| Portugal | Hospital (Operating theater) | MAS-100 air sampler | 12 ~ 170 | 30.1 | 43.8 | | - | - | - | [42] |
| | Hospital (Emergency service) | | 240 ~ 736 | 7.1 ~ 30.1 | 43.8 ~ 82.7 | *Staphylococcus* *Micrococcus* *Neisseria* | 27 ~ 933 | 7.1 ~ 31 | 43.8 ~ 82.7 | *Penicillium* spp. *Aspergillus* spp. *Cladosporium* spp. |
| | Hospital (Surgical ward) | | 99 ~ 495 | 7.1 ~ 30.1 | 43.8 ~ 82.7 | | 1 ~ 32 | 7.1 | 82.7 | |

[a] Temp.: Temperature
[b] Hum.: Humidity

# APPENDIX B: SUPPLEMENTARY INFORMATION OF CHPATER 2

**Table B1.** Bacterial percentage (%) on surfaces (restroom and skin) classified according to gender usage

| | Family [a] | Cor. | Mic. | Pro. | Fla. | Bac. | Sta. | Lac. | Str. | Bra. | Met. | Rho. | Sph. | Ent. | Mor. | Pse. | Ref. |
|---|---|---|---|---|---|---|---|---|---|---|---|---|---|---|---|---|---|
| Female | Restroom | 2.76 | 2.24 | 37.5 | 0.68 | 0.28 | 7.72 | 0.80 | 7.88 | 1.08 | 0.28 | 0.36 | 1.44 | 0.96 | 1.52 | 1.36 | [29] |
| | | 4.10 | 2.33 | 17.5 | 0.97 | 0.03 | 13.3 | 4.20 | 7.97 | 0.50 | 0.30 | 0.93 | 0.83 | 0.90 | 5.17 | 1.50 | |
| | | 3.50 | 3.30 | 20.2 | | 0.30 | 5.00 | 5.60 | 8.80 | 1.70 | 0.60 | 0.40 | 2.10 | 2.00 | 2.70 | 3.30 | |
| | | 2.15 | 2.05 | 32.6 | 0.35 | 0.20 | 7.85 | 12.9 | 7.35 | 0.70 | 0.10 | 0.25 | 0.70 | 3.50 | 1.15 | 0.60 | |
| | | 2.52 | 3.04 | 9.48 | 0.16 | | 2.36 | 2.60 | 2.76 | 0.24 | 0.24 | 0.84 | 14.4 | 0.12 | 19.0 | 1.36 | |
| | | 3.47 | 2.07 | 21.4 | 0.37 | 0.10 | 3.33 | 7.07 | 6.97 | 1.47 | 0.40 | 0.70 | 1.73 | 1.17 | 3.73 | 1.73 | |
| | | 8.53 | 2.43 | 1.70 | 0.33 | 0.03 | 2.37 | 20.3 | 1.20 | 0.53 | 0.50 | 0.17 | 1.93 | 0.33 | 3.70 | 2.40 | |
| | | 7.00 | 2.60 | 5.15 | 1.25 | 0.05 | 5.55 | 8.80 | 1.65 | 0.50 | 1.15 | 2.55 | 7.70 | 5.40 | 1.10 | 1.35 | |
| | | 1.73 | 8.83 | 5.53 | 1.93 | 0.07 | 1.00 | 1.03 | 1.67 | 0.73 | 1.10 | 4.30 | 3.87 | 1.60 | 9.77 | 1.50 | |
| | | 1.37 | 11.8 | 6.03 | 1.50 | 0.10 | 0.60 | 0.70 | 1.17 | 0.57 | 1.07 | 4.63 | 4.50 | 1.60 | 7.10 | 1.50 | |
| | Skin | 9.50 | | 24.5 | 1.10 | 1.70 | 6.70 | | 2.60 | | | 3.10 | 1.50 | 1.40 | 6.90 | 1.20 | [85] |
| | | 7.50 | | 6.20 | 2.00 | 1.90 | 7.10 | | 1.20 | | | 6.30 | 6.30 | 0.70 | 10.3 | 1.40 | |
| | | 7.80 | | 23.0 | 0.50 | 2.20 | 7.00 | | 3.50 | | | 3.70 | 3.70 | 1.20 | 7.60 | 1.20 | |
| | | | | 73.3 | | 1.10 | 3.30 | | | | | | | | 6.70 | 4.40 | [77] |
| | | 3.40 | | 64.3 | | | 27.6 | | 2.20 | | | | | | 1.10 | | |
| | | | | 73.5 | | 1.10 | 8.00 | | 1.10 | | | | | | 8.00 | | |
| | | 1.44 | 7.21 | 10.6 | 0.48 | | 3.37 | | 7.69 | | 1.92 | 0.480 | | | 5.77 | | [78] |
| | | 7.35 | 3.92 | 12.3 | | | 2.94 | 4.41 | 5.88 | | | | | 1.96 | 11.8 | 9.31 | |
| | | 26.2 | 3.47 | 12.4 | | | 16.8 | 2.48 | 5.94 | | | | | 0.50 | 14.4 | 2.97 | |
| Male | Restroom | 5.87 | 2.27 | 37.7 | 0.80 | 4.33 | 6.93 | 0.27 | 4.87 | 0.08 | 0.60 | 0.53 | 0.53 | 1.00 | 2.80 | 1.80 | [29] |
| | | 7.20 | 3.48 | 25.8 | 0.24 | 0.60 | 15.0 | 0.36 | 7.44 | 0.96 | 0.08 | 0.48 | 1.48 | 0.44 | 3.20 | 1.04 | |
| | | 6.80 | 3.90 | 17.1 | 0.90 | 0.05 | 3.70 | 0.05 | 3.90 | 1.05 | 0.40 | 2.10 | 2.20 | 0.45 | 4.55 | 1.00 | |
| | | 7.50 | 2.00 | 37.0 | 0.30 | 0.20 | 6.23 | 0.33 | 6.77 | 0.33 | 0.20 | 1.30 | 0.83 | 0.57 | 4.13 | 0.63 | |
| | | 15.1 | 9.17 | 28.9 | 0.57 | 0.03 | 4.80 | 1.27 | 4.33 | 0.23 | 0.23 | 0.90 | 0.67 | 0.87 | 5.10 | 1.40 | |
| | | 5.65 | 3.45 | 29.0 | 0.30 | 14.1 | 4.55 | 0.45 | 5.05 | 1.30 | 0.30 | 0.85 | 1.10 | 1.05 | 3.10 | 1.15 | |
| | | 27.4 | 0.56 | 4.08 | 0.32 | 0.04 | 2.24 | 0.48 | 0.76 | 0.48 | 0.12 | 0.40 | 0.48 | 0.24 | 0.36 | 0.24 | |
| | | 10.2 | 2.07 | 12.3 | 0.53 | 0.07 | 2.93 | 0.67 | 1.60 | 1.17 | 0.30 | 0.67 | 4.07 | 0.27 | 0.97 | 0.60 | |
| | | 1.90 | 9.23 | 5.53 | 1.43 | 0.10 | 1.17 | 0.47 | 1.13 | 0.37 | 0.93 | 3.33 | 3.27 | 1.00 | 11.1 | 0.83 | |
| | | 1.73 | 10.2 | 5.23 | 3.00 | 0.20 | 0.87 | 0.43 | 1.03 | 1.03 | 1.07 | 3.33 | 3.40 | 0.73 | 11.5 | 2.67 | |
| | Skin | 13.2 | | 29.6 | 0.60 | 1.80 | 6.80 | | 2.10 | | | 2.10 | 2.10 | 1.10 | 4.30 | 0.90 | [85] |
| | | 15.5 | | 19.6 | 2.20 | 2.90 | 5.50 | | 1.50 | | | 2.60 | 2.60 | 0.70 | 10.0 | 0.40 | |
| | | 11.1 | | 18.0 | 0.70 | 2.40 | 7.30 | | 4.90 | | | 4.20 | 4.20 | 1.20 | 7.00 | 1.10 | |
| | | | | 85.2 | | 1.60 | | | | 0.240 | | | | | | | [77] |
| | | | | 25.3 | | | 8.80 | | | | | | | | 2.20 | 1.10 | |
| | | 44.6 | 1.47 | 14.7 | | | 18.6 | | 1.96 | | | | | | 4.90 | | [78] |
| | | 21.2 | 1.97 | 23.2 | | | 15.8 | 0.99 | 10.8 | | | | | | 0.49 | 2.96 | |
| | | 13.5 | 1.00 | 59.5 | | | 9.50 | | 2.50 | | | | | | 1.50 | 1.00 | |

[a] Cor.: *Corynebacteriaceae*, Der.: *Dermabacteraceae*, Mic.: *Micrococcaceae*, Pro.: *Propionibacteriaceae*, Fla.: *Flavobacteriaceae*, Ali.: *Alicyclobacillaceae*, Bac.: *Bacillaceae*, Sta.: *Staphylococcaceae*, Lac.: *Lactobacillaceae*, Str.: *Streptococcaceae*, Bra.: *Bradyrhizobiaceae*, Met.: *Methylobacteriaceae*, Rho.: *Rhodobacteraceae*, Sph.: *Sphingomonadaceae*, Ent.: *Enterobacteriaceae*, Mor.: *Moraxellaceae*, and Pse.: *Pseudomonadaceae*

**Table B2.** Bacterial percentage (%) in air samples from literature review

| Family | Cor. | Der. | Mic. | Pro. | Fla. | Ali. | Bac. | Sta. | Lac. | Str. | Bra. | Met. | Rho. | Sph. | Ent. | Mor. | Pse. | Ref. |
|---|---|---|---|---|---|---|---|---|---|---|---|---|---|---|---|---|---|---|
| Residence | 0.63 | 1.90 | 43.4 | | 0.47 | | 14.6 | 12.0 | | 0.32 | | | 0.32 | | | 2.06 | 1.42 | [33] |
| | 4.00 | | 1.00 | 14.0 | | 6.00 | | 4.00 | | | 1.00 | 4.00 | 1.00 | 4.00 | 1.00 | 2.00 | 2.00 | [34] |
| Hospital | 7.00 | | 16.7 | | | | 8.60 | 58.1 | 1.30 | 0.50 | | | | | | | | [39] |
| | 5.20 | | 32.4 | | | | 6.60 | 44.8 | | | | | | | | | | |
| | | | 6.00 | | 4.00 | | | 53.0 | | | | | | | | 4.00 | 10.0 | [40] |
| | | | 12.0 | | | | 29.0 | 18.0 | | | | | | | | 12.0 | | |
| | | | 4.00 | | | | 25.0 | 21.0 | | | | | | | | 42.0 | | |
| | | | 2.00 | | 2.00 | | 8.00 | 55.0 | | | | | | | | 2.00 | 2.00 | |
| | 7.00 | | 16.7 | | | | 8.60 | 58.1 | 1.30 | 0.50 | | | | | 0.80 | | | [41] |
| | 7.40 | | 13.4 | | | | 8.90 | 57.4 | 1.50 | 1.50 | | | | | 1.50 | | | |
| | 11.6 | | 17.1 | | | | 15.0 | 44.7 | 2.40 | 1.70 | | | | | 1.00 | | | |
| | 22.9 | | 21.1 | | | | 8.30 | 43.6 | 1.40 | 0.50 | | | | | 0.50 | | | |
| | | | 42.0 | | | | | 51.0 | | | | | | | 0.10 | | | [42] |
| | | | 23.0 | | | | | 55.0 | | | | | | | 1.00 | | | |
| | | | 45.0 | | | | | 35.0 | | | | | | | | | | |
| | | | 39.0 | | | | | 39.0 | | | | | | | | | | |
| | | | 31.0 | | | | | 62.0 | | | | | | | | | | |
| | | | | | | | | 51.6 | | | | | | | | | | [43] |
| | | | | | | | | 47.8 | | | | | | | | | | |
| | | | 13.7 | | | | 14.7 | 43.8 | | | | | | | | | | [44] |
| Office | | | 18.0 | | 2.80 | | 2.80 | 16.5 | | | | | | | 0.03 | 0.10 | 4.00 | [36] |
| | | | 39.7 | | | | 23.6 | 10.4 | | | | | | | | | | [37] |
| | | | | | | | 23.1 | 15.4 | | | | | | | | | | [38] |
| Elementary school | 20.4 | | 6.90 | 2.40 | | | 6.90 | 44.4 | 1.40 | 2.30 | | | | | 0.20 | 7.00 | 1.10 | [45] |
| | 16.3 | | 22.2 | 0.62 | | | 10.2 | 43.1 | | 0.92 | | | | | | 3.07 | 0.62 | [46] |
| | 4.00 | | 12.7 | 1.18 | | | 3.06 | 65.4 | | 4.71 | | | | | 0.47 | 1.41 | 0.24 | |
| | 6.20 | | 10.8 | 1.89 | | | 6.47 | 63.1 | | 6.47 | | | | | | | | |
| | 1.43 | | 14.3 | 1.43 | | | 8.21 | 61.8 | | 7.50 | | | | | | 0.71 | | |
| | 3.40 | 0.50 | 18.8 | 1.20 | | | 2.40 | 5.30 | 0.30 | 5.70 | | 0.90 | 8.00 | 1.20 | 0.30 | 7.30 | 0.80 | [47] |
| | 3.10 | 0.40 | 14.0 | 0.90 | | | 1.00 | 4.20 | 0.30 | 2.90 | | 2.30 | 3.30 | 1.70 | 0.30 | 6.80 | 1.10 | |
| | 8.40 | | 65.6 | | | | 4.30 | 16.2 | | 2.10 | | | | | | | | [39] |
| | 0.50 | | 0.60 | | 1.30 | | 12.4 | 3.10 | 4.60 | | | | | 0.45 | 5.58 | | 2.40 | [48] |
| | 2.30 | | 1.00 | | 5.20 | | 10.8 | 3.30 | 3.10 | | | | | | 5.20 | | 1.70 | |
| | 2.00 | | 2.10 | | 1.30 | | 14.1 | 4.40 | 5.20 | | | | | | 10.1 | | 2.70 | |

**Table B2.** (continued)

| Family | Cor. | Der. | Mic. | Pro. | Fla. | Ali. | Bac. | Sta. | Lac. | Str. | Bra. | Met. | Rho. | Sph. | Ent. | Mor. | Pse. | Ref. |
|---|---|---|---|---|---|---|---|---|---|---|---|---|---|---|---|---|---|---|
| University | | | 15.1 | | 8.00 | | 0.50 | 17.1 | | | | | | | | | 7.10 | [36] |
| | | | 18.0 | | 2.80 | | 2.80 | 16.5 | | | | | | | 0.03 | 0.10 | 4.00 | |
| | | | 7.10 | | 3.70 | | 1.20 | 32.6 | | | | | | | | | 6.40 | |
| | | | 13.7 | | 1.20 | | 8.60 | 15.4 | | | | | | | 0.10 | 0.10 | 7.20 | |
| | | | 9.30 | | 4.30 | | 3.60 | 35.0 | | | | | | | | | | |
| | | | 23.7 | | 2.50 | | 1.30 | 10.3 | | | | | | | | | 3.70 | |
| | | | 15.8 | | 7.70 | | 1.30 | 32.0 | | | | | | | | | 5.10 | |
| | | | 9.70 | | 2.00 | | 1.30 | 16.2 | | | | | | | | | 1.30 | |
| | 1.40 | | 37.6 | | | | 0.80 | 55.0 | | 0.80 | | | | | | | | |
| | 7.10 | | 12.6 | | | | 5.40 | 44.3 | | | | | | | | | | |
| | | | 42.4 | | | | 12.8 | 22.0 | | | | | | | | | 1.20 | [79] |
| | | | 15.8 | | | | 34.8 | 27.1 | | | | | | | | | | |
| | 1.00 | | 26.3 | | | | 4.70 | 48.9 | | 0.60 | | | | | | | | |
| | | | | | | | | | | | | | | 4.10 | | 2.30 | | [57] |
| | | | 7.00 | | | | 35.0 | | | 13.0 | | | | | | | | [70] |
| | | | 15.0 | | | | 40.0 | | | 16.0 | | | | | | | | |
| | | | 23.7 | | 2.50 | | 1.30 | 10.3 | | | | | | | | | 3.70 | [36] |
| | 6.20 | 11.4 | 58.0 | | | | 7.40 | 15.8 | | | | | | | | | | [50] |
| | 3.50 | | 30.0 | | | | 17.0 | 18.0 | | 0.90 | | | | | | 3.00 | 14.0 | [49] |
| Public buildings [a] | 13.3 | | | 5.10 | | | 0.90 | 1.90 | | | | 8.30 | | 1.40 | | 0.90 | 3.20 | [51] |
| | 4.90 | | 0.20. | 2.30 | | | 3.60 | 0.80 | | | | 17.6 | 0.20 | 4.30 | 0.30 | | 1.00 | |
| | 1.30 | | | 0.20 | | | 0.90 | 0.20 | | | | 71.2 | 0.10 | 1.30 | 0.20 | 0.40 | 8.80 | |
| | 2.20 | | 3.60 | 0.30 | | | 0.80 | 0.20 | | | | 0.10 | 1.90 | 7.00 | 5.90 | 19.6 | 4.50 | |
| | 3.20 | | 5.10 | 1.30 | | | 1.40 | 1.30 | | | | 5.90 | 2.70 | 2.60 | 3.20 | 4.50 | 5.40 | |
| | 3.60 | | 4.70 | 3.50 | | | 2.70 | 1.20 | | | | 8.90 | 0.40 | 3.40 | 0.200 | 2.80 | 2.10 | |
| | 4.90 | | 2.90 | 1.60 | | | 1.00 | 4.30 | | | | 8.60 | 1.10 | 3.60 | 4.30 | 3.00 | 4.50 | |
| | 7.30 | | 4.30 | 0.90 | | | 1.60 | 3.60 | | | | 9.50 | 1.00 | 0.90 | | 0.50 | 0.90 | |
| | | | | | | | | | | | | 94.5 | | | | | | |
| | 6.00 | | 1.20 | 0.80 | | | 1.30 | 0.60 | | | | 6.50 | 4.20 | 2.20 | 0.60 | 15.3 | 4.00 | |
| | | | | 0.10 | | | 0.20 | | | | | 84.1 | | 0.90 | 0.60 | 0.10 | 1.00 | |
| | 6.80 | | 2.40 | 0.50 | | | 0.50 | 2.00 | | | | 2.10 | 0.60 | 2.80 | 4.60 | 8.00 | 6.70 | |
| | 2.00 | | 1.70 | 2.30 | 1.20 | | 8.90 | 1.70 | | | | 2.30 | 0.40 | 1.90 | 2.80 | 9.60 | 4.70 | |
| | 1.90 | | 2.50 | 0.30 | 1.20 | | 2.60 | 0.40 | | | | 5.60 | 2.20 | 3.90 | 2.40 | 11.4 | 5.70 | |
| | 13.9 | | 0.90 | 2.20 | 22.1 | | 0.30 | 1.10 | | | | 18.8 | 3.70 | 4.20 | 0.40 | 0.70 | 1.00 | |
| | 1.00 | | 1.70 | 1.50 | | | 2.70 | 1.10 | | | | 5.20 | 0.80 | 2.80 | 0.80 | 1.90 | 24.1 | |
| | 10.3 | | 5.90 | 1.20 | 0.20 | | 4.20 | 5.30 | | | | 0.50 | 1.30 | 2.70 | 3.50 | 5.00 | 5.60 | |
| | 1.70 | | 1.70 | | 0.10 | | 71.6 | 0.40 | | | | 1.00 | 0.30 | 0.10 | 0.30 | 0.50 | 0.10 | |
| | 0.80 | | | | 0.40 | | 5.50 | 0.10 | | | | 74.9 | | 1.80 | 0.50 | 0.10 | 1.00 | |

**Table B2.** (continued)

| Family | Cor. | Der. | Mic. | Pro. | Fla. | Ali. | Bac. | Sta. | Lac. | Str. | Bra. | Met. | Rho. | Sph. | Ent. | Mor. | Pse. | Ref. |
|---|---|---|---|---|---|---|---|---|---|---|---|---|---|---|---|---|---|---|
| | 13.3 | | 3.40 | 1.50 | | | 1.20 | 4.70 | | | | 10.8 | 0.70 | 4.70 | 0.80 | 2.40 | 2.10 | |
| | 1.40 | | 0.20 | 2.70 | | | 9.20 | 0.40 | | | | 1.80 | 0.90 | 8.60 | 2.40 | 0.30 | 10.9 | |
| | 1.00 | | 0.30 | 0.10 | | | 5.50 | 1.00 | | | | 9.00 | 1.60 | 4.30 | 0.90 | 1.10 | 2.00 | |
| | 23.0 | | | | | | 4.00 | 4.00 | | | | | | 10.0 | | 14.0 | | |
| | | | | | | | | 100 | | | | | | | | | | |
| | | | 67.0 | | | | | 7.00 | | | | | | 7.00 | | | | |
| | | | | | | | | 8.00 | | | | | | 8.00 | | 8.00 | | |
| | | | | | | | | 33.0 | | | | | | | | | | [52] |
| | | | | | | | | 60.0 | | | | | | | | | | |
| | | | | | | | | 33.0 | | | | | | | | 11.0 | | |
| | | | | | | | | | | | | | | 100 | | | | |
| | 19.0 | | | | | | | | | | | | | | | | | |
| | | | 42.6 | 2.00 | | | 5.60 | 24.1 | | | | | | | | 11.1 | 1.90 | |
| | | | 65.0 | 9.02 | | | 2.20 | | | | | | | | | 5.10 | 8.80 | |
| | | | 65.3 | 10.8 | | | 1.10 | 5.30 | | | | | 2.10 | | | 6.30 | 10.5 | |
| | | | 59.5 | 9.09 | | | 13.5 | | | | | | | 2.70 | | 8.10 | | [71] |
| | | | 68.0 | | | | 4.00 | 20.0 | | | | | | | | | | |
| | | | 73.8 | | 1.00 | | 5.80 | 8.70 | | | | | | | | 3.90 | 1.00 | |
| | | | 35.3 | | | | 1.00 | 3.80 | | | | | | | | 6.70 | | |
| | | | 50.0 | | | | 2.20 | | | | | | | 6.50 | | 19.6 | 6.50 | |

[a] Public buildings include auditorium, museum, retail store, subway station, and restaurant

**Table B3.** Bacterial percentage (%) in surface samples from literature review

| Family | Cor. | Der. | Mic. | Pro. | Fla. | Ali. | Bac. | Sta. | Lac. | Str. | Bra. | Met. | Rho. | Sph. | Ent. | Mor. | Pse. | Ref. |
|---|---|---|---|---|---|---|---|---|---|---|---|---|---|---|---|---|---|---|
| Residence | 4.00 | | | 11.0 | | 1.00 | | 2.00 | | | | 30.0 | | 5.00 | | | 2.00 | [34] |
| | 5.00 | | | 16.0 | | | | 14.0 | | | 1.00 | 1.0 | | 4.00 | | 2.00 | 2.00 | |
| | 2.00 | | 6.00 | 1.00 | | | | 1.00 | | | | 1.0 | | 5.00 | | 6.00 | 23.00 | |
| | 4.00 | | | 5.00 | | | | 1.00 | | | | 2.0 | 1.00 | 10.0 | | 1.00 | 2.00 | |
| | 5.00 | | | 8.00 | | | | 13.0 | | | | 1.0 | 1.00 | 6.00 | | 2.00 | 3.00 | |
| | | | 1.00 | 2.00 | | | | 1.00 | | | | | | 1.00 | | 4.00 | 23.00 | |
| | 2.00 | | | 15.0 | | 6.00 | | 1.00 | | | | 17.0 | | 10.0 | | | | |
| | 1.00 | | | 20.0 | | 16.0 | | 2.00 | | | 3.00 | 11.0 | | 5.00 | 2.00 | | 1.00 | |
| | 3.00 | | | | | | | | | | | 3.0 | 2.00 | 1.00 | 2.00 | 1.00 | 1.00 | |
| | | | 17.0 | | | | | | | | | | | | | | | |
| | | 32.0 | 26.3 | | | | | | | | | | | | | 33.00 | | |
| | | | 35.7 | | 13.0 | | | | | | | | | 9.30 | | 28.70 | | |
| | | | 20.0 | | | | | | | | | | | | | 50.00 | 5.70 | |
| | | | 33.0 | | | | | | | | | | | | | 62.30 | | |
| | | 30.0 | 48.3 | | | | | | | | | | | | | 8.30 | | |
| | | | 50.0 | | | | | | | | | | | 22.3 | | 16.70 | | |
| | | 39.5 | 35.5 | | | | | | | | | | | | 25.0 | | | |
| Hospital | | | | | | | | | | | | | | | | 24.00 | | [81] |
| | | | | 7.00 | 0.00 | | | | | | 16.0 | | | | | 3.00 | 4.00 | |
| | | | | 5.00 | 0.00 | | | | | | 17.0 | | | | | 2.00 | 7.00 | |
| | | | 2.36 | | 4.02 | 4.35 | | | | 1.42 | | | | | | 13.00 | 0.03 | [84] |
| | 0.35 | | 3.13 | 1.98 | 4.00 | 8.62 | 0.07 | | 0.32 | 3.48 | | | | 0.09 | | 19.10 | 0.03 | |
| Fitness center | | | 5.20 | | | | | 20.0 | 1.30 | | | | | | 72.5 | | | [82] |
| | | | | | | | | 6.80 | | | | | | | 32.8 | | | |
| | | | 2.00 | | | | | 52.7 | | | | | | | 44.9 | | | |
| | | | | | | | | 99.8 | | | | | | | | | | |
| | | | | | | | 84.5 | 13.6 | 1.80 | | | | | | | | | |
| | | | | | | | | 17.7 | | | | | | | 11.5 | | 6.30 | |
| | | | | | | | 7.10 | 3.70 | | | | | | | 14.7 | | 2.40 | |
| | | | | | | | 0.30 | 48.0 | | | | | | | 50.5 | | | |
| | | | | | | | | 32.6 | | | | | | | 66.3 | | | |

**Table B3.** Bacterial (continued)

| Family | Cor. | Der. | Mic. | Pro. | Fla. | Ali. | Bac. | Sta. | Lac. | Str. | Bra. | Met. | Rho. | Sph. | Ent. | Mor. | Pse. | Ref. |
|---|---|---|---|---|---|---|---|---|---|---|---|---|---|---|---|---|---|---|
| Museum | 3.50 | | 18.8 | | | | 59.0 | 18.7 | | | | | | | | | | [50] |
| | 1.20 | 0.90 | 45.5 | | | | 41.3 | 10.3 | | | | | | | | | | |
| Mobile device | | | 8.65 | | | | 4.33 | 51.9 | 4.33 | 6.73 | | | | | 0.48 | 2.40 | 0.48 | [83] |
| | | | 5.66 | | | | 2.52 | 52.8 | 9.43 | 10.7 | | | | | 0.63 | 1.26 | 0.63 | |
| | | | 3.00 | | | | 5.15 | 57.5 | 6.01 | 4.72 | | | | | 0.86 | 2.15 | 1.29 | |
| | | | 5.20 | | | | 4.09 | 48.4 | 5.98 | 8.19 | | | | | 1.89 | 0.79 | 0.47 | |

**Table B4.** Bacterial percentage (%) from air and surfaces classified according to age

| Family | | Cor. | Der. | Mic. | Pro. | Fla. | Ali. | Bac. | Sta. | Lac. | Str. | Bra. | Met. | Rho. | Sph. | Ent. | Mor. | Pse. | Ref. |
|---|---|---|---|---|---|---|---|---|---|---|---|---|---|---|---|---|---|---|---|
| Children | Air | 20.4 | | 6.90 | 2.40 | | | 6.90 | 44.4 | 1.40 | 2.30 | | | | | 0.20 | 7.00 | 1.10 | [45] |
| | | 16.3 | | 22.2 | 0.62 | | | 10.2 | 43.1 | | 0.92 | | | | | | 3.07 | 0.62 | [46] |
| | | 4.00 | | 12.7 | 1.18 | | | 3.06 | 65.4 | | 4.71 | | | | | 0.47 | 1.41 | 0.24 | |
| | | 6.20 | | 10.8 | 1.89 | | | 6.47 | 63.1 | | 6.47 | | | | | | | | |
| | | 1.43 | | 14.3 | 1.43 | | | 8.21 | 61.8 | | 7.50 | | | | | | 0.71 | | |
| | | 3.40 | 0.50 | 18.8 | 1.20 | | | 2.40 | 5.30 | 0.30 | 5.70 | | 0.90 | 8.00 | 1.20 | 0.30 | 7.30 | 0.80 | [47] |
| | | 3.10 | 0.40 | 14.0 | 0.90 | | | 1.00 | 4.20 | 0.30 | 2.90 | | 2.30 | 3.30 | 1.70 | 0.30 | 6.80 | 1.10 | |
| | | 8.40 | | 65.6 | | | | 4.30 | 16.2 | | 2.10 | | | | | | | | [39] |
| | | 0.50 | | 0.60 | | 1.30 | | 12.4 | 3.10 | 4.60 | | | | | 0.45 | 5.58 | | 2.40 | [48] |
| | | 2.30 | | 1.00 | | 5.20 | | 10.8 | 3.30 | 3.10 | | | | | | 5.20 | | 1.70 | |
| | | 2.00 | | 2.10 | | 1.30 | | 14.1 | 4.40 | 5.20 | | | | | | 10.1 | | 2.70 | |
| | Skin | 7.80 | | | 23.0 | 0.50 | | 2.20 | 7.00 | | 3.50 | | | 3.70 | 3.70 | 1.20 | 7.60 | 1.20 | [85] |
| | | 11.1 | | | 18.0 | 0.70 | | 2.40 | 7.30 | | 4.90 | | | 4.20 | 4.20 | 1.20 | 7.00 | 1.10 | |
| | | 9.02 | | | 1.57 | | | | 18.7 | | 18.9 | | | | | | | 2.52 | [80] |
| | | 5.86 | | | 2.03 | | | | 28.9 | | 23.2 | | | | | | | 0.77 | |
| | | 1.34 | | | 5.54 | | | | 7.15 | | 27.1 | | | | | | | 2.52 | |
| | | 3.31 | | | 6.96 | | | | 29.7 | 1.46 | 34.1 | | | | | | | | |
| | | 3.55 | | | 12.8 | | | | 12.2 | 1.30 | 39.4 | | | | | | | | |
| | | 3.75 | | | 4.93 | | | | 6.17 | 0.97 | 29.6 | | | | | | | | |
| | | | | | | | | | 9.87 | 6.10 | 5.84 | | | | | | | | |
| | | | | | | | | | 6.47 | 4.36 | 12.0 | | | | | | | | |
| | | | | | | | | | 10.1 | 2.25 | 6.86 | | | | | | | | |
| Adult | Air | 3.00 | | 53.1 | | | | 9.40 | 26.7 | 3.60 | | | | | | | | | [39] |
| | | | | 15.1 | | 8.00 | | 0.50 | 17.1 | | | | | | | | | 7.10 | [36] |
| | | | | 18.0 | | 2.80 | | 2.80 | 16.5 | | | | | | | 0.03 | 0.10 | 4.00 | |
| | | | | 7.10 | | 3.70 | | 1.20 | 32.6 | | | | | | | | | 6.40 | |
| | | | | 13.7 | | 1.20 | | 8.60 | 15.4 | | | | | | | 0.10 | 0.10 | 7.20 | |
| | | | | 9.30 | | 4.30 | | 3.60 | 35.0 | | | | | | | | | | |
| | | | | 23.7 | | 2.50 | | 1.30 | 10.3 | | | | | | | | | 3.70 | |
| | | | | 15.8 | | 7.70 | | 1.30 | 32.0 | | | | | | | | | 5.10 | |
| | | | | 9.70 | | 2.00 | | 1.30 | 16.2 | | | | | | | | | 1.30 | |
| | | 1.40 | | 37.6 | | | | 0.80 | 55.0 | | 0.800 | | | | | | | | [79] |
| | | 7.10 | | 12.6 | | | | 5.40 | 44.3 | | | | | | | | | | |
| | | | | 42.4 | | | | 12.8 | 22.0 | | | | | | | | | 1.20 | |
| | | | | 15.8 | | | | 34.8 | 27.1 | | | | | | | | | | |
| | | 1.00 | | 26.3 | | | | 4.70 | 48.9 | | 0.600 | | | | | | | | |
| | | | | | | | | | | | | | | | 4.10 | | 2.30 | | [57] |
| | | | | 7.00 | | | | 35.0 | | | 13.0 | | | | | | | | [70] |
| | | | | 15.0 | | | | 40.0 | | | 16.0 | | | | | | | | |

**Table B4.** Bacterial (continued)

| Family | Cor. | Der. | Mic. | Pro. | Fla. | Ali. | Bac. | Sta. | Lac. | Str. | Bra. | Met. | Rho. | Sph. | Ent. | Mor. | Pse. | Ref. | Family |
|---|---|---|---|---|---|---|---|---|---|---|---|---|---|---|---|---|---|---|---|
| | | 9.50 | | | 24.5 | 1.10 | | 1.70 | 6.70 | | 2.60 | | | 3.10 | 1.50 | 1.40 | 6.90 | 1.20 | |
| | | 7.50 | | | 6.20 | 2.00 | | 1.90 | 7.10 | | 1.20 | | | 6.30 | 6.30 | 0.70 | 10.3 | 1.40 | [85] |
| | | 13.2 | | | 29.6 | 0.60 | | 1.80 | 6.80 | | 2.10 | | | 2.10 | 2.10 | 1.10 | 4.30 | 0.90 | |
| | | 15.5 | | | 19.6 | 2.20 | | 2.90 | 5.50 | | 1.50 | | | 2.60 | 2.60 | 0.70 | 10.0 | 0.40 | |
| | | | | | 85.2 | | | 1.60 | | | | 0.240 | | | | | | | |
| | | | | | 73.3 | | | 1.10 | 3.30 | | | | | | | | 6.70 | 4.40 | [77] |
| | | | | | 25.3 | | | | 8.80 | | | | | | | | 2.20 | 1.10 | |
| | Skin | 3.40 | | | 64.3 | | | | 27.6 | | 2.20 | | | | | | 1.10 | | |
| | | | | | 73.5 | | | 1.10 | 8.00 | | 1.10 | | | | | | 8.00 | | |
| | | 1.44 | | 7.21 | 10.6 | 0.48 | | | 3.37 | | 7.69 | | 1.92 | 0.480 | | | 5.77 | | |
| | | 7.35 | | 3.92 | 12.3 | | | | 2.94 | 4.41 | 5.88 | | | | | 1.96 | 11.8 | 9.31 | |
| | | 26.2 | | 3.47 | 12.4 | | | | 16.8 | 2.48 | 5.94 | | | | | 0.50 | 14.4 | 2.97 | [78] |
| | | 44.6 | | 1.47 | 14.7 | | | | 18.6 | | 1.96 | | | | | | 4.90 | | |
| | | 21.2 | | 1.97 | 23.2 | | | | 15.8 | 0.99 | 10.8 | | | | | | 0.49 | 2.96 | |
| | | 13.5 | | 1.00 | 59.5 | | | | 9.50 | | 2.50 | | | | | | 1.50 | 1.00 | |

# APPENDIX C. IRB EXEMPT FOR CHAPTER 3

UNIVERSITY OF
SOUTH CAROLINA

OFFICE OF RESEARCH COMPLIANCE

**INSTITUTIONAL REVIEW BOARD FOR HUMAN RESEARCH**
**DECLARATION of NOT HUMAN SUBJECTS**

Shamia Hoque
300 Main Street
Columbia, SC 29208

Re: **Pro00117130**

Dear Dr. Shamia Hoque:

This is to certify that Research Proposal entitled ***Occupants, activities, and distance from vents influence presence, quantity and spatial distribution of particles, and microbes from indoor and outdoor sources in school buildings*** was reviewed on **11/19/2021** by the Office of Research Compliance, an administrative office that supports the University of South Carolina Institutional Review Board (USC IRB). The Office of Research Compliance, on behalf of the Institutional Review Board, has determined that the referenced study meets the Not Human Subject criteria set forth by the Code of Federal Regulations (45 CFR 46) of:

a. the specimens and/or private information/data were not collected specifically for the currently proposed research project through an interaction/intervention with living individuals AND

b. the investigator(s) including collaborators on the proposed research cannot readily ascertain the identity of the individual(s) to whom the coded private information or specimens pertain

No further oversight by the USC IRB is required; however, the investigator should inform the Office of Research Compliance prior to making any substantive changes in the research methods, as this may alter the status of the project.

If you have questions, contact Lisa M. Johnson at lisaj@mailbox.sc.edu or (803) 777-6670.

Sincerely,

Lisa M. Johnson
ORC Assistant Director and IRB Manager

# APPENDIX D. MATHEMATICAL MODEL SIMULATING FUNGAL AND BACTERIAL GROWTH ON SURFACES IN INDOOR SPACES [5]


## ABSTRACT

The growth and persistence of microbes on indoor surfaces is influenced by various properties such as temperature, surface characteristics, material type and microbial characteristics. Although studies about microbial attachment have been conducted in many different fields, study of surface microbial behavior is still insufficient to interpret how microorganisms interact with the indoor surfaces and predict temporal and spatial changes. This study simulates the fungal and bacterial growth of selected microbe: *E. coli*, *Staphylococcus* aureus, *Micrococcus*, and *Bacillus* for bacteria and *Aspergillus* and *Penicillium* for fungi. Surface properties and microbial characteristics are expressed as a function of an attachment fraction. The results show the change of bacterial density is influenced by the microbial growth and decay rate. The attachment fraction plays a dominant role. Temperature and humidity are significant factors for fungal growth. The optimum temperature and relative humidity value for fungal growth were 30℃ and 90%, respectively.



*Keywords: Microbial adhesion, surface roughness, building environment, indoor, diffusion*


[5] Seong, D. & Hoque, S.
Results in this chapter presented in Indoor Air Conference 2018, Philadelphia, Pennsylvania, USA

## D.1. INTRODUCTION

Microbial contamination on different surfaces is influenced by various properties such as temperature, type of surface materials (plastic, glass, stainless steel, or wood), surface characteristics (hydrophobicity, charge, or roughness), and microbial characteristics (hydrophobicity, flagellation or motility) [218, 332]. The basic process of bacterial attachment on the surface is a physicochemical process. The first step is a physical attachment which is a reversible interaction between the bacterial cell and the contact material surface. The second step is a chemical interaction between the microbial cell structures and molecules on the contact material surfaces [218].

Microbial attachment on the surfaces has been studied in various fields. Dental researchers evaluated the impact of surface characteristics on the bacterial adhesion of zirconia-porcelain veneer or implant [267, 318]. A study of attachment characterization of microorganisms was investigated to prevent bacterial regrowth and survival in food containers [333, 334]. Higher number of microorganisms attached on the plastic surface (polyethylene) than galvanized steel as plastic containers encouraged the bacterial attachment by supplying enough nutrients for bacterial growth [333]. Similar results were reported with higher spore attachment rate on plastic surfaces compared to steel surfaces with a working ventilation system [335]. It was also reported that bacterial adhesion patterns on the glass materials changed depending on the bacterial strains and surface characteristics [170]. Recent study examined bacterial re-aerosolization under different environmental conditions. Jana S. Kesavan and her colleagues [171] found that attached bacterial spores were affected by the relative humidity and bacterial characteristics

(existence of exosporium, hair, or basal layer). Lower humidity levels caused higher re-aerosolization and also dry-deposited particles showed more resuspension than wet-deposited particles [171].

Humidity also plays a significant role in fungal growth and persistence in indoor spaces. Fungi was commonly detected in damped environments such as water damaged places [66, 336]. An environmental assessment conducted by Riggs *et al.*[337] in Greater New Orleans after the hurricanes revealed nearly 44% homes had visible mold growth with *Aspergilli* and *Penicillium* being the dominant fungal species. Significant increases in *Aspergilli* species were also reported in homes flooded in southern Taiwan after extreme rainfall due to Typhoon Morakat [338]. Exposure to dampness becomes more significant if the concerned building is used by vulnerable population (*e.g.,* schools). Predominant indoor fungi are *Aspergillus*, *Penicillium, Cladosporium* and *Alternaria* [45].

The diversity of the microbiome in the indoor air and the influence of built environment characteristics, air quality parameters, human impact on it continues to be investigated [57, 71, 339]. However, we do not know or cannot predict how specific changes either in air quality parameters such as temperature or humidity or in design parameters such as surface type will influence the growth of specific bacteria or fungi. Being able to quantify such changes can have immediate impacts in areas such as remediation after flooding. This paper builds a mathematical model to quantify the influence of indoor air parameters and surface characteristics on fungal and bacterial growth.

## D.2. MATERIALS AND METHODS

### D.2.1. Model description

The model accounts for attachment of the microbe, growth/decay and transport. The attachment process is influenced by the surface characteristics which are surface roughness, porosity or morphology, or microbial characteristics which are mobility, flexibility, or hydrophilicity [170, 171]. **Table D1** shows the response and predictor variables. Bacterial and fungal density are the response variables. The predictor variables are the microbial growth and decay rate, time, microbial diffusivity, and fraction of attached microbes.

**Table D1.** Model parameters

| Classification | Parameter | Description | Unit |
|---|---|---|---|
| Response variables | $M_b$ | Bacterial density | g/cm$^3$ |
| | $M_u$ | Fungal density | g/cm$^3$ |
| Predictor variables | $B$ | Total bacterial density | g/cm$^3$ |
| | $U$ | Total fungal density | g/cm$^3$ |
| | $t$ | Time | h |
| | $\mu$ | Microbial growth rate | h$^{-1}$ |
| | $k_d$ | Bacterial decay rate | h$^{-1}$ |
| | $D_b$ | Bacterial diffusivity | cm$^2$/h |
| | $D_u$ | Fungal diffusivity | mm/h |
| | $f$ | Fraction of attached microbes | None |

The overall equation contains the function of attachment, growth and decay, and transport of microbes. The equation is as follows where *M* indicates either bacteria or fungi:

$$\frac{\partial M}{\partial t} = f(attachment, fate, and\ transport) \quad \text{Eq. D1}$$

There are two assumptions. The first assumption is that inactive (dead) microbes do not impact on the active ones. The second assumption is that nutrient is enough to grow

microbes, so that chemotaxis is not considered in for the 'bacteria' model. However, the second assumption is not considered in the 'fungus' model. Since microbial attachment is influenced by surface roughness and air flow rate, the number of attached microbes ($M_0$) will be described with arbitrary fraction ($f$) of suspending microbes ($M_s$).

$$M_0 = f \times M_s \qquad \text{Eq. D2}$$

The change of bacterial density on the surface can be described as follows where the bacterial growth and death is modeled as a first order reaction, $\chi$ is a chemotaxis coefficient, and $s$ is the concentration of nutrient:

$$\frac{\partial M_0}{\partial t} = \mu M_b - k_d M_b - D_b \nabla^2 b - \chi \nabla (b \nabla s) \qquad \text{Eq. D3}$$

The range of $D_b$ for the model is from $10^{-9}$~$10^{-11}$ $m^2/s$. The first and second terms on the right side describe microbial growth and decay rate, the third term represents the bacterial motility in the absence of chemotaxis (bacterial random walk), and the last term designates the bacterial flux resulted from chemotaxis [340, 341]. Since we assumed the absence of chemotaxis and that bacterial motility is described with only diffusivity, the last term is neglected for future calculations. Initial and boundary condition of the bacterial surface model are given in **Table D2**.

Fungal surface model for fate and transport is described with one-dimensional reaction diffusion model by Ito [342]. The equation is adopted as follows where $u$ is the density of the active fungus, $D_u$ is the diffusion coefficient of fungus, $n$ is the concentration of nutrients, and $\gamma$ is the death rate of fungus:

$$\frac{\partial M_u}{\partial t} = -D_u \nabla^2 u + f(u) - a(u)n - \gamma u \qquad \text{Eq. D4}$$

The first term on the right side describes the fungal random movement, the second term indicates the reaction and generation term, the third term shows the conversion from active to inactive fungus, and the last term describes the death rate of active fungi [342]. To estimate the impact of temperature and relative humidity, the following correlation is utilized:

$$\xi(T, \varphi) = a_1 \exp\left(a_2 \varphi^2 + a_3 T^2 + a_4 \varphi T + a_5 \varphi + a_6 T + a_7\right) \qquad \text{Eq. D5}$$

where, $T$ is temperature, $\varphi$ is relative humidity, and $a_n$ is model parameter. According to the analysis of Ito [342], the parameters in **Eq. D5** are: $a_1$ =0.840, $a_2$ =-132.403, $a_3$ =-0.009, $a_4$ =-0.943, $a_5$ =269.292, $a_6$ =1.350, and $a_7$ =-141.976. Initial and boundary condition of the fungal surface model are presented in **Table D2**. In absence of diffusion the change of microbial density can be determined from $M = M_0 \exp((\mu - k_d)t)$. However, combining the influence of diffusion and decay the aforementioned equations can be solved to obtain the mathematical forms shown in **Eqs. D6** and **D7** that predict bacterial and fungal density changes. The symbols $b_o$ and $u_o$ represent the initial bacterial and fungal densities.

$$M_b = b_0 \exp\big((\mu - k_d)t\big) - \frac{B}{2(\pi D_b t)^{1/2}} \exp\left(-\frac{x^2}{4 D_b t}\right) \qquad \text{Eq. D6}$$

$$M_u = u_0 \exp\big((\mu - k_d)t\big)\, \xi(T, \varphi) - \frac{U}{2(\pi D_u t)^{1/2}} \exp\left(-\frac{x^2}{4 D_u t}\right) \qquad \text{Eq. D7}$$

**Table D2.** Initial and boundary conditions

| Condition | Bacterial density | Distance | Time |
|---|---|---|---|
| Initial condition | $b = 0$<br>$u = 1$ | $0 \le x \le \mathrm{L}$ | $t = 0$ |
| Boundary condition | $b = b_0,\ u = u_0$ | $x = 0$ | $t = 0$ |
| | $\partial b/\partial x = 0,\ \partial u/\partial x = 0$ | $x = \mathrm{L}$ | $t \ge 0$ |

D.2.2. Microbial characteristics

The process of microbial attachment on the surfaces is influenced by the microbial characteristics. **Table D3** shows the microbial characteristics of the indoor microbes, *E. coli*, *Staphylococcus aureus*, *Micrococcus*, *Bacillus*, *Aspergillus*, and *Penicillium*. Bacteria have two types of shape, rod or cocci (sphere), and two different motilities, moving via flagella or fixed/floating on the surfaces. Fungi form conidiophores. Microbial growth and decay rates were obtained from the literature.

**Table D3.** Microbial characteristics

| Bacteria | Gram | Shape | Mobility | $\mu$ (/h) | $k_d$ (/h) | Ref. |
|---|---|---|---|---|---|---|
| *Escherichia coli* (*E. coli*) | (-) | Rod | Flagella | 0.37 | 0.084 | [268, 343, 344] |
| *Staphylococcus aureus* | (+) | Cocci | Nonmotile | 0.15 | 0.042[a] | [268, 345] |
| *Micrococcus* | (+) | Cocci | Nonmotile | 0.30 | 0.042 [a] | [346, 347] |
| *Bacillus subtilis* | (+) | Rod | Flagella | 0.35 | 0.0002 | [348, 349] |
| **Fungi** | | **Shape** | | **$\mu$ (/h)** | **$k_d$ (/h)** | **Ref.** |
| *Aspergillus* | | Conidiophores | | 0.148 | 0.042 [a] | [350] |
| *Penicillium* | | Conidiophores | | 0.123 | 0.042 [a] | [350] |

[a] arbitrary values

## D.3. RESULTS AND DISCUSSIONS

Bacterial behavior on the different surfaces is influenced depending on the surface conditions (roughness, hydrophobicity, or charge), surrounding indoor air quality parameters (temperature, humidity, or flow rate), and bacterial characteristics (hydrophobicity, flagellation, or motility). Surface conditions and microbial characteristics

are shown as attachment fraction ($f_{att}$) and multiplied by the number of suspended microbes in the ambient. For example, if a surface material holds all the attached microbes, the attachment fraction ($f_{att}$) is stated as 1.0. The fraction ($f_{att}$) differs depending on the surface materials, roughness, temperature, or humidity. This allows for incorporating different microbe – surface configurations into the models based on prior knowledge or simulate a required hypothetical scenario.

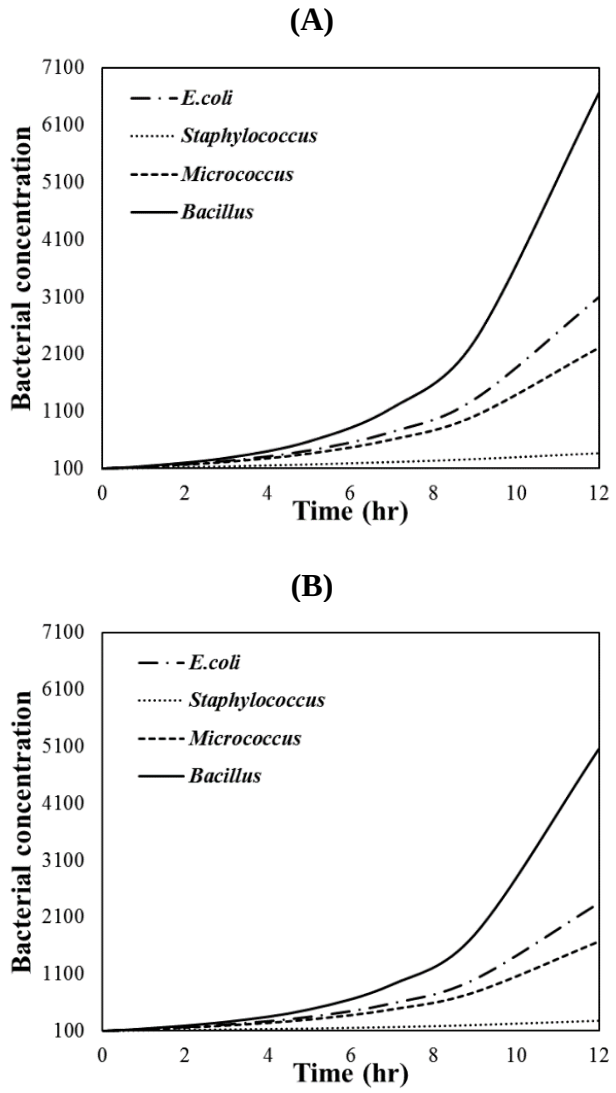


**Figure D1. (A)** The change of bacterial density if only bacterial growth and death are considered. **(B)** The change of bacterial density when the bacterial growth/death and diffusion are considered.

**Figure D1** shows the change of bacterial concentration over time when the number of air-borne bacteria near the surface is set as a hundred and all the bacteria attach onto the surface ($f_{att}$ = 1.0). This represents a scenario where boundary conditions near the surface favors the microbes 'deposition' and surface and microbial wall characteristics ensures attachment. **Figure D1(A)** indicates the change of bacterial density in absence of diffusivity. The calculation of growth and decay rate of each bacteria shows the following trend for bacterial density: *Bacillus* (0.35 g/cm$^3$) > *Micrococcus* (0.30 g/cm$^3$) > *E. coli* (0.29 g/cm$^3$) > *Staphylococcus* (0.15 g/cm$^3$). *Bacillus* has the highest growth rate whereas *Staphylococcus* shows the lowest. The overall bacterial density exponentially increases with time (since nutrient is considered to be in excess). **Figure D1(B)** shows the change of bacterial density when bacterial diffusivity is considered. The diffusion coefficient, $D_b$ was set at $3.6\times10^{-2}$ cm$^2$/h. The diffusion coefficient takes into account the influence of the boundary conditions at the air – surface interface on the microbe transport to the surface. Although the plots of **Figure D1(B)** are very similar to **Figure D1(A)**, the concentration is slightly lower due to diffusion as it now takes longer to reach the same concentrations.

**Figure D2** shows the impact of attachment fraction ($f_{att}$) on the density of *Micrococcus*. *Staphylococcus* showed the similar trends. Bacterial growth and decay rate and diffusivity are considered, and the number of suspended bacteria is assumed to be a hundred. Attachment fraction has a high impact on the bacterial concentration. As more bacteria 'attach', the higher the increase of the bacterial density and minimal influence of diffusion or growth/decay rates. This indicates the importance of further exploring the surface properties and bacterial characteristics.

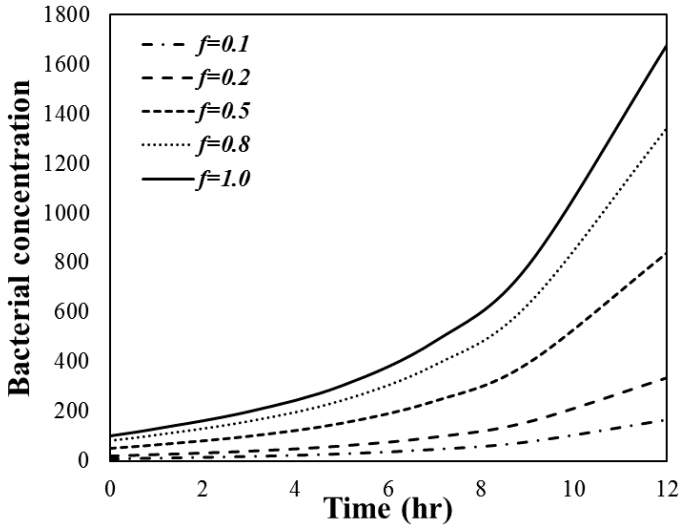


**Figure D2.** The influence of the attachment fraction (bacterial characteristics and surface properties) on the change of the *Micrococcus* concentration.

**Figure D3** shows the fungal hyphal length growth depending on temperature and relative humidity after 24 hrs. The growth rate is in mm/day. **Figure D3(A)** represents *Aspergillus*. The figure shows that growth spikes when relative humidity crosses 70%, but under coupled temperature condition the maximum growth rates occur near 30°C. **Figure D3(B)** shows similar growth rate versus humidity dependency for *Penicillium*. However, no significant temperature dependency is observed.

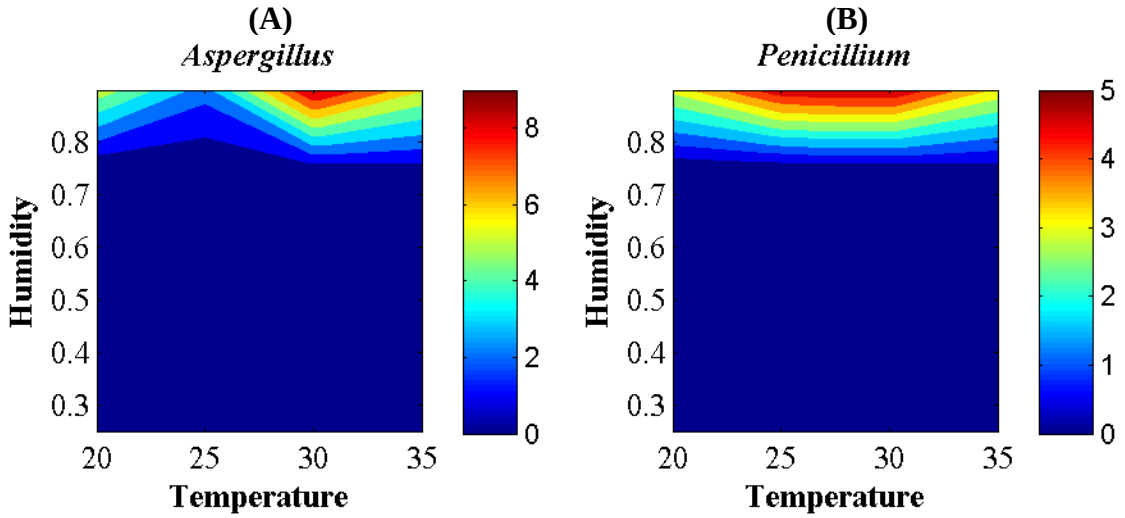


**Figure D3.** The fungal hyphal growth depending on temperature and relative humidity after 24 hours. **(A)** *Aspergillus* and **(B)** *Penicillium*.

**Figure D4** plots the significance of nutrient condition. A relative humidity value higher than 75% is considered as a limiting growth condition. **Figure D4** shows the fungal hyphal growth after 50 hours when temperature, relative humidity, and diffusivity are fixed at 30℃, 90% and 3 mm/day. The percentages in the figure indicate the concentration of nutrient *i.e.*, at 100% nutrient presence 19.7 mm growth is seen for *Aspergillus* and 5.6 mm growth in *Penicillium*. 90% nutrient indicates that sufficient nutrient is present to sustain 90% of the population. The figure shows the extent of contamination that may occur on a surface under assumed given conditions. *Penicillium* growth is much slower than *Aspergillus* due to the growth rate. Several studies investigated the influence of temperature and relative humidity on mold growth. Limiting humidity values were observed between 75~80% [351-353]. A short spore germination time was observed with increasing temperature and relative humidity [342].

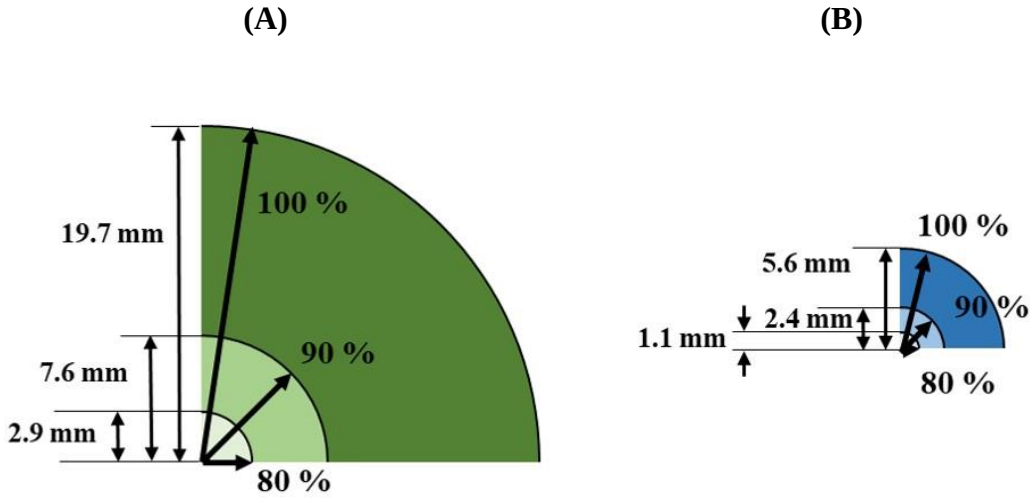


**Figure D4.** The fungal hyphal growth after 50 hours depending on the nutrient concentration at 30℃, 90% relative humidity, and 3 mm/day diffusivity. **(A)** *Aspergillus* and **(B)** *Penicillium*.

The results indicate the dominant influence of attachment fraction on change of bacterial density and the effects of temperature and humidity. Further investigation and characterization of microbe - surface interaction is required to qualify attachment fraction. Laboratory tests and field sampling data focusing on extracting information on microbial growth on surfaces can be applied to assess the models. 'Building scientists' can apply these models and the associated mathematical framework to determine building, indoor and surface conditions that control the indoor microbiome diversity and quantity. The information can be applied for HVAC operations, interior design in all buildings and specific cases will be useful for reducing transfer of infection in hospitals, day cares, and senior homes etc., where more vulnerable populations reside.

## D.4. CONCLUSIONS

This study developed a mathematical model to simulate how microbes interact with indoor surfaces. Common indoor microorganisms, such as *E. coli*, *Staphylococcus aureus*, *Micrococcus*, *Bacillus*, *Aspergillus*, and *Penicillium* are investigated. *Bacillus* shows the highest increase in density, whereas *Staphylococcus* shows the least. The attachment fraction is a major determining factor on the surface persistence of bacteria. In fungus surface model, *Aspergillus* shows higher hyphal length growth than *Penicillium* due to the different growth rates. Limiting relative humidity for fungal growth is 75%. Optimum temperature of *Aspergillus* is observed to be 30℃ while *Penicillium* is not significantly influenced by temperature. Fungal contamination spread is influenced by 'nutrition'.

# APPENDIX E. INFLUENCE OF INDOOR CONDITIONS ON MICROBIAL DIVERSITY AND QUANTITY IN SCHOOLS [6]


## ABSTRACT

HVAC systems consumes 37% of the electricity in educational buildings. Energy consumption varies depending on the ventilation strategy. School buildings have a responsibility of ensuring energy performance and maintenance of indoor environmental quality for its occupants. This study assesses the efficiency of the ventilation system in terms of the microbes present in the spaces. Microorganisms and particulate matters were sampled in classrooms, locker rooms, libraries in two high schools and an elementary school. Six bacterial species and seven fungal species were identified. The most abundant microorganisms were *Staphylococcus* sp., *Bacillus* sp., and *Micrococcus* sp. Elementary school, especially kindergarten, showed higher microbial concentration and particulate matter as a result of higher human activity. Microbial concentration was influenced by the types of room in the same building with the same ventilation system. Canonical correspondence plot (CCA) determined that gender and school type have significant effects. The presence of *Bacillus* sp., *Aerococcus* sp., *Corynebacterium* sp., and *Penicillium* sp. was significantly related to gender, while *Staphylococcus* sp. and


[6] Seong, D., Norman, R.S. & Hoque, S.
Results in this chapter presented in Indoor Air Conference 2018, Philadelphia, Pennsylvania, USA

*Alternaria* sp. were related to type of school. The presence of *Aerococcus* sp. and *Micrococcus* sp. depended on the distance from the vent location. Relatively lower number of *Aerococcus* sp. was detected when the distance between sampling site and vent was less than 2 m. *Micrococcus* sp. was generally detected when the distance was < 3.5 m. The distance from the door was not significant.

## E.1. INTRODUCTION

Poor air quality causes health problem [48, 73], discomfort [354, 355], and deterioration of learning performance [356]. More and more buildings are being designed as air-tight structures to save energy, however, this could lead to degradation of indoor air quality through containment of contaminated air in dead zones in the room, or introduce outdoor pollutants indoors depending on the ventilation condition [19, 20]. Even though ventilation systems have evolved over decades, poor air quality persists. Therefore, appropriate ventilation strategy is required to maintain air quality and prevent waste of energy.

According to the data from EIA (Energy Information Administration, US), HVAC systems consume most of the electricity following lighting, refrigeration, and computing in educational buildings in USA [357]. Schools spend approximately $130 per student for electricity [357]. School's median energy costs based on EPA data are $1.30/ft$^2$ in elementary school, $1.38/ft$^2$ in middle school, and $1.35/ft$^2$ in high school, respectively [358]. Educational buildings which include classrooms, preschool, day-care, elementary school, middle school, high school, and college/university consume 37% of total electricity consumption for HVAC systems [357]. Energy usage in schools is not only related to the

schools' operational expenditure but is also connected to reducing energy consumption and $CO_2$ emission. School as a public building has a responsibility of energy performance and indoor environmental quality [359]. A recent study has predicted that the total world energy usage will increase by 56% from 2010 to 2040 [360]. Buildings consume 50% of total building energy usage and 20% of total energy consumption in USA to operate HVAC systems [361]. According to a previous study comparing energy usage of offices in U.S. cities, energy consumption reduced 1.5~29.0% when the ventilation strategy changed from mechanical to natural ventilation [117]. HVAC systems have become essential for thermal comfort and desired indoor air quality. The increase of building's energy consumption is inevitable. Since different school levels have different human density and occupational time, consequently, different energy consumption [359], schools' requirements need to be considered before determining an energy efficient ventilation strategy which will also ensure health and productivity.

Several studies have investigated the effect of ventilation system using carbon dioxide ($CO_2$) or particulate matter as tracers/indicators [3, 362], but few studies have assessed the impact on indoor microbes. Microorganisms in an indoor space reflect the combined effects of the presence of occupants, activities, environmental parameters and specific characteristics of the space. For instance, human-related bacteria such as *Staphylococcus* sp. and *Micrococcus* ap. are frequently found in building environment [363]. Different age groups have different microbial flora [85]. Since *Lactobacillus* sp. is a vaginal microorganism, it has been frequently detected in female related spaces while *Corynebacterium* sp. has been found in male-related rooms [30]. Meadow and his colleagues confirmed that individuals have their own biological cloud and release their

distinctive microbes in the spaces [72]. Human activity changes the indoor microbial communities and concentrations [34].

Although numerous studies have found that the indoor microorganisms differ depending on the indoor conditions, current ventilation standards do not use microbial presence as a way of assessing, 'adequate ventilation' [364]. Indoor microbial communities were highly influenced by the ventilation strategy [365]. In this study, the relationship between indoor microbial characteristics and engineering controls have been investigated.

## E.2. MATERIALS AND METHODS

Microorganism and particulate matter were obtained from sampling in classrooms, locker rooms, and libraries in two high schools and an elementary school. The spatial distribution of the microbial quantity and diversity was assessed in relation to the interior orientation of engineering controls (such as vents) and select interior 'décor' such as placement of desks, bookshelves, sinks etc. All the schools were always mechanically ventilated and had windows (closed) except for the locker rooms which had no windows. Indoor microorganisms were collected through passive air sampling for 60 minutes using open Petri dishes filled with tryptic soy agar (TSA). The passive air sampling method follows the standard 1/1/1 scheme (1 hr exposure, 1 m above the floor, and 1 m far from the wall) [127]. The locations of the Petri dishes in this study were varied in relation to the HVAC system vents in order to investigate the influence of the ventilation system. Optical Particle Sizer 3330 (TSI Inc., MN, USA) was used to measure particle size distribution. Indoor environmental conditions were monitored using ABM-200 (Airflow and Environmental Meter, CPS Products, Inc., FL, USA). Temperature and humidity were

recorded typically at ~26°C and ~47%, respectively. Samples were collected from October 2017 to February 2018. Occupancy and activity were recorded. The degree of activity was rated in three levels: -1 (no activity, unoccupied), 0 (normal activity: sitting, talking, or walking), and +1 (high activity: running or most people is moving around).

Sampled Petri dishes were incubated at the room temperature for 7 days. The shape, colour, and texture of the colony were evaluated for microbial identification. Colony forming units per $m^3$ of indoor air ($CFU/m^3$) were calculated to quantify the concentration of indoor microbes applying **Eq.E1** [1, 366]:

$$CFU/m^3 = \frac{5 \times n \times 10^4}{A \times t} \qquad \text{Eq. E1}$$

where $n$ is the number of colonies on the Petri dish, $A$ is the surface area of the Petri dish ($cm^2$), and $t$ is exposure time (min).

Overall 160 air samples were collected. For the data reliability, duplicate samples were taken at the same sampling location. R 3.5.1 and Minitab (Minitab Inc., PA, USA) were used for statistical analysis. The data significance was evaluated at $p$ level of 0.05. Canonical correspondence analysis (CCA) was applied to determine the influence of sampling condition and distance from the vent. CCA represented the relationships between biological species and their environment [367]. One-way ANOVA test was applied to evaluate the differences among the samples.

## E.3. RESULTS AND DISCUSSIONS

### E.3.1. Indoor air quality

Indoor air quality was evaluated with the concentrations and types of detected microorganism, and particulate matter. Overall 160 air samples were collected. Among the samples, six different bacteria and seven different fungi were identified. Detected bacterial species were *Bacillus* sp., *Staphylococcus* sp., *Curtobacterium* sp., *Aerococcus* sp., *Micrococcus* sp., and *Corynebacterium* sp. Detected fungi were *Rhodotorula* sp., *Cochliobolus* spp., *Pithomyces* sp., *Alternaria* sp., *Ascochyta* sp., *Aspergillus* sp., and *Penicillium* spp. The most abundant microorganisms were *Staphylococcus* sp., *Bacillus* sp., and *Micrococcus* sp. This result is in accordance with other studies in the literature. *Staphylococcus* sp., *Bacillus* sp., *Corynebacterium* sp., and *Micrococcus* sp. are frequently found in indoors such as residences, hospitals, offices, or schools since they are human-related bacteria [34, 37, 42, 79]. A study conducted in air-conditioned office buildings found *Micrococcus* sp., *Bacillus* sp., *Staphylococcus* sp., *Penicillium* sp., *Aspergillus* sp., and *Rhodotorula* sp. from the air and settled dust samples [37].

Indoor microbial concentration in each school and space is described in **Figure E1(A)**. Elementary school showed a higher microbial concentration, especially in kindergarten, than high school. The averaged concentrations were 135 CFU/$m^3$ in high school and 293 CFU/$m^3$ in elementary school, respectively. The ANOVA test confirmed that human activity (*p-value* < 0.05) had a significant influence on the microbial concentration. No activity was reported in the $5^{th}$ grade classroom. **Figure E1(A)** shows that the number of microbes detected is higher in male's locker room even when both locker rooms had similar activities and occupancy rates. Gender did not significantly

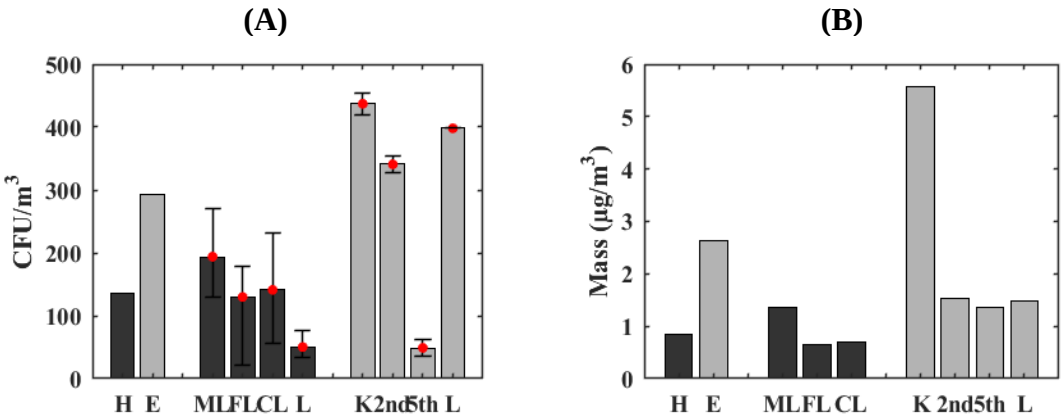


**Figure E1. (A)** Microbial concentration (CFU/$m^3$) and **(B)** $PM_{2.5}$ (µg/$m^3$) in each sampling location. H: High school, E: Elementary school, ML: Male's locker room, FL: Female's locker room, CL: Classroom, L: Library, K: Kindergarten, 2nd: $2^{nd}$ grade classroom, and 5th: $5^{th}$ grade classroom.

impact the number of detected microorganisms (CFU/$m^3$) and microbial species (*p-value* > 0.05). Fungal and bacterial concentration were highly influenced by the types of room (*p-value* < 0.05). Relatively higher fungal level was measured in library (median: 23%) than other rooms (median: 8% in locker room and 11% in classroom, respectively). **Figure E1(B)** shows the concentration of particulate matter ($PM_{2.5}$). In accordance with the indoor microbial concentration, **Figure E1(A)**, particulate matter was higher in kindergarten.

E.3.2. Influence of sampling condition

Canonical correspondence plot (**Figure E2**) showed and confirmed the relation between sampling location and microbial community. The types of room are classified into locker room, classroom, and library. Adolescence and children represented two different age groups. The three schools are: two high schools and an elementary school. Gender indicates: female only, male only, and both genders present. CCA results show that gender and types of school had a significant effect (*p-value* < 0.05). As shown in **Figure E2** the presence of *Bacillus* sp., *Aerococcus* sp., *Corynebacterium* sp., and *Penicillium* sp. is

highly related to gender, while *Staphylococcus* sp. and *Alternaria* sp. are related to types of school. Numerous studies have found that *Corynebacterium* sp. is dominant in male-occupied rooms [30, 78, 85]. *Bacillus* sp. is often found in indoor air and dust samples [79], *Aerococcus* sp. is known as an environmental species [129], and *Penicillium* sp. is one of the most common indoor fungi [129]. However, previous studies have not investigated the relation between *Bacillus* sp., *Aerococcus* sp., and *Penicillium* sp. and gender.

The presence of *Aspergillus* sp., *Rhodotorula* sp., *Ascochyta* sp., *Cochliobolus* sp., *Micrococcus* sp., and *Curtobacterium* sp. was not associated with the types of room, school, age, and gender. *Aspergillus* sp. is frequently detected indoors, while *Cochliobolus* sp. is an outdoor-related fungus [37, 129, 368]. *Rhodotorula* sp. is abundant in indoor and outdoor air samples [369].

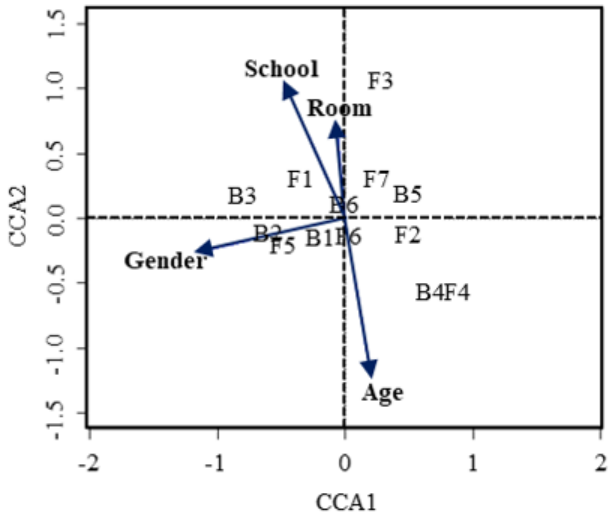


**Figure E2.** CCA plot showing overall detected microorganisms among different sampling conditions. B1: *Aerococcus* sp., B2: *Bacillus* sp., B3: *Corynebacterium* sp., B4: *Curtobacterium* sp., B5: *Micrococcus* sp., B6: *Staphylococcus* sp., F1: *Alternaria* sp., F2: *Ascochyta* sp., F3: *Aspergillus* sp., F4: *Cochliobolus* sp., F5: *Penicillium* sp., F6: *Pithomyces* sp., and F7: *Rhodotorula* sp.

E.3.3. Influence of vent location

The spatial distribution of microbial diversity and quantity was investigated to determine the influence of vent location. **Figure E3** shows the location of sampling sites, vents, doors, and windows. The ratio of detected bacteria and fungi was not significantly influenced by the distance from vents (*p-value* > 0.05). However, the presence of *Aerococcus* sp. and *Micrococcus* sp. were significantly influenced by the vent location (*p-value* < 0.05). *Aerococcus* sp. is outdoor-related species and *Micrococcus* sp. is associated with human presence [129]. Relatively lower number of *Aerococcus* sp. was detected when the distance between sampling site and vent was less than 2 m. *Micrococcus* sp. was generally detected when the distance was lower than 3.5 m. Higher number of *Micrococcus* sp. was observed > 4 m away from the closest vent. This result demonstrates a possibility

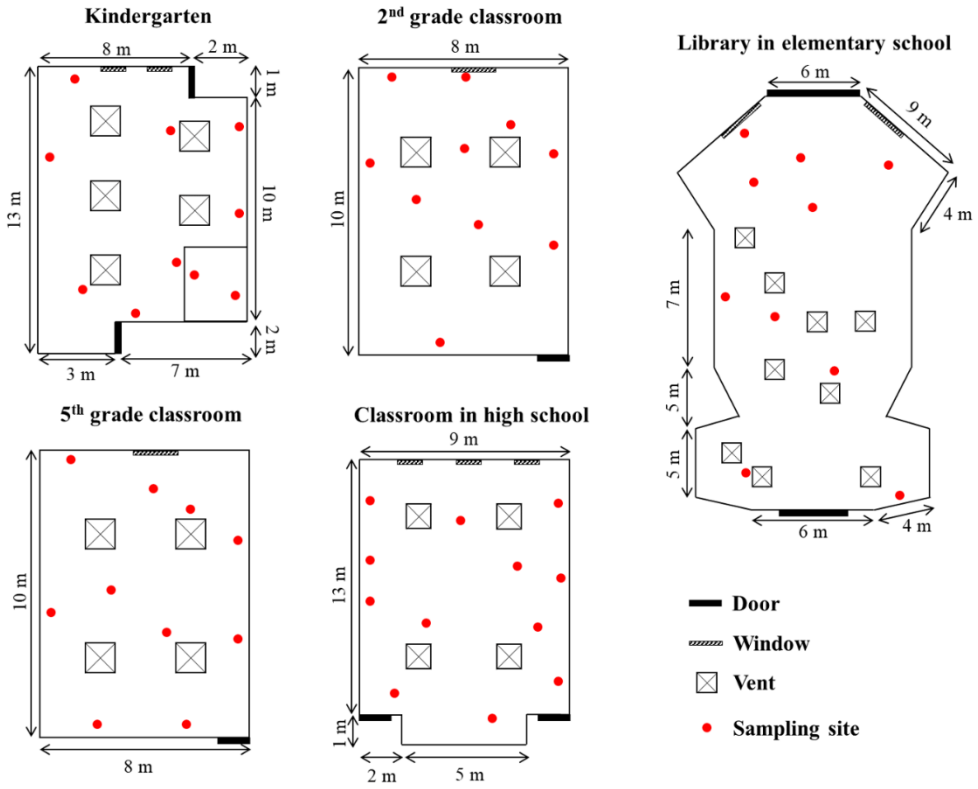


**Figure E3.** Schematic diagram of the location of vents, doors, windows, and sampling sites.

of the influence of the zones in the room with different range of velocity magnitudes influencing the presence of microbes. The number of detected bacteria ($CFU/m^3$) was highly impacted by the distance from the closest window (*p-value* < 0.05). However, each microbial species was not significantly influenced by the window location (*p-value* > 0.05). The distance between sampling site and the door was not significant among all microbial species (*p-value* > 0.05).

## E.4. CONCLUSIONS

The study investigated the microbial concentration and particulate matter in different sampling conditions. Samples were collected from two high schools and an elementary school. Air sampling from locker rooms, classrooms, and library were investigated to identify the influence of age, gender, space occupancy, and activity. Six different bacteria and seven different fungi were detected. Bacterial species were *Bacillus* sp., *Staphylococcus* sp., *Curtobacterium* sp., *Aerococcus* sp., *Micrococcus* sp., and *Corynebacterium* sp. Fungi were *Rhodotorula* sp., *Cochliobolus* spp., *Pithomyces* sp., *Alternaria* sp., *Ascochyta* sp., *Aspergillus* sp., and *Penicillium* spp. Higher microbial concentration was observed in kindergarten where the highest activity rate was measured. In agreement with previous studies, male's locker room showed relatively higher concentration of microorganisms and particulate matter [30, 72]. Our CCA result confirmed that the microbiome at different schools (high school and elementary school) and gender were significantly different. *Staphylococcus* sp. and *Alternaria* sp. are highly related to types of school, while the presence of *Bacillus* sp., *Aerococcus* sp., *Corynebacterium* sp., and *Penicillium* sp. is mainly related to gender. The analysis

determined that the ratio of bacteria and fungi was not significantly influenced by the vent location. However, several bacterial species showed differences depending on the distance from the closest vent, *Aerococcus* sp. and *Micrococcus* sp. The distance from the door was not significant among all the microbial species. *Aerococcus* sp. and *Micrococcus* sp. were detected in spaces with natural and mechanical ventilation system [47, 51].

The results of the analysis indicate that while the spaces were continually mechanically ventilated maintaining acceptable humidity and indoor temperature conditions, the effects on indoor microbial diversity and quantity needs further evaluation. Outdoor related microorganisms such as *Aerococcus* sp. and *Bacillus* sp. were continuously detected in the mechanically ventilated spaces. There was no impact of window or door locations to the presence or absence of the detected species. Understanding how other ventilation approaches such as natural, hybrid or personalized ventilation systems impact the spatial distribution of the microbiome can lead to more energy efficient designs and healthy indoor conditions. The characteristics of the microbiome can also have an influence, which remains to be investigated.

# APPENDIX F. DATA AND CODES

## F.1. Data of Chapter 2

**Table F1.** Surface bacterial diversity and their percentage (%)

| Family | Skin | Rest room | Mobile device |
|---|---|---|---|
| *Bacillaceae* | 1.00 | 1.55 | 5.00 |
| *Comamonadaceae* | 0.00 | 2.36 | 0.00 |
| *Corynebacteriaceae* | 12.36 | 9.37 | 0.00 |
| *Enterobacteriaceae* | 0.00 | 1.79 | 1.20 |
| *Lactobacillaceae* | 1.35 | 5.09 | 8.01 |
| *Micrococcaceae* | 1.28 | 6.45 | 7.00 |
| *Moraxellaceae* | 6.20 | 7.54 | 2.05 |
| *Propionibacteriaceae* | 37.37 | 26.62 | 0.00 |
| *Pseudomonadaceae* | 2.39 | 2.07 | 0.00 |
| *Rhodobacteraceae* | 1.25 | 2.15 | 0.00 |
| *Sphingomonadaceae* | 1.13 | 4.24 | 0.00 |
| *Staphylococcaceae* | 16.37 | 7.22 | 65.50 |
| *Streptococcaceae* | 13.95 | 6.24 | 9.43 |
| Others | 5.34 | 17.30 | 1.80 |

**Table F2.** Bacterial diversity of air samples from different sampling locations

| Family | Residence | Hospital | Office | School | Public building |
|---|---|---|---|---|---|
| *Alicyclobacillaceae* | 4.10 | 0.00 | 0.00 | 0.00 | 0.00 |
| *Bacillaceae* | 9.95 | 8.68 | 31.15 | 12.87 | 6.89 |
| *Bradyrhizobiaceae* | 0.00 | 0.00 | 0.00 | 0.00 | 0.00 |
| *Corynebacteriaceae* | 3.16 | 4.00 | 0.00 | 4.27 | 5.48 |
| *Dermabacteraceae* | 1.30 | 0.00 | 0.00 | 0.00 | 0.00 |
| *Enterobacteriaceae* | 0.00 | 0.00 | 0.00 | 1.23 | 1.26 |
| *Flavobacteriaceae* | 0.00 | 0.00 | 1.76 | 2.20 | 1.03 |
| *Methylobacteriaceae* | 2.73 | 0.00 | 0.00 | 0.00 | 16.07 |
| *Micrococcaceae* | 30.32 | 21.92 | 36.31 | 24.10 | 24.47 |
| *Moraxellaceae* | 2.78 | 3.92 | 0.00 | 1.58 | 6.64 |
| *Propionibacteriaceae* | 9.57 | 0.00 | 0.00 | 0.00 | 2.13 |
| *Pseudomonadaceae* | 2.34 | 0.00 | 2.52 | 2.57 | 5.24 |
| *Sphingomonadaceae* | 2.73 | 0.00 | 0.00 | 0.00 | 7.17 |
| *Staphylococcaceae* | 10.96 | 54.88 | 26.62 | 37.78 | 13.77 |
| *Streptococcaceae* | 0.00 | 0.00 | 0.00 | 3.47 | 0.00 |
| Others | 20.06 | 6.60 | 1.65 | 9.95 | 9.84 |

**Table F3.** Bacterial diversity of surface samples from different sampling locations

| Family | Residence | Hospital | Gym | Museum |
|---|---|---|---|---|
| *Alicyclobacillaceae* | 1.86 | 8.47 | 0.00 | 0.00 |
| *Bacillaceae* | 0.00 | 0.00 | 10.28 | 50.15 |
| *Bradyrhizobiaceae* | 0.00 | 21.54 | 0.00 | 0.00 |
| *Corynebacteriaceae* | 2.10 | 0.00 | 0.00 | 2.35 |
| *Dermabacteraceae* | 8.20 | 0.00 | 0.00 | 0.00 |
| *Enterobacteriaceae* | 2.34 | 0.00 | 32.78 | 0.00 |
| *Flavobacteriaceae* | 1.05 | 5.23 | 0.00 | 0.00 |
| *Methylobacteriaceae* | 5.33 | 0.00 | 0.00 | 0.00 |
| *Micrococcaceae* | 22.05 | 3.58 | 0.00 | 32.15 |
| *Moraxellaceae* | 17.38 | 39.92 | 0.00 | 0.00 |
| *Propionibacteriaceae* | 6.30 | 9.12 | 0.00 | 0.00 |
| *Pseudomonadaceae* | 5.07 | 7.22 | 0.00 | 0.00 |
| *Sphingomonadaceae* | 6.35 | 0.00 | 0.00 | 0.00 |
| *Staphylococcaceae* | 2.83 | 0.00 | 32.97 | 14.50 |
| *Streptococcaceae* | 0.00 | 3.20 | 0.00 | 0.00 |
| Others | 19.14 | 1.72 | 23.97 | 0.85 |

**Table F4.** Bacterial diversity and percentages (%) of difference age group

| Family | Children | Adult |
|---|---|---|
| *Corynebacteriaceae* | 8.18 | 7.99 |
| *Micrococcaceae* | 12.14 | 15.50 |
| *Propionibacteriaceae* | 6.07 | 24.27 |
| *Bacillaceae* | 6.06 | 7.98 |
| *Staphylococcaceae* | 32.89 | 24.53 |
| *Lactobacillaceae* | 2.25 | 0.52 |
| *Streptococcaceae* | 17.10 | 3.45 |
| *Enterobacteriaceae* | 1.76 | 0.29 |
| *Moraxellaceae* | 2.94 | 4.13 |
| *Pseudomonadaceae* | 1.35 | 2.80 |
| Others | 9.26 | 8.54 |

## F.2. Data of Chapter 3

**Table F5.** Microbial concentration (CFU/$m^3$) and relative PM concentration (µg/$m^3$)

| Sampling location | | Microbial concentration (CFU/$m^3$) | | | $PM_{2.5}$ [a] (µg/$m^3$) | | | $PM_{10}$ [a] (µg/$m^3$) | | |
|---|---|---|---|---|---|---|---|---|---|---|
| | | Indoor bacteria | Outdoor bacteria | Fungi | max.-avg. | avg. | avg.-min. | max.-avg. | avg. | avg.-min. |
| University | Lab | 4.37 | 0.00 | 0.00 | 95.58 | 59.02 | 37.54 | 184.73 | 85.66 | 47.72 |
| | Office | 47.00 | 15.41 | 5.39 | 87.10 | 48.35 | 29.96 | 171.99 | 74.82 | 49.59 |
| | Classroom (All) | 161.87 | 24.33 | 0.00 | 64.81 | 104.83 | 48.83 | 192.73 | 173.12 | 96.69 |
| | Classroom (Occupied) | 270.17 | 37.66 | 0.00 | 41.97 | 127.67 | 41.97 | 115.54 | 250.30 | 115.54 |
| | Classroom (Unoccupied) | 17.47 | 6.55 | 0.00 | 59.47 | 89.61 | 33.60 | 76.67 | 121.66 | 45.23 |
| High school | Locker room (All) | 146.57 | 27.26 | 8.85 | 30.67 | 51.79 | 25.53 | 140.82 | 134.66 | 98.55 |
| | Male's locker room | 108.43 | 26.93 | 5.82 | 12.54 | 69.92 | 12.54 | 53.64 | 221.84 | 53.64 |
| | Female's locker room | 182.70 | 27.58 | 11.72 | 7.40 | 33.67 | 7.40 | 11.37 | 47.48 | 11.37 |
| | Classroom | 169.53 | 57.94 | 21.66 | 15.62 | 26.63 | 20.13 | 164.90 | 63.26 | 49.18 |
| Elementary school | Kindergarten | 345.16 | 144.75 | 20.30 | 25.45 | 286.11 | 25.45 | 1252.48 | 4553.78 | 1252.48 |
| | 2nd grade classroom | 269.19 | 102.17 | 11.13 | 35.18 | 78.90 | 35.18 | 296.82 | 676.93 | 296.82 |
| | 5th grade classroom | 38.64 | 13.75 | 8.51 | 41.96 | 69.90 | 41.96 | 80.98 | 253.16 | 80.98 |
| | Library | 311.76 | 140.16 | 81.21 | | 75.84 | | | 240.13 | |

[a] max.-avg.: maximum of the data - average of the data, avg.: average of the data, avg.-min.: average of data - minimum of the data

**Table F6.** Indoor and outdoor bacterial concentration (CFU/$m^3$) and distance between sampling location and BAE components

| Occupancy | Room [a] | Sample # | Bacteria (CFU/$m^3$) | | Distance (m) [b] | | | | | | | | |
|---|---|---|---|---|---|---|---|---|---|---|---|---|---|
| | | | Outdoor | Indoor | v1 | v2 | v3 | v4 | v5 | d1 | d2 | w1 | w2 |
| unoccupied | 5CR | ES1 | 0.00 | 26.20 | 6.26 | 7.12 | 3.38 | 4.80 | | 3.36 | | 7.27 | |
| unoccupied | 5CR | ES2 | 13.10 | 0.00 | 7.30 | 6.00 | 5.07 | 2.89 | | 6.71 | | 4.68 | |
| unoccupied | 5CR | ES3 | 0.00 | 26.20 | 6.56 | 4.52 | 5.12 | 1.91 | | 7.45 | | 3.06 | |
| unoccupied | 5CR | ES4 | 0.00 | 13.10 | 6.18 | 3.34 | 5.78 | 2.54 | | 8.46 | | 1.84 | |
| unoccupied | 5CR | ES5 | 13.10 | 0.00 | 6.85 | 2.65 | 7.90 | 4.74 | | 11.24 | | 2.91 | |
| unoccupied | 5CR | ES6 | 0.00 | 0.00 | 2.98 | 2.67 | 5.52 | 5.36 | | 8.72 | | 6.10 | |
| unoccupied | 5CR | ES7 | 26.20 | 52.40 | 4.62 | 2.16 | 5.36 | 3.47 | | 8.34 | | 3.46 | |
| unoccupied | 5CR | ES8 | 13.10 | 26.20 | 3.66 | 5.26 | 2.17 | 4.35 | | 4.02 | | 6.65 | |
| unoccupied | 5CR | ES9 | 0.00 | 0.00 | 2.89 | 6.87 | 4.45 | 7.65 | | 5.67 | | 9.72 | |
| unoccupied | 5CR | ES10 | 0.00 | 0.00 | 4.73 | 7.71 | 3.10 | 6.83 | | 2.05 | | 9.35 | |
| unoccupied | 5CR | ES11 | 0.00 | 39.30 | 6.26 | 7.12 | 3.38 | 4.80 | | 3.36 | | 7.27 | |
| unoccupied | 5CR | ES12 | 13.10 | 78.60 | 7.30 | 6.00 | 5.07 | 2.89 | | 6.71 | | 4.68 | |
| unoccupied | 5CR | ES13 | 0.00 | 39.30 | 6.56 | 4.52 | 5.12 | 1.91 | | 7.45 | | 3.06 | |
| unoccupied | 5CR | ES14 | 0.00 | 13.10 | 6.18 | 3.34 | 5.78 | 2.54 | | 8.46 | | 1.84 | |
| unoccupied | 5CR | ES15 | 0.00 | 13.10 | 6.85 | 2.65 | 7.90 | 4.74 | | 11.24 | | 2.91 | |
| unoccupied | 5CR | ES16 | 0.00 | 39.30 | 2.98 | 2.67 | 5.52 | 5.36 | | 8.72 | | 6.10 | |
| unoccupied | 5CR | ES17 | 26.20 | 13.10 | 4.62 | 2.16 | 5.36 | 3.47 | | 8.34 | | 3.46 | |
| unoccupied | 5CR | ES18 | 0.00 | 0.00 | 3.66 | 5.26 | 2.17 | 4.35 | | 4.02 | | 6.65 | |
| unoccupied | 5CR | ES19 | 0.00 | 39.30 | 2.89 | 6.87 | 4.45 | 7.65 | | 5.67 | | 9.72 | |
| unoccupied | 5CR | ES20 | 0.00 | 78.60 | 4.73 | 7.71 | 3.10 | 6.83 | | 2.05 | | 9.35 | |
| occupied | 2CR | ES21 | 91.69 | 235.79 | 5.57 | 6.59 | 3.06 | 4.67 | | 3.09 | | 7.98 | |
| occupied | 2CR | ES22 | 26.20 | 52.40 | 6.28 | 5.66 | 4.22 | 3.22 | | 5.51 | | 5.83 | |
| occupied | 2CR | ES23 | 13.10 | 104.79 | 6.17 | 3.97 | 5.07 | 1.85 | | 7.39 | | 3.48 | |
| occupied | 2CR | ES24 | 0.00 | 183.39 | 5.25 | 3.19 | 4.48 | 1.66 | | 6.95 | | 3.76 | |
| occupied | 2CR | ES25 | 26.20 | 170.29 | 8.11 | 4.51 | 7.97 | 4.26 | | 10.51 | | 0.20 | |
| occupied | 2CR | ES26 | 1139.63 | 26.20 | 7.70 | 3.72 | 8.57 | 5.30 | | 11.50 | | 2.70 | |
| occupied | 2CR | ES27 | 26.20 | 91.69 | 3.84 | 2.20 | 5.93 | 5.03 | | 8.63 | | 5.89 | |
| occupied | 2CR | ES28 | 0.00 | 157.19 | 4.15 | 2.20 | 5.03 | 3.59 | | 7.50 | | 4.58 | |

**Table F6.** (continued)

| Occupancy | Room [a] | Sample # | Bacteria (CFU/m$^3$) | | Distance (m) [b] | | | | | | | | |
|---|---|---|---|---|---|---|---|---|---|---|---|---|---|
| | | | Outdoor | Indoor | v1 | v2 | v3 | v4 | v5 | d1 | d2 | w1 | w2 |
| occupied | 2CR | ES29 | 26.20 | 91.69 | 3.65 | 3.30 | 3.39 | 3.00 | | 5.60 | | 5.49 | |
| occupied | 2CR | ES30 | 13.10 | 39.30 | 2.92 | 6.64 | 3.92 | 7.13 | | 4.17 | | 10.27 | |
| occupied | 2CR | ES61 | 13.10 | 314.38 | 5.57 | 6.59 | 3.06 | 4.67 | | 3.09 | | 7.98 | |
| occupied | 2CR | ES62 | 65.50 | 13.10 | 6.28 | 5.66 | 4.22 | 3.22 | | 5.51 | | 5.83 | |
| occupied | 2CR | ES63 | 26.20 | 353.68 | 6.17 | 3.97 | 5.07 | 1.85 | | 7.39 | | 3.48 | |
| occupied | 2CR | ES64 | 65.50 | 65.50 | 5.25 | 3.19 | 4.48 | 1.66 | | 6.95 | | 3.76 | |
| occupied | 2CR | ES65 | 65.50 | 104.79 | 8.11 | 4.51 | 7.97 | 4.26 | | 10.51 | | 0.20 | |
| occupied | 2CR | ES66 | 117.89 | 641.86 | 7.70 | 3.72 | 8.57 | 5.30 | | 11.50 | | 2.70 | |
| occupied | 2CR | ES67 | 52.40 | 183.39 | 3.84 | 2.20 | 5.93 | 5.03 | | 8.63 | | 5.89 | |
| occupied | 2CR | ES68 | 0.00 | 0.00 | 4.15 | 2.20 | 5.03 | 3.59 | | 7.50 | | 4.58 | |
| occupied | 2CR | ES69 | 13.10 | 327.48 | 3.65 | 3.30 | 3.39 | 3.00 | | 5.60 | | 5.49 | |
| occupied | 2CR | ES70 | 39.30 | 183.39 | 2.92 | 6.64 | 3.92 | 7.13 | | 4.17 | | 10.27 | |
| occupied | K | ES31 | 104.79 | 261.98 | 2.06 | 4.93 | 8.12 | 7.74 | 10.47 | 1.86 | 10.87 | 10.41 | 11.37 |
| occupied | K | ES32 | 52.40 | 144.09 | 3.45 | 6.48 | 9.60 | 6.72 | 10.28 | 1.84 | 10.79 | 11.41 | 11.66 |
| occupied | K | ES33 | 130.99 | 65.50 | 4.59 | 5.60 | 7.93 | 3.45 | 7.12 | 5.01 | 7.62 | 9.03 | 8.69 |
| occupied | K | ES34 | 39.30 | 183.39 | 7.98 | 7.30 | 8.09 | 2.64 | 4.81 | 8.85 | 4.99 | 7.79 | 6.38 |
| occupied | K | ES35 | 91.69 | 157.19 | 10.15 | 7.94 | 6.97 | 4.46 | 1.94 | 11.84 | 1.75 | 5.46 | 3.12 |
| occupied | K | ES36 | 694.26 | 222.69 | 7.82 | 4.81 | 3.39 | 4.69 | 2.88 | 9.85 | 2.50 | 2.49 | 2.56 |
| occupied | K | ES37 | 104.79 | 170.29 | 8.99 | 5.39 | 2.44 | 8.76 | 6.95 | 11.38 | 6.71 | 3.14 | 5.75 |
| occupied | K | ES38 | 52.40 | 445.37 | 5.78 | 3.10 | 3.48 | 8.25 | 8.37 | 7.96 | 8.44 | 6.00 | 8.11 |
| occupied | K | ES39 | 327.48 | 52.40 | 5.12 | 6.40 | 8.74 | 4.11 | 7.78 | 5.02 | 8.18 | 9.72 | 9.30 |
| occupied | K | ES40 | 104.79 | 26.20 | 7.33 | 8.83 | 11.02 | 5.30 | 9.05 | 6.83 | 9.56 | 11.75 | 10.86 |
| occupied | K | ES41 | 65.50 | 432.27 | 2.06 | 4.93 | 8.12 | 7.74 | 10.47 | 1.86 | 10.87 | 10.41 | 11.37 |
| occupied | K | ES42 | 222.69 | 196.49 | 3.45 | 6.48 | 9.60 | 6.72 | 10.28 | 1.84 | 10.79 | 11.41 | 11.66 |
| occupied | K | ES43 | 52.40 | 196.49 | 4.59 | 5.60 | 7.93 | 3.45 | 7.12 | 5.01 | 7.62 | 9.03 | 8.69 |
| occupied | K | ES44 | 78.60 | 235.79 | 7.98 | 7.30 | 8.09 | 2.64 | 4.81 | 8.85 | 4.99 | 7.79 | 6.38 |
| occupied | K | ES45 | 39.30 | 327.48 | 10.15 | 7.94 | 6.97 | 4.46 | 1.94 | 11.84 | 1.75 | 5.46 | 3.12 |
| occupied | K | ES46 | 104.79 | 196.49 | 7.82 | 4.81 | 3.39 | 4.69 | 2.88 | 9.85 | 2.50 | 2.49 | 2.56 |

**Table F6.** (continued)

| Occupancy | Room [a] | Sample # | Bacteria (CFU/m$^3$) | | Distance (m) [b] | | | | | | | | |
|---|---|---|---|---|---|---|---|---|---|---|---|---|---|
| | | | Outdoor | Indoor | v1 | v2 | v3 | v4 | v5 | d1 | d2 | w1 | w2 |
| occupied | K | ES47 | 117.89 | 261.98 | 8.99 | 5.39 | 2.44 | 8.76 | 6.95 | 11.38 | 6.71 | 3.14 | 5.75 |
| occupied | K | ES48 | 78.60 | 196.49 | 5.78 | 3.10 | 3.48 | 8.25 | 8.37 | 7.96 | 8.44 | 6.00 | 8.11 |
| occupied | K | ES49 | 0.00 | 222.69 | 5.12 | 6.40 | 8.74 | 4.11 | 7.78 | 5.02 | 8.18 | 9.72 | 9.30 |
| occupied | K | ES50 | 26.20 | 13.10 | 7.33 | 8.83 | 11.02 | 5.30 | 9.05 | 6.83 | 9.56 | 11.75 | 10.86 |

[a] 5CR: 5$^{th}$ grade classroom, 2CR: 2$^{nd}$ grade classroom, K: Kindergarten
[b] v: vent, d: door, w: window

**Table F7.** Raw data of microbial concentration (CFU/m$^3$/100 cm$^2$) on different sampling sites

| Table | Door | Chair | Bookshelf | Computer | Locker | Floor | Vent |
|---|---|---|---|---|---|---|---|
| 472500 | 235500 | 1342500 | 1425000 | 69000 | 577500 | 2415000 | 321000 |
| 324000 | 1087500 | 1500 | 181500 | 1027500 | 33000 | 1920000 | 201000 |
| 645000 | 42000 | 5092500 | 187500 | 7530000 | 1500 | 3840000 | 535500 |
| 667500 | 1500 | 75000 | 1320000 | | 1500 | 385500 | 127500 |
| 1338000 | 3000 | 30000 | 91500 | | | 937500 | |
| 525000 | 447000 | 85500 | 892500 | | | 1200000 | |
| 211500 | 102000 | 1312500 | | | | | |
| 2070000 | 7500 | 3765000 | | | | | |
| 240000 | 33000 | 1500 | | | | | |
| 4500 | 42000 | 435000 | | | | | |
| 3000 | 303000 | 3000 | | | | | |
| 574500 | 7800 | | | | | | |
| 13875 | 1950000 | | | | | | |
| 885000 | | | | | | | |
| 510000 | | | | | | | |
| 256875 | | | | | | | |
| 4500 | | | | | | | |

**Table F8.** Raw data of microbial concentration (CFU/$m^3$/100 $cm^2$) on different sampling materials

| Wood | Metal | Plastic | Carpet | Tile |
|---|---|---|---|---|
| 211500 | 235500 | 472500 | 2415000 | 385500 |
| 2070000 | 1087500 | 324000 | 1920000 | 937500 |
| 240000 | 42000 | 645000 | 3840000 | 1200000 |
| 4500 | 1500 | 667500 | | |
| 3000 | 3000 | 1338000 | | |
| 574500 | 447000 | 525000 | | |
| 13875 | 102000 | 1342500 | | |
| 885000 | 7500 | 1500 | | |
| 510000 | 33000 | 5092500 | | |
| 256875 | 42000 | 75000 | | |
| 4500 | 91500 | 30000 | | |
| 303000 | 892500 | 85500 | | |
| 7800 | 577500 | 69000 | | |
| 1950000 | 33000 | 1027500 | | |
| 1312500 | 1500 | 7530000 | | |
| 3765000 | 1500 | 321000 | | |
| 1500 | | 201000 | | |
| 435000 | | 535500 | | |
| 3000 | | 127500 | | |
| 1425000 | | | | |
| 181500 | | | | |
| 187500 | | | | |
| 1320000 | | | | |

## F.3. R Codes of Chapter 3

### F.3.1. Normality and ANOVA test

```
library(ggplot2)
library(ggpubr)
library(tidyverse)
library(broom)
library(AICcmodavg)
library(dplyr)
library(devtools)
library(gplots)
mydata<-read.csv(file.choose(),header=TRUE,sep=",")
## CHECK DATA, VISUAL METHODS
# DENSITY PLOT - library(ggpubr)
ggdensity(mydata$CFU,xlab = "CFU")
# Q-Q PLOT - library(ggpubr):ggqqplot() or library(car):qqPlot()
ggqqplot(mydata$CFU)
# HISTOGRAM
hist(mydata$CFU)
hist(mydata$logCFU)
# NORMALITY TEST
shapiro.test(mydata$CFU)
shapiro.test(mydata$logCFU)
## ANOVA, ONE-WAY
one.way <- aov(CFU2 ~ MICROBIOME, data=mydata)
summary(one.way)
# ANOVA PLOT
par(mfrow=c(2,2))
plot(one.way)
par(mfrow=c(1,1))
# TUKEY
one.way.tukey <- aov(OUT ~ as.factor(VENT), data=mydata)
tukey.one.way<-TukeyHSD(one.way.tukey)
tukey.one.way
tukey.plot.test<-aov(OUT ~ as.factor(VENT), data=mydata)
plot(tukey.plot.test, las = 1)
```

### F.3.2. Mann-Whitney-Wilcox Test

```
library(ggplot2)

dat <- read.csv(file.choose(),header=TRUE,sep=",")

test <- wilcox.test(dat$out ~ dat$l1)
```

### F.3.3. Spearman's rank correlation

```
mydata<-read.csv(file.choose(),header=TRUE,sep=",")
# VISUALIZE DATA USING SCATTER PLOTS
library(ggplot2)
library(ggpubr)
ggscatter(mydata, x = "PM2.5", y = "In",
                                    add = "reg.line", conf.int = TRUE,
                                    cor.coef = TRUE, cor.method = "pearson",
                                    xlab = "PM2.5 (ug/m^3)",
                                    ylab = "Indoor related bacteria (CFU/m^3)")
# PEARSON CORRELATION TEST (WHEN NORMALLY DISTRIBUTED)
P_res <- cor.test(mydata$PM2.5, mydata$In, method = "pearson")
# KENDALL RANK CORRELATION TST (ESTIMATE A RANK-BASED MEASURE OF ASSOCIATION)
K_res <- cor.test(mydata$PM2.5, mydata$In, method = "kendall")
# SPEARMAN RANK CORRELATION COEFFICIENT (ESTIMATE A RANK-BASED MEASURE OF ASSOCIATION)
S_res <- cor.test(mydata$PM2.5, mydata$In, method = "spearman")
mat_1 <- as.dist(round(cor(mydata),2))
# VISUALIZE CORRELATION MATRIX
install.packages("GGally")
library(GGally)
# TILE
tiff("spearman(1).tiff", units = "in", width = 5, height = 5, res = 300)
ggcorr(mydata, method = c("pairwise","spearman"),
                    nbreaks = NULL, digits = 2, low = "#3B9AB2",
                    mid = "#EEEEEE", high = "#F21A00",
                    geom = "tile", label = FALSE,
                    label_alpha = FALSE)
dev.off()
# CIRCLE, 6 COLORS
tiff("spearman(2).tiff", units = "in", width = 5, height = 5, res = 300)
ggcorr(mydata, method = c("pairwise","spearman"),
                    nbreaks = 6,
                    low = "steelblue", mid = "white", high = "darkred",
                    geom = "circle")
dev.off()
# TILE WITH LABELS
tiff("spearman(3).tiff", units = "in", width = 5, height = 5, res = 300)
ggcorr(mydata, method = c("pairwise","spearman"),
                    nbreaks = 6, digits = 2,
                    low = "#3B9AB2", mid = "#EEEEEE", high = "#F21A00",
                    geom = "tile", label = TRUE, label_size = 3, color = "grey50")
dev.off()
```

## F.3.4. Clustering analysis

```
library(tidyverse)              # data manipulation
library(cluster)                # clustering algorithm
library(factoextra)             # clustering algorithm & visualization
library(ggplot2)
library(ggfortify)
library(gridExtra)
df <- read.csv(file.choose(),header=TRUE,row.names=1,sep=",")
df <- na.omit(df)               # remove any missing value that might be present in the data
df <- scale(df)
head(df)
k2 <- kmeans(df, center = 2, nstart = 25)
k3 <- kmeans(df, center = 3, nstart = 25)
k4 <- kmeans(df, center = 4, nstart = 25)
k5 <- kmeans(df, center = 5, nstart = 25)
p1 <- fviz_cluster(k2, geom = "point", data = df) + ggtitle("k = 2")
p2 <- fviz_cluster(k3, geom = "point", data = df) + ggtitle("k = 3")
p3 <- fviz_cluster(k4, geom = "point", data = df) + ggtitle("k = 4")
p4 <- fviz_cluster(k5, geom = "point", data = df) + ggtitle("k = 5")
grid.arrange(p1, p2, p3, p4, nrow = 2)
# COMPUTE PCA AND EXTRACT INDIVIDUAL COORDINATES
# DIMENSION REDUCTION USING PCA
res.pca <- prcomp(df)
# COORDINATES OF INDIVIDUALS
ind.coord <- as.data.frame(get_pca_ind(res.pca)$coord)
# ADD CLUSTERS OBTAINED USING THE K-MEANS ALGORITHM
ind.coord$cluster <- factor(k2$cluster)
# PERCENTAGE OF VARIANCE EXPLAINED BY DIMENSIONS
eigenvalue <- round(get_eigenvalue(res.pca),1)
variance.percent <- eigenvalue$variance.percent
# head(eigenvalue)
eigenvalue
ind.coord
# DETERMINING OPTIMAL CLUSTERS - ELBOW METHOD
set.seed(123)
wss <- function(k) {
  kmeans(df, k, nstart = 10)$tot.withinss
}
k.values <- 1:15
wss_values <- map_dbl(k.values, wss)
plot(k.values, wss_values,
     type="b", pch = 19, frame = FALSE,
     xlab="Number of clusters K",
     ylab="Total within-clusters sum of squares")
set.seed(123)
fviz_nbclust(df, kmeans, method = "wss")
```

### F.3.5. Heatmap

```
library(RColorBrewer)

df <- read.csv(file.choose(),header=TRUE,sep=",")
df <- na.omit(df)
df <- scale(df)

heatmap(df,
                                    Colv = NA, Rowv = NA,
                                    trace = "none",
                                    col = colorRampPalette(brewer.pal(8,"Blues"))(5))
legend(x = "right", legend=c("1","2","3","4","5"),
                                    cex = 0.8, fill = colorRampPalette(brewer.pal(8,"Blues"))(5))
```

## F.4. Data of Chapter 4 & 5

**Table F9.** QCM-D data of VACV during attachment and detachment experiments

| Flow rate (µL/min) | Sensor | Attachment Detachment | Flow | | Slope (K) | | Viscosity (kg/m/s) | | Elasticity (kg/m/s²) | | Wall shear stress (kg/m/s²) | | Δ*f* (Hz) | | Δ*D* (×10⁻⁶) | | Δ*m* (ng/cm²) | |
|---|---|---|---|---|---|---|---|---|---|---|---|---|---|---|---|---|---|---|
| | | | Re | Shear Stress (kg/m/s²) | avg. | std. | avg. | std. | avg. | std. | avg. | std. | avg. | std. | avg. | std. | avg. | std. |
| 100 | Gold | ATT1 | 3.30 | 0.05 | 0.20 | 0.06 | 9.65E-04 | 1.97E-04 | 131526 | 221826 | 0.05 | 0.01 | -22.66 | 6.62 | 3.31 | 1.64 | 601.07 | 482.84 |
| | | ATT2 | 3.30 | 0.05 | 0.11 | 0.01 | 1.10E-03 | 2.32E-04 | 176753 | 285035 | 0.05 | 0.01 | -22.66 | 6.62 | 3.31 | 1.64 | 601.07 | 482.84 |
| | | ATT3 | 3.30 | 0.05 | 0.11 | 0.01 | | | | | | | | | | | | |
| | | FR 100_1 | 3.30 | 0.05 | 0.92 | 0.77 | 1.16E-03 | 1.87E-04 | 214426 | 350482 | 0.06 | 0.01 | -17.22 | 7.55 | 2.11 | 1.66 | 674.15 | |
| | | FR 100_2 | 3.30 | 0.05 | 0.91 | 0.78 | 1.16E-03 | 1.30E-04 | 326130 | 556065 | 0.06 | 0.01 | -17.22 | 7.55 | 2.11 | 1.66 | 674.15 | |
| | | FR 100_3 | 3.30 | 0.05 | 0.91 | 0.78 | | | | | | | | | | | | |
| | | FR 100_4 | 3.30 | 0.05 | 0.91 | 0.78 | | | | | | | | | | | | |
| | | FR 200 | 6.61 | 0.10 | 0.33 | 0.35 | 1.16E-03 | 1.30E-04 | 326130 | 556065 | 0.11 | 0.01 | -17.44 | 7.72 | 2.04 | 1.65 | 691.53 | |
| | | FR 300 | 9.91 | 0.15 | 0.33 | 0.35 | 1.16E-03 | 1.30E-04 | 326130 | 556065 | 0.11 | 0.01 | -17.30 | 7.84 | 1.59 | 1.67 | 677.58 | |
| | | FR 500 | 16.52 | 0.24 | 0.33 | 0.35 | 1.16E-03 | 1.30E-04 | 326130 | 556065 | 0.11 | 0.01 | -17.04 | 8.04 | 1.61 | 1.66 | 667.28 | |
| | | FR 700 | 23.12 | 0.34 | 0.33 | 0.35 | 1.16E-03 | 1.30E-04 | 326130 | 556065 | 0.11 | 0.01 | -16.92 | 7.91 | 1.81 | 1.59 | 655.84 | |
| | | FR 1000 | 33.03 | 0.49 | 0.23 | 0.18 | 1.16E-03 | 1.30E-04 | 326130 | 556065 | 0.56 | 0.06 | -15.18 | 7.66 | 1.38 | 1.37 | | |

**Table F9.** (continued)

| Flow rate (µL/min) | Sensor | Attachment Detachment | Flow | | Slope (K) | | Viscosity (kg/m/s) | | Elasticity (kg/m/s²) | | Wall shear stress (kg/m/s²) | | Δ*f* (Hz) | | Δ*D* (×10⁻⁶) | | Δ*m* (ng/cm²) | |
|---|---|---|---|---|---|---|---|---|---|---|---|---|---|---|---|---|---|---|
| | | | Re | Shear Stress (kg/m/s²) | avg. | std. | avg. | std. | avg. | std. | avg. | std. | avg. | std. | avg. | std. | avg. | std. |
| 100 | $SiO_2$ | ATT1 | 3.30 | 0.05 | 0.05 | 0.01 | 1.50E-03 | 1.66E-03 | 624431 | 767773 | 0.07 | 0.08 | -12.72 | 3.55 | 1.99 | 0.16 | 295.85 | 28.29 |
| | | ATT2 | 3.30 | 0.05 | 0.23 | 0.08 | 2.08E-03 | 1.09E-03 | 563646 | 552259 | 0.10 | 0.05 | -12.72 | 3.55 | 1.99 | 0.16 | 295.85 | 28.29 |
| | | ATT3 | 3.30 | 0.05 | 0.96 | 1.07 | 1.61E-03 | 4.28E-04 | 543720 | 552253 | 0.08 | 0.02 | -12.72 | 3.55 | 1.99 | 0.16 | 295.85 | 28.29 |
| | | FR 100_1 | 3.30 | 0.05 | 0.13 | 0.02 | 4.46E-04 | | 332260 | | 0.02 | | -3.51 | 3.85 | 0.84 | 0.22 | 45.36 | 29.16 |
| | | FR 100_2 | 3.30 | 0.05 | 0.25 | 0.23 | | | | | | | | | | | | |
| | | FR 100_3 | 3.30 | 0.05 | 0.25 | 0.23 | | | | | | | | | | | | |
| | | FR 100_4 | 3.30 | 0.05 | 0.25 | 0.23 | | | | | | | | | | | | |
| | | FR 200 | 6.61 | 0.10 | 0.22 | 0.25 | 4.46E-04 | | 332260 | | 0.04 | | -3.46 | 3.84 | 0.83 | 0.22 | 43.88 | 29.45 |
| | | FR 300 | 9.91 | 0.15 | 0.22 | 0.25 | 4.46E-04 | | 332260 | | 0.04 | | -3.39 | 3.76 | 0.79 | 0.19 | 40.74 | 27.28 |
| | | FR 500 | 16.52 | 0.24 | 0.22 | 0.25 | 4.46E-04 | | 332260 | | 0.04 | | -3.41 | 3.73 | 0.76 | 0.19 | 40.32 | 23.89 |
| | | FR 700 | 23.12 | 0.34 | 0.21 | 0.26 | 4.46E-04 | | 332260 | | 0.04 | | -3.70 | 3.58 | 0.72 | 0.23 | 34.52 | 0.23 |
| | | FR 1000 | 33.03 | 0.49 | 0.21 | 0.26 | 4.46E-04 | | 332260 | | 0.04 | | -3.50 | 3.57 | 0.64 | 0.33 | 25.16 | 17.98 |

**Table F9.** (continued)

| Flow rate (µL/min) | Sensor | Attachment Detachment | Flow | | Slope (K) | | Viscosity (kg/m/s) | | Elasticity (kg/m/s²) | | Wall shear stress (kg/m/s²) | | Δ*f* (Hz) | | Δ*D* (×10⁻⁶) | | Δ*m* (ng/cm²) | |
|---|---|---|---|---|---|---|---|---|---|---|---|---|---|---|---|---|---|---|
| | | | Re | Shear Stress (kg/m/s²) | avg. | std. | avg. | std. | avg. | std. | avg. | std. | avg. | std. | avg. | std. | avg. | std. |
| 100 | Glass | ATT1 | 3.30 | 0.05 | 0.10 | 0.01 | 2.00E-03 | 5.38E-04 | 339923 | 308603 | 0.10 | 0.03 | -36.50 | 2.81 | 3.96 | 0.60 | 2706.73 | 836.17 |
| | | ATT2 | 3.30 | 0.05 | 0.10 | 0.01 | | | | | | | | | | | | |
| | | ATT3 | 3.30 | 0.05 | 0.10 | 0.01 | | | | | | | | | | | | |
| | | FR 100_1 | 3.30 | 0.05 | 0.24 | 0.12 | 2.50E-03 | 1.11E-03 | 483804 | 403174 | 0.12 | 0.05 | -27.77 | 3.48 | 1.90 | 0.61 | 2014.06 | 715.49 |
| | | FR 100_2 | 3.30 | 0.05 | 0.21 | 0.04 | 2.65E-03 | 1.03E-03 | 518608 | 434061 | 0.13 | 0.05 | -27.77 | 3.48 | 1.90 | 0.61 | 2014.06 | 715.49 |
| | | FR 100_3 | 3.30 | 0.05 | 0.21 | 0.04 | | | | | | | | | | | | |
| | | FR 100_4 | 3.30 | 0.05 | 0.21 | 0.04 | | | | | | | | | | | | |
| | | FR 200 | 6.61 | 0.10 | 0.24 | 0.05 | 2.85E-03 | 1.35E-03 | 595305 | 506462 | 0.28 | 0.13 | -27.58 | 3.61 | 1.88 | 0.56 | 2030.83 | 729.31 |
| | | FR 300 | 9.91 | 0.15 | 0.21 | 0.01 | 2.86E-03 | 1.38E-03 | 617748 | 525908 | 0.42 | 0.20 | -27.57 | 3.45 | 1.85 | 0.57 | 2006.48 | 693.86 |
| | | FR 500 | 16.52 | 0.24 | 0.21 | 0.01 | 2.86E-03 | 1.38E-03 | 617748 | 525908 | 0.42 | 0.20 | -27.55 | 3.51 | 1.83 | 0.58 | 2025.92 | 728.94 |
| | | FR 700 | 23.12 | 0.34 | 0.21 | 0.01 | 2.86E-03 | 1.38E-03 | 617748 | 525908 | 0.42 | 0.20 | -27.22 | 3.45 | 1.78 | 0.57 | 1998.38 | 702.47 |
| | | FR 1000 | 33.03 | 0.49 | 0.21 | 0.01 | 2.86E-03 | 1.38E-03 | 617748 | 525908 | 0.42 | 0.20 | -26.96 | 3.77 | 1.74 | 0.62 | 2035.13 | 755.58 |

**Table F9.** (continued)

| Flow rate (µL/min) | Sensor | Attachment Detachment | Flow | | Slope (K) | | Viscosity (kg/m/s) | | Elasticity (kg/m/s²) | | Wall shear stress (kg/m/s²) | | Δ*f* (Hz) | | Δ*D* (×10⁻⁶) | | Δ*m* (ng/cm²) | |
|---|---|---|---|---|---|---|---|---|---|---|---|---|---|---|---|---|---|---|
| | | | Re | Shear Stress (kg/m/s²) | avg. | std. | avg. | std. | avg. | std. | avg. | std. | avg. | std. | avg. | std. | avg. | std. |
| 100 | SS | ATT1 | 3.30 | 0.05 | 0.21 | 0.01 | 1.43E-03 | 4.19E-04 | 85052 | 133812 | 0.07 | 0.02 | -30.70 | 3.61 | 5.72 | 0.73 | 3268.06 | 122.71 |
| | | ATT2 | 3.30 | 0.05 | 0.19 | 0.07 | 1.48E-03 | 3.42E-04 | 77346 | 114141 | 0.07 | 0.02 | -30.70 | 3.61 | 5.72 | 0.73 | 3268.06 | 122.71 |
| | | ATT3 | 3.30 | 0.05 | 0.19 | 0.07 | | | | | | | | | | | | |
| | | FR 100_1 | 3.30 | 0.05 | 0.45 | 0.17 | 1.40E-03 | 1.74E-04 | 76602 | 114071 | 0.07 | 0.01 | -33.44 | 4.13 | 5.34 | 0.76 | 3149.43 | 210.81 |
| | | FR 100_2 | 3.30 | 0.05 | 0.24 | 0.18 | 1.40E-03 | 1.70E-04 | 82635 | 124510 | 0.07 | 0.01 | -33.44 | 4.13 | 5.34 | 0.76 | 3149.43 | 210.81 |
| | | FR 100_3 | 3.30 | 0.05 | 0.24 | 0.18 | | | | | | | | | | | | |
| | | FR 100_4 | 3.30 | 0.05 | 0.24 | 0.18 | | | | | | | | | | | | |
| | | FR 200 | 6.61 | 0.10 | 0.23 | 0.10 | 1.56E-03 | 3.76E-04 | 86878 | 134408 | 0.15 | 0.04 | -33.57 | 4.17 | 5.34 | 0.75 | 3157.09 | 217.97 |
| | | FR 300 | 9.91 | 0.15 | 0.27 | 0.11 | 1.58E-03 | 4.13E-04 | 86269 | 134959 | 0.23 | 0.06 | -33.38 | 4.49 | 5.15 | 1.07 | 3170.45 | 225.50 |
| | | FR 500 | 16.52 | 0.24 | 0.27 | 0.11 | 1.58E-03 | 4.13E-04 | 86269 | 134959 | 0.23 | 0.06 | -33.43 | 4.52 | 5.12 | 1.08 | 3184.07 | 254.38 |
| | | FR 700 | 23.12 | 0.34 | 0.27 | 0.11 | 1.58E-03 | 4.13E-04 | 86269 | 134959 | 0.23 | 0.06 | -33.02 | 4.82 | 5.16 | 1.02 | 3234.87 | 192.58 |
| | | FR 1000 | 33.03 | 0.49 | 0.27 | 0.11 | 1.58E-03 | 4.13E-04 | 86269 | 134959 | 0.23 | 0.06 | -32.76 | 5.18 | 5.12 | 1.05 | 3328.67 | 112.00 |

**Table F9.** (continued)

| Flow rate (µL/min) | Sensor | Attachment Detachment | Flow | | Slope (K) | | Viscosity (kg/m/s) | | Elasticity (kg/m/s²) | | Wall shear stress (kg/m/s²) | | Δ*f* (Hz) | | Δ*D* (×10⁻⁶) | | Δ*m* (ng/cm²) | |
|---|---|---|---|---|---|---|---|---|---|---|---|---|---|---|---|---|---|---|
| | | | Re | Shear Stress (kg/m/s²) | avg. | std. | avg. | std. | avg. | std. | avg. | std. | avg. | std. | avg. | std. | avg. | std. |
| 50 | Gold | ATT1 | 1.65 | 0.02 | 0.16 | 0.07 | 1.83E-03 | 3.44E-04 | 330279 | 249467 | 0.04 | 0.01 | -28.10 | 2.79 | 3.01 | 0.18 | 886.76 | 366.52 |
| | | ATT2 | 1.65 | 0.02 | 0.06 | 0.01 | 2.18E-03 | 2.00E-04 | 391129 | 312939 | 0.05 | 0.00 | -28.10 | 2.79 | 3.01 | 0.18 | 886.76 | 366.52 |
| | | ATT3 | 1.65 | 0.02 | 0.06 | 0.01 | | | | | | | | | | | | |
| | | DET1 | 1.65 | 0.02 | 3.64 | 5.69 | 2.36E-03 | 9.24E-05 | 411301 | 330920 | 0.06 | 0.00 | -23.36 | 3.39 | 1.27 | 0.21 | 612.39 | 261.48 |
| | | DET2 | 1.65 | 0.02 | 0.41 | 0.16 | 3.43E-03 | 6.31E-04 | 639784 | 367723 | 0.08 | 0.02 | -23.36 | 3.39 | 1.27 | 0.21 | 612.39 | 261.48 |
| | | DET3 | 1.65 | 0.02 | 0.41 | 0.16 | | | | | | | | | | | | |
| | | DET4 | 1.65 | 0.02 | 0.41 | 0.16 | | | | | | | | | | | | |
| | | DET5 | 1.65 | 0.02 | 0.41 | 0.16 | | | | | | | | | | | | |
| | | DET6 | 1.65 | 0.02 | 0.41 | 0.16 | | | | | | | | | | | | |
| 50 | $SiO_2$ | ATT1 | 1.65 | 0.02 | 0.08 | 0.03 | 1.67E-03 | 4.66E-04 | 127792 | 119485 | 0.04 | 0.01 | -21.86 | 3.43 | 3.78 | 0.81 | 570.37 | 92.13 |
| | | ATT2 | 1.65 | 0.02 | 0.20 | 0.02 | 1.67E-03 | 4.04E-04 | 161279 | 134243 | 0.04 | 0.01 | -21.86 | 3.43 | 3.78 | 0.81 | 570.37 | 92.13 |
| | | ATT3 | 1.65 | 0.02 | 0.20 | 0.02 | | | | | | | | | | | | |
| | | DET1 | 1.65 | 0.02 | 0.13 | 0.03 | 1.61E-03 | 3.50E-04 | 156689 | 129486 | 0.04 | 0.01 | -7.67 | 2.63 | 1.34 | 0.46 | 149.98 | 5.45 |
| | | DET2 | 1.65 | 0.02 | 0.43 | 0.06 | 1.66E-03 | 4.24E-04 | 158868 | 132084 | 0.04 | 0.01 | -7.67 | 2.63 | 1.34 | 0.46 | 149.98 | 5.45 |
| | | DET3 | 1.65 | 0.02 | 0.12 | 0.02 | 1.61E-03 | 4.61E-04 | 179779 | 154427 | 0.04 | 0.01 | -7.67 | 2.63 | 1.34 | 0.46 | 149.98 | 5.45 |
| | | DET4 | 1.65 | 0.02 | 0.17 | 0.11 | 1.58E-03 | 4.57E-04 | 186085 | 158894 | 0.04 | 0.01 | -7.67 | 2.63 | 1.34 | 0.46 | 149.98 | 5.45 |
| | | DET5 | 1.65 | 0.02 | 0.12 | 0.03 | 1.53E-03 | 4.63E-04 | 192059 | 163685 | 0.04 | 0.01 | -7.67 | 2.63 | 1.34 | 0.46 | 149.98 | 5.45 |
| | | DET6 | 1.65 | 0.02 | 0.12 | 0.03 | | | | | | | | | | | | |

**Table F9.** (continued)

| Flow rate (µL/min) | Sensor | Attachment Detachment | Flow | | Slope (K) | | Viscosity (kg/m/s) | | Elasticity (kg/m/s²) | | Wall shear stress (kg/m/s²) | | Δ*f* (Hz) | | Δ*D* (×10⁻⁶) | | Δ*m* (ng/cm²) | |
|---|---|---|---|---|---|---|---|---|---|---|---|---|---|---|---|---|---|---|
| | | | Re | Shear Stress (kg/m/s²) | avg. | std. | avg. | std. | avg. | std. | avg. | std. | avg. | std. | avg. | std. | avg. | std. |
| 50 | Glass | ATT1 | 1.65 | 0.02 | 0.13 | 0.04 | 1.30E-03 | 2.53E-04 | 19759 | 13746 | 0.03 | 0.01 | -40.42 | 7.39 | 4.08 | 0.41 | 1523.88 | 373.64 |
| | | ATT2 | 1.65 | 0.02 | 0.09 | 0.02 | 1.44E-03 | 1.25E-04 | 18396 | 7532 | 0.04 | 0.00 | -40.42 | 7.39 | 4.08 | 0.41 | 1523.88 | 373.64 |
| | | ATT3 | 1.65 | 0.02 | 0.09 | 0.08 | 1.75E-03 | 2.25E-04 | 37581 | 17493 | 0.04 | 0.01 | -40.42 | 7.39 | 4.08 | 0.41 | 1523.88 | 373.64 |
| | | DET1 | 1.65 | 0.02 | 0.15 | 0.18 | 2.02E-03 | 5.88E-04 | 72853 | 67808 | 0.05 | 0.01 | -34.63 | 10.09 | 1.68 | 0.59 | 968.91 | 72.50 |
| | | DET2 | 1.65 | 0.02 | 0.53 | 0.42 | 2.16E-03 | 5.00E-04 | 68426 | 58964 | 0.05 | 0.01 | -34.63 | 10.09 | 1.68 | 0.59 | 968.91 | 72.50 |
| | | DET3 | 1.65 | 0.02 | 0.62 | 0.54 | 3.43E-03 | 2.12E-03 | 353133 | 432281 | 0.08 | 0.05 | -34.63 | 10.09 | 1.68 | 0.59 | 968.91 | 72.50 |
| | | DET4 | 1.65 | 0.02 | 0.62 | 0.54 | | | | | | | | | | | | |
| | | DET5 | 1.65 | 0.02 | 0.62 | 0.54 | | | | | | | | | | | | |
| | | DET6 | 1.65 | 0.02 | 0.62 | 0.54 | | | | | | | | | | | | |
| 50 | SS | ATT1 | 1.65 | 0.02 | 0.19 | 0.06 | 1.52E-03 | 5.91E-04 | 139239 | 122840 | 0.04 | 0.01 | -24.58 | 4.41 | 4.10 | 1.47 | 797.06 | 52.12 |
| | | ATT2 | 1.65 | 0.02 | 0.11 | 0.02 | 1.71E-03 | 5.46E-04 | 140966 | 108991 | 0.04 | 0.01 | -24.58 | 4.41 | 4.10 | 1.47 | 797.06 | 52.12 |
| | | ATT3 | 1.65 | 0.02 | 0.11 | 0.02 | | | | | | | | | | | | |
| | | DET1 | 1.65 | 0.02 | 0.50 | 0.20 | 1.74E-03 | 5.08E-04 | 133821 | 103801 | 0.04 | 0.01 | -26.15 | 4.83 | 3.57 | 2.00 | 750.95 | 76.74 |
| | | DET2 | 1.65 | 0.02 | 1.76 | 2.12 | 1.88E-03 | 7.06E-04 | 148324 | 115001 | 0.05 | 0.02 | -26.15 | 4.83 | 3.57 | 2.00 | 750.95 | 76.74 |
| | | DET3 | 1.65 | 0.02 | 0.09 | 0.02 | 2.06E-03 | 9.45E-04 | 193563 | 162121 | 0.05 | 0.02 | -26.15 | 4.83 | 3.57 | 2.00 | 750.95 | 76.74 |
| | | DET4 | 1.65 | 0.02 | 0.09 | 0.02 | | | | | | | | | | | | |
| | | DET5 | 1.65 | 0.02 | 0.09 | 0.02 | | | | | | | | | | | | |
| | | DET6 | 1.65 | 0.02 | 0.09 | 0.02 | | | | | | | | | | | | |

**Table F9.** (continued)

| Flow rate (µL/min) | Sensor | Attachment Detachment | Flow | | Slope (K) | | Viscosity (kg/m/s) | | Elasticity (kg/m/s²) | | Wall shear stress (kg/m/s²) | | Δ*f* (Hz) | | Δ*D* (×10⁻⁶) | | Δ*m* (ng/cm²) | |
|---|---|---|---|---|---|---|---|---|---|---|---|---|---|---|---|---|---|---|
| | | | Re | Shear Stress (kg/m/s²) | avg. | std. | avg. | std. | avg. | std. | avg. | std. | avg. | std. | avg. | std. | avg. | std. |
| 200 | Gold | ATT1 | 6.61 | 0.10 | 0.10 | 0.02 | 1.62E-03 | 3.35E-04 | 307206 | 501032 | 0.16 | 0.03 | -26.22 | 2.65 | 2.88 | 0.14 | 1079.08 | 549.52 |
| | | ATT2 | 6.61 | 0.10 | 0.11 | 0.04 | 1.54E-03 | 9.77E-05 | 266750 | 424877 | 0.15 | 0.01 | -26.22 | 2.65 | 2.88 | 0.14 | 1079.08 | 549.52 |
| | | ATT3 | 6.61 | 0.10 | 0.11 | 0.04 | | | | | | | | | | | | |
| | | DET1 | 6.61 | 0.10 | 0.21 | 0.06 | 1.60E-03 | 6.14E-06 | 267252 | 415196 | 0.16 | 0.00 | -19.76 | 2.74 | 1.03 | 0.05 | 561.11 | 213.01 |
| | | DET2 | 6.61 | 0.10 | 0.33 | 0.03 | 2.47E-03 | 4.25E-04 | 512203 | 814940 | 0.24 | 0.04 | -19.76 | 2.74 | 1.03 | 0.05 | 561.11 | 213.01 |
| | | DET3 | 6.61 | 0.10 | 0.33 | 0.03 | | | | | | | | | | | | |
| | | DET4 | 6.61 | 0.10 | 0.33 | 0.03 | | | | | | | | | | | | |
| | | DET5 | 6.61 | 0.10 | 0.33 | 0.03 | | | | | | | | | | | | |
| | | DET6 | 6.61 | 0.10 | 0.33 | 0.03 | | | | | | | | | | | | |
| 200 | $SiO_2$ | ATT1 | 6.61 | 0.10 | 0.18 | 0.01 | 1.94E-03 | 8.95E-04 | 268111 | 241740 | 0.19 | 0.09 | -19.56 | 3.87 | 5.25 | 1.50 | 614.41 | |
| | | ATT2 | 6.61 | 0.10 | 0.61 | 0.74 | 1.72E-03 | 5.43E-04 | 240263 | 207134 | 0.17 | 0.05 | -19.56 | 3.87 | 5.25 | 1.50 | 614.41 | |
| | | ATT3 | 6.61 | 0.10 | 0.65 | 0.76 | 1.36E-03 | 3.27E-04 | 226269 | 195656 | 0.13 | 0.03 | -19.56 | 3.87 | 5.25 | 1.50 | 614.41 | |
| | | DET1 | 6.61 | 0.10 | 0.22 | 0.02 | 1.43E-03 | 4.15E-04 | 144116 | 197658 | 0.14 | 0.04 | -3.84 | 6.30 | 2.30 | 1.47 | 166.80 | |
| | | DET2 | 6.61 | 0.10 | 0.32 | 0.21 | 1.47E-03 | 4.81E-04 | 150347 | 205989 | 0.14 | 0.05 | -3.84 | 6.30 | 2.30 | 1.47 | 166.80 | |
| | | DET3 | 6.61 | 0.10 | 0.16 | 0.02 | 1.25E-03 | 2.66E-04 | 172688 | 242694 | 0.12 | 0.03 | -3.84 | 6.30 | 2.30 | 1.47 | 166.80 | |
| | | DET4 | 6.61 | 0.10 | 0.16 | 0.02 | | | | | | | | | | | | |
| | | DET5 | 6.61 | 0.10 | 0.16 | 0.02 | | | | | | | | | | | | |
| | | DET6 | 6.61 | 0.10 | 0.16 | 0.02 | | | | | | | | | | | | |

**Table F9.** (continued)

| Flow rate (µL/min) | Sensor | Attachment Detachment | Flow | | Slope (K) | | Viscosity (kg/m/s) | | Elasticity (kg/m/s²) | | Wall shear stress (kg/m/s²) | | Δ*f* (Hz) | | Δ*D* (×10⁻⁶) | | Δ*m* (ng/cm²) | |
|---|---|---|---|---|---|---|---|---|---|---|---|---|---|---|---|---|---|---|
| | | | Re | Shear Stress (kg/m/s²) | avg. | std. | avg. | std. | avg. | std. | avg. | std. | avg. | std. | avg. | std. | avg. | std. |
| 200 | Glass | ATT1 | 6.61 | 0.10 | 0.12 | 0.03 | 1.89E-03 | 9.99E-04 | 111088 | 172669 | 0.18 | 0.10 | -40.13 | 5.11 | 4.68 | 0.79 | 1919.70 | 610.57 |
| | | ATT2 | 6.61 | 0.10 | 0.25 | 0.25 | 1.85E-03 | 7.57E-04 | 83447 | 117194 | 0.18 | 0.07 | -40.13 | 5.11 | 4.68 | 0.79 | 1919.70 | 610.57 |
| | | ATT3 | 6.61 | 0.10 | 0.25 | 0.25 | | | | | | | | | | | | |
| | | DET1 | 6.61 | 0.10 | 0.12 | 0.04 | 1.46E-03 | 8.32E-05 | 18272 | 7964 | 0.14 | 0.01 | -32.69 | 5.79 | 1.90 | 0.83 | 1552.73 | 229.92 |
| | | DET2 | 6.61 | 0.10 | 0.53 | 0.07 | 1.51E-03 | 8.60E-05 | 20221 | 8430 | 0.15 | 0.01 | -32.69 | 5.79 | 1.90 | 0.83 | 1552.73 | 229.92 |
| | | DET3 | 6.61 | 0.10 | 0.32 | 0.20 | 1.56E-03 | 6.67E-05 | 12941 | 14745 | 0.15 | 0.01 | -32.69 | 5.79 | 1.90 | 0.83 | 1552.73 | 229.92 |
| | | DET4 | 6.61 | 0.10 | 0.32 | 0.20 | | | | | | | | | | | | |
| | | DET5 | 6.61 | 0.10 | 0.32 | 0.20 | | | | | | | | | | | | |
| | | DET6 | 6.61 | 0.10 | 0.32 | 0.20 | | | | | | | | | | | | |
| 200 | Glass | ATT1 | 6.61 | 0.10 | 0.12 | 0.03 | 1.89E-03 | 9.99E-04 | 111088 | 172669 | 0.18 | 0.10 | -40.13 | 5.11 | 4.68 | 0.79 | 1919.70 | 610.57 |
| | | ATT2 | 6.61 | 0.10 | 0.25 | 0.25 | 1.85E-03 | 7.57E-04 | 83447 | 117194 | 0.18 | 0.07 | -40.13 | 5.11 | 4.68 | 0.79 | 1919.70 | 610.57 |
| | | ATT3 | 6.61 | 0.10 | 0.25 | 0.25 | | | | | | | | | | | | |
| | | DET1 | 6.61 | 0.10 | 0.12 | 0.04 | 1.46E-03 | 8.32E-05 | 18272 | 7964 | 0.14 | 0.01 | -32.69 | 5.79 | 1.90 | 0.83 | 1552.73 | 229.92 |
| | | DET2 | 6.61 | 0.10 | 0.53 | 0.07 | 1.51E-03 | 8.60E-05 | 20221 | 8430 | 0.15 | 0.01 | -32.69 | 5.79 | 1.90 | 0.83 | 1552.73 | 229.92 |
| | | DET3 | 6.61 | 0.10 | 0.32 | 0.20 | 1.56E-03 | 6.67E-05 | 12941 | 14745 | 0.15 | 0.01 | -32.69 | 5.79 | 1.90 | 0.83 | 1552.73 | 229.92 |
| | | DET4 | 6.61 | 0.10 | 0.32 | 0.20 | | | | | | | | | | | | |
| | | DET5 | 6.61 | 0.10 | 0.32 | 0.20 | | | | | | | | | | | | |
| | | DET6 | 6.61 | 0.10 | 0.32 | 0.20 | | | | | | | | | | | | |

**Table F10.** QCM-D data of MV during attachment and detachment experiments

| Flow rate (µL/min) | Sensor | Attachment Detachment | Flow | | Slope (K) | | Viscosity (kg/m/s) | | Elasticity (kg/m/s²) | | Wall shear stress (kg/m/s²) | | Δ*f* (Hz) | | Δ*D* (×10⁻⁶) | | Δ*m* (ng/cm²) | |
|---|---|---|---|---|---|---|---|---|---|---|---|---|---|---|---|---|---|---|
| | | | Re | Shear Stress (kg/m/s²) | avg. | std. | avg. | std. | avg. | std. | avg. | std. | avg. | std. | avg. | std. | avg. | std. |
| 100 | Gold | ATT1 | 3.30 | 0.05 | 0.16 | 0.01 | 1.68E-03 | 3.83E-04 | 96640 | 132591 | 0.08 | 0.02 | -60.66 | 6.05 | 10.09 | 0.99 | 3498.48 | 292.16 |
| | | ATT2 | 3.30 | 0.05 | 0.16 | 0.01 | | | | | | | | | | | | |
| | | ATT3 | 3.30 | 0.05 | 0.16 | 0.01 | | | | | | | | | | | | |
| | | FR 100_1 | 3.30 | 0.05 | 0.30 | 0.06 | 1.75E-03 | 3.52E-04 | 100094 | 128378 | 0.08 | 0.02 | -35.48 | 2.67 | 2.27 | 0.64 | 1470.98 | 24.73 |
| | | FR 100_2 | 3.30 | 0.05 | 0.02 | 0.03 | 1.57E-03 | 1.53E-04 | 61494 | 41936 | 0.08 | 0.01 | -35.48 | 2.67 | 2.27 | 0.64 | 1470.98 | 24.73 |
| | | FR 100_3 | 3.30 | 0.05 | 0.26 | 0.21 | 1.57E-03 | 1.53E-04 | 64343 | 39512 | 0.08 | 0.01 | -35.48 | 2.67 | 2.27 | 0.64 | 1470.98 | 24.73 |
| | | FR 100_4 | 3.30 | 0.05 | 0.66 | 0.57 | 1.71E-03 | 4.83E-05 | 52241 | 49842 | 0.08 | 0.00 | -35.48 | 2.67 | 2.27 | 0.64 | 1470.98 | 24.73 |
| | | FR 200 | 6.61 | 0.10 | 0.45 | 0.18 | 1.79E-03 | 2.30E-05 | 18475 | 9375 | 0.17 | 0.00 | -34.92 | 2.35 | 2.03 | 0.43 | 1445.55 | 24.65 |
| | | FR 300 | 9.91 | 0.15 | 0.45 | 0.18 | 1.79E-03 | 2.30E-05 | 18475 | 9375 | 0.17 | 0.00 | -34.24 | 1.54 | 1.87 | 0.27 | 1449.67 | 36.59 |
| | | FR 500 | 16.52 | 0.24 | 0.33 | 0.12 | 1.80E-03 | 2.86E-05 | 12991 | 2431 | 0.44 | 0.01 | -33.75 | 1.26 | 1.75 | 0.26 | 1468.79 | 63.18 |
| | | FR 700 | 23.12 | 0.34 | 0.33 | 0.12 | 1.80E-03 | 2.86E-05 | 12991 | 2431 | 0.44 | 0.01 | -33.26 | 0.95 | 1.64 | 0.29 | 1442.66 | 38.87 |
| | | FR 1000 | 33.03 | 0.49 | 0.33 | 0.12 | 1.80E-03 | 2.86E-05 | 12991 | 2431 | 0.44 | 0.01 | -32.85 | 0.80 | 1.55 | 0.29 | 1441.22 | 42.53 |

**Table F10.** (continued)

| Flow rate (µL/min) | Sensor | Attachment Detachment | Flow | | Slope (K) | | Viscosity (kg/m/s) | | Elasticity (kg/m/s²) | | Wall shear stress (kg/m/s²) | | Δ*f* (Hz) | | Δ*D* (×10⁻⁶) | | Δ*m* (ng/cm²) | |
|---|---|---|---|---|---|---|---|---|---|---|---|---|---|---|---|---|---|---|
| | | | Re | Shear Stress (kg/m/s²) | avg. | std. | avg. | std. | avg. | std. | avg. | std. | avg. | std. | avg. | std. | avg. | std. |
| 100 | $SiO_2$ | ATT1 | 3.30 | 0.05 | 0.17 | 0.01 | 1.90E-03 | 3.33E-04 | 235036 | 191611 | 0.09 | 0.02 | -58.48 | 9.28 | 10.11 | 0.66 | 1382.39 | 256.55 |
| | | ATT2 | 3.30 | 0.05 | 0.54 | 0.36 | 1.84E-03 | 3.19E-04 | 232843 | 190214 | 0.09 | 0.02 | -58.48 | 9.28 | 10.11 | 0.66 | 1382.39 | 256.55 |
| | | ATT3 | 3.30 | 0.05 | 0.54 | 0.36 | | | | | | | | | | | | |
| | | FR 100_1 | 3.30 | 0.05 | 0.31 | 0.09 | 1.70E-03 | 3.25E-04 | 216893 | 179200 | 0.08 | 0.02 | -22.71 | 7.98 | 2.76 | 0.43 | 462.58 | 225.68 |
| | | FR 100_2 | 3.30 | 0.05 | 0.03 | 0.02 | 1.50E-03 | 2.03E-04 | 141794 | 108184 | 0.07 | 0.01 | -22.71 | 7.98 | 2.76 | 0.43 | 462.58 | 225.68 |
| | | FR 100_3 | 3.30 | 0.05 | 0.26 | 0.06 | 1.39E-03 | 1.73E-04 | 103374 | 80414 | 0.07 | 0.01 | -22.71 | 7.98 | 2.76 | 0.43 | 462.58 | 225.68 |
| | | FR 100_4 | 3.30 | 0.05 | 0.58 | 0.22 | 1.51E-03 | 4.61E-04 | 201181 | 173792 | 0.07 | 0.02 | -22.71 | 7.98 | 2.76 | 0.43 | 462.58 | 225.68 |
| | | FR 200 | 6.61 | 0.10 | 0.40 | 0.27 | 1.51E-03 | 4.64E-04 | 225961 | 193965 | 0.15 | 0.05 | -22.80 | 8.53 | 2.63 | 0.46 | 465.80 | 247.52 |
| | | FR 300 | 9.91 | 0.15 | 0.40 | 0.27 | 1.51E-03 | 4.64E-04 | 225961 | 193965 | 0.15 | 0.05 | -22.10 | 7.92 | 2.45 | 0.35 | 435.52 | 214.20 |
| | | FR 500 | 16.52 | 0.24 | 0.40 | 0.27 | 1.51E-03 | 4.64E-04 | 225961 | 193965 | 0.15 | 0.05 | -21.57 | 7.27 | 2.31 | 0.34 | 414.65 | 183.57 |
| | | FR 700 | 23.12 | 0.34 | 0.40 | 0.27 | 1.51E-03 | 4.64E-04 | 225961 | 193965 | 0.15 | 0.05 | -21.00 | 7.20 | 2.14 | 0.46 | 393.26 | 171.18 |
| | | FR 1000 | 33.03 | 0.49 | 0.40 | 0.27 | 1.51E-03 | 4.64E-04 | 225961 | 193965 | 0.15 | 0.05 | -20.40 | 7.20 | 2.09 | 0.44 | 378.88 | 173.18 |

**Table F10.** (continued)

| Flow rate (µL/min) | Sensor | Attachment Detachment | Flow | | Slope (K) | | Viscosity (kg/m/s) | | Elasticity (kg/m/s²) | | Wall shear stress (kg/m/s²) | | Δ*f* (Hz) | | Δ*D* (×10⁻⁶) | | Δ*m* (ng/cm²) | |
|---|---|---|---|---|---|---|---|---|---|---|---|---|---|---|---|---|---|---|
| | | | Re | Shear Stress (kg/m/s²) | avg. | std. | avg. | std. | avg. | std. | avg. | std. | avg. | std. | avg. | std. | avg. | std. |
| 100 | Glass | ATT1 | 3.30 | 0.05 | 0.16 | 0.02 | 1.53E-03 | 1.41E-04 | 22003 | 6710 | 0.07 | 0.01 | -64.39 | 10.70 | 10.31 | 0.48 | 3909.32 | 651.42 |
| | | ATT2 | 3.30 | 0.05 | 0.16 | 0.02 | 1.53E-03 | 1.41E-04 | 22003 | 6710 | 0.07 | 0.01 | -64.39 | 10.70 | 10.31 | 0.48 | 3909.32 | 651.42 |
| | | ATT3 | 3.30 | 0.05 | 0.16 | 0.02 | 1.53E-03 | 1.41E-04 | 22003 | 6710 | 0.07 | 0.01 | -64.39 | 10.70 | 10.31 | 0.48 | 3909.32 | 651.42 |
| | | FR 100_1 | 3.30 | 0.05 | 0.40 | 0.05 | 1.61E-03 | 1.97E-04 | 26134 | 10833 | 0.08 | 0.01 | -42.92 | 12.05 | 3.28 | 0.31 | 2153.31 | 323.51 |
| | | FR 100_2 | 3.30 | 0.05 | 0.05 | 0.04 | 1.51E-03 | 2.01E-04 | 39651 | 18337 | 0.07 | 0.01 | -42.92 | 12.05 | 3.28 | 0.31 | 2153.31 | 323.51 |
| | | FR 100_3 | 3.30 | 0.05 | 1.10 | 0.98 | 1.53E-03 | 2.21E-04 | 43036 | 16611 | 0.07 | 0.01 | -42.92 | 12.05 | 3.28 | 0.31 | 2153.31 | 323.51 |
| | | FR 100_4 | 3.30 | 0.05 | 1.64 | 0.62 | 1.65E-03 | 2.97E-04 | 25643 | 12632 | 0.08 | 0.01 | -42.92 | 12.05 | 3.28 | 0.31 | 2153.31 | 323.51 |
| | | FR 200 | 6.61 | 0.10 | 0.31 | 0.14 | 1.70E-03 | 3.69E-04 | 13381 | 8922 | 0.17 | 0.04 | -42.25 | 12.45 | 3.15 | 0.36 | 2163.40 | 372.27 |
| | | FR 300 | 9.91 | 0.15 | 0.31 | 0.14 | 1.70E-03 | 3.69E-04 | 13381 | 8922 | 0.17 | 0.04 | -41.52 | 13.22 | 3.01 | 0.43 | 2118.34 | 327.58 |
| | | FR 500 | 16.52 | 0.24 | 0.31 | 0.14 | 1.70E-03 | 3.69E-04 | 13381 | 8922 | 0.17 | 0.04 | -41.22 | 13.35 | 2.88 | 0.53 | 2157.16 | 397.92 |
| | | FR 700 | 23.12 | 0.34 | 0.31 | 0.14 | 1.70E-03 | 3.69E-04 | 13381 | 8922 | 0.17 | 0.04 | -40.84 | 13.70 | 2.75 | 0.60 | 2160.64 | 396.91 |
| | | FR 1000 | 33.03 | 0.49 | 0.31 | 0.14 | 1.70E-03 | 3.69E-04 | 13381 | 8922 | 0.17 | 0.04 | -40.65 | 13.70 | 2.80 | 0.46 | 2231.06 | 541.04 |

**Table F10.** (continued)

| Flow rate (µL/min) | Sensor | Attachment Detachment | Flow | | Slope (K) | | Viscosity (kg/m/s) | | Elasticity (kg/m/s²) | | Wall shear stress (kg/m/s²) | | Δ*f* (Hz) | | Δ*D* (×10⁻⁶) | | Δ*m* (ng/cm²) | |
|---|---|---|---|---|---|---|---|---|---|---|---|---|---|---|---|---|---|---|
| | | | Re | Shear Stress (kg/m/s²) | avg. | std. | avg. | std. | avg. | std. | avg. | std. | avg. | std. | avg. | std. | avg. | std. |
| 100 | SS | ATT1 | 3.30 | 0.05 | 0.15 | 0.00 | 1.73E-03 | 3.68E-04 | 112834 | 159076 | 0.08 | 0.02 | -64.74 | 1.85 | 9.85 | 0.16 | 2859.11 | 1074.60 |
| | | ATT2 | 3.30 | 0.05 | 0.17 | 0.04 | 1.77E-03 | 4.25E-04 | 112682 | 158811 | 0.09 | 0.02 | -64.74 | 1.85 | 9.85 | 0.16 | 2859.11 | 1074.60 |
| | | ATT3 | 3.30 | 0.05 | 0.17 | 0.04 | | | | | | | | | | | | |
| | | FR 100_1 | 3.30 | 0.05 | 0.21 | 0.16 | 1.74E-03 | 1.46E-04 | 78547 | 85122 | 0.08 | 0.01 | -39.02 | 1.55 | 1.90 | 0.03 | 1659.31 | 52.79 |
| | | FR 100_2 | 3.30 | 0.05 | 0.10 | 0.14 | 1.65E-03 | 1.23E-04 | 69185 | 51122 | 0.08 | 0.01 | -39.02 | 1.55 | 1.90 | 0.03 | 1659.31 | 52.79 |
| | | FR 100_3 | 3.30 | 0.05 | 0.69 | 0.46 | 1.64E-03 | 1.28E-04 | 71907 | 48628 | 0.08 | 0.01 | -39.02 | 1.55 | 1.90 | 0.03 | 1659.31 | 52.79 |
| | | FR 100_4 | 3.30 | 0.05 | 1.10 | 0.11 | 1.74E-03 | 8.92E-05 | 57706 | 60750 | 0.08 | 0.00 | -39.02 | 1.55 | 1.90 | 0.03 | 1659.31 | 52.79 |
| | | FR 200 | 6.61 | 0.10 | 0.22 | 0.08 | 1.83E-03 | 1.20E-04 | 8460 | 1548 | 0.18 | 0.01 | -38.55 | 1.71 | 1.82 | 0.09 | 1635.64 | 45.26 |
| | | FR 300 | 9.91 | 0.15 | 0.28 | 0.09 | 1.83E-03 | 1.20E-04 | 8460 | 1548 | 0.27 | 0.02 | -37.41 | 2.67 | 1.30 | 0.75 | 1631.49 | 48.28 |
| | | FR 500 | 16.52 | 0.24 | 0.28 | 0.09 | 1.83E-03 | 1.20E-04 | 8460 | 1548 | 0.27 | 0.02 | -36.97 | 3.09 | 1.16 | 0.91 | 1638.82 | 65.90 |
| | | FR 700 | 23.12 | 0.34 | 0.28 | 0.09 | 1.83E-03 | 1.20E-04 | 8460 | 1548 | 0.27 | 0.02 | -36.72 | 3.10 | 1.11 | 0.91 | 1637.06 | 65.40 |
| | | FR 1000 | 33.03 | 0.49 | 0.28 | 0.09 | 1.83E-03 | 1.20E-04 | 8460 | 1548 | 0.27 | 0.02 | -36.38 | 3.24 | 1.01 | 0.98 | 1615.39 | 34.53 |

**Table F10.** (continued)

| Flow rate (µL/min) | Sensor | Attachment Detachment | Flow | | Slope (K) | | Viscosity (kg/m/s) | | Elasticity (kg/m/s²) | | Wall shear stress (kg/m/s²) | | Δ*f* (Hz) | | Δ*D* (×10⁻⁶) | | Δ*m* (ng/cm²) | |
|---|---|---|---|---|---|---|---|---|---|---|---|---|---|---|---|---|---|---|
| | | | Re | Shear Stress (kg/m/s²) | avg. | std. | avg. | std. | avg. | std. | avg. | std. | avg. | std. | avg. | std. | avg. | std. |
| 50 | Gold | ATT1 | 1.65 | 0.02 | 0.17 | 0.00 | 1.29E-03 | 1.24E-05 | 9398 | 322 | 0.03 | 0.00 | -44.84 | 2.81 | 7.99 | 0.42 | 4067.90 | 179.78 |
| | | ATT2 | 1.65 | 0.02 | 0.17 | 0.00 | | | | | | | | | | | | |
| | | ATT3 | 1.65 | 0.02 | 0.17 | 0.00 | | | | | | | | | | | | |
| | | DET1 | 1.65 | 0.02 | 0.32 | 0.06 | 1.35E-03 | 1.22E-05 | 12496 | 378 | 0.03 | 0.00 | -24.18 | 0.77 | 2.47 | 0.45 | 1879.94 | 117.38 |
| | | DET2 | 1.65 | 0.02 | 0.06 | 0.04 | 1.33E-03 | 7.15E-06 | 20602 | 1775 | 0.03 | 0.00 | -24.18 | 0.77 | 2.47 | 0.45 | 1879.94 | 117.38 |
| | | DET3 | 1.65 | 0.02 | 0.37 | 0.03 | 1.32E-03 | 3.85E-06 | 25153 | 890 | 0.03 | 0.00 | -24.18 | 0.77 | 2.47 | 0.45 | 1879.94 | 117.38 |
| | | DET4 | 1.65 | 0.02 | 2.27 | 0.79 | 1.34E-03 | 1.40E-06 | 19341 | 1768 | 0.03 | 0.00 | -24.18 | 0.77 | 2.47 | 0.45 | 1879.94 | 117.38 |
| | | DET5 | 1.65 | 0.02 | 0.38 | 0.05 | 1.35E-03 | 1.08E-05 | 13388 | 1478 | 0.03 | 0.00 | -24.18 | 0.77 | 2.47 | 0.45 | 1879.94 | 117.38 |
| | | DET6 | 1.65 | 0.02 | 0.54 | 0.21 | 1.35E-03 | 1.22E-05 | 10436 | 3713 | 0.03 | 0.00 | -24.18 | 0.77 | 2.47 | 0.45 | 1879.94 | 117.38 |
| 50 | $SiO_2$ | ATT1 | 1.65 | 0.02 | 0.17 | 0.01 | 1.79E-03 | 3.52E-04 | 211640 | 178882 | 0.04 | 0.01 | -45.65 | 7.24 | 9.08 | 0.65 | 1184.12 | 250.38 |
| | | ATT2 | 1.65 | 0.02 | 0.61 | 0.18 | 1.75E-03 | 2.86E-04 | 211283 | 174552 | 0.04 | 0.01 | -45.65 | 7.24 | 9.08 | 0.65 | 1184.12 | 250.38 |
| | | ATT3 | 1.65 | 0.02 | 0.29 | 0.12 | 1.64E-03 | 2.72E-04 | 207419 | 172127 | 0.04 | 0.01 | -45.65 | 7.24 | 9.08 | 0.65 | 1184.12 | 250.38 |
| | | DET1 | 1.65 | 0.02 | 0.36 | 0.16 | 1.51E-03 | 2.51E-04 | 184695 | 152653 | 0.04 | 0.01 | -16.23 | 4.85 | 3.25 | 0.43 | 396.16 | 127.38 |
| | | DET2 | 1.65 | 0.02 | 0.10 | 0.08 | 1.41E-03 | 2.08E-04 | 148663 | 119535 | 0.03 | 0.01 | -16.23 | 4.85 | 3.25 | 0.43 | 396.16 | 127.38 |
| | | DET3 | 1.65 | 0.02 | 0.24 | 0.08 | 1.31E-03 | 1.76E-04 | 113205 | 90647 | 0.03 | 0.00 | -16.23 | 4.85 | 3.25 | 0.43 | 396.16 | 127.38 |
| | | DET4 | 1.65 | 0.02 | 1.13 | 0.64 | 1.42E-03 | 5.05E-04 | 183664 | 170574 | 0.03 | 0.01 | -16.23 | 4.85 | 3.25 | 0.43 | 396.16 | 127.38 |
| | | DET5 | 1.65 | 0.02 | 0.26 | 0.02 | 1.45E-03 | 5.56E-04 | 210107 | 186998 | 0.04 | 0.01 | -16.23 | 4.85 | 3.25 | 0.43 | 396.16 | 127.38 |
| | | DET6 | 1.65 | 0.02 | 0.26 | 0.02 | | | | | | | | | | | | |

**Table F10.** (continued)

| Flow rate (µL/min) | Sensor | Attachment Detachment | Flow | | Slope (K) | | Viscosity (kg/m/s) | | Elasticity (kg/m/s²) | | Wall shear stress (kg/m/s²) | | Δ*f* (Hz) | | Δ*D* (×10⁻⁶) | | Δ*m* (ng/cm²) | |
|---|---|---|---|---|---|---|---|---|---|---|---|---|---|---|---|---|---|---|
| | | | Re | Shear Stress (kg/m/s²) | avg. | std. | avg. | std. | avg. | std. | avg. | std. | avg. | std. | avg. | std. | avg. | std. |
| 50 | Glass | ATT1 | 1.65 | 0.02 | 0.16 | 0.01 | 1.43E-03 | 1.60E-05 | 16864 | 993 | 0.03 | 0.00 | -56.18 | 2.20 | 9.14 | 0.30 | 3643.89 | 89.40 |
| | | ATT2 | 1.65 | 0.02 | 0.16 | 0.01 | | | | | | | | | | | | |
| | | ATT3 | 1.65 | 0.02 | 0.16 | 0.01 | | | | | | | | | | | | |
| | | DET1 | 1.65 | 0.02 | 0.37 | 0.06 | 1.51E-03 | 2.05E-05 | 21367 | 267 | 0.04 | 0.00 | -35.58 | 3.09 | 3.05 | 0.68 | 1934.31 | 207.81 |
| | | DET2 | 1.65 | 0.02 | 0.04 | 0.03 | 1.45E-03 | 2.88E-05 | 29310 | 338 | 0.04 | 0.00 | -35.58 | 3.09 | 3.05 | 0.68 | 1934.31 | 207.81 |
| | | DET3 | 1.65 | 0.02 | 0.60 | 0.08 | 1.45E-03 | 2.81E-05 | 32445 | 2235 | 0.04 | 0.00 | -35.58 | 3.09 | 3.05 | 0.68 | 1934.31 | 207.81 |
| | | DET4 | 1.65 | 0.02 | 1.82 | 0.05 | 1.48E-03 | 2.29E-05 | 23744 | 1446 | 0.04 | 0.00 | -35.58 | 3.09 | 3.05 | 0.68 | 1934.31 | 207.81 |
| | | DET5 | 1.65 | 0.02 | 0.40 | 0.06 | 1.57E-03 | 9.20E-06 | 14580 | 1656 | 0.04 | 0.00 | -35.58 | 3.09 | 3.05 | 0.68 | 1934.31 | 207.81 |
| | | DET6 | 1.65 | 0.02 | 0.40 | 0.06 | | | | | | | | | | | | |
| 50 | SS | ATT1 | 1.65 | 0.02 | 0.15 | 0.00 | 1.45E-03 | 1.43E-05 | 17323 | 1309 | 0.04 | 0.00 | -59.80 | 0.69 | 9.16 | 0.41 | 3452.24 | 201.50 |
| | | ATT2 | 1.65 | 0.02 | 0.15 | 0.00 | | | | | | | | | | | | |
| | | ATT3 | 1.65 | 0.02 | 0.15 | 0.00 | | | | | | | | | | | | |
| | | DET1 | 1.65 | 0.02 | 0.20 | 0.06 | 1.59E-03 | 3.48E-05 | 25247 | 3078 | 0.04 | 0.00 | -33.18 | 1.21 | 1.88 | 0.32 | 1676.51 | 82.91 |
| | | DET2 | 1.65 | 0.02 | 0.07 | 0.06 | 1.54E-03 | 7.31E-05 | 29904 | 1374 | 0.04 | 0.00 | -33.18 | 1.21 | 1.88 | 0.32 | 1676.51 | 82.91 |
| | | DET3 | 1.65 | 0.02 | 0.28 | 0.15 | 1.52E-03 | 5.87E-05 | 35333 | 2621 | 0.04 | 0.00 | -33.18 | 1.21 | 1.88 | 0.32 | 1676.51 | 82.91 |
| | | DET4 | 1.65 | 0.02 | 0.96 | 0.15 | 1.58E-03 | 4.02E-05 | 23293 | 4777 | 0.04 | 0.00 | -33.18 | 1.21 | 1.88 | 0.32 | 1676.51 | 82.91 |
| | | DET5 | 1.65 | 0.02 | 0.26 | 0.05 | 1.65E-03 | 5.69E-05 | 10349 | 4479 | 0.04 | 0.00 | -33.18 | 1.21 | 1.88 | 0.32 | 1676.51 | 82.91 |
| | | DET6 | 1.65 | 0.02 | 0.26 | 0.05 | | | | | | | | | | | | |

**Table F10.** (continued)

| Flow rate (µL/min) | Sensor | Attachment Detachment | Flow | | Slope (K) | | Viscosity (kg/m/s) | | Elasticity (kg/m/s²) | | Wall shear stress (kg/m/s²) | | Δ*f* (Hz) | | Δ*D* (×10⁻⁶) | | Δ*m* (ng/cm²) | |
|---|---|---|---|---|---|---|---|---|---|---|---|---|---|---|---|---|---|---|
| | | | Re | Shear Stress (kg/m/s²) | avg. | std. | avg. | std. | avg. | std. | avg. | std. | avg. | std. | avg. | std. | avg. | std. |
| 200 | Gold | ATT1 | 6.61 | 0.10 | 0.17 | 0.02 | 1.30E-03 | 8.47E-05 | 11662 | 3650 | 0.13 | 0.01 | -39.13 | 7.26 | 6.89 | 0.53 | 3496.06 | 503.24 |
| | | ATT2 | 6.61 | 0.10 | 0.17 | 0.02 | | | | | | | | | | | | |
| | | ATT3 | 6.61 | 0.10 | 0.17 | 0.02 | | | | | | | | | | | | |
| | | DET1 | 6.61 | 0.10 | 0.28 | 0.06 | 1.35E-03 | 1.09E-04 | 15462 | 5193 | 0.13 | 0.01 | -24.49 | 6.82 | 2.91 | 0.17 | 1796.99 | 308.53 |
| | | DET2 | 6.61 | 0.10 | 0.06 | 0.08 | 1.35E-03 | 1.25E-04 | 28134 | 11275 | 0.13 | 0.01 | -24.49 | 6.82 | 2.91 | 0.17 | 1796.99 | 308.53 |
| | | DET3 | 6.61 | 0.10 | 0.65 | 0.26 | 1.36E-03 | 1.36E-04 | 29970 | 11756 | 0.13 | 0.01 | -24.49 | 6.82 | 2.91 | 0.17 | 1796.99 | 308.53 |
| | | DET4 | 6.61 | 0.10 | 5.10 | 4.23 | 1.38E-03 | 1.53E-04 | 22747 | 9199 | 0.13 | 0.01 | -24.49 | 6.82 | 2.91 | 0.17 | 1796.99 | 308.53 |
| | | DET5 | 6.61 | 0.10 | 0.34 | 0.01 | 1.40E-03 | 1.90E-04 | 16966 | 7578 | 0.14 | 0.02 | -24.49 | 6.82 | 2.91 | 0.17 | 1796.99 | 308.53 |
| | | DET6 | 6.61 | 0.10 | 0.34 | 0.01 | | | | | | | | | | | | |
| 200 | $SiO_2$ | ATT1 | 6.61 | 0.10 | 0.24 | 0.01 | 1.67E-03 | 5.15E-05 | 404188 | 229703 | 0.16 | 0.01 | -30.03 | 7.62 | 7.82 | 0.73 | 753.53 | 22.74 |
| | | ATT2 | 6.61 | 0.10 | 0.87 | 0.24 | 1.39E-03 | 2.12E-04 | 366096 | 183584 | 0.14 | 0.02 | -30.03 | 7.62 | 7.82 | 0.73 | 753.53 | 22.74 |
| | | ATT3 | 6.61 | 0.10 | 0.35 | 0.18 | 1.14E-03 | 3.94E-04 | 341713 | 166712 | 0.11 | 0.04 | -30.03 | 7.62 | 7.82 | 0.73 | 753.53 | 22.74 |
| | | DET1 | 6.61 | 0.10 | 0.14 | 0.05 | 9.64E-04 | 4.91E-04 | 306479 | 146140 | 0.09 | 0.05 | -7.80 | 2.39 | 3.28 | 0.72 | 222.45 | 33.32 |
| | | DET2 | 6.61 | 0.10 | 0.07 | 0.07 | 8.52E-04 | 4.54E-04 | 222771 | 123674 | 0.08 | 0.04 | -7.80 | 2.39 | 3.28 | 0.72 | 222.45 | 33.32 |
| | | DET3 | 6.61 | 0.10 | 0.39 | 0.08 | 7.71E-04 | 3.82E-04 | 213612 | 130821 | 0.07 | 0.04 | -7.80 | 2.39 | 3.28 | 0.72 | 222.45 | 33.32 |
| | | DET4 | 6.61 | 0.10 | 1.16 | 0.84 | 6.98E-04 | 3.16E-04 | 235695 | 113569 | 0.07 | 0.03 | -7.80 | 2.39 | 3.28 | 0.72 | 222.45 | 33.32 |
| | | DET5 | 6.61 | 0.10 | 1.00 | 1.04 | 6.90E-04 | 3.10E-04 | 237274 | 111778 | 0.07 | 0.03 | -7.80 | 2.39 | 3.28 | 0.72 | 222.45 | 33.32 |
| | | DET6 | 6.61 | 0.10 | 1.00 | 1.04 | | | | | | | | | | | | |

**Table F10.** (continued)

| Flow rate (µL/min) | Sensor | Attachment Detachment | Flow | | Slope (K) | | Viscosity (kg/m/s) | | Elasticity (kg/m/s²) | | Wall shear stress (kg/m/s²) | | Δ*f* (Hz) | | Δ*D* (×10⁻⁶) | | Δ*m* (ng/cm²) | |
|---|---|---|---|---|---|---|---|---|---|---|---|---|---|---|---|---|---|---|
| | | | Re | Shear Stress (kg/m/s²) | avg. | std. | avg. | std. | avg. | std. | avg. | std. | avg. | std. | avg. | std. | avg. | std. |
| 200 | Glass | ATT1 | 6.61 | 0.10 | 0.16 | 0.01 | 1.35E-03 | 7.09E-05 | 12519 | 2403 | 0.13 | 0.01 | -47.45 | 6.83 | 8.04 | 0.64 | 3665.57 | 247.26 |
| | | ATT2 | 6.61 | 0.10 | 0.16 | 0.01 | 1.35E-03 | 7.09E-05 | 16594 | 3073 | 0.13 | 0.01 | -47.45 | 6.83 | 8.04 | 0.64 | 3665.57 | 247.26 |
| | | ATT3 | 6.61 | 0.10 | 0.16 | 0.01 | | | | | | | | | | | | |
| | | DET1 | 6.61 | 0.10 | 0.22 | 0.05 | 1.42E-03 | 8.85E-05 | 23518 | 5639 | 0.14 | 0.01 | -31.92 | 5.97 | 3.43 | 0.66 | 2181.07 | 289.24 |
| | | DET2 | 6.61 | 0.10 | 0.07 | 0.08 | 1.38E-03 | 7.75E-05 | 25109 | 5261 | 0.13 | 0.01 | -31.92 | 5.97 | 3.43 | 0.66 | 2181.07 | 289.24 |
| | | DET3 | 6.61 | 0.10 | 0.58 | 0.34 | 1.38E-03 | 8.33E-05 | 19068 | 3042 | 0.13 | 0.01 | -31.92 | 5.97 | 3.43 | 0.66 | 2181.07 | 289.24 |
| | | DET4 | 6.61 | 0.10 | 2.09 | 0.50 | 1.40E-03 | 9.02E-05 | 12743 | 2157 | 0.14 | 0.01 | -31.92 | 5.97 | 3.43 | 0.66 | 2181.07 | 289.24 |
| | | DET5 | 6.61 | 0.10 | 0.40 | 0.02 | 1.43E-03 | 1.09E-04 | 12743 | 2157 | 0.14 | 0.01 | -31.92 | 5.97 | 3.43 | 0.66 | 2181.07 | 289.24 |
| | | DET6 | 6.61 | 0.10 | 0.40 | 0.02 | | | | | | | | | | | | |
| 200 | SS | ATT1 | 6.61 | 0.10 | 0.15 | 0.01 | 1.74E-03 | 3.01E-04 | 208588 | 169730 | 0.17 | 0.03 | -53.10 | 4.92 | 8.14 | 0.42 | 1257.41 | 64.96 |
| | | ATT2 | 6.61 | 0.10 | 0.15 | 0.01 | | | | | | | | | | | | |
| | | ATT3 | 6.61 | 0.10 | 0.15 | 0.01 | | | | | | | | | | | | |
| | | DET1 | 6.61 | 0.10 | 0.04 | 0.04 | 1.91E-03 | 3.04E-04 | 218399 | 171927 | 0.19 | 0.03 | -25.51 | 5.73 | 2.13 | 0.22 | 479.09 | 67.87 |
| | | DET2 | 6.61 | 0.10 | 0.19 | 0.19 | 1.81E-03 | 2.39E-04 | 159593 | 116248 | 0.18 | 0.02 | -25.51 | 5.73 | 2.13 | 0.22 | 479.09 | 67.87 |
| | | DET3 | 6.61 | 0.10 | 0.92 | 0.23 | 2.07E-03 | 4.28E-04 | 238339 | 188658 | 0.20 | 0.04 | -25.51 | 5.73 | 2.13 | 0.22 | 479.09 | 67.87 |
| | | DET4 | 6.61 | 0.10 | 0.15 | 0.02 | 2.38E-03 | 8.21E-04 | 372306 | 321831 | 0.23 | 0.08 | -25.51 | 5.73 | 2.13 | 0.22 | 479.09 | 67.87 |
| | | DET5 | 6.61 | 0.10 | 0.15 | 0.02 | | | | | | | | | | | | |
| | | DET6 | 6.61 | 0.10 | 0.15 | 0.02 | | | | | | | | | | | | |

**Table F11.** QCM-D data of Bacteria during attachment and detachment experiments

| Flow rate (µL/min) | Sensor | Attachment Detachment | Flow | | Slope (K) | | Viscosity (kg/m/s) | | Elasticity (kg/m/s²) | | Wall shear stress (kg/m/s²) | | Δ*f* (Hz) | | Δ*D* (×10⁻⁶) | | Δ*m* (ng/cm²) | |
|---|---|---|---|---|---|---|---|---|---|---|---|---|---|---|---|---|---|---|
| | | | Re | Shear Stress (kg/m/s²) | avg. | std. | avg. | std. | avg. | std. | avg. | std. | avg. | std. | avg. | std. | avg. | std. |
| 100 | Gold | ATT1 | 3.30 | 0.05 | 0.28 | 0.08 | 1.08E-03 | 5.41E-05 | 7339 | 5759 | 0.05 | 0.00 | -27.10 | 0.68 | 5.63 | 0.65 | 2001.16 | 107.50 |
| | | ATT2 | 3.30 | 0.05 | 0.15 | 0.04 | 1.32E-03 | 2.56E-05 | 26122 | 6197 | 0.06 | 0.00 | -27.10 | 0.68 | 5.63 | 0.65 | 2001.16 | 107.50 |
| | | ATT3 | 3.30 | 0.05 | 0.15 | 0.04 | | | | | | | | | | | | |
| | | FR 100_1 | 3.30 | 0.05 | 0.93 | 0.50 | 1.36E-03 | 6.88E-05 | 27347 | 10581 | 0.07 | 0.00 | -15.97 | 0.63 | 1.18 | 0.05 | 1423.69 | 337.64 |
| | | FR 100_2 | 3.30 | 0.05 | 0.35 | 0.15 | 1.30E-03 | 7.77E-05 | 15309 | 12304 | 0.06 | 0.00 | -15.97 | 0.63 | 1.18 | 0.05 | 1423.69 | 337.64 |
| | | FR 100_3 | 3.30 | 0.05 | 0.44 | 0.02 | 1.29E-03 | 6.25E-05 | 11855 | 6414 | 0.06 | 0.00 | -15.97 | 0.63 | 1.18 | 0.05 | 1423.69 | 337.64 |
| | | FR 100_4 | 3.30 | 0.05 | 0.44 | 0.02 | | | | | | | | | | | | |
| | | FR 200 | 6.61 | 0.10 | 0.20 | 0.11 | 1.30E-03 | 1.10E-04 | 4369 | 3968 | 0.13 | 0.01 | -15.74 | 0.65 | 1.14 | 0.03 | 1447.66 | 363.93 |
| | | FR 300 | 9.91 | 0.15 | 0.20 | 0.11 | 1.30E-03 | 1.10E-04 | 4369 | 3968 | 0.13 | 0.01 | -15.58 | 0.62 | 1.12 | 0.05 | 1429.30 | 355.71 |
| | | FR 500 | 16.52 | 0.24 | 0.20 | 0.11 | 1.30E-03 | 1.10E-04 | 4369 | 3968 | 0.13 | 0.01 | -15.17 | 0.59 | 1.05 | 0.05 | 1379.04 | 326.11 |
| | | FR 700 | 23.12 | 0.34 | 0.20 | 0.11 | 1.30E-03 | 1.10E-04 | 4369 | 3968 | 0.13 | 0.01 | -14.58 | 0.68 | 0.89 | 0.14 | 1379.97 | 305.64 |
| | | FR 1000 | 33.03 | 0.49 | 0.20 | 0.11 | 1.30E-03 | 1.10E-04 | 4369 | 3968 | 0.13 | 0.01 | -13.66 | 1.10 | 0.68 | 0.34 | 1256.87 | 238.80 |

**Table F11.** (continued)

| Flow rate (µL/min) | Sensor | Attachment Detachment | Flow | | Slope (K) | | Viscosity (kg/m/s) | | Elasticity (kg/m/s²) | | Wall shear stress (kg/m/s²) | | Δ*f* (Hz) | | Δ*D* (×10⁻⁶) | | Δ*m* (ng/cm²) | |
|---|---|---|---|---|---|---|---|---|---|---|---|---|---|---|---|---|---|---|
| | | | Re | Shear Stress (kg/m/s²) | avg. | std. | avg. | std. | avg. | std. | avg. | std. | avg. | std. | avg. | std. | avg. | std. |
| 100 | $SiO_2$ | ATT1 | 3.30 | 0.05 | 0.27 | 0.10 | 1.59E-03 | 3.87E-04 | 122991 | 117649 | 0.08 | 0.02 | -37.00 | 12.00 | 5.83 | 0.50 | 899.05 | 29.04 |
| | | ATT2 | 3.30 | 0.05 | 0.38 | 0.30 | 1.56E-03 | 4.34E-04 | 116484 | 123153 | 0.08 | 0.02 | -37.00 | 12.00 | 5.83 | 0.50 | 899.05 | 29.04 |
| | | ATT3 | 3.30 | 0.05 | 0.13 | 0.02 | 1.69E-03 | 2.12E-04 | 142513 | 106719 | 0.08 | 0.01 | -37.00 | 12.00 | 5.83 | 0.50 | 899.05 | 29.04 |
| | | FR 100_1 | 3.30 | 0.05 | 0.68 | 0.54 | 1.71E-03 | 1.44E-04 | 158900 | 119026 | 0.08 | 0.01 | -15.00 | 11.42 | 1.57 | 0.48 | 218.80 | 77.09 |
| | | FR 100_2 | 3.30 | 0.05 | 0.22 | 0.27 | 1.55E-03 | 1.22E-04 | 121181 | 65321 | 0.08 | 0.01 | -15.00 | 11.42 | 1.57 | 0.48 | 218.80 | 77.09 |
| | | FR 100_3 | 3.30 | 0.05 | 0.37 | 0.04 | 1.55E-03 | 2.13E-04 | 114541 | 51516 | 0.08 | 0.01 | -15.00 | 11.42 | 1.57 | 0.48 | 218.80 | 77.09 |
| | | FR 100_4 | 3.30 | 0.05 | 0.82 | 0.29 | 1.70E-03 | 3.94E-04 | 198384 | 206037 | 0.08 | 0.02 | -15.00 | 11.42 | 1.57 | 0.48 | 218.80 | 77.09 |
| | | FR 200 | 6.61 | 0.10 | 0.16 | 0.07 | 1.61E-03 | 5.06E-04 | 197785 | 209262 | 0.16 | 0.05 | -14.36 | 11.43 | 1.49 | 0.48 | 206.01 | 80.45 |
| | | FR 300 | 9.91 | 0.15 | 0.16 | 0.07 | 1.61E-03 | 5.06E-04 | 197785 | 209262 | 0.16 | 0.05 | -13.94 | 11.49 | 1.44 | 0.48 | 193.84 | 82.61 |
| | | FR 500 | 16.52 | 0.24 | 0.16 | 0.07 | 1.61E-03 | 5.06E-04 | 197785 | 209262 | 0.16 | 0.05 | -13.30 | 11.54 | 1.29 | 0.62 | 174.04 | 71.00 |
| | | FR 700 | 23.12 | 0.34 | 0.16 | 0.07 | 1.61E-03 | 5.06E-04 | 197785 | 209262 | 0.16 | 0.05 | -12.70 | 11.52 | 1.18 | 0.67 | 105.96 | |
| | | FR 1000 | 33.03 | 0.49 | 0.16 | 0.07 | 1.61E-03 | 5.06E-04 | 197785 | 209262 | 0.16 | 0.05 | -11.52 | 11.51 | 0.98 | 0.83 | 92.42 | |

**Table F11.** (continued)

| Flow rate (µL/min) | Sensor | Attachment Detachment | Flow | | Slope (K) | | Viscosity (kg/m/s) | | Elasticity (kg/m/s²) | | Wall shear stress (kg/m/s²) | | Δ*f* (Hz) | | Δ*D* (×10⁻⁶) | | Δ*m* (ng/cm²) | |
|---|---|---|---|---|---|---|---|---|---|---|---|---|---|---|---|---|---|---|
| | | | Re | Shear Stress (kg/m/s²) | avg. | std. | avg. | std. | avg. | std. | avg. | std. | avg. | std. | avg. | std. | avg. | std. |
| 100 | Glass | ATT1 | 3.30 | 0.05 | 0.27 | 0.07 | 1.05E-03 | 2.92E-05 | 2333 | 1898 | 0.05 | 0.00 | -42.30 | 3.73 | 5.46 | 0.30 | 2715.70 | 354.40 |
| | | ATT2 | 3.30 | 0.05 | 0.10 | 0.02 | 1.36E-03 | 9.08E-05 | 12979 | 4627 | 0.07 | 0.00 | -42.30 | 3.73 | 5.46 | 0.30 | 2715.70 | 354.40 |
| | | ATT3 | 3.30 | 0.05 | 0.10 | 0.02 | | | | | | | | | | | | |
| | | FR 100_1 | 3.30 | 0.05 | 0.65 | 0.40 | 1.47E-03 | 1.13E-04 | 18500 | 4585 | 0.07 | 0.01 | -24.16 | 2.77 | 2.11 | 0.34 | 1984.14 | 183.60 |
| | | FR 100_2 | 3.30 | 0.05 | 0.24 | 0.16 | 1.41E-03 | 8.61E-05 | 26674 | 7379 | 0.07 | 0.00 | -24.16 | 2.77 | 2.11 | 0.34 | 1984.14 | 183.60 |
| | | FR 100_3 | 3.30 | 0.05 | 0.40 | 0.02 | 1.40E-03 | 9.63E-05 | 28172 | 9088 | 0.07 | 0.00 | -24.16 | 2.77 | 2.11 | 0.34 | 1984.14 | 183.60 |
| | | FR 100_4 | 3.30 | 0.05 | 1.57 | 0.44 | 1.39E-03 | 9.91E-05 | 17433 | 12720 | 0.07 | 0.00 | -24.16 | 2.77 | 2.11 | 0.34 | 1984.14 | 183.60 |
| | | FR 200 | 6.61 | 0.10 | 0.17 | 0.01 | 1.33E-03 | 9.78E-05 | 6805 | 2150 | 0.13 | 0.01 | -23.90 | 2.71 | 2.09 | 0.31 | 1976.36 | 184.69 |
| | | FR 300 | 9.91 | 0.15 | 0.17 | 0.01 | 1.33E-03 | 9.78E-05 | 6805 | 2150 | 0.13 | 0.01 | -23.64 | 2.75 | 2.05 | 0.32 | 1962.19 | 175.40 |
| | | FR 500 | 16.52 | 0.24 | 0.17 | 0.01 | 1.33E-03 | 9.78E-05 | 6805 | 2150 | 0.13 | 0.01 | -23.33 | 2.79 | 2.02 | 0.32 | 1964.92 | 143.41 |
| | | FR 700 | 23.12 | 0.34 | 0.17 | 0.01 | 1.33E-03 | 9.78E-05 | 6805 | 2150 | 0.13 | 0.01 | -23.00 | 2.82 | 1.99 | 0.32 | 1918.57 | 95.93 |
| | | FR 1000 | 33.03 | 0.49 | 0.17 | 0.01 | 1.33E-03 | 9.78E-05 | 6805 | 2150 | 0.13 | 0.01 | -22.44 | 2.80 | 1.88 | 0.28 | 1966.06 | 139.91 |

**Table F11.** (continued)

| Flow rate (µL/min) | Sensor | Attachment Detachment | Flow | | Slope (K) | | Viscosity (kg/m/s) | | Elasticity (kg/m/s²) | | Wall shear stress (kg/m/s²) | | Δ*f* (Hz) | | Δ*D* (×10⁻⁶) | | Δ*m* (ng/cm²) | |
|---|---|---|---|---|---|---|---|---|---|---|---|---|---|---|---|---|---|---|
| | | | Re | Shear Stress (kg/m/s²) | avg. | std. | avg. | std. | avg. | std. | avg. | std. | avg. | std. | avg. | std. | avg. | std. |
| 100 | SS | ATT1 | 3.30 | 0.05 | 0.29 | 0.02 | 9.37E-04 | 1.45E-04 | 37634 | 63299 | 0.05 | 0.01 | -26.62 | 11.29 | 5.50 | 0.50 | 1985.35 | 144.86 |
| | | ATT2 | 3.30 | 0.05 | 0.29 | 0.01 | 1.05E-03 | 2.90E-04 | 44145 | 58579 | 0.05 | 0.01 | -26.62 | 11.29 | 5.50 | 0.50 | 1985.35 | 144.86 |
| | | ATT3 | 3.30 | 0.05 | 0.17 | 0.03 | 1.21E-03 | 2.05E-04 | 70457 | 83874 | 0.06 | 0.01 | -26.62 | 11.29 | 5.50 | 0.50 | 1985.35 | 144.86 |
| | | FR 100_1 | 3.30 | 0.05 | 0.30 | 0.02 | 1.33E-03 | 1.91E-04 | 81633 | 88229 | 0.06 | 0.01 | -11.79 | 10.61 | 2.11 | 0.44 | 1535.78 | 89.17 |
| | | FR 100_2 | 3.30 | 0.05 | 0.11 | 0.06 | 1.23E-03 | 2.09E-04 | 69556 | 75316 | 0.06 | 0.01 | -11.79 | 10.61 | 2.11 | 0.44 | 1535.78 | 89.17 |
| | | FR 100_3 | 3.30 | 0.05 | 0.50 | 0.03 | 1.02E-03 | 4.68E-04 | 48938 | 63461 | 0.05 | 0.02 | -11.79 | 10.61 | 2.11 | 0.44 | 1535.78 | 89.17 |
| | | FR 100_4 | 3.30 | 0.05 | 0.50 | 0.03 | | | | | | | | | | | | |
| | | FR 200 | 6.61 | 0.10 | 0.46 | 0.28 | 9.54E-04 | 5.96E-04 | 33303 | 34319 | 0.09 | 0.06 | -11.54 | 10.67 | 2.31 | 0.48 | 1418.29 | 179.66 |
| | | FR 300 | 9.91 | 0.15 | 0.46 | 0.28 | 9.54E-04 | 5.96E-04 | 33303 | 34319 | 0.09 | 0.06 | -11.37 | 10.63 | 2.36 | 0.48 | 1393.36 | 142.70 |
| | | FR 500 | 16.52 | 0.24 | 0.25 | 0.07 | 9.64E-04 | 6.04E-04 | 35958 | 32266 | 0.23 | 0.15 | -11.14 | 10.58 | 2.45 | 0.36 | 1351.76 | 181.45 |
| | | FR 700 | 23.12 | 0.34 | 0.20 | 0.08 | 9.64E-04 | 6.04E-04 | 35958 | 32266 | 0.23 | 0.15 | -10.86 | 10.60 | 2.48 | 0.39 | 1474.23 | |
| | | FR 1000 | 33.03 | 0.49 | 0.13 | 0.04 | 9.64E-04 | 6.04E-04 | 37256 | 30962 | 0.47 | 0.29 | -10.23 | 10.87 | 2.48 | 0.49 | 1423.86 | |

**Table F11.** (continued)

| Flow rate (µL/min) | Sensor | Attachment Detachment | Flow | | Slope (K) | | Viscosity (kg/m/s) | | Elasticity (kg/m/s²) | | Wall shear stress (kg/m/s²) | | Δ*f* (Hz) | | Δ*D* (×10⁻⁶) | | Δ*m* (ng/cm²) | |
|---|---|---|---|---|---|---|---|---|---|---|---|---|---|---|---|---|---|---|
| | | | Re | Shear Stress (kg/m/s²) | avg. | std. | avg. | std. | avg. | std. | avg. | std. | avg. | std. | avg. | std. | avg. | std. |
| 50 | Gold | ATT1 | 1.65 | 0.02 | 1.56 | 2.34 | 1.06E-03 | 3.69E-05 | 3867 | 3330 | 0.03 | 0.00 | -13.63 | 3.29 | 4.34 | 1.70 | 2666.11 | 529.61 |
| | | ATT2 | 1.65 | 0.02 | 0.84 | 0.21 | 1.09E-03 | 2.83E-05 | 8962 | 4335 | 0.03 | 0.00 | -13.63 | 3.29 | 4.34 | 1.70 | 2666.11 | 529.61 |
| | | ATT3 | 1.65 | 0.02 | 0.31 | 0.15 | 1.15E-03 | 2.65E-05 | 16504 | 3532 | 0.03 | 0.00 | -13.63 | 3.29 | 4.34 | 1.70 | 2666.11 | 529.61 |
| | | DET1 | 1.65 | 0.02 | 0.57 | 0.15 | 1.17E-03 | 2.74E-05 | 17987 | 3679 | 0.03 | 0.00 | -9.26 | 2.45 | 1.16 | 0.08 | 2177.87 | 1456.10 |
| | | DET2 | 1.65 | 0.02 | 0.44 | 0.33 | 1.16E-03 | 3.21E-05 | 15065 | 6340 | 0.03 | 0.00 | -9.26 | 2.45 | 1.16 | 0.08 | 2177.87 | 1456.10 |
| | | DET3 | 1.65 | 0.02 | 0.58 | 0.11 | 1.14E-03 | 5.05E-05 | 10398 | 10430 | 0.03 | 0.00 | -9.26 | 2.45 | 1.16 | 0.08 | 2177.87 | 1456.10 |
| | | DET4 | 1.65 | 0.02 | 0.58 | 0.11 | | | | | | | | | | | | |
| | | DET5 | 1.65 | 0.02 | 0.58 | 0.11 | | | | | | | | | | | | |
| | | DET6 | 1.65 | 0.02 | 0.58 | 0.11 | | | | | | | | | | | | |
| 50 | SiO2 | ATT1 | 1.65 | 0.02 | 0.27 | 0.20 | 9.96E-04 | 8.55E-05 | 21790 | 22512 | 0.02 | 0.00 | -9.23 | 3.90 | 4.05 | 1.18 | 428.99 | |
| | | ATT2 | 1.65 | 0.02 | 0.50 | 0.70 | 1.15E-03 | 1.67E-04 | 102408 | 136524 | 0.03 | 0.00 | -9.23 | 3.90 | 4.05 | 1.18 | 428.99 | |
| | | ATT3 | 1.65 | 0.02 | 0.60 | 0.28 | 1.06E-03 | 1.90E-05 | 91542 | 121157 | 0.03 | 0.00 | -9.23 | 3.90 | 4.05 | 1.18 | 428.99 | |
| | | DET1 | 1.65 | 0.02 | 0.18 | 0.05 | 1.08E-03 | 1.78E-05 | 65205 | 104047 | 0.03 | 0.00 | 3.02 | 7.12 | 1.16 | 0.59 | | |
| | | DET2 | 1.65 | 0.02 | 0.14 | 0.10 | 1.07E-03 | 1.27E-05 | 65067 | 104162 | 0.03 | 0.00 | 3.02 | 7.12 | 1.16 | 0.59 | | |
| | | DET3 | 1.65 | 0.02 | 0.57 | 0.36 | 1.06E-03 | 2.33E-05 | 63782 | 105267 | 0.03 | 0.00 | 3.02 | 7.12 | 1.16 | 0.59 | | |
| | | DET4 | 1.65 | 0.02 | 0.28 | 0.08 | 1.06E-03 | 2.65E-05 | 63528 | 105488 | 0.03 | 0.00 | 3.02 | 7.12 | 1.16 | 0.59 | | |
| | | DET5 | 1.65 | 0.02 | 0.28 | 0.08 | | | | | | | | | | | | |
| | | DET6 | 1.65 | 0.02 | 0.28 | 0.08 | | | | | | | | | | | | |

**Table F11.** (continued)

| Flow rate (µL/min) | Sensor | Attachment Detachment | Flow | | Slope (K) | | Viscosity (kg/m/s) | | Elasticity (kg/m/s²) | | Wall shear stress (kg/m/s²) | | Δ*f* (Hz) | | Δ*D* (×10⁻⁶) | | Δ*m* (ng/cm²) | |
|---|---|---|---|---|---|---|---|---|---|---|---|---|---|---|---|---|---|---|
| | | | Re | Shear Stress (kg/m/s²) | avg. | std. | avg. | std. | avg. | std. | avg. | std. | avg. | std. | avg. | std. | avg. | std. |
| 50 | Glass | ATT1 | 1.65 | 0.02 | 0.29 | 0.07 | 1.04E-03 | 1.56E-05 | 3814 | 2805 | 0.03 | 0.00 | -14.11 | 4.01 | 3.92 | 1.04 | 3313.88 | 179.18 |
| | | ATT2 | 1.65 | 0.02 | 0.96 | 0.87 | 1.05E-03 | 9.33E-06 | 5914 | 1814 | 0.03 | 0.00 | -14.11 | 4.01 | 3.92 | 1.04 | 3313.88 | 179.18 |
| | | ATT3 | 1.65 | 0.02 | 0.10 | 0.10 | 1.11E-03 | 2.74E-05 | 8679 | 2377 | 0.03 | 0.00 | -14.11 | 4.01 | 3.92 | 1.04 | 3313.88 | 179.18 |
| | | DET1 | 1.65 | 0.02 | 0.30 | 0.02 | 1.14E-03 | 3.48E-05 | 9197 | 1732 | 0.03 | 0.00 | -7.40 | 2.06 | 1.43 | 0.37 | 3502.31 | 873.16 |
| | | DET2 | 1.65 | 0.02 | 0.04 | 0.04 | 1.11E-03 | 5.20E-05 | 7208 | 3579 | 0.03 | 0.00 | -7.40 | 2.06 | 1.43 | 0.37 | 3502.31 | 873.16 |
| | | DET3 | 1.65 | 0.02 | 0.63 | 0.07 | 1.10E-03 | 6.51E-05 | 5719 | 4638 | 0.03 | 0.00 | -7.40 | 2.06 | 1.43 | 0.37 | 3502.31 | 873.16 |
| | | DET4 | 1.65 | 0.02 | 0.46 | 0.55 | 1.09E-03 | 6.71E-05 | 5001 | 5278 | 0.03 | 0.00 | -7.40 | 2.06 | 1.43 | 0.37 | 3502.31 | 873.16 |
| | | DET5 | 1.65 | 0.02 | 0.46 | 0.55 | | | | | | | | | | | | |
| | | DET6 | 1.65 | 0.02 | 0.46 | 0.55 | | | | | | | | | | | | |
| 50 | SS | ATT1 | 1.65 | 0.02 | 0.27 | 0.05 | 1.08E-03 | 7.00E-05 | 8194 | 9548 | 0.03 | 0.00 | -11.82 | 4.92 | 4.11 | 1.21 | 2205.66 | 313.48 |
| | | ATT2 | 1.65 | 0.02 | 1.17 | 0.70 | 1.09E-03 | 5.68E-05 | 10404 | 7531 | 0.03 | 0.00 | -11.82 | 4.92 | 4.11 | 1.21 | 2205.66 | 313.48 |
| | | ATT3 | 1.65 | 0.02 | 0.37 | 0.12 | 1.13E-03 | 3.95E-05 | 15269 | 3274 | 0.03 | 0.00 | -11.82 | 4.92 | 4.11 | 1.21 | 2205.66 | 313.48 |
| | | DET1 | 1.65 | 0.02 | 0.40 | 0.06 | 1.15E-03 | 5.42E-05 | 17951 | 3433 | 0.03 | 0.00 | -8.12 | 1.99 | 1.84 | 0.55 | 1694.42 | |
| | | DET2 | 1.65 | 0.02 | 1.75 | 0.33 | 1.15E-03 | 4.83E-05 | 16467 | 1068 | 0.03 | 0.00 | -8.12 | 1.99 | 1.84 | 0.55 | 1694.42 | |
| | | DET3 | 1.65 | 0.02 | 0.44 | 0.23 | 1.14E-03 | 4.49E-05 | 14796 | 2230 | 0.03 | 0.00 | -8.12 | 1.99 | 1.84 | 0.55 | 1694.42 | |
| | | DET4 | 1.65 | 0.02 | 0.21 | 0.19 | 1.13E-03 | 3.80E-05 | 12594 | 5968 | 0.03 | 0.00 | -8.12 | 1.99 | 1.84 | 0.55 | 1694.42 | |
| | | DET5 | 1.65 | 0.02 | 0.21 | 0.19 | | | | | | | | | | | | |
| | | DET6 | 1.65 | 0.02 | 0.21 | 0.19 | | | | | | | | | | | | |

**Table F11.** (continued)

| Flow rate (µL/min) | Sensor | Attachment Detachment | Flow | | Slope (K) | | Viscosity (kg/m/s) | | Elasticity (kg/m/s²) | | Wall shear stress (kg/m/s²) | | Δ*f* (Hz) | | Δ*D* (×10⁻⁶) | | Δ*m* (ng/cm²) | |
|---|---|---|---|---|---|---|---|---|---|---|---|---|---|---|---|---|---|---|
| | | | Re | Shear Stress (kg/m/s²) | avg. | std. | avg. | std. | avg. | std. | avg. | std. | avg. | std. | avg. | std. | avg. | std. |
| 200 | Gold | ATT1 | 6.61 | 0.10 | 0.20 | 0.04 | 1.06E-03 | 7.59E-05 | 3022 | 5073 | 0.10 | 0.01 | -15.25 | 4.20 | 3.54 | 1.69 | 3105.64 | 530.29 |
| | | ATT2 | 6.61 | 0.10 | 0.75 | 1.07 | 1.11E-03 | 6.05E-05 | 5575 | 5268 | 0.11 | 0.01 | -15.25 | 4.20 | 3.54 | 1.69 | 3105.64 | 530.29 |
| | | ATT3 | 6.61 | 0.10 | 0.26 | 0.09 | 1.13E-03 | 4.66E-05 | 7203 | 5993 | 0.11 | 0.00 | -15.25 | 4.20 | 3.54 | 1.69 | 3105.64 | 530.29 |
| | | DET1 | 6.61 | 0.10 | 0.31 | 0.09 | 1.14E-03 | 5.19E-05 | 8507 | 6903 | 0.11 | 0.01 | -7.46 | 3.95 | 0.80 | 0.65 | 1810.60 | 413.28 |
| | | DET2 | 6.61 | 0.10 | 2.02 | 2.66 | 1.14E-03 | 5.21E-05 | 8937 | 6607 | 0.11 | 0.01 | -7.46 | 3.95 | 0.80 | 0.65 | 1810.60 | 413.28 |
| | | DET3 | 6.61 | 0.10 | 1.93 | 2.74 | 1.12E-03 | 7.05E-05 | 4684 | 4084 | 0.11 | 0.01 | -7.46 | 3.95 | 0.80 | 0.65 | 1810.60 | 413.28 |
| | | DET4 | 6.61 | 0.10 | 0.20 | 0.12 | 1.11E-03 | 7.47E-05 | 3537 | 4635 | 0.11 | 0.01 | -7.46 | 3.95 | 0.80 | 0.65 | 1810.60 | 413.28 |
| | | DET5 | 6.61 | 0.10 | 0.20 | 0.12 | | | | | | | | | | | | |
| | | DET6 | 6.61 | 0.10 | 0.20 | 0.12 | | | | | | | | | | | | |
| 200 | $SiO_2$ | ATT1 | 6.61 | 0.10 | 0.16 | 0.17 | 1.75E-03 | 8.05E-04 | 209036 | 152333 | 0.17 | 0.08 | -4.76 | 1.34 | 3.92 | 2.72 | 296.28 | 163.24 |
| | | ATT2 | 6.61 | 0.10 | 1.00 | 1.16 | 1.55E-03 | 5.82E-04 | 182302 | 126942 | 0.15 | 0.06 | -4.76 | 1.34 | 3.92 | 2.72 | 296.28 | 163.24 |
| | | ATT3 | 6.61 | 0.10 | 0.64 | 0.33 | 1.17E-03 | 2.97E-04 | 148580 | 78079 | 0.11 | 0.03 | -4.76 | 1.34 | 3.92 | 2.72 | 296.28 | 163.24 |
| | | DET1 | 6.61 | 0.10 | 0.34 | 0.20 | 1.05E-03 | 4.14E-04 | 132863 | 57754 | 0.10 | 0.04 | 6.36 | 7.89 | 1.18 | 1.82 | | |
| | | DET2 | 6.61 | 0.10 | 0.29 | 0.27 | 1.05E-03 | 4.14E-04 | 132863 | 57754 | 0.10 | 0.04 | 6.36 | 7.89 | 1.18 | 1.82 | | |
| | | DET3 | 6.61 | 0.10 | 0.49 | 0.38 | 1.05E-03 | 4.14E-04 | 132863 | 57754 | 0.10 | 0.04 | 6.36 | 7.89 | 1.18 | 1.82 | | |
| | | DET4 | 6.61 | 0.10 | 0.26 | 0.23 | 1.05E-03 | 4.14E-04 | 132863 | 57754 | 0.10 | 0.04 | 6.36 | 7.89 | 1.18 | 1.82 | | |
| | | DET5 | 6.61 | 0.10 | 0.26 | 0.23 | | | | | | | | | | | | |
| | | DET6 | 6.61 | 0.10 | 0.26 | 0.23 | | | | | | | | | | | | |

**Table F11.** (continued)

| Flow rate (µL/min) | Sensor | Attachment Detachment | Flow | | Slope (K) | | Viscosity (kg/m/s) | | Elasticity (kg/m/s²) | | Wall shear stress (kg/m/s²) | | Δ*f* (Hz) | | Δ*D* (×10⁻⁶) | | Δ*m* (ng/cm²) | |
|---|---|---|---|---|---|---|---|---|---|---|---|---|---|---|---|---|---|---|
| | | | Re | Shear Stress (kg/m/s²) | avg. | std. | avg. | std. | avg. | std. | avg. | std. | avg. | std. | avg. | std. | avg. | std. |
| 200 | Glass | ATT1 | 6.61 | 0.10 | 0.27 | 0.05 | 1.17E-03 | 1.99E-04 | 42585 | 70407 | 0.11 | 0.02 | -17.59 | 12.74 | 3.79 | 2.43 | 3804.19 | 211.59 |
| | | ATT2 | 6.61 | 0.10 | 0.19 | 0.01 | 1.24E-03 | 1.76E-04 | 40100 | 59060 | 0.12 | 0.02 | -17.59 | 12.74 | 3.79 | 2.43 | 3804.19 | 211.59 |
| | | ATT3 | 6.61 | 0.10 | 0.19 | 0.01 | | | | | | | | | | | | |
| | | DET1 | 6.61 | 0.10 | 0.25 | 0.04 | 1.27E-03 | 1.63E-04 | 35623 | 47953 | 0.12 | 0.02 | -8.18 | 8.34 | 1.14 | 1.38 | 3080.61 | 219.18 |
| | | DET2 | 6.61 | 0.10 | 0.11 | 0.13 | 1.24E-03 | 1.85E-04 | 34700 | 48713 | 0.12 | 0.02 | -8.18 | 8.34 | 1.14 | 1.38 | 3080.61 | 219.18 |
| | | DET3 | 6.61 | 0.10 | 0.57 | 0.05 | 1.22E-03 | 2.01E-04 | 32898 | 50196 | 0.12 | 0.02 | -8.18 | 8.34 | 1.14 | 1.38 | 3080.61 | 219.18 |
| | | DET4 | 6.61 | 0.10 | 0.12 | 0.17 | 1.22E-03 | 2.05E-04 | 31891 | 51074 | 0.12 | 0.02 | -8.18 | 8.34 | 1.14 | 1.38 | 3080.61 | 219.18 |
| | | DET5 | 6.61 | 0.10 | 0.12 | 0.17 | | | | | | | | | | | | |
| | | DET6 | 6.61 | 0.10 | 0.12 | 0.17 | | | | | | | | | | | | |
| 200 | SS | ATT1 | 6.61 | 0.10 | 0.29 | 0.03 | 1.16E-03 | 1.68E-04 | 71498 | 110514 | 0.11 | 0.02 | -12.21 | 6.97 | 3.88 | 2.62 | 2804.79 | |
| | | ATT2 | 6.61 | 0.10 | 0.43 | 0.18 | 1.22E-03 | 1.37E-04 | 62608 | 84583 | 0.12 | 0.01 | -12.21 | 6.97 | 3.88 | 2.62 | 2804.79 | |
| | | ATT3 | 6.61 | 0.10 | 0.43 | 0.18 | | | | | | | | | | | | |
| | | DET1 | 6.61 | 0.10 | 0.34 | 0.02 | 1.23E-03 | 1.17E-04 | 54929 | 65902 | 0.12 | 0.01 | -6.76 | 6.42 | 1.49 | 1.91 | 2043.11 | |
| | | DET2 | 6.61 | 0.10 | 0.84 | 0.34 | 1.23E-03 | 1.52E-04 | 130242 | 201580 | 0.12 | 0.01 | -6.76 | 6.42 | 1.49 | 1.91 | 2043.11 | |
| | | DET3 | 6.61 | 0.10 | 0.78 | 0.72 | 1.23E-03 | 1.52E-04 | 130242 | 201580 | 0.12 | 0.01 | -6.76 | 6.42 | 1.49 | 1.91 | 2043.11 | |
| | | DET4 | 6.61 | 0.10 | 0.78 | 0.72 | | | | | | | | | | | | |
| | | DET5 | 6.61 | 0.10 | 0.78 | 0.72 | | | | | | | | | | | | |
| | | DET6 | 6.61 | 0.10 | 0.78 | 0.72 | | | | | | | | | | | | |

**Table F12.** QCM-D data of BSA during attachment and detachment experiments

| Flow rate (µL/min) | Sensor | Attachment Detachment | Flow | | Slope (K) | | Viscosity (kg/m/s) | | Elasticity (kg/m/s²) | | Wall shear stress (kg/m/s²) | | Δ*f* (Hz) | | Δ*D* (×10⁻⁶) | | Δ*m* (ng/cm²) | |
|---|---|---|---|---|---|---|---|---|---|---|---|---|---|---|---|---|---|---|
| | | | Re | Shear Stress (kg/m/s²) | avg. | std. | avg. | std. | avg. | std. | avg. | std. | avg. | std. | avg. | std. | avg. | std. |
| 100 | Gold | ATT1 | 3.30 | 0.05 | 1.39 | 1.02 | 3.13E-03 | 5.93E-05 | 22927 | 6419 | 0.15 | 0.00 | -26.40 | 0.77 | 0.50 | 0.02 | 94.49 | 2.76 |
| | | ATT2 | 3.30 | 0.05 | 0.30 | 0.51 | 2.94E-03 | 5.62E-05 | 22671 | 3399 | 0.14 | 0.00 | -26.40 | 0.77 | 0.50 | 0.02 | 94.49 | 2.76 |
| | | ATT3 | 3.30 | 0.05 | 0.30 | 0.51 | | | | | | | | | | | | |
| | | FR 100_1 | 3.30 | 0.05 | 0.41 | 0.22 | 2.90E-03 | 9.50E-05 | 10618 | 11981 | 0.14 | 0.00 | -25.38 | 0.97 | 0.20 | 0.03 | 90.83 | 3.46 |
| | | FR 100_2 | 3.30 | 0.05 | 0.24 | 0.27 | 2.97E-03 | 1.90E-04 | 10618 | 11981 | 0.14 | 0.01 | -25.38 | 0.97 | 0.20 | 0.03 | 90.83 | 3.46 |
| | | FR 100_3 | 3.30 | 0.05 | 0.24 | 0.27 | | | | | | | | | | | | |
| | | FR 100_4 | 3.30 | 0.05 | 0.24 | 0.27 | | | | | | | | | | | | |
| | | FR 200 | 6.61 | 0.10 | 0.12 | 0.05 | 3.16E-03 | 4.62E-04 | 10618 | 11981 | 0.31 | 0.04 | -25.18 | 1.32 | 0.18 | 0.02 | 90.11 | 4.72 |
| | | FR 300 | 9.91 | 0.15 | 0.11 | 0.04 | 3.20E-03 | 4.06E-04 | 9545 | 13499 | 0.47 | 0.06 | -24.97 | 1.51 | 0.15 | 0.02 | 89.38 | 5.39 |
| | | FR 500 | 16.52 | 0.24 | 0.12 | 0.06 | 3.71E-03 | 3.10E-04 | 9545 | 13499 | 0.90 | 0.08 | -24.59 | 1.58 | 0.10 | 0.00 | 88.00 | 5.65 |
| | | FR 700 | 23.12 | 0.34 | 0.12 | 0.06 | 3.71E-03 | 3.10E-04 | 9545 | 13499 | 0.90 | 0.08 | -24.14 | 1.63 | 0.02 | 0.01 | 86.41 | 5.84 |
| | | FR 1000 | 33.03 | 0.49 | 0.12 | 0.06 | 3.71E-03 | 3.10E-04 | 9545 | 13499 | 0.90 | 0.08 | -23.23 | 1.81 | -0.08 | 0.04 | 83.16 | 6.47 |

**Table F12.** (continued)

| Flow rate (µL/min) | Sensor | Attachment Detachment | Flow | | Slope (K) | | Viscosity (kg/m/s) | | Elasticity (kg/m/s²) | | Wall shear stress (kg/m/s²) | | Δ*f* (Hz) | | Δ*D* (×10⁻⁶) | | Δ*m* (ng/cm²) | |
|---|---|---|---|---|---|---|---|---|---|---|---|---|---|---|---|---|---|---|
| | | | Re | Shear Stress (kg/m/s²) | avg. | std. | avg. | std. | avg. | std. | avg. | std. | avg. | std. | avg. | std. | avg. | std. |
| 100 | $SiO_2$ | ATT1 | 3.30 | 0.05 | 0.16 | 0.15 | 1.18E-02 | 5.24E-03 | 1367495 | 1760721 | 0.57 | 0.25 | -35.85 | 13.12 | 0.60 | 0.20 | 128.29 | 46.97 |
| | | ATT2 | 3.30 | 0.05 | 0.02 | 0.02 | 1.05E-02 | 4.32E-03 | 1365632 | 1762699 | 0.51 | 0.21 | -35.85 | 13.12 | 0.60 | 0.20 | 128.29 | 46.97 |
| | | ATT3 | 3.30 | 0.05 | 0.02 | 0.02 | | | | | | | | | | | | |
| | | FR 100_1 | 3.30 | 0.05 | 0.17 | 0.10 | 9.70E-03 | 3.01E-03 | 679227 | 529008 | 0.47 | 0.15 | -30.98 | 10.60 | 0.14 | 0.02 | 110.89 | 37.92 |
| | | FR 100_2 | 3.30 | 0.05 | 0.10 | 0.14 | 1.07E-02 | 1.53E-03 | 651257 | 576032 | 0.52 | 0.07 | -30.98 | 10.60 | 0.14 | 0.02 | 110.89 | 37.92 |
| | | FR 100_3 | 3.30 | 0.05 | 0.10 | 0.14 | | | | | | | | | | | | |
| | | FR 100_4 | 3.30 | 0.05 | 0.10 | 0.14 | | | | | | | | | | | | |
| | | FR 200 | 6.61 | 0.10 | 0.10 | 0.11 | 2.17E-02 | 8.40E-03 | 1380139 | 2382602 | 2.11 | 0.82 | -30.12 | 10.54 | 0.09 | 0.06 | 107.79 | 37.73 |
| | | FR 300 | 9.91 | 0.15 | 0.11 | 0.10 | 1.74E-02 | 5.31E-03 | 5274870 | 9128475 | 2.53 | 0.77 | -29.61 | 10.58 | 0.03 | 0.14 | 105.98 | 37.86 |
| | | FR 500 | 16.52 | 0.24 | 0.11 | 0.10 | 1.74E-02 | 5.31E-03 | 5274870 | 9128475 | 2.53 | 0.77 | -29.15 | 10.51 | -0.03 | 0.15 | 104.32 | 37.63 |
| | | FR 700 | 23.12 | 0.34 | 0.11 | 0.10 | 1.74E-02 | 5.31E-03 | 5274870 | 9128475 | 2.53 | 0.77 | -28.55 | 10.51 | -0.12 | 0.22 | 102.17 | 37.61 |
| | | FR 1000 | 33.03 | 0.49 | 0.11 | 0.10 | 1.74E-02 | 5.31E-03 | 5274870 | 9128475 | 2.53 | 0.77 | -27.76 | 10.82 | -0.14 | 0.08 | 99.36 | 38.74 |

**Table F12.** (continued)

| Flow rate (µL/min) | Sensor | Attachment Detachment | Flow | | Slope (K) | | Viscosity (kg/m/s) | | Elasticity (kg/m/s²) | | Wall shear stress (kg/m/s²) | | Δ*f* (Hz) | | Δ*D* (×10⁻⁶) | | Δ*m* (ng/cm²) | |
|---|---|---|---|---|---|---|---|---|---|---|---|---|---|---|---|---|---|---|
| | | | Re | Shear Stress (kg/m/s²) | avg. | std. | avg. | std. | avg. | std. | avg. | std. | avg. | std. | avg. | std. | avg. | std. |
| 100 | Glass | ATT1 | 3.30 | 0.05 | 0.42 | 0.18 | 3.58E-03 | 3.61E-04 | 27759 | 9094 | 0.17 | 0.02 | -29.61 | 4.57 | 0.61 | 0.05 | 105.97 | 16.37 |
| | | ATT2 | 3.30 | 0.05 | 0.03 | 0.04 | 3.49E-03 | 3.41E-05 | 46699 | 13856 | 0.17 | 0.00 | -29.61 | 4.57 | 0.61 | 0.05 | 105.97 | 16.37 |
| | | ATT3 | 3.30 | 0.05 | 0.03 | 0.04 | | | | | | | | | | | | |
| | | FR 100_1 | 3.30 | 0.05 | 1.17 | 0.90 | 3.47E-03 | 1.92E-04 | 33076 | 20842 | 0.17 | 0.01 | -27.39 | 5.67 | 0.23 | 0.15 | 98.02 | 20.29 |
| | | FR 100_2 | 3.30 | 0.05 | 0.19 | 0.26 | 3.48E-03 | 1.69E-04 | 18968 | 25040 | 0.17 | 0.01 | -27.39 | 5.67 | 0.23 | 0.15 | 98.02 | 20.29 |
| | | FR 100_3 | 3.30 | 0.05 | 0.19 | 0.26 | | | | | | | | | | | | |
| | | FR 100_4 | 3.30 | 0.05 | 0.19 | 0.26 | | | | | | | | | | | | |
| | | FR 200 | 6.61 | 0.10 | 0.11 | 0.06 | 4.62E-03 | 9.52E-04 | 3325 | 5062 | 0.45 | 0.09 | -26.93 | 5.91 | 0.21 | 0.15 | 96.38 | 21.15 |
| | | FR 300 | 9.91 | 0.15 | 0.11 | 0.06 | 4.62E-03 | 9.52E-04 | 3325 | 5062 | 0.45 | 0.09 | -26.51 | 6.11 | 0.18 | 0.15 | 94.88 | 21.88 |
| | | FR 500 | 16.52 | 0.24 | 0.11 | 0.06 | 4.62E-03 | 9.52E-04 | 3325 | 5062 | 0.45 | 0.09 | -26.17 | 6.16 | 0.13 | 0.12 | 93.68 | 22.06 |
| | | FR 700 | 23.12 | 0.34 | 0.11 | 0.06 | 4.62E-03 | 9.52E-04 | 3325 | 5062 | 0.45 | 0.09 | -25.71 | 6.40 | 0.07 | 0.12 | 92.02 | 22.92 |
| | | FR 1000 | 33.03 | 0.49 | 0.11 | 0.06 | 4.62E-03 | 9.52E-04 | 3325 | 5062 | 0.45 | 0.09 | -24.83 | 6.70 | -0.06 | 0.19 | 88.86 | 23.97 |

**Table F12.** (continued)

| Flow rate (µL/min) | Sensor | Attachment Detachment | Flow | | Slope (K) | | Viscosity (kg/m/s) | | Elasticity (kg/m/s²) | | Wall shear stress (kg/m/s²) | | Δ*f* (Hz) | | Δ*D* (×10⁻⁶) | | Δ*m* (ng/cm²) | |
|---|---|---|---|---|---|---|---|---|---|---|---|---|---|---|---|---|---|---|
| | | | Re | Shear Stress (kg/m/s²) | avg. | std. | avg. | std. | avg. | std. | avg. | std. | avg. | std. | avg. | std. | avg. | std. |
| 100 | SS | ATT1 | 3.30 | 0.05 | 0.11 | 0.08 | 3.23E-03 | 5.19E-04 | 18237 | 6452 | 0.16 | 0.03 | -29.38 | 3.97 | 0.63 | 0.11 | 105.15 | 14.20 |
| | | ATT2 | 3.30 | 0.05 | 0.02 | 0.02 | 2.94E-03 | 2.32E-04 | 25812 | 7059 | 0.14 | 0.01 | -29.38 | 3.97 | 0.63 | 0.11 | 105.15 | 14.20 |
| | | ATT3 | 3.30 | 0.05 | 0.02 | 0.02 | | | | | | | | | | | | |
| | | FR 100_1 | 3.30 | 0.05 | 0.90 | 0.63 | 2.83E-03 | 1.63E-04 | 19358 | 13818 | 0.14 | 0.01 | -27.28 | 4.33 | 0.25 | 0.14 | 97.65 | 15.49 |
| | | FR 100_2 | 3.30 | 0.05 | 0.07 | 0.04 | 2.90E-03 | 1.44E-05 | 13163 | 17868 | 0.14 | 0.00 | -27.28 | 4.33 | 0.25 | 0.14 | 97.65 | 15.49 |
| | | FR 100_3 | 3.30 | 0.05 | 0.07 | 0.04 | 2.95E-03 | 7.86E-05 | 5152 | 4757 | 0.14 | 0.00 | -27.28 | 4.33 | 0.25 | 0.14 | 97.65 | 15.49 |
| | | FR 100_4 | 3.30 | 0.05 | 0.07 | 0.04 | | | | | | | | | | | | |
| | | FR 200 | 6.61 | 0.10 | 0.06 | 0.02 | 3.11E-03 | 1.61E-04 | 2500 | 3042 | 0.30 | 0.02 | -26.51 | 4.45 | 0.21 | 0.13 | 94.87 | 15.94 |
| | | FR 300 | 9.91 | 0.15 | 0.06 | 0.02 | 3.11E-03 | 1.61E-04 | 2500 | 3042 | 0.30 | 0.02 | -25.90 | 4.60 | 0.17 | 0.14 | 92.69 | 16.47 |
| | | FR 500 | 16.52 | 0.24 | 0.06 | 0.02 | 3.11E-03 | 1.61E-04 | 2500 | 3042 | 0.30 | 0.02 | -25.39 | 4.59 | 0.15 | 0.12 | 90.87 | 16.42 |
| | | FR 700 | 23.12 | 0.34 | 0.06 | 0.02 | 3.11E-03 | 1.61E-04 | 2500 | 3042 | 0.30 | 0.02 | -24.75 | 4.74 | 0.09 | 0.14 | 88.57 | 16.97 |
| | | FR 1000 | 33.03 | 0.49 | 0.06 | 0.02 | 3.11E-03 | 1.61E-04 | 2500 | 3042 | 0.30 | 0.02 | -23.87 | 4.94 | -0.03 | 0.19 | 85.45 | 17.69 |

**Table F12.** (continued)

| Flow rate (µL/min) | Sensor | Attachment Detachment | Flow | | Slope (K) | | Viscosity (kg/m/s) | | Elasticity (kg/m/s²) | | Wall shear stress (kg/m/s²) | | Δ*f* (Hz) | | Δ*D* (×10⁻⁶) | | Δ*m* (ng/cm²) | |
|---|---|---|---|---|---|---|---|---|---|---|---|---|---|---|---|---|---|---|
| | | | Re | Shear Stress (kg/m/s²) | avg. | std. | avg. | std. | avg. | std. | avg. | std. | avg. | std. | avg. | std. | avg. | std. |
| 50 | Gold | ATT1 | 1.65 | 0.02 | 1.80 | 1.00 | 3.23E-03 | 3.91E-04 | 18341 | 3971 | 0.08 | 0.01 | -31.89 | 3.97 | 0.68 | 0.16 | 114.12 | 14.19 |
| | | ATT2 | 1.65 | 0.02 | 0.13 | 0.11 | 2.94E-03 | 6.97E-05 | 23301 | 5950 | 0.07 | 0.00 | -31.89 | 3.97 | 0.68 | 0.16 | 114.12 | 14.19 |
| | | ATT3 | 1.65 | 0.02 | 0.13 | 0.11 | | | | | | | | | | | | |
| | | DET1 | 1.65 | 0.02 | 0.36 | 0.09 | 2.90E-03 | 1.86E-04 | 14161 | 11524 | 0.07 | 0.00 | -28.48 | 2.99 | 0.22 | 0.08 | 101.92 | 10.69 |
| | | DET2 | 1.65 | 0.02 | 0.03 | 0.03 | 3.51E-03 | 2.00E-04 | 3618 | 4063 | 0.09 | 0.00 | -28.48 | 2.99 | 0.22 | 0.08 | 101.92 | 10.69 |
| | | DET3 | 1.65 | 0.02 | 0.03 | 0.03 | | | | | | | | | | | | |
| | | DET4 | 1.65 | 0.02 | 0.03 | 0.03 | | | | | | | | | | | | |
| | | DET5 | 1.65 | 0.02 | 0.03 | 0.03 | | | | | | | | | | | | |
| | | DET6 | 1.65 | 0.02 | 0.03 | 0.03 | | | | | | | | | | | | |
| 50 | $SiO_2$ | ATT1 | 1.65 | 0.02 | 0.14 | 0.02 | 1.67E-02 | 9.00E-03 | 1276303 | 1527652 | 0.41 | 0.22 | -40.37 | 15.33 | 0.67 | 0.24 | 144.49 | 54.88 |
| | | ATT2 | 1.65 | 0.02 | 0.05 | 0.03 | 8.79E-03 | 1.15E-03 | 396490 | 233298 | 0.21 | 0.03 | -40.37 | 15.33 | 0.67 | 0.24 | 144.49 | 54.88 |
| | | ATT3 | 1.65 | 0.02 | 0.05 | 0.03 | | | | | | | | | | | | |
| | | DET1 | 1.65 | 0.02 | 0.29 | 0.19 | 7.55E-03 | 7.95E-04 | 196847 | 12426 | 0.18 | 0.02 | -33.36 | 12.25 | 0.10 | 0.00 | 119.39 | 43.83 |
| | | DET2 | 1.65 | 0.02 | 0.10 | 0.09 | 8.87E-03 | 1.07E-03 | 148977 | 55272 | 0.22 | 0.03 | -33.36 | 12.25 | 0.10 | 0.00 | 119.39 | 43.83 |
| | | DET3 | 1.65 | 0.02 | 0.01 | 0.00 | 2.19E-02 | 6.25E-04 | 345274 | 171084 | 0.53 | 0.02 | -33.36 | 12.25 | 0.10 | 0.00 | 119.39 | 43.83 |
| | | DET4 | 1.65 | 0.02 | 0.01 | 0.00 | | | | | | | | | | | | |
| | | DET5 | 1.65 | 0.02 | 0.01 | 0.00 | | | | | | | | | | | | |
| | | DET6 | 1.65 | 0.02 | 0.01 | 0.00 | | | | | | | | | | | | |

**Table F12.** (continued)

| Flow rate (µL/min) | Sensor | Attachment Detachment | Flow | | Slope (K) | | Viscosity (kg/m/s) | | Elasticity (kg/m/s²) | | Wall shear stress (kg/m/s²) | | Δ*f* (Hz) | | Δ*D* (×10⁻⁶) | | Δ*m* (ng/cm²) | |
|---|---|---|---|---|---|---|---|---|---|---|---|---|---|---|---|---|---|---|
| | | | Re | Shear Stress (kg/m/s²) | avg. | std. | avg. | std. | avg. | std. | avg. | std. | avg. | std. | avg. | std. | avg. | std. |
| 50 | Glass | ATT1 | 1.65 | 0.02 | 1.59 | 0.94 | 3.48E-03 | 2.28E-04 | 25312 | 12842 | 0.08 | 0.01 | -31.41 | 0.84 | 0.73 | 0.04 | 112.40 | 3.00 |
| | | ATT2 | 1.65 | 0.02 | 0.04 | 0.05 | 3.21E-03 | 1.16E-04 | 35492 | 9327 | 0.08 | 0.00 | -31.41 | 0.84 | 0.73 | 0.04 | 112.40 | 3.00 |
| | | ATT3 | 1.65 | 0.02 | 0.04 | 0.05 | | | | | | | | | | | | |
| | | DET1 | 1.65 | 0.02 | 1.01 | 1.44 | 3.15E-03 | 1.19E-04 | 29944 | 4539 | 0.08 | 0.00 | -28.58 | 1.61 | 0.19 | 0.02 | 102.30 | 5.78 |
| | | DET2 | 1.65 | 0.02 | 0.07 | 0.02 | 3.65E-03 | 3.31E-04 | 176 | 297 | 0.09 | 0.01 | -28.58 | 1.61 | 0.19 | 0.02 | 102.30 | 5.78 |
| | | DET3 | 1.65 | 0.02 | 0.07 | 0.02 | | | | | | | | | | | | |
| | | DET4 | 1.65 | 0.02 | 0.07 | 0.02 | | | | | | | | | | | | |
| | | DET5 | 1.65 | 0.02 | 0.07 | 0.02 | | | | | | | | | | | | |
| | | DET6 | 1.65 | 0.02 | 0.07 | 0.02 | | | | | | | | | | | | |
| 50 | SS | ATT1 | 1.65 | 0.02 | 0.64 | 0.57 | 3.66E-03 | 6.55E-04 | 18637 | 17954 | 0.09 | 0.02 | -37.19 | 0.71 | 0.78 | 0.10 | 133.10 | 2.55 |
| | | ATT2 | 1.65 | 0.02 | 0.01 | 0.00 | 3.29E-03 | 4.80E-04 | 25951 | 14135 | 0.08 | 0.01 | -37.19 | 0.71 | 0.78 | 0.10 | 133.10 | 2.55 |
| | | ATT3 | 1.65 | 0.02 | 0.01 | 0.00 | | | | | | | | | | | | |
| | | DET1 | 1.65 | 0.02 | 0.80 | 0.72 | 3.30E-03 | 4.95E-04 | 13045 | 7545 | 0.08 | 0.01 | -36.08 | 0.98 | 0.39 | 0.05 | 129.14 | 3.50 |
| | | DET2 | 1.65 | 0.02 | 0.10 | 0.11 | 3.55E-03 | 5.53E-04 | 3547 | 6144 | 0.09 | 0.01 | -36.08 | 0.98 | 0.39 | 0.05 | 129.14 | 3.50 |
| | | DET3 | 1.65 | 0.02 | 0.10 | 0.11 | | | | | | | | | | | | |
| | | DET4 | 1.65 | 0.02 | 0.10 | 0.11 | | | | | | | | | | | | |
| | | DET5 | 1.65 | 0.02 | 0.10 | 0.11 | | | | | | | | | | | | |
| | | DET6 | 1.65 | 0.02 | 0.10 | 0.11 | | | | | | | | | | | | |

**Table F12.** (continued)

| Flow rate (µL/min) | Sensor | Attachment Detachment | Flow | | Slope (K) | | Viscosity (kg/m/s) | | Elasticity (kg/m/s²) | | Wall shear stress (kg/m/s²) | | Δ*f* (Hz) | | Δ*D* (×10⁻⁶) | | Δ*m* (ng/cm²) | |
|---|---|---|---|---|---|---|---|---|---|---|---|---|---|---|---|---|---|---|
| | | | Re | Shear Stress (kg/m/s²) | avg. | std. | avg. | std. | avg. | std. | avg. | std. | avg. | std. | avg. | std. | avg. | std. |
| 200 | Gold | ATT1 | 6.61 | 0.10 | 0.04 | 0.02 | 4.05E-03 | 3.61E-03 | 216078 | 295217 | 0.39 | 0.35 | -14.42 | 0.53 | 0.37 | 0.00 | 51.61 | 1.90 |
| | | ATT2 | 6.61 | 0.10 | 0.01 | 0.00 | 4.41E-03 | 3.08E-03 | 290208 | 379289 | 0.43 | 0.30 | -14.42 | 0.53 | 0.37 | 0.00 | 51.61 | 1.90 |
| | | ATT3 | 6.61 | 0.10 | 0.01 | 0.00 | | | | | | | | | | | | |
| | | DET1 | 6.61 | 0.10 | 0.31 | 0.36 | 5.20E-03 | 4.22E-03 | 380966 | 525280 | 0.51 | 0.41 | -12.66 | 0.55 | 0.04 | 0.06 | 45.31 | 1.97 |
| | | DET2 | 6.61 | 0.10 | 0.07 | 0.03 | 5.34E-03 | 4.02E-03 | 380749 | 525587 | 0.52 | 0.39 | -12.66 | 0.55 | 0.04 | 0.06 | 45.31 | 1.97 |
| | | DET3 | 6.61 | 0.10 | 0.07 | 0.03 | | | | | | | | | | | | |
| | | DET4 | 6.61 | 0.10 | 0.07 | 0.03 | | | | | | | | | | | | |
| | | DET5 | 6.61 | 0.10 | 0.07 | 0.03 | | | | | | | | | | | | |
| | | DET6 | 6.61 | 0.10 | 0.07 | 0.03 | | | | | | | | | | | | |
| 200 | $SiO_2$ | ATT1 | 6.61 | 0.10 | 0.06 | 0.03 | 1.29E-02 | 4.33E-03 | 1686153 | 1321761 | 1.26 | 0.42 | -35.26 | 11.43 | 0.46 | 0.17 | 126.18 | 40.89 |
| | | ATT2 | 6.61 | 0.10 | 0.05 | 0.06 | 1.22E-02 | 4.34E-03 | 1729331 | 1305738 | 1.19 | 0.42 | -35.26 | 11.43 | 0.46 | 0.17 | 126.18 | 40.89 |
| | | ATT3 | 6.61 | 0.10 | 0.05 | 0.06 | 1.39E-02 | 4.76E-03 | 1635772 | 1201590 | 1.35 | 0.46 | -35.26 | 11.43 | 0.46 | 0.17 | 126.18 | 40.89 |
| | | DET1 | 6.61 | 0.10 | 0.19 | 0.02 | 2.25E-02 | 1.38E-02 | | | 2.19 | 1.34 | -28.56 | 8.60 | -0.01 | 0.08 | 102.22 | 30.78 |
| | | DET2 | 6.61 | 0.10 | 0.01 | 0.00 | 3.35E-02 | 3.67E-03 | | | 3.26 | 0.36 | -28.56 | 8.60 | -0.01 | 0.08 | 102.22 | 30.78 |
| | | DET3 | 6.61 | 0.10 | 0.01 | 0.00 | | | | | | | | | | | | |
| | | DET4 | 6.61 | 0.10 | 0.01 | 0.00 | | | | | | | | | | | | |
| | | DET5 | 6.61 | 0.10 | 0.01 | 0.00 | | | | | | | | | | | | |
| | | DET6 | 6.61 | 0.10 | 0.01 | 0.00 | | | | | | | | | | | | |

**Table F12.** (continued)

| Flow rate (µL/min) | Sensor | Attachment Detachment | Flow | | Slope (K) | | Viscosity (kg/m/s) | | Elasticity (kg/m/s²) | | Wall shear stress (kg/m/s²) | | Δ*f* (Hz) | | Δ*D* (×10⁻⁶) | | Δ*m* (ng/cm²) | |
|---|---|---|---|---|---|---|---|---|---|---|---|---|---|---|---|---|---|---|
| | | | Re | Shear Stress (kg/m/s²) | avg. | std. | avg. | std. | avg. | std. | avg. | std. | avg. | std. | avg. | std. | avg. | std. |
| 200 | Glass | ATT1 | 6.61 | 0.10 | 0.32 | 0.44 | 5.20E-03 | 3.36E-03 | 216993 | 307590 | 0.51 | 0.33 | -20.70 | 4.48 | 0.41 | 0.14 | 74.09 | 16.03 |
| | | ATT2 | 6.61 | 0.10 | 0.03 | 0.02 | 4.88E-03 | 2.80E-03 | 207374 | 232165 | 0.47 | 0.27 | -20.70 | 4.48 | 0.41 | 0.14 | 74.09 | 16.03 |
| | | ATT3 | 6.61 | 0.10 | 0.05 | 0.01 | 5.12E-03 | 3.13E-03 | 225867 | 262377 | 0.50 | 0.30 | -20.70 | 4.48 | 0.41 | 0.14 | 74.09 | 16.03 |
| | | DET1 | 6.61 | 0.10 | 0.41 | 0.07 | 5.79E-03 | 3.52E-03 | 247635 | 273955 | 0.56 | 0.34 | -18.57 | 4.74 | -0.09 | 0.10 | 66.47 | 16.98 |
| | | DET2 | 6.61 | 0.10 | 0.33 | 0.36 | 6.03E-03 | 3.15E-03 | 247658 | 273923 | 0.59 | 0.31 | -18.57 | 4.74 | -0.09 | 0.10 | 66.47 | 16.98 |
| | | DET3 | 6.61 | 0.10 | 0.33 | 0.36 | | | | | | | | | | | | |
| | | DET4 | 6.61 | 0.10 | 0.33 | 0.36 | | | | | | | | | | | | |
| | | DET5 | 6.61 | 0.10 | 0.33 | 0.36 | | | | | | | | | | | | |
| | | DET6 | 6.61 | 0.10 | 0.33 | 0.36 | | | | | | | | | | | | |
| 200 | SS | ATT1 | 6.61 | 0.10 | 0.15 | 0.10 | 7.87E-03 | 3.27E-03 | 285472 | 307502 | 0.76 | 0.32 | -15.90 | 6.64 | 0.27 | 0.06 | 56.90 | 23.78 |
| | | ATT2 | 6.61 | 0.10 | 0.03 | 0.03 | 6.81E-03 | 2.13E-03 | 469378 | 567450 | 0.66 | 0.21 | -15.90 | 6.64 | 0.27 | 0.06 | 56.90 | 23.78 |
| | | ATT3 | 6.61 | 0.10 | 0.03 | 0.03 | | | | | | | | | | | | |
| | | DET1 | 6.61 | 0.10 | 0.12 | 0.15 | 1.02E-02 | 5.98E-03 | 1124263 | 1562063 | 1.00 | 0.58 | -18.11 | 5.88 | 0.10 | 0.01 | 64.83 | 21.06 |
| | | DET2 | 6.61 | 0.10 | 0.02 | 0.02 | 1.92E-02 | 1.58E-02 | | | 1.86 | 1.53 | -18.11 | 5.88 | 0.10 | 0.01 | 64.83 | 21.06 |
| | | DET3 | 6.61 | 0.10 | 0.02 | 0.02 | | | | | | | | | | | | |
| | | DET4 | 6.61 | 0.10 | 0.02 | 0.02 | | | | | | | | | | | | |
| | | DET5 | 6.61 | 0.10 | 0.02 | 0.02 | | | | | | | | | | | | |
| | | DET6 | 6.61 | 0.10 | 0.02 | 0.02 | | | | | | | | | | | | |

# F.5. MATLAB Codes of Chapter 5

## F.5.1. Generate scatter plots

```
clc; clear; close all;
FileName = 'D:\2.Publication\2020_QCMD\DfindFiles\Final_all.xlsx';
SaveDir = 'D:\2.Publication\2020_QCMD\DfindFiles\FIGURE\fdvm_v2_flow vs interact surface\';

Ref = xlsread(FileName,'ReVisEla (2)_norepeat (2)','E4:E484');
wsf = xlsread(FileName,'ReVisEla (2)_norepeat (2)','F4:F484');
all = xlsread(FileName,'ReVisEla (2)_norepeat (2)','G4:AL484');

for p = 1:1:4
if p == 1
name = 'VACV';
elseif p == 2
name = 'MV';
elseif p == 3
name = 'BAC';
else
name = 'BSA';
end

data = all(120*(p-1)+1:120*p,:);
slo = data(:,1);
vis = data(:,5);
ela = data(:,9);
rey = data(:,13);
shr = data(:,17);
fre = data(:,21);
dis = data(:,25);
mas = data(:,29);

SaveImg = [SaveDir,name,'AllTests_(1)k-m'];
figure = figure('InvertHardcopy','off','Color',[1 1 1]);
AX = axes('Parent',figure);
scatter(slo,mas,8,'c','MarkerFaceColor','k','MarkerEdgeColor','k');
box(AX,'on');
set(AX,'LineWidth',0.5,'FontName','Arial','FontSize',8);
xlabel('K','FontWeight','Bold','FontSize',9);
ylabel('mass','FontWeight','Bold','FontSize',9);
set(gcf,'Units','inches','Position', [0 0 1.8 1.5],'PaperUnits','Inches','PaperSize',[1.8 1.5]);
saveas(gcf,SaveImg,'tiff');
clearvars figure AX SaveImg
close;

clearvars sensor d s slo vis ela rey shr fre dis mas
end
clearvars data name
```

## F.5.2. Generate plots with arrows

```
clc; clear; close all;

FileName = 'D:\2.Publication\2020_QCMD\DfindFiles\Final_all.xlsx';

clr1 = [.0 .0 .0; .3 .7 .9; 1 .7 .2; .9 .1 .2];
clr2 = [.3 .3 .3; .1 .5 .7; .8 .5 .0; .8 .0 .1];
y1 = [6;6;5;5;0;0;4;4;3;3;2;2;1;1];
y2 = [8;8;7;7;6;6;5;5;4;4;3;3;2;2;1;1];

for a = 1:1:2
if a == 1
k_all = xlsread(FileName,'Sheet3 (2)_k','G3:J158');
SaveDir = 'D:\2.Publication\2020_QCMD\DfindFiles\FIGURE\Slope PLOTS\arrows\111021\111021_k_';
xxlim = [0.001 3.75];
xname = 'K';
xtickrng = [(0.001:0.001:0.009),(0.01:0.01:0.09),(0.1:0.1:1)];
xticklab = {'10^-^3','','','','','','','','','10^-^2','','','','','','','','','10^-^1','','','','','','','','','10^0'};
else
k_all = xlsread(FileName,'Sheet3 (2)_w','G3:J158');
SaveDir = 'D:\2.Publication\2020_QCMD\DfindFiles\FIGURE\Slope PLOTS\arrows\111021\111021_w_';
xxlim = [0.01 3.75];
xname = '\tau_w';
xtickrng = [(0.01:0.01:0.09),(0.1:0.1:1)];
xticklab = {'10^-^2','','','','','','','','','10^-^1','','','','','','','','','10^0'};
end

for p = 1:1:4
if p == 1
name = 'VACV';
k = k_all(1:38,:);
elseif p == 2
name = 'MV';
k = k_all(40:77,:);
elseif p == 3
name = 'BAC';
k = k_all(79:116,:);
else
name = 'BSA';
k = k_all(118:155,:);
end

for test = 1:1:4
if test == 4
x = k(4:12,:);
n = 8;
y = y2;
ytk = (1:1:n);
yylim = [0 9];
position = [0 0 1.75 2];
paper = [1.75 2];
ylb = {'FR1000','FR700','FR500','FR300','FR200','FR100(3)','FR100(2)','FR100(1)'};
else
x = k(13*test-12:13*test-6,:);
n = 6;
y = y1;
ytk = (1:1:n);
yylim = [1 7];
position = [0 0 1.62 1.75];
paper = [1.62 1.75];
ylb = {'','DET(3)','DET(2)','DET(1)','ATT(2)','ATT(1)'};
end
```

```
for sensor = 1:1:4
SaveImg = [SaveDir,name,'_test_',num2str(test),'_s(',num2str(sensor),')'];
figure = figure('InvertHardcopy','off','Color',[1 1 1]);
AX = axes('Parent',figure);
hold on
if test ~= 4
for i = 1:1:n
if i <= 2
plot(x(i:i+1,sensor),y(2*i-1:2*i),'Color',[192/255 0 0],'LineWidth',1);
scatter(x(i,sensor),y(2*i-1),8,'c','MarkerFaceColor',[192/255 0 0],'MarkerEdgeColor',[192/255 0 0]);
if x(i,sensor) > x(i+1,sensor)
scatter(x(i+1,sensor),y(2*i),15,'<','MarkerFaceColor',[192/255 0 0],'MarkerEdgeColor',[192/255 0 0]);
elseif x(i,sensor) < x(i+1,sensor)
scatter(x(i+1,sensor),y(2*i),15,'>','MarkerFaceColor',[192/255 0 0],'MarkerEdgeColor',[192/255 0 0]);
end


elseif i >= 4
plot(x(i:i+1,sensor),y(2*i-1:2*i),'Color',[0 112/255 192/255],'LineWidth',1);
scatter(x(i,sensor),y(2*i-1),8,'c','MarkerFaceColor',[0 112/255 192/255],'MarkerEdgeColor',[0 112/255 192/255]);
if x(i,sensor) > x(i+1,sensor)
scatter(x(i+1,sensor),y(2*i),15,'<','MarkerFaceColor',[0 112/255 192/255],'MarkerEdgeColor',[0 112/255 192/255]);
elseif x(i,sensor) < x(i+1,sensor)
scatter(x(i+1,sensor),y(2*i),15,'>','MarkerFaceColor',[0 112/255 192/255],'MarkerEdgeColor',[0 112/255 192/255]);
end
end
end
else
for i = 1:1:n
plot(x(i:i+1,sensor),y(2*i-1:2*i),'Color',[0 112/255 192/255],'LineWidth',1);
scatter(x(i,sensor),y(2*i-1),8,'c','MarkerFaceColor',[0 112/255 192/255],'MarkerEdgeColor',[0 112/255 192/255]);
if x(i,sensor) > x(i+1,sensor)
scatter(x(i+1,sensor),y(2*i),15,'<','MarkerFaceColor',[0 112/255 192/255],'MarkerEdgeColor',[0 112/255 192/255]);
elseif x(i,sensor) < x(i+1,sensor)
scatter(x(i+1,sensor),y(2*i),15,'>','MarkerFaceColor',[0 112/255 192/255],'MarkerEdgeColor',[0 112/255 192/255]);
end
end
end
hold off
box(AX,'on');
xlim(xxlim); ylim(yylim);
set(AX,'xscale','log')
set(AX,'LineWidth',0.5,'FontName','Arial','FontSize',9,...
'YTick',ytk,'YTickLabel',ylb,'XTick',xtickrng,'XTickLabel',xticklab);
xlabel(xname,'FontWeight','Bold','FontSize',9);
set(gcf,'Units','inches','Position',position,'PaperUnits','Inches','PaperSize',paper);
saveas(gcf,SaveImg,'tiff');
clearvars figure AX SaveImg sensor dat ad
close;
end
clearvars t att det
end
clearvars k p
end
clearvars k_all SaveDir xxlim xtickrng xticklab
end
```

### F.5.3. Generate surface shear stress plots

```
clc; clear; close all;

FileName = 'D:\2.Publication\2020_QCMD\DfindFiles\Final_all.xlsx';
SaveDir = 'D:\2.Publication\2020_QCMD\DfindFiles\FIGURE\DetMass\112221_DetMass_';

all = xlsread(FileName,'ReVisEla (2)_norepeat_mass&WCA','AP4:BE15');
clr1 = [.0 .0 .0; .3 .7 .9; 1 .7 .2; .9 .1 .2];
clr2 = [.3 .3 .3; .1 .5 .7; .8 .5 .0; .8 .0 .1];
t = xlsread(FileName,'ReVisEla (2)_norepeat_mass&WCA','AO4:AO15');

for p = 1:1:4
if p == 1
s = 'VACV';
elseif p == 2
s = 'MV';
elseif p == 3
s = 'BAC';
else
s = 'BSA';
end

data = all(:,4*p-3:4*p);

SaveImg = [SaveDir,'Shear_Particle_Surface_',s];
figure = figure('InvertHardcopy','off','Color',[1 1 1]);
AX = axes('Parent',figure);
hold on
for i = 1:1:4
scatter(t,data(:,i),8,'c','MarkerFaceColor',clr1(i,:),'MarkerEdgeColor',clr2(i,:));
plot(t,data(:,i),'LineWidth',1,'Color',clr1(i,:));
end
hold off
box(AX,'on');
xlim([0 0.6]);
if p == 4
ylim([0 3]);
else
ylim([0 .6]);
end
set(AX,'LineWidth',0.5,'FontName','Arial','FontSize',12);
xlabel('\tau_f (kg/m/s^2)','FontWeight','Bold','FontSize',14);
ylabel('\tau_s (kg/m/s^2)','FontWeight','Bold','FontSize',14);
set(gcf,'Units','inches','Position', [0 0 3.5 2.3],'PaperUnits','Inches','PaperSize',[3.5 2.3]);
saveas(gcf,SaveImg,'tiff');
clearvars figure AX SaveImg i
close;

clearvars sensor d s slo vis ela rey shr fre dis mas Ref wsf
clearvars data name
end
```

## F.5.4. Generate plots for clustering analysis

```
clc; clear; close all;

FileDir = 'D:\2.Publication\2020_QCMD\DfindFiles\Clustering\Clustering analysis.xlsx';
SaveDir = 'D:\2.Publication\2020_QCMD\DfindFiles\FIGURE\Clustering\';

bclr = [0 0 0; .278 .722 .878; .988 .745 .196; .906 .114 .212];
m_clr = [0.5 0.5 0.5; .463 .671 .863; .992 .875 .616; .929 .380 .447];

shape = 'c'; sz = 20;

for i = 1:1:4
if i == 1
sheet = 'Sheet1';
name = 'kw_';
elseif i == 2
sheet = 'Sheet1_log';
name = 'kw_log_';
elseif i == 3
sheet = 'Sheet2';
name = 'All_';
else
sheet = 'Sheet2_log';
name = 'All_log_';
end
[data] = xlsread(FileDir,sheet,'B15:K299');
[prct] = xlsread(FileDir,sheet,'C7:C8');
p = data(:,1); s = data(:,2); ad = data(:,3);
x = data(:,4); y = data(:,5); cl = data(:,end);
xmin = floor(min(x)*10)/10-0.5; xmax = round(max(x),1)+0.5;
ymin = floor(min(y)*10)/10-0.5; ymax = round(max(y),1)+0.5;
xlb = ['Dim1 - ',num2str(prct(1)),'%'];
ylb = ['Dim2 - ',num2str(prct(2)),'%'];
lx = [xmin xmax; 0 0]; ly = [0 0; ymin ymax];
for k = 1:1:4
if k == 1
img = 'microbes'; dat = p;
elseif k == 2
img = 'sensor'; dat = s;
elseif k == 3
img = 'attdet'; dat = ad;
else
img = 'cluster'; dat = cl;
end
```

```
SaveImgName = [SaveDir,name,img];
figure = figure('InvertHardcopy','off','Color','none');
AX = axes('Parent',figure);
hold on;
plot(lx(1,:),ly(1,:),':','LineWidth',0.5,'Color',[0.5 0.5 0.5]);
plot(lx(2,:),ly(2,:),':','LineWidth',0.5,'Color',[0.5 0.5 0.5]);
for iii = 1:1:length(dat)
n = dat(iii);
scatter(x(iii),y(iii),sz,shape,'filled','MarkerFaceColor',...
bclr(n,:),'MarkerEdgeColor','k');
clearvars n
end
hold off;
box(AX,'on');
xlim([xmin xmax]);
ylim([ymin ymax]);
set(AX,'LineWidth',0.5,'FontName','Arial','FontSize',11);
xlabel(xlb,'FontSize',13,'FontWeight','Bold');
ylabel(ylb,'FontSize',13,'FontWeight','Bold');
set(gcf,'Units','inches','Position', [0 0 4 3],'PaperUnits','Inches','PaperSize',[4 3]);
export_fig(SaveImgName,'-dpng','-transparent','-nocrop','-r300');
close;
clearvars figure AX SaveImgName iii img dat
end
clearvars sheet name data prct p s ad x y cl
end
```